# A Matrix Converter for Variable Speed AC Motor Drives

Patrick W Wheeler BEng(Hons)

September 1993

A thesis submitted to the University of Bristol in accordance with the requirements for the degree of Doctor of Philosophy in the Faculty of Engineering, Department of Electrical Engineering, September 1993.

# ABSTRACT

The matrix converter offers an all silicon solution to the variable speed AC motor drive problem. The large reactive components required in rectifier/inverter circuits are not needed and therefore a compact and reliable converter can be built. The matrix converter has a number of other advantages over the inverter drive, including four quadrant operation with natural regenerative operation.

With the control methods currently being introduced for use with AC machine drives the induction motor is becoming increasingly popular in applications where DC machines have been used in the past. AC induction motors have the advantages of lower cost and maintenance as well as a greater reliability than DC motors. These advantages are due to the absence of the brushes that are required in DC motors. If AC motor drives could be made in a cheaper and more compact form then it may be possible to expand the market even further into the areas currently occupied by DC drives. In the future the matrix converter may offer this exciting prospect.

This thesis considers the present and future prospects of the matrix converter. Problems associated with control, current commutation and supply harmonics are addressed. The building and testing of a microprocessor controlled PWM matrix converter is described. Alternative uses of the circuit and control theory are also considered.

With the price of semiconductors falling and the reduction in device switching times it may not be long before the matrix converter's silicon solution to AC motor control problems may be commercially viable.

# Claims

A general PWM control algorithm for matrix converters has been developed. A suitable microcontroller has been identified from a range of 16-bit processors compatible with the matrix converter control process. It has been demonstrated that present day high performance micro-controllers can offer adequate performance to meet the needs of matrix converter control. Therefore the use of the matrix converter is no longer impeded by the requirement for high processing power.

A study has been made of modern semiconductor power switching devices, and the IGBT chosen as the most suitable device for switching power converters of this type at the present time. The design of a suitable bi-directional switch for use in matrix converter circuits has been considered. A gate drive circuit that is capable of meeting the requirements of the converter has been developed.

The problems associated with current commutation between switches in the matrix converter have been addressed. A state machine categorisation of existing and new solutions has been developed. The technique of semi-soft current commutation has been introduced and implemented using Logic Array technology.

The semiconductor losses in the matrix converter have been modelled and quantified. Methods for the minimisation of the losses have been introduced. The benefits of these loss reduction methods have been quantified. It has been shown that the matrix converter losses are lower than those in a rectifier/inverter circuit at the higher switching frequencies being used in today's AC drives.

The switching frequency input current harmonics have been calculated, modelled and measured. Guidelines and techniques for input filter design to meet future European EMC regulations have been developed.

A 3.5kWatt experimental matrix converter has been built and tested. The practical results have been found to agree with the analysis and predictions, proving the validity of the simulation and mathematical modelling of the converter. Novel uses of matrix converter control theory have been proposed. Practical commercial applications of the matrix converter technology have been considered.

# Acknowledgements

I would like to thank Dr. Duncan Grant for giving me the opportunity to carry out this research and for being an excellent supervisor. The support for this work from the Science and Engineering Research Council and Control Techniques plc. under the PEDDs LINK scheme and the CASE studentship award scheme is gratefully acknowledged (Grant No. GR/H23436). I would also like to thank all the members of the Industrial Electronics Group who have given advice and encouragement to me throughout the project. Many thanks also go to the workshop technicians and Mr. Bill York for their work in the construction of the experimental matrix converter and the associated test equipment. Finally, thanks to Karen for proof-reading this thesis.

## Author's Declaration

Unless otherwise acknowledged, the contents of this thesis are the original and sole work of the author. No portion of the work in this thesis has been submitted by the author in support of an application for any other degree or qualification, at this or any other University or institution of learning. The views expressed in this thesis are those of the author and not of the University.

Patrick W Wheeler

## Copyright © 1993

# Contents

# List of Figures

# List of Tables

# Publications

The following papers have been written as part of the work leading to this thesis.

Wheeler P.W. and Grant D.A., "Reducing the Semiconductor Losses in a Matrix Converter", IEE Colloquium on Variable Speed Drives, 1992.

Wheeler P.W. and Grant D.A., "A Low Loss Matrix Converter for Variable-Speed Drives", European Power Electronics Conference, Brighton, September 1993.

Wheeler P.W., Zhang H. and Grant D.A., "A Theoretical and Practical Investigation of Switching Frequency Harmonics in a Matrix Converter", Universities Power Electronics Conference, Stafford, September 1993.

(Winner of the Prize for Best Paper at the Conference)

Chapter 1

# Introduction

## 1.1 Introduction

In 1888 the induction machine was invented by Tesla [1] and for the next 75 years it was used as a fixed speed motor. The robust and maintenance free structure of the induction machine made it very popular within the fixed speed constraints. The introduction of the DC machine drives seemed to fulfil the need for variable speed motors, however DC machines suffer from the need to have commutation brushes that require regular maintenance. Even so, the days of the induction machine in many applications seemed numbered until the advancement of silicon technology reached the point, in the 1960s, where efficient variable speed drives for induction machines became feasible [2].

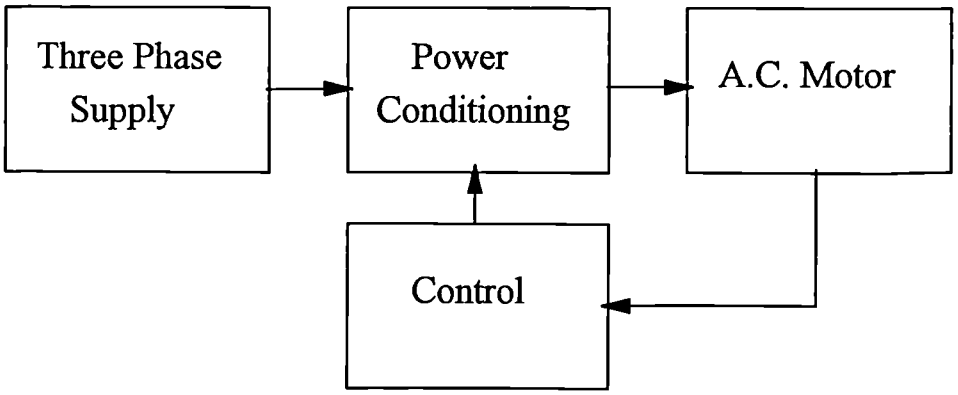


**Figure 1.1. The Layout of a General A.C. Motor Drive**

The solution to the problem of controlling the speed of a three phase induction motor is summarised in figure 1.1. A fixed frequency three phase mains supply must be altered with some form of power conditioning circuit in such a way that the machine will turn at the desired speed. A controller may then be implemented to adjust the operating parameters of the system.

There are many possible circuits for achieving this power conditioning. This thesis will consider a direct conversion circuit that consists of nine fully controllable bi-directional switches, as shown in figure 1.2. This circuit, commonly called a matrix converter, allows any input line to be connected to any output line for any given period of time. It is possible to open and close the switches in a suitable sequence that will generate the required output waveforms.

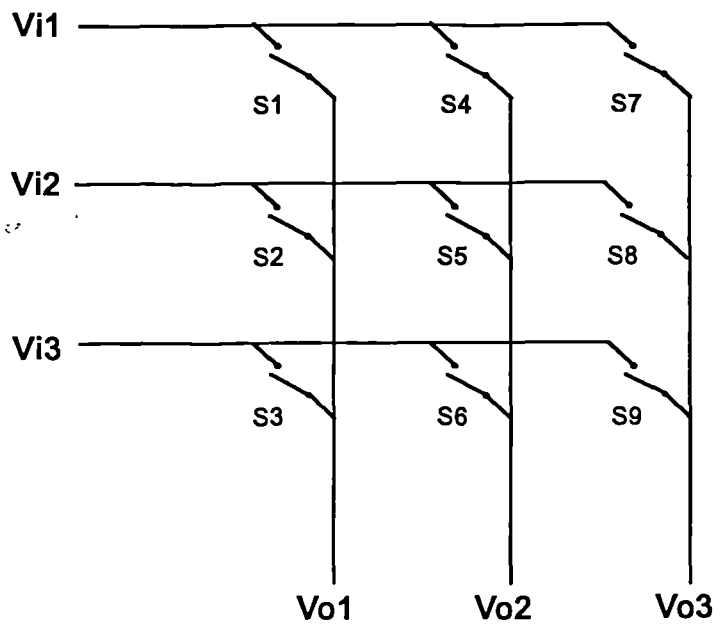


**Figure 1.2. The Matrix Converter Switch Layout**

The matrix converter has a number of distinct advantages over the commonly used rectifier/inverter circuit:

- Natural regeneration.
- No requirement for large reactive components.
- Sinusoidal input currents with displacement factor control.

This introduction will describe the alternatives to the matrix converter and will consider the development of matrix converter technology over the last twenty years. The structure of the thesis will also be outlined.

## 1.2 Solutions to the Variable Speed AC Drives Problem

Besides the matrix converter there are three other basic power circuits that may be used as variable speed drives for AC motors:

- The Rectifier and Inverter
- The Back-to-Back Converter
- The Resonant Converter

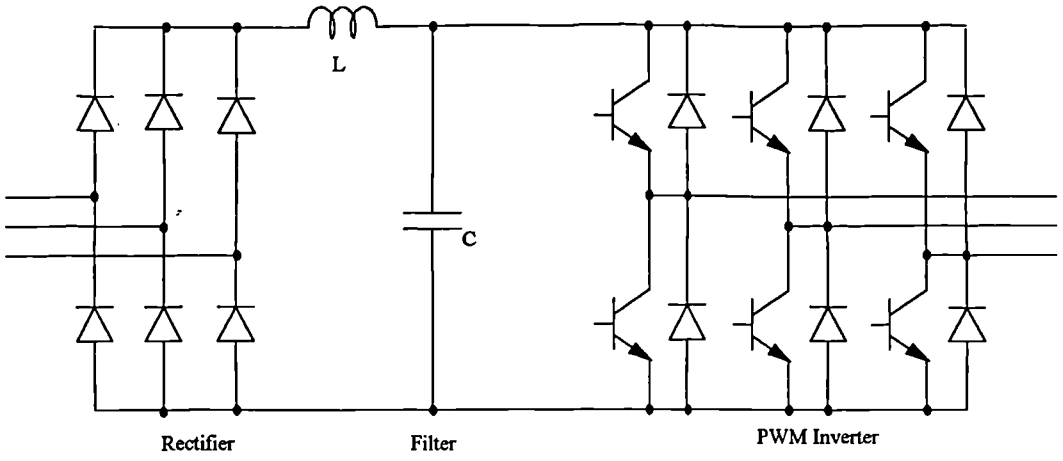


**Figure 1.3. A Voltage Source Inverter Circuit**

This section will consider each of these alternative circuits, giving a brief account of the merits and disadvantages of each configuration.

### 1.2.1 The Rectifier/Inverter

The inverter is the most common commercial AC variable speed drive system used today [3]. The circuit generally consists of a diode bridge rectifier input stage; a large capacitor to smooth the DC Link voltage, that also circulates the switching frequency, and a controllable output-bridge. The output-bridge may be configured as a Voltage Source Inverter (VSI) [4], or a Current Source Inverter (CSI), [5]. A typical rectifier/inverter circuit is shown in figure 1.3.

Progress in power switching device and microprocessor technology has made the use of inverters in industrial applications more widespread. In the last few years much work has been done to improve the performance and efficiency of the inverter [6-8].

In the last 10 years new control methods, such as field orientation control, have been used to enhance the performance of inverter drives [9-11]. This has enabled the AC motor to offer the degree of control that was previously only available with DC motors.

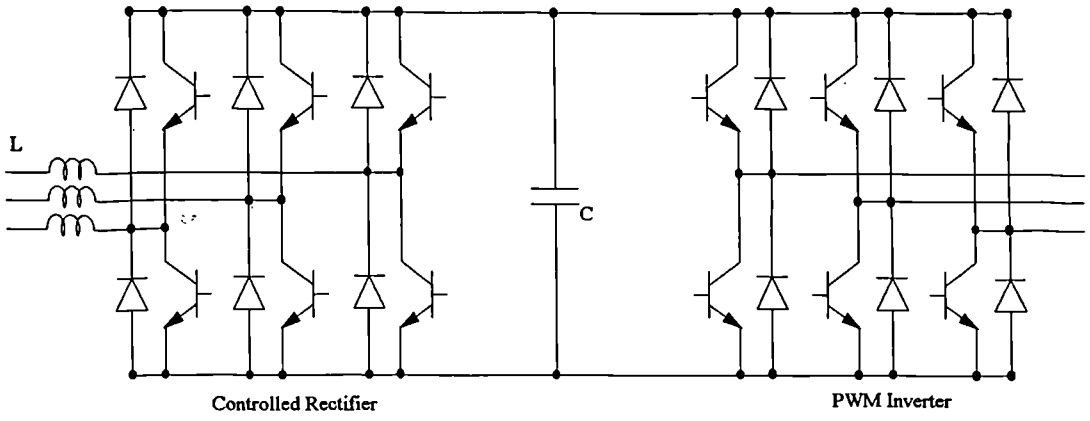


**Figure 1.4. A Double-Bridge, Controlled Rectifier/Inverter Circuit**

### 1.2.2 The Double-Bridge Converter

The input currents drawn by a bridge rectifier are far from sinusoidal and there is no natural means of regeneration into the mains when the inverter is used to brake the motor. A solution to these problems can be found if a controlled bridge is used in place of the diode bridge rectifier. The output-bridge associated control can remain independent of this input-bridge, therefore existing control methods can be used. The addition of this controlled rectifier to the inverter circuit forms the so called "back-to-back" or "double-bridge" converter. A typical controlled double-bridge circuit is shown in figure 1.4.

With correct control this form of input-bridge is capable of sinusoidal input currents. If a control loop is implemented to maintain the DC link voltage at a given voltage then the drive also becomes naturally regenerative. Many methods of control for the input-bridge have been proposed [12-14], including some based on matrix converter control theory. The double-bridge circuit requires twice as many switching devices as the rectifier/inverter circuit and still requires a large DC link capacitor as well as input line inductors.

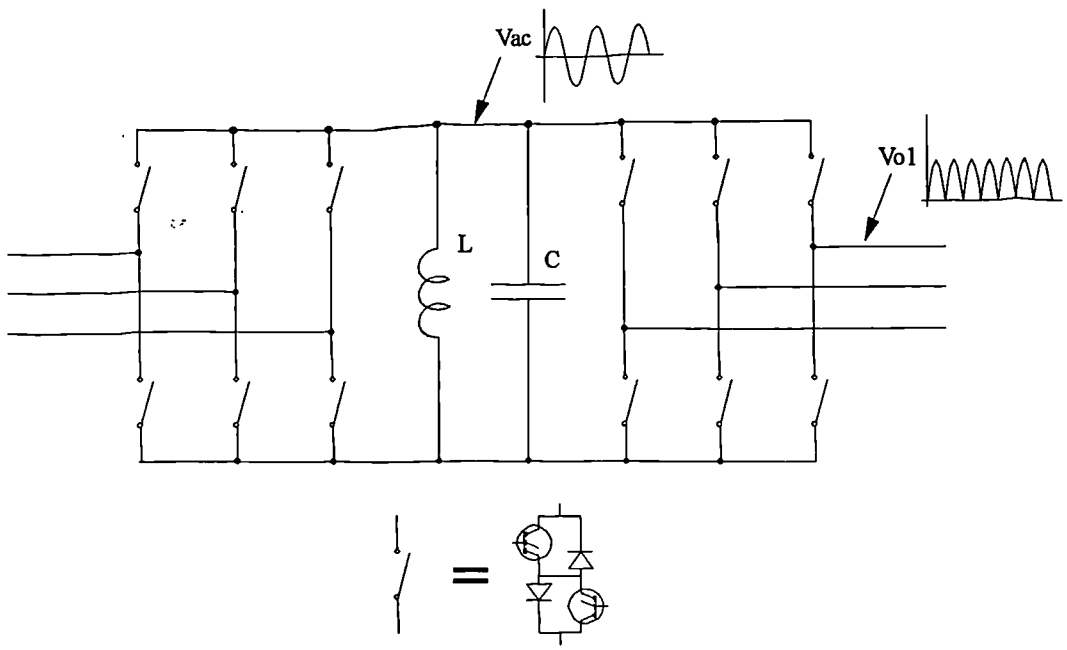


**Figure 1.5. A Parallel Resonant AC Voltage Link Converter**

### 1.2.3 The Resonant Converter

In an attempt to reduce the switching losses inherent in the structure of most power converters whilst increasing the switching frequency, to reduce the filtering requirements, the concept of introducing resonance to the DC link has been proposed. In these converters a capacitor and an inductor are used to sustain a high frequency resonance in the voltage or current waveforms of the DC link. The output-bridge can then be used as a high frequency to low average frequency converter, with the switch state changes taking place at the zero crossings [15]. This will minimise the switching losses and the associated stresses placed on the switching elements.

It is possible to have either the voltage or the current resonating by using a parallel or series resonant circuit. The resonance is either an AC waveform or an AC waveform superimposed on a DC level so that the current or voltage will never fall below zero. This gives four basic circuit configurations for a resonant converter:

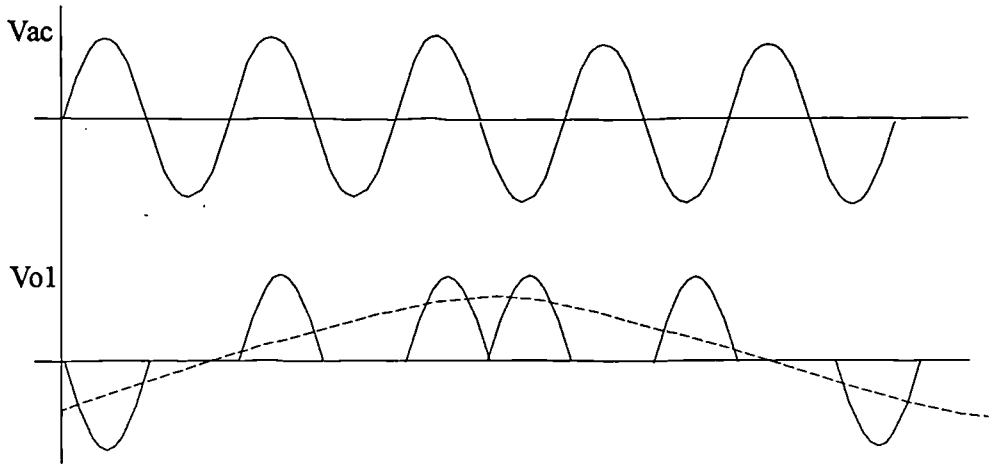


**Figure 1.6. Typical Waveforms for a Parallel Resonant AC Converter**

- Parallel Resonant AC Voltage Link
- Parallel Resonant DC Voltage Link
- Series Resonant AC Current Link
- Series Resonant DC Current Link

### 1.2.3.1 Parallel Resonant AC Voltage Link Converter

The parallel resonant AC voltage link is the simplest of the possible resonant link converter structures. The circuit is shown in figure 1.5. The high frequency resonance in the link voltage is caused by the reaction between the inductor and the capacitor [16-19]. The output-bridge is then used to switch sections of the high frequency link voltage of a given polarity between the output lines to give the desired average output voltage waveform, as shown in figure 1.6. This form of converter requires fully controllable bi-directional switches. The device utilisation is poor due to the high device voltage ratings required by the resonant peak voltage. For these reasons a more cost effective form of the resonant converter must be considered.

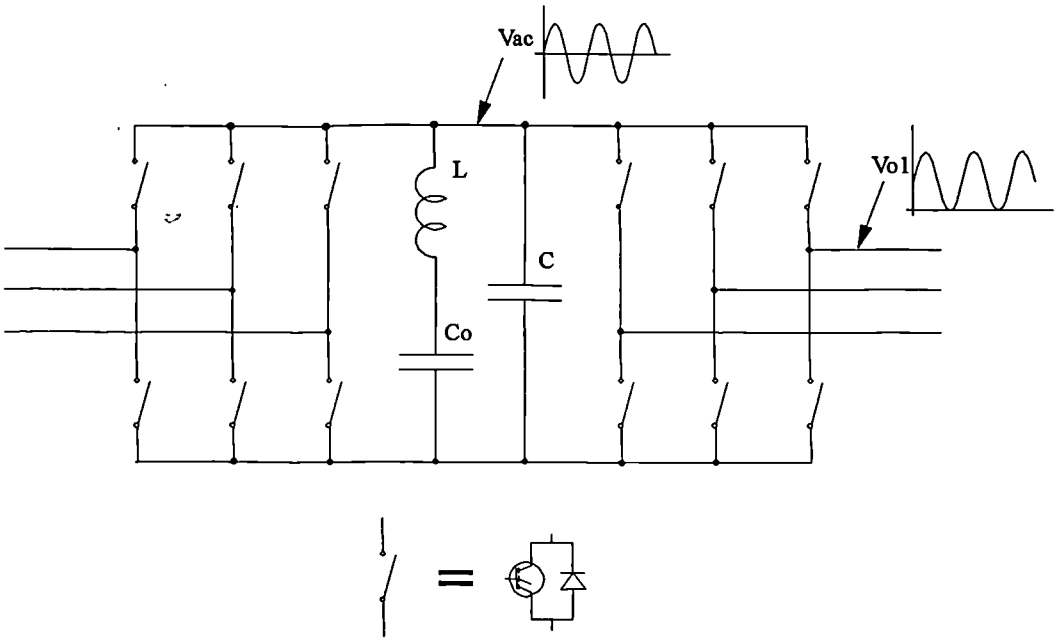


**Figure 1.7. A Parallel Resonant DC Voltage Link Converter**

### 1.2.3.2 Parallel Resonant DC Voltage Link Converter

To avoid the requirement for bi-directional switches, a DC bias can be added to the resonant voltage by the addition of an extra capacitor, as shown in figure 1.7. The link voltage will now take the form of a biased sine wave [20-24]. In the implementation of this circuit care must be taken to ensure that the link voltage actually reaches zero every cycle. The requirement for a bidirectional switch has therefore been removed. This form of the converter still suffers from poor device utilisation because of the high peak voltages in the link. This effect may be reduced with an active clamp circuit that will limit the maximum link voltage to a pre-set level of 700V [25,26]. Using this technique it is possible to reduce the required device voltage rating by 50%, making it comparable with the device requirements of a conventional inverter output-bridge.

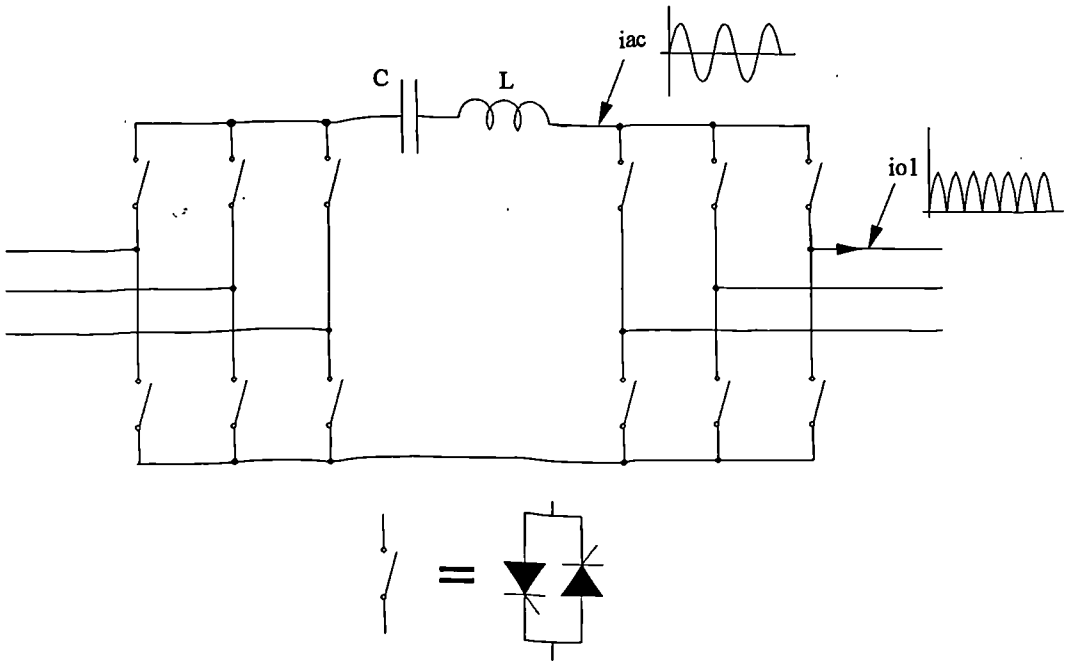


**Figure 1.8. A Series Resonant AC Current Link Converter**

### 1.2.3.3 Series Resonant AC Current Link Converter

If the resonant circuit is built as a series circuit instead of a parallel circuit then a resonant current link may be formed [27-29], as shown in figure 1.8. Since the current will pass through zero the switch state changes can take place in a zero current switching mode. This zero current position will also allow the use of thyristor type devices because the current will pass through zero at the time of switching. Thyristors have the advantage of large current carrying capabilities at a lower cost than in a MOS controlled device structure. Because the current is bidirectional a pair of back to back thyristors will be required. The major problem with the series resonant circuit at high power levels is the design of the magnetic components.

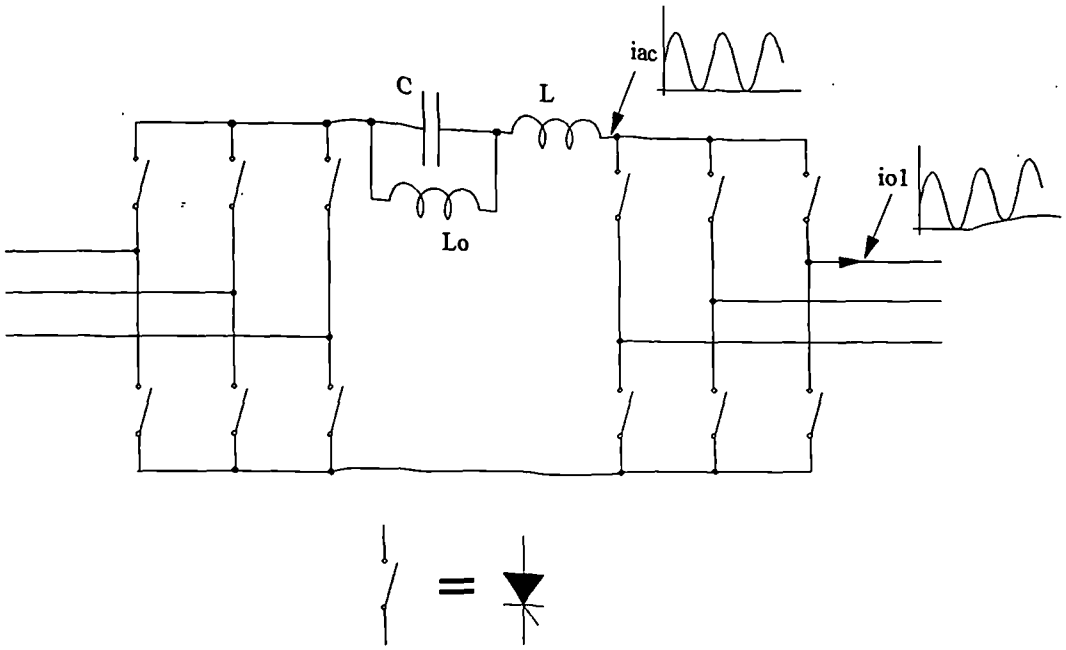


**Figure 1.9. A Series Resonant DC Current Link Converter**

### 1.2.3.4 Series Resonant DC Current Link Converter

In the same way as a DC voltage bias can be added to the resonant AC voltage in the parallel arrangement, a DC current bias may be introduced to the resonant current link [30,31]. This may be done with the addition of an inductor in parallel with the resonating capacitor as shown in figure 1.9. The current flowing in this inductor requires careful regulation to ensure that the current will reach zero every cycle. As in the previous circuit it will then be possible to switch at the zero current intervals. Since the current will also be positive the switches may now be implemented as single thyristors, making the bridge circuit relatively simple.

The increase in the required current handling capabilities of the switching devices will not be as serious as the voltage problems in the parallel circuit because high current devices carry a lower premium than higher voltage devices, however a current clamp may be added to reduce the maximum resonant current. One possible method of achieving this is by placing a clamp thyristor across the capacitor and part of the resonant inductor [32,33].

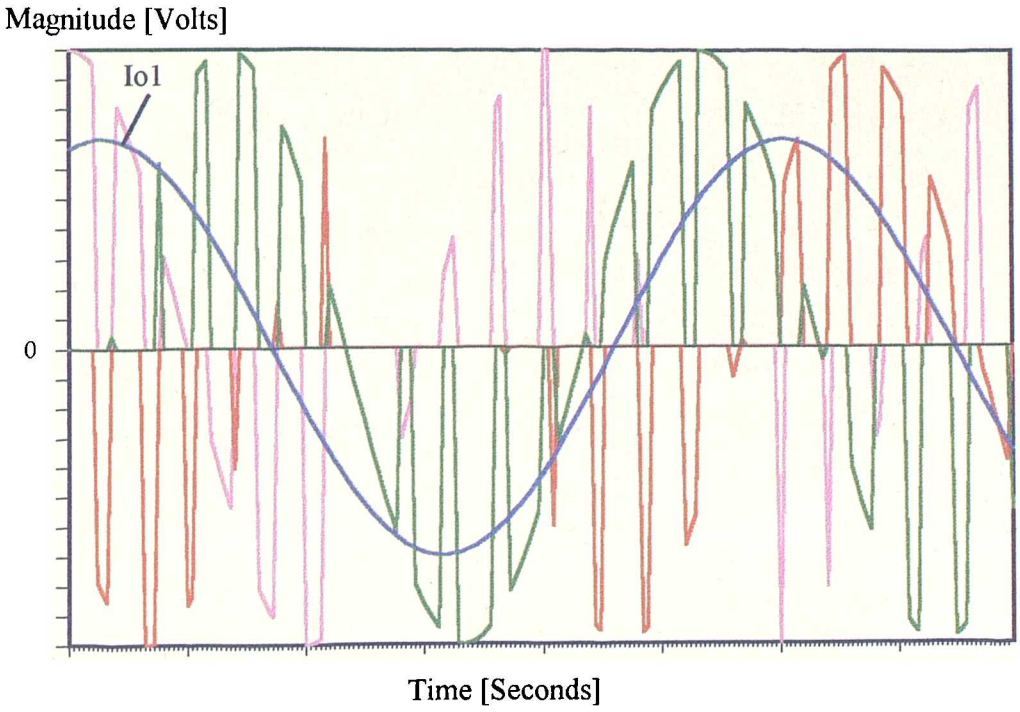


**Figure 1.10. An Output Voltage Waveform Form a Matrix Converter With a Very Low Switching Frequency**

## 1.3 A Review of Matrix Converter Technology

The fully controllable matrix converter circuit was first proposed in a book by Gjugyi and Pelly in 1976 [35]. They stated that if fully controllable bi-directional power switching devices became available then the principle of Cycloconverter operation could be extended to cover an unrestricted output frequency range. This can be achieved by opening and closing the switches in a suitable sequence that will generate the required output voltage waveforms, as shown in figure 1.10. Table 1.1 compares the characteristics of the matrix converter circuit to the alternatives described in the previous section.

The first papers about the practical realisation of the circuit were published by Daniels and Slattery in 1978. They started by introducing a single phase output matrix converter [36]. This work was then extended to cover a full three phase to three phase converter [37]. Power transistors were used to form the switches and attempts were made to classify the behaviour of the switches.

| | Back-to-Back | Inverter | Matrix | Resonant | | | |
|---|---|---|---|---|---|---|---|
| | | | | Series AC | Parallel AC | Series DC | Parallel DC |
| **No. of Active Devices** | 12 | 6 | 18 | 12 (24)[1] Thyristors | 12 (24)[1] | 6 (12)[1] Thyristors | 6 (12)[1] |
| **No. Reactive Components[2]** | 4 | >1 | 0 | 2 | 2 | 3 | 3 |
| **Input Current Quality** | Good, Sinusoidal | Poor | Good, Sinusoidal | Poor (Good) | Poor (Good) | Poor (Good) | Poor (Good) |
| **Silicon Device Ratings** | Medium | Medium | Medium/ Low | High Current | High Voltage | High Current[3] | High Voltage[3] |
| **Regenerative** | Yes, Controlled | No | Yes, Naturally | No (Yes) | No (Yes) | No (Yes) | No (Yes) |

**Table 1.1. Comparison of Switching Power Converter Topologies**

These converters worked on making use of the input lines with the maximum voltage difference at any given time and then using the required proportion of this voltage between the output lines to satisfy the demand from the control circuit. For this reason the low order harmonics in input currents to the converter resemble those of a rectifier [38].

### 1.3.1 PWM Control Algorithms

In 1980 Venturini proposed a PWM control algorithm that allowed the converter to draw sinusoidal input current and produce sinusoidal output voltages, albeit at the relatively low input to output voltage ratio of 0.5 [39]. Venturini and others then proceeded to analyse the mathematics of the control algorithm and consider the

---

[1] Bracketed numbers refer to circuits including a regenerative rectifier bridge.

[2] Ignores relatively small input filter components.

[3] Can be reduced with the use of active clamping

operation of the circuit [40-46]. The PWM techniques described in these papers also allow the control of the input displacement factor with limits imposed by the nature of the load. The ideas originally proposed by Venturini were then extended to allow the voltage ratio to be increase to 0.866. This is achieved with the inclusion of the third harmonics of the input and output frequencies on all the output waveforms [38,47-49].

The control of the input displacement angle can be achieved by defining two converter control algorithms [50]. The first algorithm passes the output displacement angle to the input terminals of the converter and the second inverts the intput displacement angle in comparison to the output displacement angle. By combining the converter algorithms in defined proportions it is possible to control the input displacement angle within the magnitude constraints dictated by the nature of the load [38,39,51,52].

Alternative schemes involving the generation of PWM waveforms in single and multiple stages were proposed by Ziogas et al in 1985 [53,54]. The multiple stage control techniques generally consist of an imaginary rectification stage followed by an imaginary inverter stage [38,55]. These control schemes require less computational work than the algorithm proposed by Venturini. Unfortunately these methods are unable to deliver all the desirable characteristics of sinusoidal input currents, controllable input displacement factor and low output voltage subharmonics.

### 1.3.2 Scalar Control Algorithms

Scalar control algorithms based on the principles used by Daniels and Slattery [37] have been proposed which enable the drawing of sinusoidal input currents. These algorithms use a principle of making the current drawn from each phase proportional to the input voltage on each phase in every switching cycle [56-60]. However these algorithms are very numerically intensive, requiring very powerful micro-processors or the off-line calculation of control variables. They also require accurate tracking of all three of the input voltage waveforms, which leads to higher hardware costs.

### 1.3.3 Space Vector Modulation

Space Vector Modulation (SVM) has been used in the micro-processor control of inverters. SVM has the advantage of reducing the software overheads in the processor to a minimum whilst maintaining functionality. The principles of SVM have been manipulated and introduced to matrix converter control [61-63] and refined [64-66]. These methods can be derived from the enhanced Venturini control algorithm [67], and are a convenient tool for the implementation of a matrix converter with real time calculation of switching periods.

### 1.3.4 Practical Bi-Directional Switches

For the purpose of mathematical analysis and computer simulation the nine bi-directional switches in the converter may be considered as perfect. If real power semiconductor devices are used then the non-ideal characteristics may cause short circuits between the input lines or open circuits between the output lines. These conditions must be controlled if the matrix converter is to be a viable commercial proposition [68,69]. Some techniques for overcoming these situations have been proposed [65,70,71], but it has so far proved difficult to define a fail-safe method of commutating the current between switches.

The design of the bi-directional switches must also be considered. Until semi-conductor device technology reaches the point where a fully controlled bi-directional switch with reverse voltage blocking capabilities is realistically realisable these switches must be constructed from discrete devices [70-72]. The bi-directional switches may be formed by placing an active device across a diode bridge or by using a back-to-back pair of active devices with anti-parallel diodes for reverse voltage blocking [66,70,73-75].

### 1.3.5 The Uses of Matrix Converter Control Theory

The ideal matrix converter circuit was proposed as the most general form of power converter circuit by Wood in 1978 [76,77]. These ideas have led to the suggestion of a simplified form matrix converter control theory being used in the control of controlled rectifiers and inverters [49,78-80]. This may be achieved by setting the

input or output frequency to zero accordingly. The circuit may also be simplified so that the converter may be used as a three phase to single phase converter [81-83].

The circuit has also been suggested as being useful as an active filter to correct harmonics drawn by rectifier configurations [84,85], and as an input displacement factor controller for Cycloconverters [86].

## 1.4 Conclusions

A brief outline the state of matrix converter technology today has been given. The important aspects in the development of the circuit and the various methods of controlling it over the last twenty years have been chronicled. Alternative solutions to the problem of three phase induction motor speed control have been briefly introduced.

## 1.5 The Thesis Layout

**Chapter 2:** The intrinsic limit on the maximum output voltage of a matrix converter is considered. A control algorithm is described which is capable of achieving the maximum output voltage. The operation of the control algorithm is examined and there is discussion of methods for adaptation to non-ideal conditions.

**Chapter 3:** A suitable state of the art micro-controller for the matrix converter and other PWM converters is identified. The implementation of the control algorithm discussed in Chapter 2 is explained and an overview of the software design is given.

**Chapter 4:** The design of the semiconductor switches for a matrix converter is considered. The building of the bi-directional switch from currently available discrete devices is described. The choice of controllable semi-conductor device from the ever increasing range of power devices is examined. Methods of driving MOS controlled semiconductor devices are investigated.

**Chapter 5:** The current commutation problems involved in using real semiconductor components instead of perfect switches is addressed. The existing solutions to the current commutation problem are categorised and the basic

principles involved are extended to generate new commutation methods with considerable practical advantages. The implementation of these methods as state machines on programmable logic arrays is described.

**Chapter 6:** A model of the semiconductor losses in a matrix converter is developed. This model is used to compare the losses in a matrix converter to those in a rectifier/inverter circuit. Methods of reducing the switching losses in a matrix converter are proposed.

**Chapter 7:** The development of a mathematical model of the input current waveform is described. The model includes the switching frequency harmonics and the side harmonics to the switching frequency harmonics. The model is verified using both practical and simulation results.

**Chapter 8:** A summary of the conductive EMC regulations is given. The regulations of special significance to the matrix converter are identified. Consideration is given to the design and analysis of possible filter configurations to meet the current and future regulations.

**Chapter 9:** The building of a 5kWatt experimental matrix converter is chronicled. Practical results from the converter are presented and analysed.

**Chapter 10:** The idea of the general matrix converter as the most general form of switching power converter is proposed. The degeneration of the matrix converter circuit and control theory to other forms of switching power converter is considered.

**Chapter 11:** The thesis is concluded with possible uses of the matrix converter and the possible areas for further research in this subject.

# Bibliography


[1] Beckhard A.J., "Nikola Tesla: Electrical Genius", 1953.

[2] Rogers G.J., "Linearised Analysis of Induction Motor Transients", Proc. IEE, Vol.122, No.10, Oct. 1965, pp1917-1926.

[3] Control Techniques, "Drives and Servos Year Book, 1990-1991", 1989.

[4] Rajashekara K.S., Rajagopalan V., Sévigny A. and Vithayathil J., "DC Line Filter Design Considerations in Three-Phase Voltage Source Inverter-Fed Induction Motor Drive Systems", IEEE Transactions on Industrial Applications, Vol.1A-23, No.4, 1987, pp.673-680.

[5] Jarc D.A. and Novarny D.W., A Graphical Approach to AC Drive Classification", IEEE Transactions on Industrial Applications, Vol.1A-23, No.6, 1987, pp.1029-1035.

[6] Brichant F., "Force-Commutated Inverters", North Oxford Academic, 1984.

[7] Enjeti P. and Shireen W., "A New Technique to Reject DC-Link Voltage Ripple for Inverters Operating on Programmed PWM Waveforms", IEEE, 1990, pp.705-712.

[8] Carrara G., Gardella S., Marchesoni M., Salutri R. and Sciutto G., "A New Multilevel PWM Method: A Theoretical Analysis", IEEE Transactions on Power Electronics, Vol.7, No.3, July1992, pp.497-505.

[9] Ohm D.Y., "Principles of Vector Control: Part1", PCIM, August 1990, pp.41-44.

[10] Ohm D.Y., "Principles of Vector Control: Part2", PCIM, September 1990, pp.32-36.

[11] Vas P., "Vector Control of AC Machines", Claredon: Oxford, 1990.

[12] Jones R. and Jones S.R., "A Unity Power Factor Sinusoidal Supply Side Converter for Industrial Applications", IEE Colloquium on Variable Speed Drives, 1992.

[13] Habetler T.G., "Rectifier/Inverter Reactive Component Minimisation", IEEE Transactions on Industrial Applications, Vol.25, No.2, March 1989, pp.307-316

[14] Joos G., Zargari N.R. and Ziogas P.D., "A New Class of Current Controlled Suppressed-Link AC to AC Frequency Changers", IEEE, 1991, pp.830-837.

[15] Lipo T.A., "Resonant Link Converters: A New Direction in Solid State Power Conversion", Second International Conference on Electrical Drives, 1989.

[16] Sood P.K. and Lipo T.A., "Power Conversion Distribution System Using a High Frequency AC Link", IEEE Trans. on Ind. Applications, Vol.24, No.2, March 1988, pp.288-299.

[17] Sood P.K., Lipo T.A. and Hansen I.G., "A Versatile power Converter for High Frequency Link Systems", IEEE Trans. On Power Electronics, Vol.3, No.4, Oct. 1988, pp.383-390.

[18] Sul S.K. and Lipo T.A., "Design and Performance of a High Freq. Link Induction Motor Drive Operating at Unity Power Factor", IEEE Trans. on Ind. Applications, Vol.26, No.3, May 1990, pp.434-440.

[19] Sul S.K. and Lipo T.A., "Design and Performance of a High Frequency Link Induction Motor Drive Operating at Unity Power Factor", Conf. Record IAS Annual Meeting, Vol.1, Oct. 1988, pp.308-313.

[20] Cho J.G., Hu D.Y. and Cho G.H., "Three Phase Sine Wave Voltage Source Inverter Using the Soft Switched Resonant Poles", IECON 1989, Vol.1, pp.48-53.

[21] Cho J.G, Kim H.S. and Cho G.H., "Novel Soft Switching PWM Converter Using A New Parallel Resonant DC-Link", PESC 1991, pp.241-247.

[22] Divan D.M. and Skibinski G., "Zero Switching Loss Inverters For High Power Applications", Conf. Record of the IAS Annual Meeting, 1987, pp.627-634.

[23] Divan D.M. and Skibinski G., "Zero Switching Loss Inverters For High Power Applications", IEEE Trans. on Ind. Applications, Vol.25, No.4, 1989, pp.634-643

[24] Divan D.M., "The Resonant DC Link Converter - A New Concept in Static Power Conversion", IEEE Trans. on Ind. Applications, Vol.25, No.2, March 1989, PP.317-325.

[25] Divan D.M., Venkataramanan G and De Doncker R.W, "Design Methodologies for soft Switched Inverters", Conf. Record of the IAS Annual Meeting, 1988, pp.758-766.

[26] Habetler T.G. and Divan M.D., "Angle Controlled Current Regulated Rectifiers For AC/AC Converters", PESC. 1989, Vol.2, pp.704-710.

[27] Huisman H., "A Three Phase to Three Phase Series Resonant Power Converter With Optimal Input Current Waveforms. Part.2: Application and Results", IEEE Transactions on Power Electronics, Vol.35, No.2, May 1988, pp.269-277.

[28] Huisman H., "A Three Phase to Three Phase Series Resonant Power Converter With Optimal Input Current Waveforms. Part.1: Control Strategy", IEEE Transactions on Power Electronics, Vol.35, No.2, May 1988, pp.263-268.

[29] Klaassens J.B., "DC to AC Series Resonant Converter System with High Freq. Generating Multiphase AC Waveforms for Multi-kilowatt Power Levels", IEEE Trans. on Power Electronics, Vol.2, No.3, July 1987, pp.247-256.

[30] Klaassens J.B. and Beer F., "Three-Phase AC to AC Series Resonant Converter With a Reduced Number of Thyristors", Conf. Record PESC 1989, pp.376-384.

[31] Lai J.S. and Bose B.K., "An Improved Resonant DC Link Inverter For Induction Motor Drives", Conf. Record IAS Annual Meeting, Vol.1, Oct. 1988, pp.742-748.

[32] Lai J.S. and Bose B.K., "An Induction Motor Drive Using An Improved High Frequency Resonant D.C. Link Inverter", Conf. Record PESC 1990, pp.792-799.

[33] Murai Y. and Lipo T.A., "High Frequency Series Resonant DC Link Conversion", Conf. Record IAS Annual Meeting, Vol.1, Oct. 1988, pp.772-779.

[34] Murai Y., Abeyratne S.G., Lipo T.A. and Caldeira P., "Dual Flow Pulse Trimming Concept for a Series Resonant DC Link Power Conversion", PESC 1991, pp.254-260.

[35] Gjugyi L and Pelly B, "Static Power Frequency Changers", New York : Wiley, 1976.

[36] Daniels A.R and Slattery D.T, " New Power Converter Technique Employing Power Transistors", Proc. IEE, Vol.125, No.2, Feb. 1978, pp.146-150.

[37] Daniels A.R and Slattery D.T, " Application of Power Transistors to Polyphase Regenerative Power Converters", Proc. IEE, Vol.125, No.7, July 1978, pp.643-647.

[38] Maytum K.J and Colman D, "The Implementation and Future Potential of the Venturini Converter", Proc. of Drives, Motors and Controls, 1983, pp.108-117.

[39] Venturini M, "A New Sine Wave in Sine Wave Out, Conversion Technique Which Eliminates Reactive Elements", Proceedings Powercon 7 (San Diego,CA), 1980, pp.E3_1-E3_15.

[40] Alesina A. and Venturini M., "The Generalised Transformer : A New Bidirectional Sinusoidal Waveform Frequency Converter With Continuous Variable Adjustable Input Power Factor", Proc. of PESC Conference Record, 1980, pp.242-252.

[41] Alesina A. and Venturini M., "Solid-State Power Conversion : A Fourier Analysis Approach to Generalised Transformer Synthesis", IEEE Trans. on Circuits and Systems, Vol. cas28, No.4, April 1981, pp.319-330.

[42] Venturini M, "Convertitore diretto AC-AC di elevata potenza", Italian Patent 20777a-79, Mar.6,1979.

[43] Braun M and Hasse K, "A Direct Frequency Changer with Control of Input Reactive Power", Proc. IFAC, Control in Power Electronics and Electrical Drive, 1983, pp.187-194.

[44] Kwon W.H and Cho G.H, "Analysis of Non-Ideal Step Down Matrix Converter Based on Circuit DQ Transformation", PESC 1991, pp.825-829.

[45] Kwon W.H and Cho G.H, "Static and Dynamic Characteristics of Non-Ideal Step Up Nine Switch Matrix Converter", EPE Firenze, 1991, Vol.4, pp.418-423.

[46] Oyama J et al, "New Control Strategy for Matrix Converter", Conf Record PESC 1989, pp.360-367.

[47] Alesina A. and Venturini M., "Intrinsic Amplitude Limits and Optimum Design of 9-Switches Direct PWM AC to AC Converters", PESC Conference Record 1988, pp.1284-1291.

[48] Venturini et al., "Method and apparatus for the conversion of a polyphase voltage system", U.S. Patent no.4628425, Dec.1986.

[49] Holmes D.G and Lipo T.A, "Implementation of a Controlled Rectifier using AC-AC Matrix Converter Theory", Conf. Record PESC 1989, pp.353-359.

[50] Asher G.M., Davis R.M. and Vasquez-Borquez, "Operation of the Naturally Commutating Hidden Link Converter Feeding a Cage Induction Motor", Conf. on Power Electronics and Variable Speed Drives, 1988, pp.130-133.

[51] Rodriguez J, "A new control technique for AC-AC converters", Proc. IFAC, Control in Power Electronics and Electrical Drive, 1983, pp.203-208.

[52] Ishida M, Iwasaki M, Ohkuma S and Iwata K, "Waveform Control of PWM Cycloconverters with Sinusoidal Input Current, Sinusoidal Output Voltage and Variable Input Displacement Factor", Electrical Eng. in Japan, Vol.107, No.3, 1987, pp.95-103.

[53] Ziogas P.D, Khan S.I and Rashid M.H, "Some Improved Forced Commutated Cycloconverter Structures", IEEE Trans. on Ind. Applications, Oct 1985, Vol.IA-21, No.5, pp.1242-1253.

[54] Ziogas P.D, Khan S.I and Rashid M.H, "Analysis and Design of Forced Commutated Cycloconverter Structures With Improved Transfer Characteristics", IEEE Trans. on Ind. Electronics, Vol.IE-33, No3, Aug.86, pp.271-280.

[55] Neft C.L and Schauder C.D, "Theory and Design of a 30-Hp Matrix Converter", IEEE-IAS, Vol.1 , 1988, pp.934-939.

[56] Ishiguro A et al., "A new method of PWM control for forced commutated Cycloconverters using microprocessors", Conf Record, IEEE-IAS Annual Meeting, 1988, pp.712-721.

[57] Ishiguro A and Furuhashi T, "A Novel Control Method for Forced Commutated Cycloconverters Using Instantaneous Values of Input Line-to-Line Voltages ", IEEE Trans. on Ind. Electronics, Vol.38, No.3, June 1991, pp.166-172.

[58] Kim Y and Ehsani M, "New Modulation Methods for Forced Commutated Direct Frequency Changers", IEEE, 1989, pp.798-809.

[59] Roy G et al., "Asynchronous Operation of Cycloconverter with Improved Voltage Gain by Employing a Scalar Control Algorithm", IEEE-IAS, Oct.1987, pp.891-898.

[60] Roy G and April G.E, "Cycloconverter Operation under a New Scalar Control Algorithm", Conf. Record PESC 1989, pp.368-375.

[61] Valle J.del, Arias D, Yeves F and Martinez P.M, "Four Quadrant Speed Control Of Induction Motor by Unrestricted Frequency Changer", IECON 1987, Vol.1, pp.422-429.

[62] Huber L and Borojevic D, "Space Vector Modulation for Forced Commutated Cycloconverters", IEEE, 1989, pp.871-876.

[63] Huber L, Borojevic D and Burany N, "Voltage Space Vector Based PWM Control of FCCs", IECON 1989, Vol.1, pp.48-53.

[64] Huber L., Borojevic D and Burany N, "Digital Implementation of the Space Vector Modulator for Forced Commutated Cycloconverters", Conf. Record on Power Electronics and Variable Speed Drives, July 1990, pp.63-68.

[65] Huber L, Borojevic D and Burany N, "Analysis, Design and Implementation of the Space Vector Modulation for Forced Commutated Cycloconverters", IEE Proceedings Part B 1992.

[66] Huber L, Borojevic D, Zhuang X F and Lee F C, "Design and Implementation of a Three Phase Matrix Converter with Input Power Correction", IEEE 1993 pp.860-865.

[67] Holmes D.G., " the General Relationship between Regular-Sampled Pulse Width Modulation and Space Vector Modulation for Hard Switching Converters" Space Vector Modulation", IEEE, 1992, pp.-.

[68] Ma X, " High Performance PWM Frequency Changers ", IEEE Trans. Industrial Applications, Vol. 1a-22, Mar./Apr. 1986, pp.267-280.

[69] Lipo T.A., "Recent Progress in the Development of Solid State AC Motor Drives", IEE Trans. on Power Electronics, Vol.3, No.2, April 1988, pp.105-117.

[70] Beasant R.R., Beatie W.C. and Refsum A., "An Approach to the Realisation of a High Power Venturini Converter", IEEE, April 1990, pp.291-297.

[71] Burany N, "Safe Control of Four Quadrant Switches", IEEE IAS Annual Meeting, 1989, pp.1190-1194.

[72] Bose B.K, "Recent Progress in Power Electronics", IEEE Transactions on Power Electronics, Jan. 1992, pp.2-17.

[73] Merwe D.J.van der, "A New System for Controlling the Speed, Direction and Torque of the Squirrel Cage Induction Motor", Patent Application No. 864255, April 1986.

[74] Beauregard F, Roy G and April G.E, "Design Consideration Related to the Use of Power MOSFETs in High Performance AC to AC Converters", Proc. of Powercon, Munich, May 11-13, 1987.

[75] Spath H and Sohner W, "The Unrestricted Frequency Changer for Feeding Induction Machines", Arch. Electrotech, Vol.71, 1988, No.6, pp.441-450.

[76] Wood P, "General Theory of Switching Power Converters", Proc. of PESC Conference Record (San Diego) 1979, pp.3-10.

[77] Wood P, "Switching Power Converters", (book), Van Nostrand Reinhold Company, 1981.

[78] Holmes D.G and Lipo T.A, "Implementation of a Controlled Rectifier using AC-AC Matrix Converter Theory ", IEEE Trans. on Power Electronics, Vol.7, No.1, January 1992, pp.240-250.

[79] Holmes D.G, "A New Modulation Algorithm for Voltage and Current Source Inverters, based on AC-AC Matrix Converter Theory", IEEE 1990 pp.1190-1195.

[80] Holmes D.G, "A Unified Modulation Algorithm for Voltage and Current Source Inverters based on AC-AC Matrix Converter Theory", IEEE 1992 pp.31-40.

[81] Khan S.I, Ziogas P.D and Rashid M.H, "Forced Commutated Cycloconverters for High Frequency Link Applications", IEEE Trans. on Ind. Applications, Vol.1A-23, 1987, pp.661-672.

[82] Khoei A and Yuvarajan S, "Single Phase AC-AC Converters Using Power MOSFET's", IEEE Trans. on Industrial Electronics, Vol.35, No.3, 1988, pp.442-443.

[83] Tenti P, Malesani L and Rossetto L, "Optimum Control of PWM Multi-converter Systems", IEEE-IAS, 1988, pp.888-894.

[84] Tenti P, "Optimum Control of N-input K-Output Matrix Converters", IEEE Transactions on Power Electronics, Vol. 7, No. 4, Oct. 1992, pp.707-713.

[85] Madangpal S and Cathey J.J, "Suppression of Converter Introduced Harmonics Currents Using a FFC", IEEE Trans. on Energy Conversion., Vol.5, No.4, 1990, pp.643-649.

[86] Nomura H, Fujiwara K and Kawakami H, "A Power Factor Compensator Using a Forced Commutated Cycloconverter", IEEE Trans. on Ind. Applications, Vol.26, No.4, 1990, pp.769-775.

[87] Bedford B.D and Hoft R.G, "Principles of Inverter Circuits", New York: Wiley, 1964.

Chapter 2

# The Control Algorithm

### 2.1 Introduction

This chapter considers the maximum output voltage limitations of a matrix converter. A possible PWM control scheme to realise this maximum output voltage is described. The effect of the control scheme on the input and output waveforms of the converter is considered. A method of control for the input displacement factor of the converter is described.

## 2.2 The Intrinsic Maximum Output Voltage

### 2.2.1 Calculating the Maximum Output Voltage

The output voltage of a matrix converter is generated by sequentially closing and opening the switches between the input and output lines. The output voltage waveform must always be within the envelope of the three phase input voltage waveforms, as shown in figure 2.1. The maximum output voltage swing is therefore the instantaneous minimum difference between the input line voltages. This limitation is shown mathematically in equation 2.1.

$$\min_{\{0<\omega_i t<2\pi\}}\left[V_{i,\max}-V_{i,\min}\right]=\max_{\{0<\omega_i t<2\pi\}}\left[V_{o,\max}-V_{o,\min}\right] \tag{2.1}$$

Let x be the instantaneous potential difference between any two of the matrix converter input or output lines, and $V_y$ denote either input or output voltages.

$$\begin{aligned} x_y &= V_{y,\min}-V_{y,\max} \\ &= V_y.\left[\cos\left(\omega_y t\right)-\cos\left(\omega_y t+\tfrac{2\pi}{3}\right)\right] \end{aligned} \tag{2.2}$$

The minimum and maximum differences can then be found by finding the minimum and maximum values of the difference equation.

$$\begin{aligned} \frac{dx_y}{dt} &= V_y.\omega_y.\left[\sin\left(\omega_y t\right)-\sin\left(\omega_y t+\tfrac{2\pi}{3}\right)\right] \\ &= 0 \end{aligned}$$

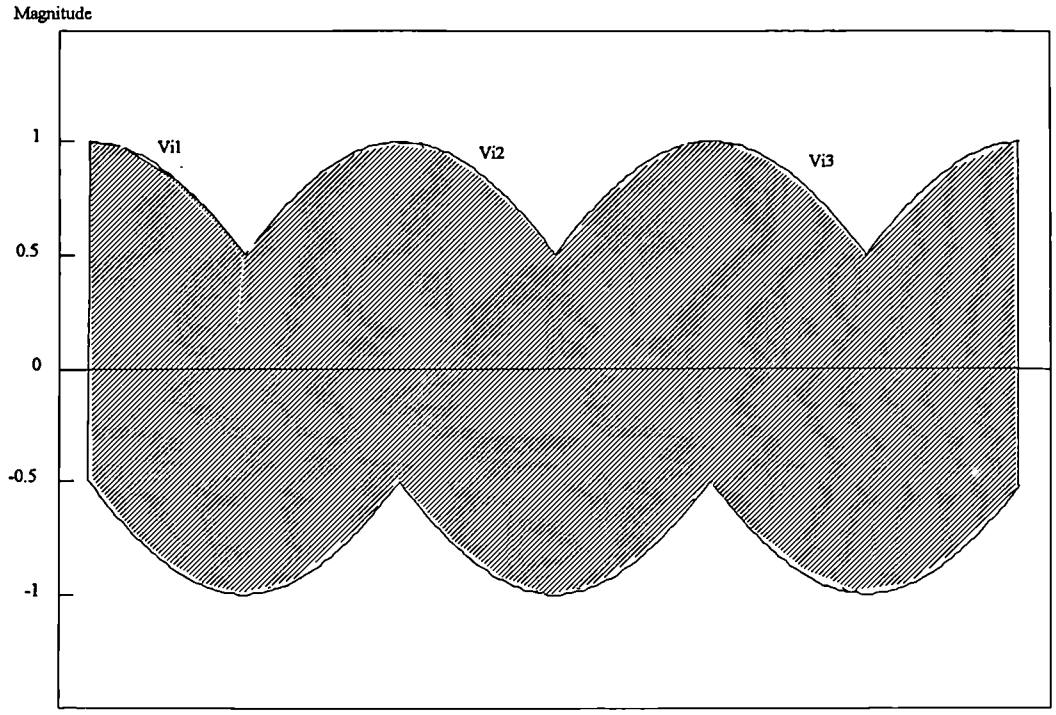


**Figure 2.1. Area of Possible Instantaneous Input and Output Voltages**

Therefore:

$$V_y.\omega_y = 0$$
$$\sin(\omega_y t) = \sin(\omega_y t + \tfrac{2\pi}{3}) \qquad (2.3)$$

The useful solutions to equations 2.3 are then:

$$\omega_{y1} t = 0$$
$$\omega_{y2} t = \tfrac{\pi}{6}$$

Substituting these values into equation 2.2 we find that the minimum difference between the input lines is:

$$x_{i,\min} = \tfrac{3}{2} V_i \qquad (2.4)$$

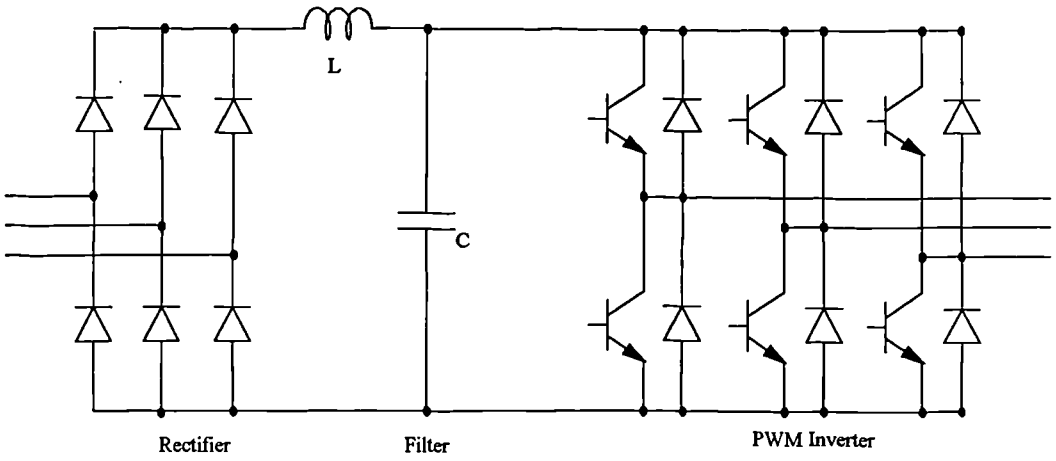


**Figure 2.2. An Inverter Circuit**

And, the maximum difference between the output lines will be:

$$x_{o,\max} = \sqrt{3}.V_o \tag{2.5}$$

By substituting equations 2.4 and 2.5 into equation 2.1 we find the intrinsic maximum output voltage of an ideal matrix converter.

$$\tfrac{3}{2}V_{i,\max} = \sqrt{3}.V_{o,\max}$$
$$V_{o,\max} = 0.866.V_i$$

This intrinsic maximum output voltage limitation is a limitation imposed due to the structure of a matrix converter and will apply to any control algorithm adopted which allows unlimited control of output frequency, assuming an ideal matrix converter with no reactive components connected to the input lines.

### 2.2.2 Effects of the Maximum Output Voltage

As described in the previous section the maximum output voltage of a matrix converter is equal to 0.866 of the input voltage. In an ac. motor drive application the limit on the output voltage would reduce the torque available from the motor if compared to an inverter system. This would require the motor to be overrated slightly for a given application to achieve the same performance. The motor rating will be dealt with in more depth later in this thesis.

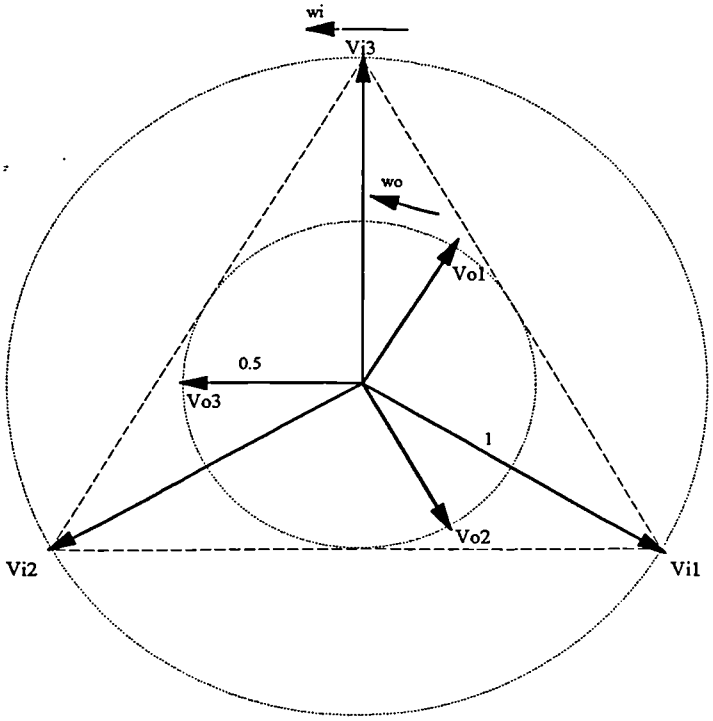


**Figure 2.3. The Phasor Diagram for the Venturini Converter**

A rectifier/inverter configuration shown in figure 2.2 maintains a one to one ratio between input and output voltage by boosting the dc voltage level after the rectification stage. The voltage boosting effect is achieved using the effect of the capacitance in the dc link.

## 2.3 Methods of Realising Maximum Output Voltage

### 2.3.1 The Venturini Converter

When the matrix converter concept was first examined by Venturini [1],[2],[3] it was thought that the maximum average output voltage would be equal to 0.5 of the input voltage. The assumption was that the average output voltage could not exceed the minimum level of the input voltage.

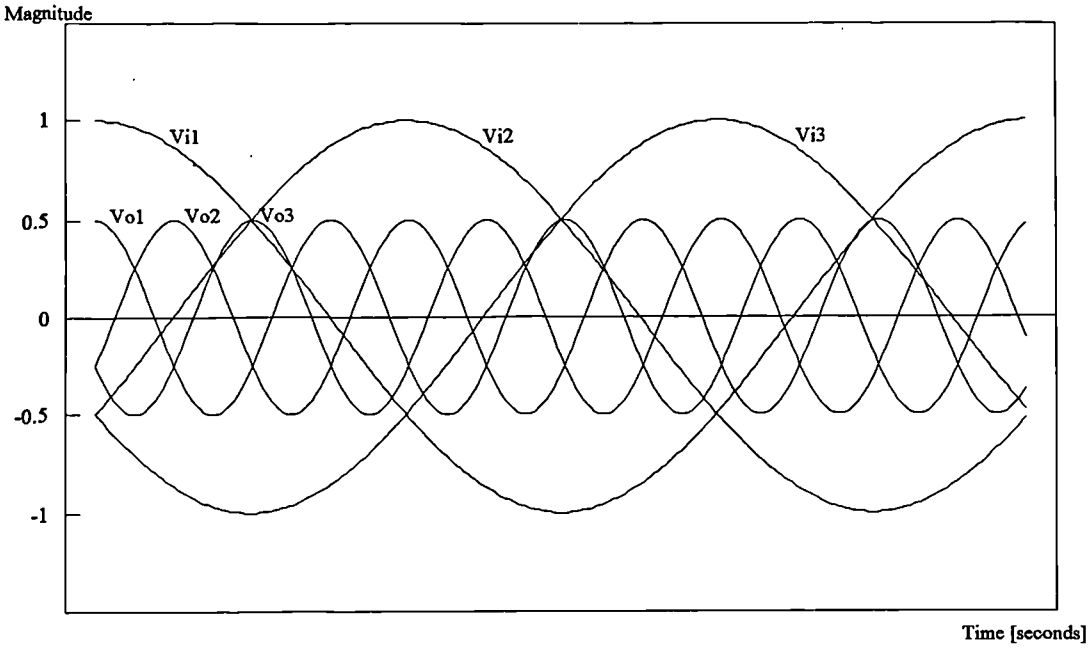


**Figure 2.4. The Venturini Converter Input and Output Voltage Waveforms**

$$V_{o1} = 0.5V_i.\cos(\omega_o t)$$

The theory behind this assumption can be shown with the aid of a phasor diagram. The average output voltage waveform is taken as the continuous output waveform of the converter ignoring the superimposed switching frequency. This average output voltage causes the continuous output current to flow in the motor windings.

Consider the input voltages of the converter to be three phasors of unity magnitude. Each phasor is displaced by an angle of $\frac{2\pi}{3}$ from each other. The set of phasors are on a plane rotating at the input frequency, $\omega_i$. Also consider the average output voltages to be represented by three phasors rotating on a second plane at the converter output frequency, $\omega_o$. The relative magnitude of the output voltage phasors to the input voltage phasors represents the relative magnitude of the fundamental input and output voltage waveforms of the matrix converter.

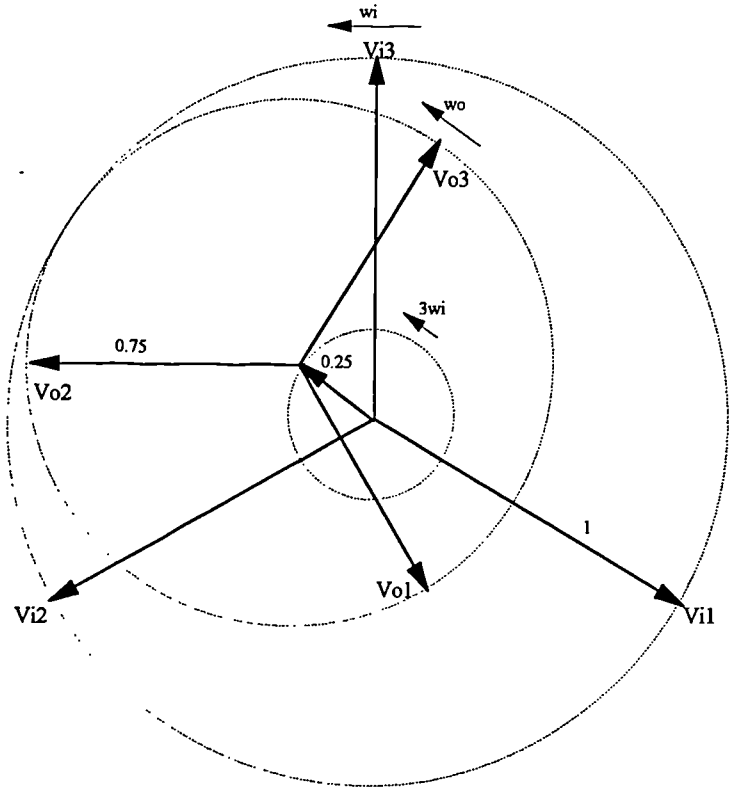


**Figure 2.5. The Phasor Diagram for a Matrix Converter with Added Input Voltage Waveform Third Harmonic**

The phasors for the Venturini converter [1] can be drawn as shown in figure 2.3. The dotted circles on the phasor diagrams represent the loci of the phasors as they rotate. The neutral points of the input and output voltage phasor sets are at the same point. This limitation explains why a maximum output voltage of only half the input voltage is achievable using this scheme. The two sets of waveforms are shown in the time domain in figure 2.4.

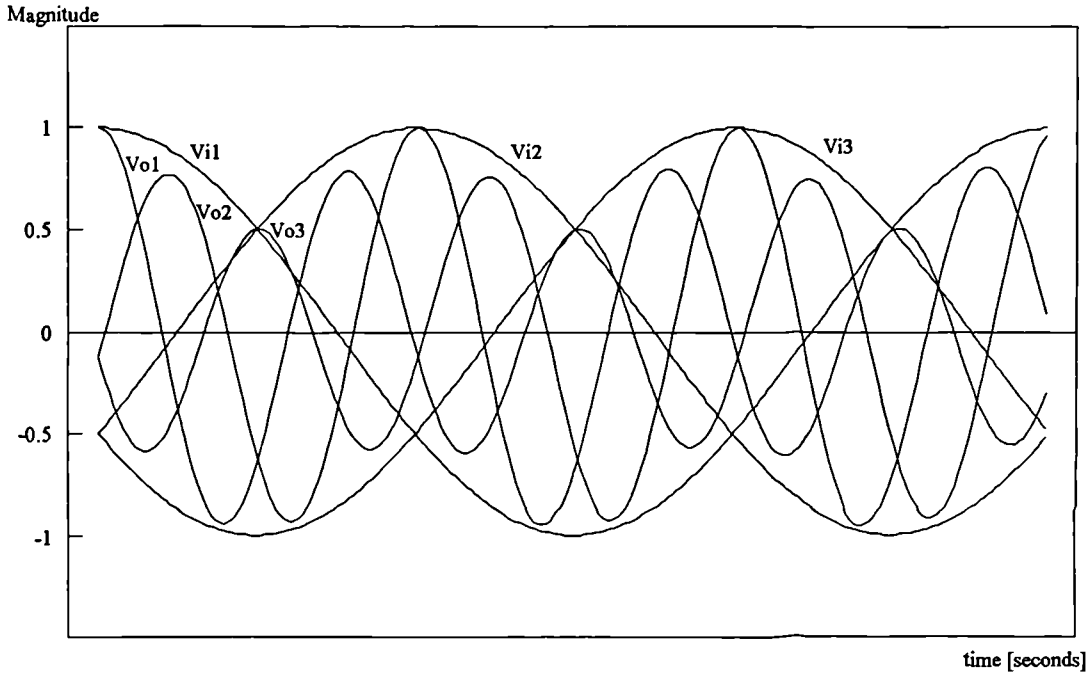


**Figure 2.6. Input and Output Voltage Waveforms for Converter with Added Input Voltage Waveform Third Harmonic**

$$V_{o1} = V_i\left[0.75.\cos(\omega_o t) + 0.25.\cos(3\omega_i t)\right]$$

### 2.3.2 The Addition of The Third Harmonic of the Input Waveform

If the third harmonic of the input voltage waveform is added to each of the output waveforms then the maximum output voltage becomes 0.75 of the input voltage [4]. The third harmonic moves the imaginary neutral point of the output voltage waveform as shown by the single phasor in figure 2.5. In drive applications this common mode third harmonic will not affect the operation or performance of the motor. This is because no neutral is connected between the input and output of the matrix converter. The time domain waveforms for the addition of the third harmonic of the input voltage waveform are shown in figure 2.6.

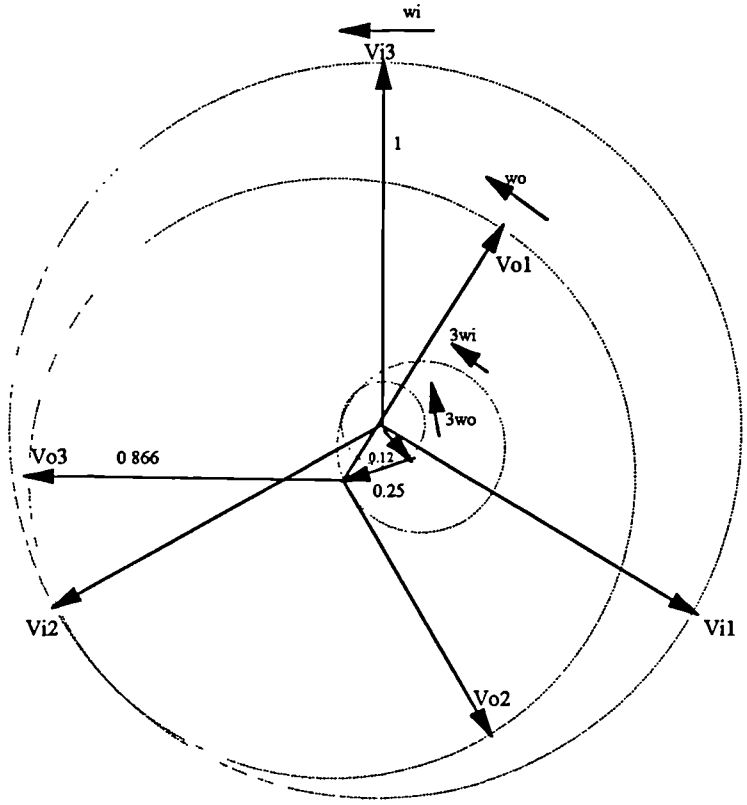


**Figure 2.7. The Phasor Diagram for a Matrix Converter with Added Input and Output Voltage Waveform Third Harmonics**

### 2.3.3 The Addition of The Third Harmonic of the Output Waveform

Besides the third harmonic of the input voltage, the third harmonic of the output voltage waveform may be added to each of the fundamental output voltage waveforms [5]. The addition of this output frequency third harmonic will increase the maximum output voltage of the matrix converter to 0.866 of the input voltage. The addition of these two third harmonic phasors is shown in figure 2.7. The introduction of the third harmonic is used in inverters [6]. The third harmonic phasors will rotate in such a manner that the loci of the average output voltage phasors will never pass outside the loci of the input voltage phasors. The effect of this process is shown in the time domain representation of the voltage waveforms in figure 2.8.

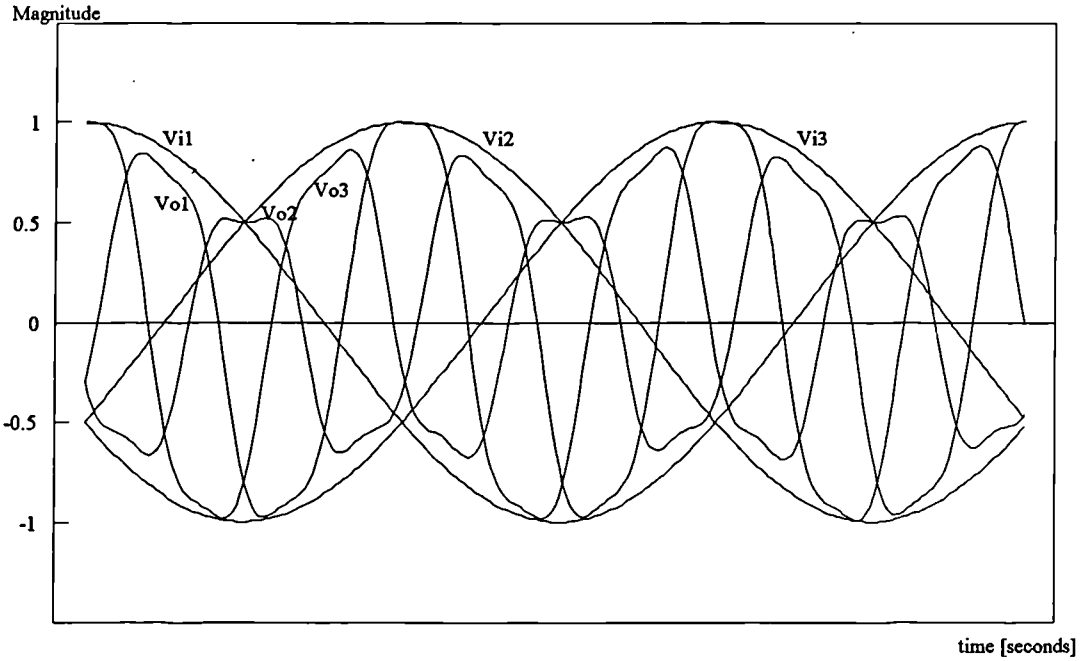


**Figure 2.8. Input and Output Voltage Waveforms for Converter with Added Input and Output Voltage Waveform Third Harmonics**

$$V_{o1} = V_i\left[0.866.\cos(\omega_o t) + 0.25.\cos(3\omega_i t) - 0.12.\cos(3\omega_o t)\right]$$

## 2.4 Construction of a Control Algorithm

By writing mathematical equations for the ideal input and output waveforms a control algorithm can be generated. A construction mechanism involving the internal creation of an imaginary dc link provides a useful tool in the derivation of the control matrix.

### 2.4.1 Input and Output Waveforms

The input waveforms to the converter are assumed to be a three phase sinusoidal set as defined in equation 2.6.

$$\mathbf{V_i(t)} = \begin{bmatrix} V_{i1}(t) \\ V_{i2}(t) \\ V_{i3}(t) \end{bmatrix} = V_i. \begin{bmatrix} \cos(\omega_i t) \\ \cos(\omega_i t + \frac{2\pi}{3}) \\ \cos(\omega_i t + \frac{4\pi}{3}) \end{bmatrix} \qquad (2.6)$$

As discussed in the previous section, the average output voltage waveforms are a three phase set. The addition of third harmonics of the input and output frequencies allows the maximum possible output magnitude to be achieved. The required output waveforms can therefore be defined.

$$\mathbf{V_o(t)} = \begin{bmatrix} V_{o1}(t) \\ V_{o2}(t) \\ V_{o3}(t) \end{bmatrix}$$

$$= 0.866V_i.\begin{bmatrix} \cos(\omega_o t) \\ \cos(\omega_o t + \frac{2\pi}{3}) \\ \cos(\omega_o t + \frac{4\pi}{3}) \end{bmatrix} + \left(0.25V_i.\cos(3\omega_i t) - 0.12V_i.\cos(3\omega_o t)\right).\begin{bmatrix} 1 \\ 1 \\ 1 \end{bmatrix} \tag{2.7}$$

### 2.4.2 Defining a Control Matrix

A three by three control matrix, **G(t)**, can then be defined to link the input and output voltage matrices.

$$\mathbf{V_o(t) = G(t).V_i(t)} \tag{2.8}$$

This control matrix consists of nine elements. Each element consists of a sum of sinusoidal functions with a total magnitude that varies between -0.5 and 0.5. These continuous functions can be used to verify the operation of the control matrix. A matrix of duty cycles for each switch may then be derived from the control matrix. The duty cycle matrix will be considered after the control matrix has been constructed.

### 2.4.3 The Derivation of a Control Matrix

For the purpose of developing and proving the adopted control algorithm for the matrix converter a high switching frequency has been assumed. This assumption allows all the control, input and output waveforms to be considered as continuous. The effects of the switching frequency on the converter will be dealt later in the thesis.

The switches in the converter are considered to be perfect. The input voltage waveforms are initially considered to be a set of perfect sinusoids. In deriving the control matrix the load is initially considered to be purely resistive.

To derive a possible control matrix consider the action of the rectifier/inverter circuit in figure 2.2. The transition between the input and output waveforms is a two stage operation. The first stage is rectification from three phase ac to dc. The second stage is the chopping of the dc voltage to three phase ac of the required frequency. These two stages can be used to construct a matrix converter control matrix. The first part of the control matrix, **H(t),** will create an imaginary dc link. The second half, **F(t),** will generate the required three phase output voltage waveforms from this imaginary dc link.

$$\mathbf{G(t) = F(t).H(t)} \tag{2.9}$$

Due to the nature of matrix multiplication the imaginary rectification stage requires the three functions in each row of the control matrix to be the input waveform functions as shown in equation 2.10. The output of the converter with this control matrix would be dc voltages.

$$\mathbf{H(t)} = \frac{2}{3}.\begin{bmatrix} \cos(\omega_i t) & \cos(\omega_i t + \frac{2\pi}{3}) & \cos(\omega_i t + \frac{4\pi}{3}) \\ \cos(\omega_i t) & \cos(\omega_i t + \frac{2\pi}{3}) & \cos(\omega_i t + \frac{4\pi}{3}) \\ \cos(\omega_i t) & \cos(\omega_i t + \frac{2\pi}{3}) & \cos(\omega_i t + \frac{4\pi}{3}) \end{bmatrix} \tag{2.10}$$

Calculating the output of the converter under the operation of the imaginary rectification control matrix, **H(t)**, will give the imaginary dc link as shown in equation 2.11. The double frequency terms will cancel due to the fact that the sum of three sine functios all $\frac{2\pi}{3}$ out of phase with each other is equal to zero.

$$\mathbf{V}_{o,dc}(t) = \mathbf{H}(t).\mathbf{V}_i(t) = V_i.\begin{bmatrix}1\\1\\1\end{bmatrix} \tag{2.11}$$

The imaginary dc link can then be modulated by the second control matrix, **F(t)**, to form the output voltage waveforms. The three functions in each column of this second matrix will be of the same form as the rows in the output voltage matrix.

$$\begin{aligned}\mathbf{F}(t) = 0.866.&\begin{bmatrix}\cos(\omega_o t) & \cos(\omega_o t) & \cos(\omega_o t)\\ \cos(\omega_o t+\frac{2\pi}{3}) & \cos(\omega_o t+\frac{2\pi}{3}) & \cos(\omega_o t+\frac{4\pi}{3})\\ \cos(\omega_o t+\frac{4\pi}{3}) & \cos(\omega_o t+\frac{4\pi}{3}) & \cos(\omega_o t+\frac{4\pi}{3})\end{bmatrix}\\ + 0.25.&\begin{bmatrix}\cos(3\omega_i t) & \cos(3\omega_i t) & \cos(3\omega_i t)\\ \cos(3\omega_i t) & \cos(3\omega_i t) & \cos(3\omega_i t)\\ \cos(3\omega_i t) & \cos(3\omega_i t) & \cos(3\omega_i t)\end{bmatrix}\\ + 0.12.&\begin{bmatrix}\cos(3\omega_o t) & \cos(3\omega_o t) & \cos(3\omega_o t)\\ \cos(3\omega_o t) & \cos(3\omega_o t) & \cos(3\omega_o t)\\ \cos(3\omega_o t) & \cos(3\omega_o t) & \cos(3\omega_o t)\end{bmatrix}\end{aligned} \tag{2.12}$$

Calculating the converter output for a converter with the dc input described by equation 2.11 will give the required average output voltage waveforms required to achieve the maximum possible output voltage magnitude.

$$\begin{aligned}\mathbf{V}_o(t) &= \mathbf{F}(t).\mathbf{V}_{o,dc}(t)\\ &= 0.866V_i.\begin{bmatrix}\cos(\omega_o t)\\ \cos(\omega_o t+\frac{2\pi}{3})\\ \cos(\omega_o t+\frac{4\pi}{3})\end{bmatrix} + \left(0.25V_i.\cos(3\omega_i t) - 0.12V_i.\cos(3\omega_o t)\right).\begin{bmatrix}1\\1\\1\end{bmatrix}\end{aligned} \tag{2.13}$$

The two imaginary control matrices given in equations 2.10 and 2.12 may be combined to give the single control matrix, **G(t)**.

$$\mathbf{G(t) = F(t).H(t)}$$

$$= \frac{1}{3}0.866.\begin{bmatrix} \cos((\omega_i+\omega_o)t) & \cos((\omega_i+\omega_o)t+\frac{2\pi}{3}) & \cos((\omega_i+\omega_o)t+\frac{4\pi}{3}) \\ \cos((\omega_i+\omega_o)t+\frac{2\pi}{3}) & \cos((\omega_i+\omega_o)t+\frac{4\pi}{3}) & \cos((\omega_i+\omega_o)t) \\ \cos((\omega_i+\omega_o)t+\frac{4\pi}{3}) & \cos((\omega_i+\omega_o)t) & \cos((\omega_i+\omega_o)t+\frac{2\pi}{3}) \end{bmatrix}$$

$$+\frac{1}{3}0.25.\begin{bmatrix} \cos(4\omega_i t) & \cos(4\omega_i t+\frac{2\pi}{3}) & \cos(4\omega_i t+\frac{4\pi}{3}) \\ \cos(4\omega_i t) & \cos(4\omega_i t+\frac{2\pi}{3}) & \cos(4\omega_i t+\frac{4\pi}{3}) \\ \cos(4\omega_i t) & \cos(4\omega_i t+\frac{2\pi}{3}) & \cos(4\omega_i t+\frac{4\pi}{3}) \end{bmatrix}$$

$$-\frac{1}{3}0.12.\begin{bmatrix} \cos((3\omega_o+\omega_i)t) & \cos((3\omega_o+\omega_i)t+\frac{4\pi}{3}) & \cos((3\omega_o+\omega_i)t+\frac{2\pi}{3}) \\ \cos((3\omega_o+\omega_i)t) & \cos((3\omega_o+\omega_i)t+\frac{4\pi}{3}) & \cos((3\omega_o+\omega_i)t+\frac{2\pi}{3}) \\ \cos((3\omega_o+\omega_i)t) & \cos((3\omega_o+\omega_i)t+\frac{4\pi}{3}) & \cos((3\omega_o+\omega_i)t+\frac{2\pi}{3}) \end{bmatrix}$$

$$+\frac{1}{3}0.866.\begin{bmatrix} \cos((\omega_i-\omega_o)t) & \cos((\omega_i-\omega_o)t-\frac{2\pi}{3}) & \cos((\omega_i-\omega_o)t-\frac{4\pi}{3}) \\ \cos((\omega_i-\omega_o)t-\frac{2\pi}{3}) & \cos((\omega_i-\omega_o)t-\frac{4\pi}{3}) & \cos((\omega_i-\omega_o)t) \\ \cos((\omega_i-\omega_o)t-\frac{4\pi}{3}) & \cos((\omega_i-\omega_o)t) & \cos((\omega_i-\omega_o)t-\frac{2\pi}{3}) \end{bmatrix}$$

$$+\frac{1}{3}0.25.\begin{bmatrix} \cos(2\omega_i t) & \cos(2\omega_i t-\frac{2\pi}{3}) & \cos(2\omega_i t-\frac{4\pi}{3}) \\ \cos(2\omega_i t) & \cos(2\omega_i t-\frac{2\pi}{3}) & \cos(2\omega_i t-\frac{4\pi}{3}) \\ \cos(2\omega_i t) & \cos(2\omega_i t-\frac{2\pi}{3}) & \cos(2\omega_i t-\frac{4\pi}{3}) \end{bmatrix}$$

$$-\frac{1}{3}0.12.\begin{bmatrix} \cos((3\omega_o-\omega_i)t) & \cos((3\omega_o-\omega_i)t-\frac{4\pi}{3}) & \cos((3\omega_o-\omega_i)t-\frac{2\pi}{3}) \\ \cos((3\omega_o-\omega_i)t) & \cos((3\omega_o-\omega_i)t-\frac{4\pi}{3}) & \cos((3\omega_o-\omega_i)t-\frac{2\pi}{3}) \\ \cos((3\omega_o-\omega_i)t) & \cos((3\omega_o-\omega_i)t-\frac{4\pi}{3}) & \cos((3\omega_o-\omega_i)t-\frac{2\pi}{3}) \end{bmatrix}$$

(2.14)

## 2.5 The Matrix Converter Input and Output Waveforms

The operation of the control matrix described by equation 2.14 will be verified by matrix multiplication. The nature of the output voltage waveforms and the input current waveforms can be checked assuming ideal input voltage waveforms, ideal switches and an ideal resistive load.

### 2.5.1 The Output Voltage Waveforms

The validity of the control matrix may be shown by performing the appropriate matrix multiplications. The input voltage waveforms are assumed to be sinusoidal and at a fixed frequency. The switching frequency is again considered to be high so that the output voltage waveforms may be considered continuous at the output frequencies. The output voltages can be found by substituting the control matrix given in equation 2.14 and the ideal input voltage matrix given in equation 2.6 into equation 2.8.

$$\mathbf{V_o(t)} = \mathbf{G(t)}.\begin{bmatrix} V_i.\cos(\omega_i t) \\ V_i.\cos(\omega_i t + \frac{2\pi}{3}) \\ V_i.\cos(\omega_i t + \frac{4\pi}{3}) \end{bmatrix}$$

$$= V_i.0.866.\begin{bmatrix} \cos(\omega_o t) \\ \cos(\omega_o t + \frac{2\pi}{3}) \\ \cos(\omega_o t + \frac{4\pi}{3}) \end{bmatrix} + \left(V_i.0.25.\cos(3\omega_o t) - V_i.0.12.\cos(3\omega_i t)\right).\begin{bmatrix} 1 \\ 1 \\ 1 \end{bmatrix} \tag{2.15}$$

The matrix manipulations for these calculations are given in appendix A.

### 2.5.2 The Input Current Waveforms

Assume that the output voltage waveforms are perfect as described in equation 2.15. Consider a matrix converter connected to a three phase resistive load as shown in figure 2.9. The output currents may be considered to be a three phase set of sinusoids because the zero sequence third harmonics will cancel.

$$\mathbf{I_o(t)} = \begin{bmatrix} I_{o1}(t) \\ I_{o2}(t) \\ I_{o3}(t) \end{bmatrix} = \xi.V_i.\begin{bmatrix} \cos(\omega_o t) \\ \cos(\omega_o t + \frac{2\pi}{3}) \\ \cos(\omega_o t + \frac{4\pi}{3}) \end{bmatrix} \tag{2.16}$$

Where $\xi$ is a scaling factor that is determined by the size and nature of the load.

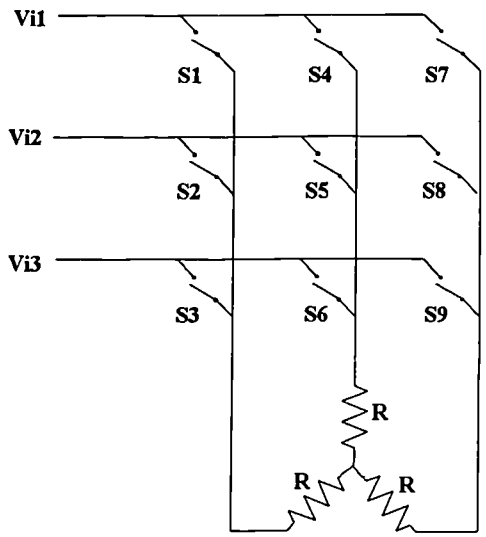


**Figure 2.9. A Matrix Converter Connected to a Resistive Load**

The current drawn from the input lines is constructed from the output current by the action of the control matrix in the reverse manner to the construction of the output voltage of the matrix converter from the input voltage waveforms. The nature of the input current may therefore be determined by the multiplication of the transpose of the control matrix and the output currents.

$$\mathbf{I}_i(\mathbf{t}) = \begin{bmatrix} I_{i1}(t) \\ I_{i2}(t) \\ I_{i2}(t) \end{bmatrix} = \mathbf{G}^{\mathrm{T}}(\mathbf{t}).\mathbf{I}_o(\mathbf{t}) \tag{2.17}$$

If the control matrix given in equation 2.14 and the ideal output current defined in equation 2.16 are substituted into equation 2.17 then the ideal continuous model of the input currents may be calculated.

$$\mathbf{I}_i(\mathbf{t}) = \mathbf{G}^{\mathrm{T}}(\mathbf{t}).\mathbf{I}_o(\mathbf{t}) = \xi.V_i.\begin{bmatrix} \cos(\omega_i t) \\ \cos(\omega_i t + \frac{2\pi}{3}) \\ \cos(\omega_i t + \frac{4\pi}{3}) \end{bmatrix} \tag{2.18}$$

The matrix manipulations for these calculations are given in appendix A.

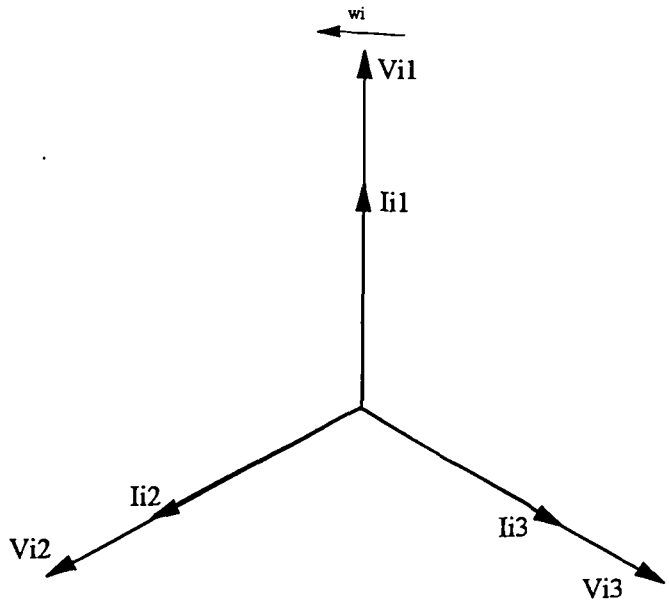


**Figure 2.10. Input Current and Voltage Phasors for a Resistive Load**

Because the load has been assumed to be purely resistive the output currents are in phase with the output voltages. Using this assumption the input currents have been shown to be in phase with the input voltages as shown in figure 2.10. If a real load is considered then the output currents and voltages will not be in phase. This can be used to control the input displacement factor.

## 2.6 The Input Displacement Factor

If a motor is connected to a three phase supply then there will be a displacement between the input current and voltage waveforms. The manipulation of the control matrix of the matrix converter allows this input displacement to be altered. The input displacement factor (d.f.) is taken to be the cosine of the angle, $\gamma$, between the voltage and current input frequency waveforms. The output displacement factor is the cosine of the angle between the fundamental output voltage and current waveforms. This is shown in the time domain in figure 2.11.

$$d.f. = \cos(\gamma) \tag{2.19}$$

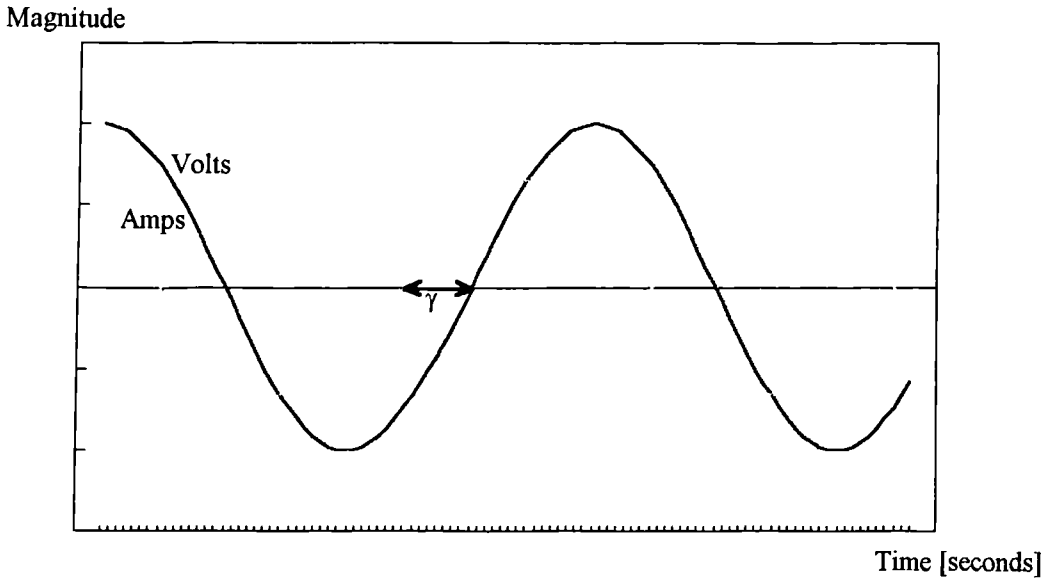


**Figure 2.11. Displacement Factor Between Current and Voltage Waveforms**

This section deals with this displacement factor and its effect on the operation of a matrix converter under the proposed PWM control scheme [7],[8].

### 2.6.1 The Converter Load Model

A simple, but valid model for the load presented by an induction motor to a matrix converter is a set of three resistors in series with three inductors as shown in figure 2.12. Assuming sinusoidal output voltage waveforms, the output voltage and current phasors for such a load can be drawn as shown in figure 2.13. The angle $\gamma$ is the angle between the voltage and current waveforms at the converter's output frequency. Equation 2.16 can then be rewritten to include this displacement angle.

$$\mathbf{I_o(t)} = \begin{bmatrix} I_{o1}(t) \\ I_{o2}(t) \\ I_{o3}(t) \end{bmatrix} = \xi.V_i.\begin{bmatrix} \cos(\omega_o t - \gamma) \\ \cos(\omega_o t + \frac{2\pi}{3} - \gamma) \\ \cos(\omega_o t + \frac{4\pi}{3} - \gamma) \end{bmatrix} \tag{2.20}$$

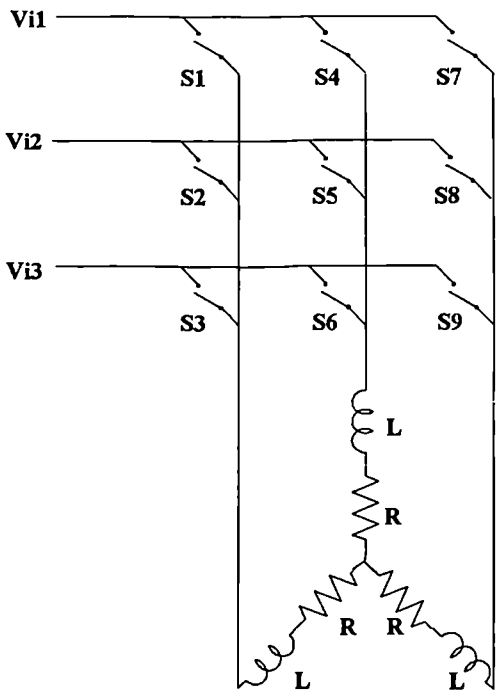


**Figure 2.12. Simple Load Model for an Induction Motor Connected to a Matrix Converter**

### 2.6.2 The Division of the Control Matrix

The control matrix, **G(t)**, given in equation 2.14 may be split into two parts:

- A Positive Converter Control Matrix
- A Negative Converter Control Matrix

The positive half of the control matrix, $\mathbf{G}_1(t)$, consists of the functions containing frequencies that are the sum of the input frequency and the required output frequencies.

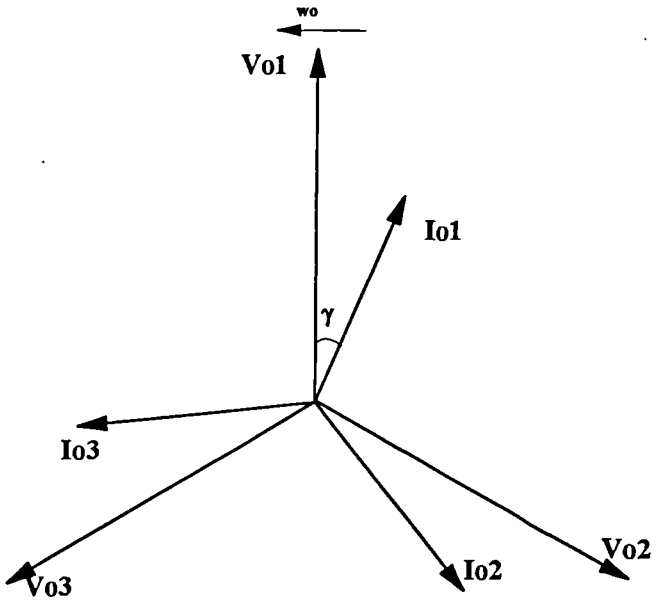


**Figure 2.13. Output Current and Voltage Phasors for a Real Three Phase Load**

$$G_1(t) = \frac{1}{3}0.866.\begin{bmatrix} \cos((\omega_i+\omega_o)t) & \cos((\omega_i+\omega_o)t+\frac{2\pi}{3}) & \cos((\omega_i+\omega_o)t+\frac{4\pi}{3}) \\ \cos((\omega_i+\omega_o)t+\frac{2\pi}{3}) & \cos((\omega_i+\omega_o)t+\frac{4\pi}{3}) & \cos((\omega_i+\omega_o)t) \\ \cos((\omega_i+\omega_o)t+\frac{4\pi}{3}) & \cos((\omega_i+\omega_o)t) & \cos((\omega_i+\omega_o)t+\frac{2\pi}{3}) \end{bmatrix}$$

$$+\frac{1}{3}0.25.\begin{bmatrix} \cos(4\omega_i t) & \cos(4\omega_i t+\frac{2\pi}{3}) & \cos(4\omega_i t+\frac{4\pi}{3}) \\ \cos(4\omega_i t) & \cos(4\omega_i t+\frac{2\pi}{3}) & \cos(4\omega_i t+\frac{4\pi}{3}) \\ \cos(4\omega_i t) & \cos(4\omega_i t+\frac{2\pi}{3}) & \cos(4\omega_i t+\frac{4\pi}{3}) \end{bmatrix}$$

$$-\frac{1}{3}0.12.\begin{bmatrix} \cos((3\omega_o+\omega_i)t) & \cos((3\omega_o+\omega_i)t+\frac{4\pi}{3}) & \cos((3\omega_o+\omega_i)t+\frac{2\pi}{3}) \\ \cos((3\omega_o+\omega_i)t) & \cos((3\omega_o+\omega_i)t+\frac{4\pi}{3}) & \cos((3\omega_o+\omega_i)t+\frac{2\pi}{3}) \\ \cos((3\omega_o+\omega_i)t) & \cos((3\omega_o+\omega_i)t+\frac{4\pi}{3}) & \cos((3\omega_o+\omega_i)t+\frac{2\pi}{3}) \end{bmatrix}$$

(2.21)

The negative half of the control matrix, $G_2(t)$, consists of the functions containing frequencies that are the difference between the input frequency and the required output frequencies.

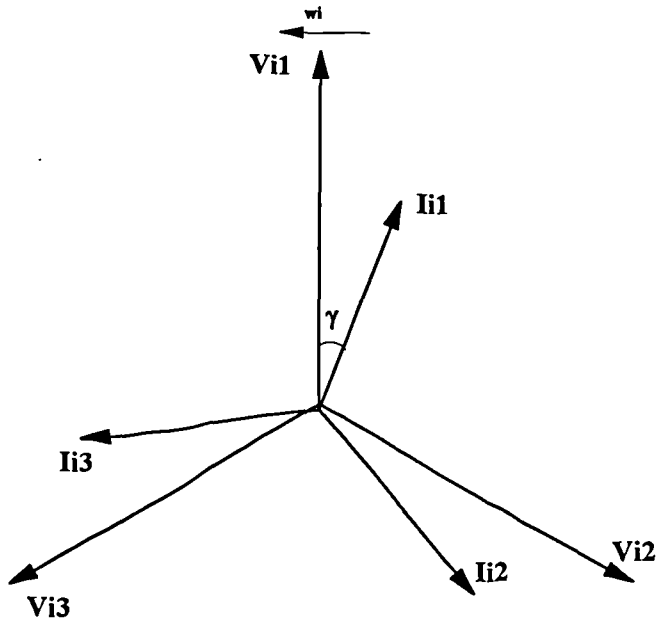


**Figure 2.14. Input Current and Voltage Phasors With Lagging Displacement Factor**

$$G_2(t) = +\frac{1}{3}0.866.\begin{bmatrix} \cos((\omega_i-\omega_o)t) & \cos((\omega_i-\omega_o)t-\frac{2\pi}{3}) & \cos((\omega_i-\omega_o)t-\frac{4\pi}{3}) \\ \cos((\omega_i-\omega_o)t-\frac{2\pi}{3}) & \cos((\omega_i-\omega_o)t-\frac{4\pi}{3}) & \cos((\omega_i-\omega_o)t) \\ \cos((\omega_i-\omega_o)t-\frac{4\pi}{3}) & \cos((\omega_i-\omega_o)t) & \cos((\omega_i-\omega_o)t-\frac{2\pi}{3}) \end{bmatrix}$$

$$+\frac{1}{3}0.25.\begin{bmatrix} \cos(2\omega_i t) & \cos(2\omega_i t-\frac{2\pi}{3}) & \cos(2\omega_i t-\frac{4\pi}{3}) \\ \cos(2\omega_i t) & \cos(2\omega_i t-\frac{2\pi}{3}) & \cos(2\omega_i t-\frac{4\pi}{3}) \\ \cos(2\omega_i t) & \cos(2\omega_i t-\frac{2\pi}{3}) & \cos(2\omega_i t-\frac{4\pi}{3}) \end{bmatrix}$$

$$-\frac{1}{3}0.12.\begin{bmatrix} \cos((3\omega_o-\omega_i)t) & \cos((3\omega_o-\omega_i)t-\frac{4\pi}{3}) & \cos((3\omega_o-\omega_i)t-\frac{2\pi}{3}) \\ \cos((3\omega_o-\omega_i)t) & \cos((3\omega_o-\omega_i)t-\frac{4\pi}{3}) & \cos((3\omega_o-\omega_i)t-\frac{2\pi}{3}) \\ \cos((3\omega_o-\omega_i)t) & \cos((3\omega_o-\omega_i)t-\frac{4\pi}{3}) & \cos((3\omega_o-\omega_i)t-\frac{2\pi}{3}) \end{bmatrix} \quad (2.22)$$

Due to the nature of the multiplication of sets of three phase waveforms and the way in which the double frequency terms cancel it is possible to analyse the operation of these two halves of the control matrix separately.

### 2.6.3 Waveforms Obtained with a Resistive Load

Repeating the output voltage analysis given in section 2.5.1 for each of the two halves of the control matrix shows that the ideal output voltage waveforms would be identical to the result obtained for the complete control matrix. This is shown in equation 2.23. This output voltage analysis is independent of the output displacement factor. This is because the output voltage may be considered as a function of the input voltage and the control matrix, and not the output current.

$$\mathbf{V}_{o,G}(\mathbf{t}) = \mathbf{G}(\mathbf{t}).\mathbf{V}_i(\mathbf{t})$$

$$= V_i.0.866.\begin{bmatrix} \cos(\omega_o t) \\ \cos(\omega_o t + \frac{2\pi}{3}) \\ \cos(\omega_o t + \frac{4\pi}{3}) \end{bmatrix} + \left(V_i.0.25.\cos(3\omega_o t) - V_i.0.12.\cos(3\omega_i t)\right).\begin{bmatrix} 1 \\ 1 \\ 1 \end{bmatrix}$$

$$\mathbf{V}_{o,G_1}(\mathbf{t}) = \mathbf{G}_1(\mathbf{t}).\mathbf{V}_i(\mathbf{t})$$

$$= V_i.0.866.\begin{bmatrix} \cos(\omega_o t) \\ \cos(\omega_o t + \frac{2\pi}{3}) \\ \cos(\omega_o t + \frac{4\pi}{3}) \end{bmatrix} + \left(V_i.0.25.\cos(3\omega_o t) - V_i.0.12.\cos(3\omega_i t)\right).\begin{bmatrix} 1 \\ 1 \\ 1 \end{bmatrix}$$

$$\mathbf{V}_{o,G_2}(\mathbf{t}) = \mathbf{G}_2(\mathbf{t}).\mathbf{V}_i(\mathbf{t})$$

$$= V_i.0.866.\begin{bmatrix} \cos(\omega_o t) \\ \cos(\omega_o t + \frac{2\pi}{3}) \\ \cos(\omega_o t + \frac{4\pi}{3}) \end{bmatrix} + \left(V_i.0.25.\cos(3\omega_o t) - V_i.0.12.\cos(3\omega_i t)\right).\begin{bmatrix} 1 \\ 1 \\ 1 \end{bmatrix} \quad (2.23)$$

Repeating the input current analysis for a resistive load as given in section 2.5.2 for each of the two halves of the control matrix would also yield the same result as the whole control matrix.

$$\mathbf{I}_{1,G}(\mathbf{t}) = \mathbf{G}^{\mathrm{T}}(\mathbf{t}).\mathbf{I}_o(\mathbf{t}) = \xi.V_i.\begin{bmatrix}\cos(\omega_i t)\\ \cos(\omega_i t+\frac{2\pi}{3})\\ \cos(\omega_i t+\frac{4\pi}{3})\end{bmatrix}\mathbf{I}$$

$$_{1,G_1}(\mathbf{t}) = \mathbf{G_1}^{\mathrm{T}}(\mathbf{t}).\mathbf{I}_o(\mathbf{t}) = \xi.V_i.\begin{bmatrix}\cos(\omega_i t)\\ \cos(\omega_i t+\frac{2\pi}{3})\\ \cos(\omega_i t+\frac{4\pi}{3})\end{bmatrix}$$

$$\mathbf{I}_{1,G_2}(\mathbf{t}) = \mathbf{G_2}^{\mathrm{T}}(\mathbf{t}).\mathbf{I}_o(\mathbf{t}) = \xi.V_i.\begin{bmatrix}\cos(\omega_i t)\\ \cos(\omega_i t+\frac{2\pi}{3})\\ \cos(\omega_i t+\frac{4\pi}{3})\end{bmatrix} \qquad (2.24)$$

### 2.6.4 Waveforms Obtain with the Motor Model Load

The input current is a function of the output current. The output displacement factor will therefore affect the nature of the input currents. The input current analysis given in equation 2.24 may then be repeated for the control matrix $\mathbf{G_1(t)}$. The modified output currents given for the inductive load in equation 2.20 are used to model the load effect of a motor on the converter's input currents.

$$\begin{aligned}\mathbf{I}_{11}(\mathbf{t}) &= \mathbf{G}_1^{\mathrm{T}}(\mathbf{t}).\mathbf{I}_o(\mathbf{t})\\ &= \mathbf{G}_1^{\mathrm{T}}(\mathbf{t}).\xi.V_i.\begin{bmatrix}\cos(\omega_o t-\gamma)\\ \cos(\omega_o t+\frac{2\pi}{3}-\gamma)\\ \cos(\omega_o t+\frac{4\pi}{3}-\gamma)\end{bmatrix}\\ &= \xi.V_i.\begin{bmatrix}\cos(\omega_i t-\gamma)\\ \cos(\omega_i t+\frac{2\pi}{3}-\gamma)\\ \cos(\omega_i t+\frac{4\pi}{3}-\gamma)\end{bmatrix}\end{aligned} \qquad (2.25)$$

As can be seen from equation 2.25, the positive converter control matrix, $\mathbf{G_1(t)}$, would demand an input current with a displacement factor from the supply voltage equal to the output displacement factor. A load with a lagging displacement factor, such as a motor, would therefore have a lagging supply displacement factor. This is shown in phasor diagram form in figure 2.14.

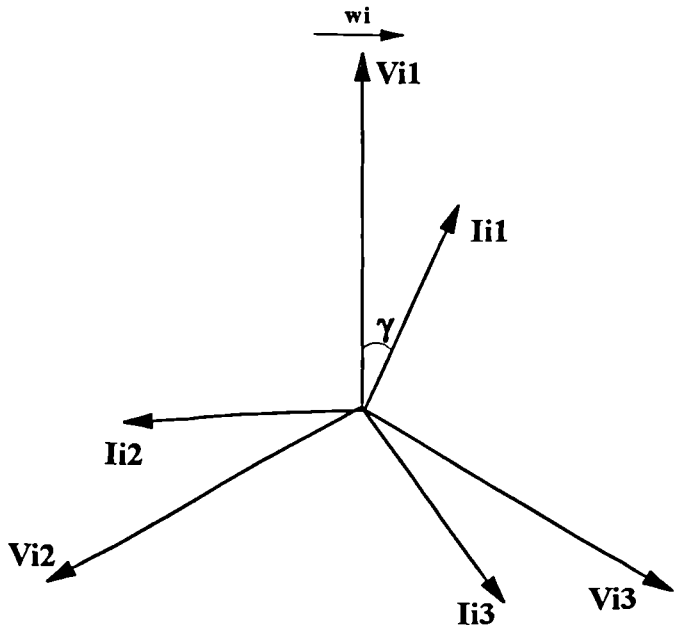


**Figure 2.15. Input Current and Voltage Phasors With Leading Displacement Factor**

The input current analysis may be repeated for the negative going converter control matrix, $\mathbf{G_2(t)}$.

$$\begin{aligned}\mathbf{I_{i2}(t)} &= \mathbf{G_2^T(t).I_o(t)} \\ &= \mathbf{G_2^T(t)}.\xi.V_i.\begin{bmatrix}\cos(\omega_o t-\gamma)\\ \cos(\omega_o t+\frac{2\pi}{3}-\gamma)\\ \cos(\omega_o t+\frac{4\pi}{3}-\gamma)\end{bmatrix} \\ &= \xi.V_i.\begin{bmatrix}\cos(\omega_i t+\gamma)\\ \cos(\omega_i t+\frac{2\pi}{3}+\gamma)\\ \cos(\omega_i t+\frac{4\pi}{3}+\gamma)\end{bmatrix}\end{aligned} \tag{2.26}$$

As can be seen from equation 2.26, the negative converter control matrix generates an input displacement factor of the opposite sign to the output displacement factor. If this negative control matrix was used to implement a matrix converter then the input current would lead the input voltage by the same angle as the output current

lags the output voltage. This leading input displacement factor is shown in phasor diagram form in figure 2.15.

### 2.6.5 Control of the Input Displacement Factor

As shown in equation 2.25, the positive control matrix, $\mathbf{G_1(t)}$, will give a converter with an input displacement factor that lags at the same angle as the output displacement factor. The negative control matrix, $\mathbf{G_2(t)}$, will give a converter with an input displacement factor that leads at the same angle as the output displacement factor lags. If a matrix converter were to be implemented with one of these two control matrices alone then these input displacement factors would result.

A matrix converter could be implemented in which the positive and negative control matrices are averaged. The output voltage waveform can then be found as shown in equation 2.27.

$$\mathbf{V_o(t)} = \left(\tfrac{1}{2}.\mathbf{G_1(t)} + \tfrac{1}{2}.\mathbf{G_2(t)}\right).\mathbf{V_i(t)} \tag{2.27}$$

The input currents may then be analysed as previously done in equation 2.26, but with the new averaged control matrix.

$$\mathbf{I_i(t)} = \left(\tfrac{1}{2}.\mathbf{G_1(t)} + \tfrac{1}{2}.\mathbf{G_2(t)}\right)^{T}.\mathbf{I_o(t)} \tag{2.28}$$

The input current phasors for each control matrix operating alone would effectively be halved and then combined. This situation would give a matrix converter with a unity input displacement factor. The phase angle between the input current and voltage waveforms in each phase would be zero. The phasor diagram for this would take the same form as the input waveforms for a resistive load shown in figure 2.11.

The positive and negative control matrices may be averaged unequally: This would give an output voltage as defined below.

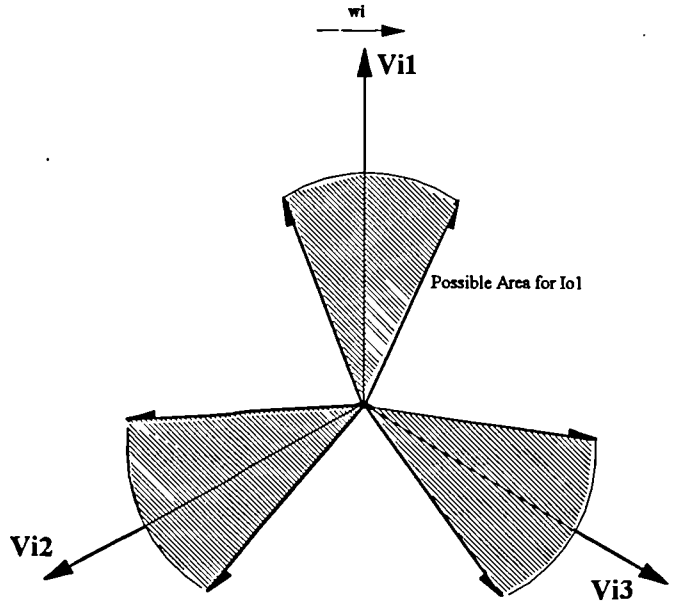


**Figure 2.16. Phasor Diagram Showing Areas for Possible Output Current Phasors**

$$\mathbf{V_o}(t) = \left(\alpha.\mathbf{G_1}(t) + (1-\alpha).\mathbf{G_2}(t)\right).\mathbf{V_i}(t) \tag{2.29}$$

where: $\alpha = 0 \rightarrow 1$

This output voltage waveform would lead to a set of input currents with variable displacement from the input voltage.

$$\mathbf{I_i}(t) = \left(\alpha.\mathbf{G_1}(t) + (1-\alpha).\mathbf{G_2}(t)\right)^{T}.\mathbf{I_o}(t) \tag{2.30}$$

By varying $\alpha$ between zero and one it follows that the input displacement factor will vary between $\gamma$ leading and $\gamma$ lagging. This will give a possible range of input current displacement angles as shown by the areas on the phasor diagram in figure 2.16.

## 2.7 Waveform Quality with Harmonic Distortion in the Supply

So far it has been assumed that the three phase input voltage waveforms from the mains supply are perfectly sinusoidal and matched. In any real supply these voltage

waveforms may be unbalanced or distorted. The harmonic distortion will affect the performance of the matrix converter. This section will examine the consequences of this distortion and unbalance on the input and output waveform quality of a matrix converter.

### 2.7.1 Harmonic Distortion of the Input Voltage Waveforms

The distortion in the input voltage waveforms is due to the use of electrical equipment with non-sinusoidal input currents and unbalanced supply demands. The maximum amount of harmonic distortion that may be generated by any one piece of equipment is defined by legislation [9]. The superposition of these harmonics from many different pieces of equipment can lead to a significant amount of harmonic distortion. In the research environment it is possible to obtain results at certain times of the day when the distortion is low. However, this is not a viable solution in industrial applications.

The equations for input voltage waveforms given in equation 2.6 may be modified to model the distortion.

$$\mathbf{V}_{\mathbf{i,real}}(\mathbf{t}) = V_i . \begin{bmatrix} \cos(\omega_i t) + (\text{harmonic distortion}) \\ \cos(\omega_i t + \frac{2\pi}{3}) + (\text{harmonic distortion}) \\ \cos(\omega_i t + \frac{2\pi}{3}) + (\text{harmonic distortion}) \end{bmatrix} \tag{2.31}$$

For the purpose of examining the effects of the harmonic distortion on the performance of a matrix converter let us take an input voltage waveform that has a significant 5th harmonic, as shown in equation 2.32. The variable β represents the relative magnitude of the harmonic to the fundamental. The arguments presented would apply to any other harmonic or combination of harmonics.

$$\mathbf{V}_{\mathbf{i},5th}(\mathbf{t}) = V_i . \begin{bmatrix} \cos(\omega_i t) \\ \cos(\omega_i t + \frac{2\pi}{3}) \\ \cos(\omega_i t + \frac{4\pi}{3}) \end{bmatrix} + V_i . \begin{bmatrix} \beta.\cos(5\omega_i t) \\ \beta.\cos(5\omega_i t + \frac{2\pi}{3}) \\ \beta.\cos(5\omega_i t + \frac{4\pi}{3}) \end{bmatrix} \tag{2.32}$$

### 2.7.2 Effect of Harmonics on the Converter if No Action is Taken

The output voltage waveform analysis presented in equation 2.15 may be repeated using the modified input waveforms defined in equation 2.32.

$$\begin{aligned}
\mathbf{V_o(t)} &= \mathbf{G(t)}.V_i.\begin{bmatrix}\cos(\omega_i t)\\ \cos(\omega_i t+\frac{2\pi}{3})\\ \cos(\omega_i t+\frac{4\pi}{3})\end{bmatrix}+\begin{bmatrix}\beta.\cos(5\omega_i t)\\ \beta.\cos(5\omega_i t+\frac{2\pi}{3})\\ \beta.\cos(5\omega_i t+\frac{4\pi}{3})\end{bmatrix}\\
&= V_i.0.866.\begin{bmatrix}\cos(\omega_o t)\\ \cos(\omega_o t+\frac{2\pi}{3})\\ \cos(\omega_o t+\frac{4\pi}{3})\end{bmatrix}+V_i.0.25.\cos(3\omega_o t)-V_i.0.12.\cos(3\omega_i t)\\
&+\beta.V_i.0.866.\begin{bmatrix}\cos((4\omega_i+\omega_o)t)\\ \cos((4\omega_i+\omega_o)t+\frac{2\pi}{3})\\ \cos((4\omega_i+\omega_o)t+\frac{4\pi}{3})\end{bmatrix}\\
&+\beta.V_i.0.866.\begin{bmatrix}\cos((\omega_o-4\omega_i)t)\\ \cos((\omega_o-4\omega_i)t+\frac{2\pi}{3})\\ \cos((\omega_o-4\omega_i)t+\frac{4\pi}{3})\end{bmatrix}\\
&+\beta.V_i.0.25.\{\cos((3\omega_o-4\omega)_i t)+\cos((3\omega_o+4\omega_i)t)\}.\begin{bmatrix}1\\1\\1\end{bmatrix}\\
&-\beta.V_i.0.12.\{\cos(7\omega_i t)+\cos(-\omega_i t)\}.\begin{bmatrix}1\\1\\1\end{bmatrix}
\end{aligned} \tag{2.33}$$

The 5th harmonic causes some differential and common mode distortion of the output voltage waveforms. The differential mode would cause distortion in the output current waveforms. The common mode functions would cancel in the output currents in the same way as would the common mode third harmonics in the ideal output voltage waveforms. The ideal output currents described by equation 2.16 are therefore modified accordingly.

$$\mathbf{I_o(t)} = \xi.V_i.\begin{bmatrix}\cos(\omega_o t)\\ \cos(\omega_o t+\frac{2\pi}{3})\\ \cos(\omega_o t+\frac{4\pi}{3})\end{bmatrix}+\beta.\xi.V_i.\begin{bmatrix}\cos((4\omega_i+\omega_o)t)\\ \cos((4\omega_i+\omega_o)t+\frac{2\pi}{3})\\ \cos((4\omega_i+\omega_o)t+\frac{4\pi}{3})\end{bmatrix}$$
$$+\beta.\xi.V_i.\begin{bmatrix}\cos((\omega_o-4\omega_i)t)\\ \cos((\omega_o-4\omega_i)t+\frac{2\pi}{3})\\ \cos((\omega_o-4\omega_i)t+\frac{4\pi}{3})\end{bmatrix} \quad (2.34)$$

This distortion in the output current waveforms imposed on the converter will lead to distortion of the input current supply waveforms. These input currents may be found by repeating the input current analysis in equation 2.18 using the distorted output currents in equation 2.34.

$$\mathbf{I_i(t)} = \mathbf{G^T(t).I_o(t)}$$
$$= \xi.V_i.\begin{bmatrix}\cos(\omega_i t)\\ \cos(\omega_i t+\frac{2\pi}{3})\\ \cos(\omega_i t+\frac{4\pi}{3})\end{bmatrix}+\beta.\xi.V_i.\begin{bmatrix}2.\cos(3\omega_i t)\\ 2.\cos(3\omega_i t+\frac{2\pi}{3})\\ 2.\cos(3\omega_i t+\frac{4\pi}{3})\end{bmatrix}$$
$$+\beta.\xi.V_i.\begin{bmatrix}\cos(5\omega_i t)\\ \cos(5\omega_i t+\frac{2\pi}{3})\\ \cos(5\omega_i t+\frac{4\pi}{3})\end{bmatrix}+\beta.\xi.V_i.\begin{bmatrix}\cos(5\omega_i t+2\omega_o t)\\ \cos(5\omega_i t+2\omega_o t+\frac{2\pi}{3})\\ \cos(5\omega_i t+2\omega_o t+\frac{4\pi}{3})\end{bmatrix} \quad (2.35)$$

The ideal sinusoidal input currents have been lost due to this distortion. The matrix converter will also add to the distortion due to the currents it will present to the mains supply.

### 2.7.3 The Correction of the Converter Waveforms

If a motor was to be controlled by a matrix converter then it is preferable that the output voltage waveforms are approximately sinusoidal. This would lead to sinusoidal output current waveforms. It is possible to modify the control matrix, given in equation 2.12, to take into account the input voltage harmonic distortion. This modification will enable the converter to produce the ideal output waveforms. The control matrix, **G(t),** for the correction of the 5th harmonic distortion can be

derived using the techniques described in section 2.4.3. This modified control matrix is shown in equation 2.36.

$$
\begin{aligned}
\mathbf{G(t)} &= \mathbf{F(t).H(t)} \\
&= \frac{1}{3}0.866.\begin{bmatrix} \cos((\omega_i+\omega_o)t) & \cos((\omega_i+\omega_o)t+\frac{2\pi}{3}) & \cos((\omega_i+\omega_o)t+\frac{4\pi}{3}) \\ \cos((\omega_i+\omega_o)t+\frac{2\pi}{3}) & \cos((\omega_i+\omega_o)t+\frac{4\pi}{3}) & \cos((\omega_i+\omega_o)t) \\ \cos((\omega_i+\omega_o)t+\frac{4\pi}{3}) & \cos((\omega_i+\omega_o)t) & \cos((\omega_i+\omega_o)t+\frac{2\pi}{3}) \end{bmatrix} \\
&+ \frac{\beta}{3}0.866.\begin{bmatrix} \cos((5\omega_i+\omega_o)t) & \cos((5\omega_i+\omega_o)t-\frac{2\pi}{3}) & \cos((5\omega_i+\omega_o)t-\frac{4\pi}{3}) \\ \cos((5\omega_i+\omega_o)t-\frac{2\pi}{3}) & \cos((5\omega_i+\omega_o)t-\frac{4\pi}{3}) & \cos((5\omega_i+\omega_o)t) \\ \cos((5\omega_i+\omega_o)t-\frac{4\pi}{3}) & \cos((5\omega_i+\omega_o)t) & \cos((5\omega_i+\omega_o)t-\frac{2\pi}{3}) \end{bmatrix} \\
&+ \frac{1}{3}0.25.\begin{bmatrix} \cos(4\omega_i t) & \cos(4\omega_i t+\frac{2\pi}{3}) & \cos(4\omega_i t+\frac{4\pi}{3}) \\ \cos(4\omega_i t) & \cos(4\omega_i t+\frac{2\pi}{3}) & \cos(4\omega_i t+\frac{4\pi}{3}) \\ \cos(4\omega_i t) & \cos(4\omega_i t+\frac{2\pi}{3}) & \cos(4\omega_i t+\frac{4\pi}{3}) \end{bmatrix} \\
&- \frac{1}{3}0.12.\begin{bmatrix} \cos((3\omega_o+\omega_i)t) & \cos((3\omega_o+\omega_i)t+\frac{4\pi}{3}) & \cos((3\omega_o+\omega_i)t+\frac{2\pi}{3}) \\ \cos((3\omega_o+\omega_i)t) & \cos((3\omega_o+\omega_i)t+\frac{4\pi}{3}) & \cos((3\omega_o+\omega_i)t+\frac{2\pi}{3}) \\ \cos((3\omega_o+\omega_i)t) & \cos((3\omega_o+\omega_i)t+\frac{4\pi}{3}) & \cos((3\omega_o+\omega_i)t+\frac{2\pi}{3}) \end{bmatrix} \\
&+ \frac{1}{3}0.866.\begin{bmatrix} \cos((\omega_i-\omega_o)t) & \cos((\omega_i-\omega_o)t-\frac{2\pi}{3}) & \cos((\omega_i-\omega_o)t-\frac{4\pi}{3}) \\ \cos((\omega_i-\omega_o)t-\frac{2\pi}{3}) & \cos((\omega_i-\omega_o)t-\frac{4\pi}{3}) & \cos((\omega_i-\omega_o)t) \\ \cos((\omega_i-\omega_o)t-\frac{4\pi}{3}) & \cos((\omega_i-\omega_o)t) & \cos((\omega_i-\omega_o)t-\frac{2\pi}{3}) \end{bmatrix} \\
&+ \frac{\beta}{3}0.866.\begin{bmatrix} \cos((5\omega_i-\omega_o)t) & \cos((5\omega_i-\omega_o)t-\frac{2\pi}{3}) & \cos((5\omega_i-\omega_o)t-\frac{4\pi}{3}) \\ \cos((5\omega_i-\omega_o)t-\frac{2\pi}{3}) & \cos((5\omega_i-\omega_o)t-\frac{4\pi}{3}) & \cos((5\omega_i-\omega_o)t) \\ \cos((5\omega_i-\omega_o)t-\frac{4\pi}{3}) & \cos((5\omega_i-\omega_o)t) & \cos((5\omega_i-\omega_o)t-\frac{2\pi}{3}) \end{bmatrix} \\
&+ \frac{1}{3}0.25.\begin{bmatrix} \cos(2\omega_i t) & \cos(2\omega_i t-\frac{2\pi}{3}) & \cos(2\omega_i t-\frac{4\pi}{3}) \\ \cos(2\omega_i t) & \cos(2\omega_i t-\frac{2\pi}{3}) & \cos(2\omega_i t-\frac{4\pi}{3}) \\ \cos(2\omega_i t) & \cos(2\omega_i t-\frac{2\pi}{3}) & \cos(2\omega_i t-\frac{4\pi}{3}) \end{bmatrix} \\
&- \frac{1}{3}0.12.\begin{bmatrix} \cos((3\omega_o-\omega_i)t) & \cos((3\omega_o-\omega_i)t-\frac{4\pi}{3}) & \cos((3\omega_o-\omega_i)t-\frac{2\pi}{3}) \\ \cos((3\omega_o-\omega_i)t) & \cos((3\omega_o-\omega_i)t-\frac{4\pi}{3}) & \cos((3\omega_o-\omega_i)t-\frac{2\pi}{3}) \\ \cos((3\omega_o-\omega_i)t) & \cos((3\omega_o-\omega_i)t-\frac{4\pi}{3}) & \cos((3\omega_o-\omega_i)t-\frac{2\pi}{3}) \end{bmatrix}
\end{aligned}
\tag{2.36}
$$

Using this modified control matrix to correct the effect on the output voltage waveform of the input voltage harmonics would give ideal sinusoidal output currents.

Unfortunately the modifications to the control matrix will modify the input currents drawn by the matrix converter. A repeat of the input current analysis will show that these input current harmonics are at the same frequency and are in phase with the input voltage harmonics.

$$\mathbf{I_i(t)} = \xi.V_i.\begin{bmatrix}\cos(\omega_i t)\\ \cos(\omega_i t+\frac{2\pi}{3})\\ \cos(\omega_i t+\frac{4\pi}{3})\end{bmatrix}+\beta.\xi.V_i.\begin{bmatrix}\cos(5\omega_i t)\\ \cos(5\omega_i t+\frac{2\pi}{3})\\ \cos(5\omega_i t+\frac{4\pi}{3})\end{bmatrix} \tag{2.37}$$

The control algorithm may be adapted in a similar way to that explained above to cope with many waveform distortion effects. If the output currents are non-sinusoidal due to the effects of the load then the output voltage generated by the converter may be altered to compensate. This adaptation of the control algorithm would lead to a distortion of the input current waveforms.

As a general rule, if the control algorithm is adapted to correct output voltage distortion then the input currents will no longer be sinusoidal. If the input currents are corrected by the adaptation of the control waveforms then the output voltage waveforms will be distorted.

## 2.8 Waveform Quality with an Unbalanced Supply

### 2.8.1 Unbalanced Supply Voltage Waveforms

The three phase mains voltage supply may be significantly unbalanced due to unbalanced loads that may be connected. The effect of this may be modelled by rewriting equation 2.6. Let x and y denote the relative higher voltages on the second and third input lines in comparison to the first input line, as shown in figure 2.17.

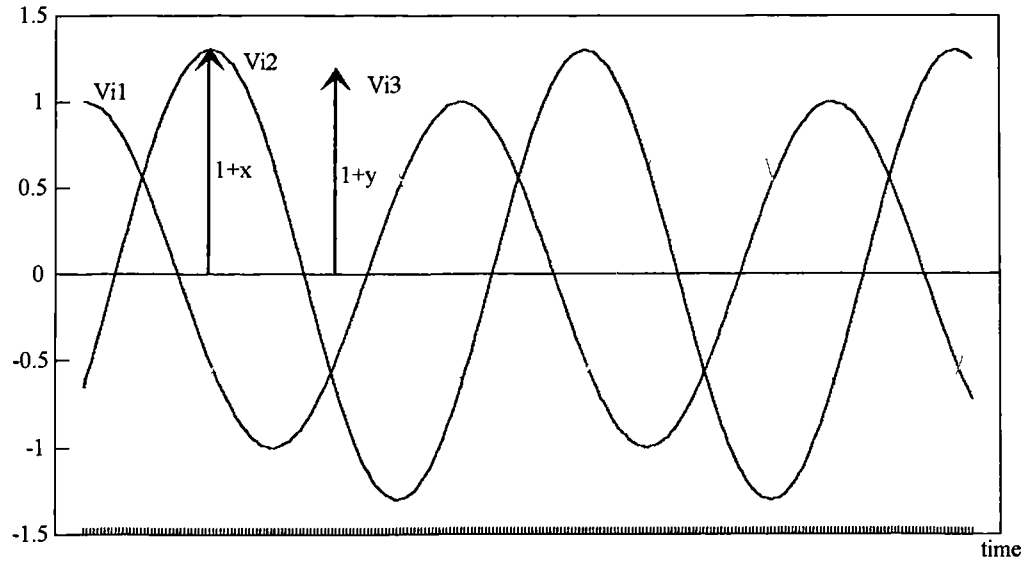


**Figure 2.17. Input Voltage Waveforms with an Unbalanced Supply**

$$\mathbf{V_i(t)} = \begin{bmatrix} V_{i1}(t) \\ V_{i2}(t) \\ V_{i3}(t) \end{bmatrix} = V_i \cdot \begin{bmatrix} \cos(\omega_i t) \\ (1+x).\cos(\omega_i t + \frac{2\pi}{3}) \\ (1+y).\cos(\omega_i t + \frac{2\pi}{3}) \end{bmatrix} \tag{2.38}$$

### 2.8.2 The Effect of an Unbalanced Supply

The output voltage analysis described in equation 2.15 may be repeated using the modified input waveforms from equation 2.38. For simplicity the input voltage is assumed to have unbalance caused by one line, therefore x equals zero. If all three input voltage waveforms are unbalanced with respect to each other then they could be modelled using superposition.

$$\mathbf{V_o(t)} = \mathbf{G(t)}.V_i.\begin{bmatrix} \cos(\omega_i t) \\ \cos(\omega_i t + \frac{2\pi}{3}) \\ (1+y)\cos(\omega_i t + \frac{4\pi}{3}) \end{bmatrix}$$

$$= V_i.0.866.\left(1+\tfrac{y}{3}\right).\begin{bmatrix} \cos(\omega_o t) \\ \cos(\omega_o t + \frac{2\pi}{3}) \\ \cos(\omega_o t + \frac{4\pi}{3}) \end{bmatrix}$$

$$+\left(V_i.0.25.\left(1+\tfrac{y}{3}\right).\cos(3\omega_o t) - V_i.0.12.\left(1+\tfrac{y}{3}\right).\cos(3\omega_i t)\right).\begin{bmatrix} 1 \\ 1 \\ 1 \end{bmatrix}$$

$$+V_i.0.866.y.\begin{bmatrix} \cos(2\omega_i t + \omega_o t + \frac{2\pi}{3}) + \cos(\omega_o t - 2\omega_i t + \frac{4\pi}{3}) \\ \cos(2\omega_i t + \omega_o t + \frac{4\pi}{3}) + \cos(\omega_o t - 2\omega_i t) \\ \cos(2\omega_i t + \omega_o t) + \cos(\omega_o t - 2\omega_i t + \frac{2\pi}{3}) \end{bmatrix}$$

$$+V_i.0.25.y.\begin{bmatrix} \cos(5\omega_i t + \frac{2\pi}{3}) + \cos(\omega_i t + \frac{4\pi}{3}) \\ \cos(5\omega_i t + \frac{4\pi}{3}) + \cos(\omega_i t) \\ \cos(5\omega_i t) + \cos(\omega_i t + \frac{2\pi}{3}) \end{bmatrix}$$

$$+V_i.0.12.y.\begin{bmatrix} \cos(2\omega_i t + 3\omega_o t) + \cos(3\omega_o t - 2\omega_i t) \\ \cos(2\omega_i t + 3\omega_o t + \frac{4\pi}{3}) + \cos(3\omega_o t - 2\omega_i t + \frac{2\pi}{3}) \\ \cos(2\omega_i t + 3\omega_o t + \frac{2\pi}{3}) + \cos(3\omega_o t - 2\omega_i t + \frac{4\pi}{3}) \end{bmatrix} \quad (2.39)$$

This distortion of the output voltage waveforms will cause distortion of the output current waveforms. This output current distortion will cause distortion in the input current waveforms.

### 2.8.3 Correcting the Effects of an Unbalanced Supply

The elements of the control matrix, **G(t)**, which are involved in the manipulation of the unbalanced input line may be multiplied by the reciprocal of the relative magnitude of the unbalanced voltage waveform.

$$\mathbf{G(t)} = \frac{1}{3}0.866.\begin{bmatrix} \cos((\omega_i+\omega_o)t) & \cos((\omega_i+\omega_o)t+\frac{2\pi}{3}) & (\frac{1}{1+y}).\cos((\omega_i+\omega_o)t+\frac{4\pi}{3}) \\ \cos((\omega_i+\omega_o)t+\frac{2\pi}{3}) & \cos((\omega_i+\omega_o)t+\frac{4\pi}{3}) & (\frac{1}{1+y}).\cos((\omega_i+\omega_o)t) \\ \cos((\omega_i+\omega_o)t+\frac{4\pi}{3}) & \cos((\omega_i+\omega_o)t) & (\frac{1}{1+y}).\cos((\omega_i+\omega_o)t+\frac{2\pi}{3}) \end{bmatrix}$$

$$+\frac{1}{3}0.25.\begin{bmatrix} \cos(4\omega_i t) & \cos(4\omega_i t+\frac{2\pi}{3}) & (\frac{1}{1+y}).\cos(4\omega_i t+\frac{4\pi}{3}) \\ \cos(4\omega_i t) & \cos(4\omega_i t+\frac{2\pi}{3}) & (\frac{1}{1+y}).\cos(4\omega_i t+\frac{4\pi}{3}) \\ \cos(4\omega_i t) & \cos(4\omega_i t+\frac{2\pi}{3}) & (\frac{1}{1+y}).\cos(4\omega_i t+\frac{4\pi}{3}) \end{bmatrix}$$

$$-\frac{1}{3}0.12.\begin{bmatrix} \cos((3\omega_o+\omega_i)t) & \cos((3\omega_o+\omega_i)t+\frac{4\pi}{3}) & (\frac{1}{1+y}).\cos((3\omega_o+\omega_i)t+\frac{2\pi}{3}) \\ \cos((3\omega_o+\omega_i)t) & \cos((3\omega_o+\omega_i)t+\frac{4\pi}{3}) & (\frac{1}{1+y}).\cos((3\omega_o+\omega_i)t+\frac{2\pi}{3}) \\ \cos((3\omega_o+\omega_i)t) & \cos((3\omega_o+\omega_i)t+\frac{4\pi}{3}) & (\frac{1}{1+y}).\cos((3\omega_o+\omega_i)t+\frac{2\pi}{3}) \end{bmatrix}$$

$$+\frac{1}{3}0.866.\begin{bmatrix} \cos((\omega_i-\omega_o)t) & \cos((\omega_i-\omega_o)t-\frac{2\pi}{3}) & (\frac{1}{1+y}).\cos((\omega_i-\omega_o)t-\frac{4\pi}{3}) \\ \cos((\omega_i-\omega_o)t-\frac{2\pi}{3}) & \cos((\omega_i-\omega_o)t-\frac{4\pi}{3}) & (\frac{1}{1+y}).\cos((\omega_i-\omega_o)t) \\ \cos((\omega_i-\omega_o)t-\frac{4\pi}{3}) & \cos((\omega_i-\omega_o)t) & (\frac{1}{1+y}).\cos((\omega_i-\omega_o)t-\frac{2\pi}{3}) \end{bmatrix}$$

$$+\frac{1}{3}0.25.\begin{bmatrix} \cos(2\omega_i t) & \cos(2\omega_i t-\frac{2\pi}{3}) & (\frac{1}{1+y}).\cos(2\omega_i t-\frac{4\pi}{3}) \\ \cos(2\omega_i t) & \cos(2\omega_i t-\frac{2\pi}{3}) & (\frac{1}{1+y}).\cos(2\omega_i t-\frac{4\pi}{3}) \\ \cos(2\omega_i t) & \cos(2\omega_i t-\frac{2\pi}{3}) & (\frac{1}{1+y}).\cos(2\omega_i t-\frac{4\pi}{3}) \end{bmatrix}$$

$$-\frac{1}{3}0.12.\begin{bmatrix} \cos((3\omega_o-\omega_i)t) & \cos((3\omega_o-\omega_i)t-\frac{4\pi}{3}) & (\frac{1}{1+y}).\cos((3\omega_o-\omega_i)t-\frac{2\pi}{3}) \\ \cos((3\omega_o-\omega_i)t) & \cos((3\omega_o-\omega_i)t-\frac{4\pi}{3}) & (\frac{1}{1+y}).\cos((3\omega_o-\omega_i)t-\frac{2\pi}{3}) \\ \cos((3\omega_o-\omega_i)t) & \cos((3\omega_o-\omega_i)t-\frac{4\pi}{3}) & (\frac{1}{1+y}).\cos((3\omega_o-\omega_i)t-\frac{2\pi}{3}) \end{bmatrix}$$

(2.40)

This scaling will eliminate the effect of the unbalance in the output voltage waveforms. The output voltage analysis described in equation 2.15 can be repeated using the input voltages given in equation 2.37 and the control matrix given in equation 2.40. This analysis would result in the ideal output voltage waveforms as described in equation 2.7. If switching frequency harmonics are ignored then the output currents are sinusoidal, as described in equation 2.8.

The input current analysis may then be repeated. As previously suggested the correction of the output voltage waveforms will result in distortion of the input current waveforms. Similar methods may be employed to correct the input current waveforms, but this would cause distortion in the output voltage waveforms.

$$\mathbf{I_i(t)} = \xi.V_i.\left(\frac{1+\frac{2}{3}y}{1+y}\right).\begin{bmatrix} \cos(\omega_i t) \\ \cos(\omega_i t+\frac{2\pi}{3}) \\ \left(\frac{1}{1+y}\right)\cos(\omega_i t+\frac{4\pi}{3}) \end{bmatrix}$$
$$+\left(\frac{y}{1+y}\right)\begin{bmatrix} \cos(\omega_i t+2\omega_o t+\frac{2\pi}{3}) & \cos(\omega_i t-2\omega_o t) \\ \cos(\omega_i t+2\omega_o t+\frac{4\pi}{3}) & \cos(\omega_i t-2\omega_o t+\frac{2\pi}{3}) \\ \cos(\omega_i t+2\omega_o t) & \cos(\omega_i t-2\omega_o t+\frac{4\pi}{3}) \end{bmatrix} \quad (2.41)$$

This unbalanced load analysis has assumed a restive load and only one unbalanced input voltage waveform. The principles of superposition may be used if all the lines are unbalanced. The analysis is still valid if an inductive load is used.

If the control algorithm was digitally implemented then these adaptations to the control algorithm could be performed by the control software. This would allow the converter to adapt to the prevailing conditions at any time.

## 2.9 Conclusions

The maximum output voltage limitation of a matrix converter has been examined. The intrinsic maximum output voltage limit for a matrix converter is 0.866 of the input voltage. The theory and historical evolution in obtaining this maximum output voltage has been discussed. A control algorithm capable of achieving the maximum output voltage may be derived using a two stage rectifier/inverter model.

It is possible to verify the operation of the proposed control matrix mathematically using ideal input and output waveforms. The ability of the control matrix to control the input displacement factor of the converter has been explored. The control algorithm is capable of input displacement factors between the output displacement factor lagging and the output displacement factor leading.

The control matrix may be adapted to deal with distortion in the input voltage waveforms. In a digital implementation this adaptation could be a continuous operation which would allow the converter to cope with the changes in the input voltage waveforms that may be experienced over a period of time.

# Bibliography


[1] Venturini M, "A New Sine In Sine Out, Conversion Technique Which Eliminates Reactive Components", Proceedings Powercon 7 (San Diego, CA), 1980, pp.E3_1-E3_15.

[2] Alesina A and Venturini M, "The Generalised Transformer: A New Bidirectional Sinusoidal Waveform Frequency Converter With Continuous Variable Adjustable Input Power Factor", Proc. of PESC Conference Record, 1980, pp.242-252.

[3] Alesina A and Venturini M, "Solid-State Power Conversion : A Fourier Analysis Approach to Generalised Transformer Synthesis", IEEE Trans. on Circuits and Systems, Vol. cas28, No.4, April 1981, pp.319-330.

[4] Ziogas P.D, Khan S.I and Rashid M.H, "Some Improved Forced Commutated Cycloconverter Structures", IEEE Trans. on Ind. Applications, Oct 1985, Vol.1A-21, No.5, pp.1242-1253.

[5] Alesina A and Venturini M, "Intrinsic Amplitude Limits and Optimum Design of 9-Switches Direct PWM AC to AC Converters", PESC Conference Record 1988, pp.1284-1291.

[6] Control Techniques, "Drives and Servos Year Book, 1990-1991", 1989.

[7] Lipo T.A., "Recent Progress in the Development of Solid State AC Motor Drives", IEE Trans. on Power Electronics, Vol.3, No.2, April 1988, pp.105-117.

[8] Maytum K.J and Colman D, "The Implementation and Future Potential of the Venturini Converter", Proc. of Drives, Motors and Controls, 1983, pp.108-117.

[9] Electricity Association, "Limits for Harmonics in the UK Electricity Supply System", G.5/3, Engineering Publications, 1976.

[10] Gjugyi L and Pelly B, "Static Power Frequency Changers", New York : Wiley, 1976.

Chapter 3

# Microcontrollers and Program Design

## 3.1 Introduction

To implement the control algorithm described in Chapter 2 on a matrix converter some form of controller must be provided. Analogue control would require a large volume of hardware and would be inflexible to changes in control strategy [1]. Digital control was therefore chosen for the prototype matrix converters.

A high switching frequency was considered important to minimise the size of the converter's input filters. The calculations in the control algorithm would therefore require a powerful processor. It was felt that a single microchip solution would be preferable to allow for maximum flexibility of programming and simplicity of hardware design.

This chapter deals with the choosing of a suitable processor. It considers the implementation of the control algorithm on the chosen processor and describes the design of the program structure.

## 3.2 Microcontrollers

A group of processors on the market called "microcontrollers" combine a microprocessor with a number of timers and other peripheral devices. These microcontrollers have the advantage of low software overheads for timer functions and reaction to external events. The peripherals usually include some on-board analogue to digital converters.

The lower end of the microcontroller family consists of comparatively slow 4 bit controllers suitable for central heating control systems and low cost embedded applications. The bulk of microcontrollers are 8 bit controllers used in embedded applications in everything from food mixers to cars [2]. These 8 bit processors can be reasonably powerful and may be found in many existing power converters. In recent years a range of 16 bit microcontrollers has been released by the major manufacturers. During the next few years their market share is expected to increase dramatically [2] as shown in figure 3.1.

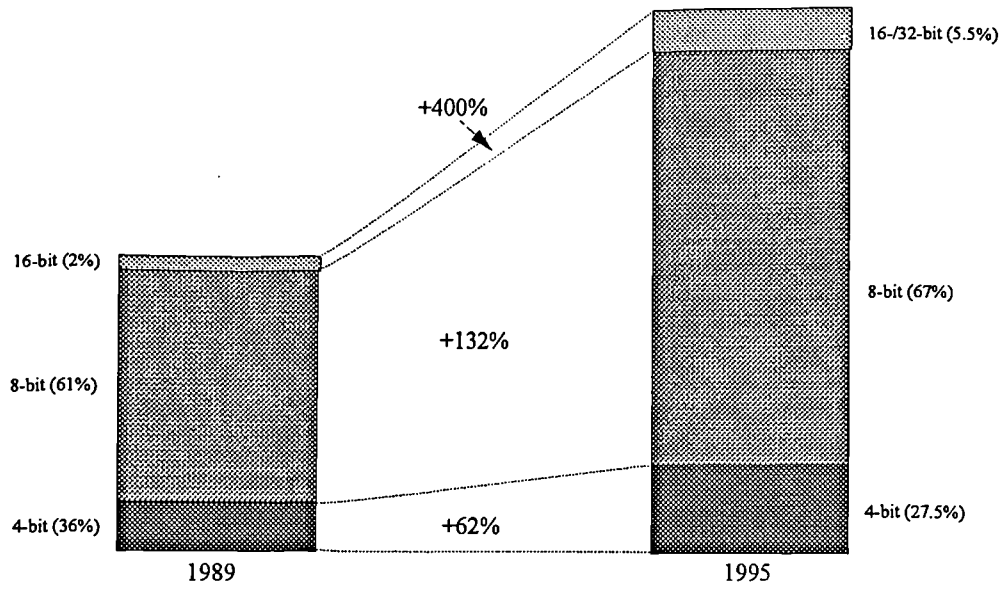


**Figure 3.1. Comparative Percentage World Sales of the Members of the Microcontroller Family**

At the time of investigation three of these new generation 16 bit microcontrollers were being introduced.

- TMS320E14 from Texas Instruments.
- MC68332 from the 68000 family by Motorola.
- SAB80C166 from Siemens.

### 3.2.1 The Texas Instruments TMS320E10

The TMS320E10 is a 16 bit microprocessor based on the established TMS320 digital signal processor family. According to the User's Guide [4] it has been designed to combine the high performance of a DSP with the on-chip peripherals of a microcontroller. This DSP engine provides the controller with an efficient and small instruction set. The on-board barrel multiplier and short instruction cycle times mean that this processor is capable of implementing complex control algorithms with high speed and accuracy.

The controller has an on-board Event Manager that is well suited to PWM wave-form production, with 10 bit resolution at 25kHz. There are only 6 high resolution

PWM output channels on the processor. This limitation would mean that the implementation of the matrix converter would require additional external hardware to generate the three extra PWM waveforms.

The TMS320C14/E14 belongs to the TMS320 family and therefore is backwardly software compatible with all preceding processors in the family. Future upgrades to the controller family will also be software compatible leading to long term stability in user's architecture investments. The TMS320C14 became available in early 1992. Before this development would have been slow as only the EPROM version was available. The key features of the microcontroller are listed in Table 3.1.

| | |
|---|---|
| CPU clock Frequency | 25.6MHz |
| Average Instruction time | 160ns |
| Multiply Instruction Time | 160ns |
| Division Instruction Time | N/A |
| PWM output channels | 6 |
| Minimum Pulse Width | 40ns in high resolution mode,<br>(160ns in standard mode) |
| Number of Timers | 4 |
| Package | 68 pin leaded chip carrier packages. |
| Number of Interrupts | 15 |
| Input/Output | 16 discrete I/O pins |
| Serial Ports | 2 |

**Table 3.1. Features of the TMS320C14/E14 Microcontroller**

### 3.2.2 The Motorola MC68300

The Motorola MC68332 16 bit microcontroller was based on the MC68020 family [6]. It is the first in a proposed MC68300 family of embedded controllers. An impressive array of on-board peripherals is boasted. These include a time processor unit [7], a system integration module [8] and a queued serial module [9], each of which comes with an independent set of manuals! It is mainly aimed at the automotive industry, but is capable of many highly complex timing applications.

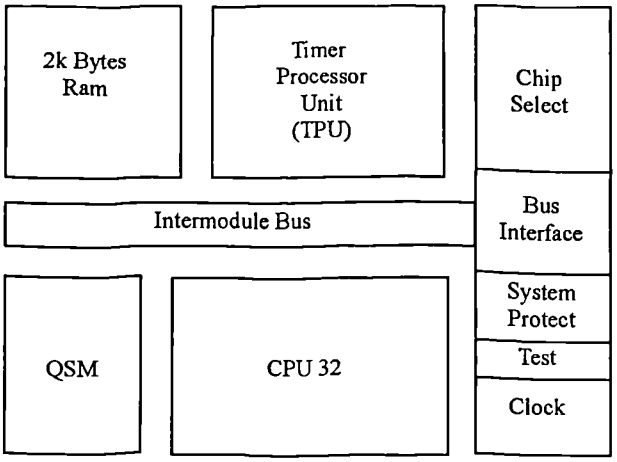


**Figure 3.2. A Functional Block Diagram of the MC68332**

The PWM generation unit is flexible and has an integrated automatic update facility to reduce software overheads. The functional block diagram for the controller is shown in figure 3.2. The backward compatibility with the MC68000 processors leads to a large and inefficient instruction set in comparison to other similar controllers. Future derivatives of this processor will have a higher clock frequency leading to a reduced instruction cycle time. The features of this controller are summarised in table 3.2.

| | |
|---|---|
| CPU Clock Frequency | 32.77MHz |
| Average Instruction time | 400ns (many 600ns or more) |
| Multiply Instruction Time | 3200ns for 16x16 (1600ns for 8x8) |
| PWM output channels | 16 |
| Minimum Pulse Width | 1920ns |
| Number of Timers | 2 |
| Serial Ports | 2 |
| Package | 132 pin plastic quad flat pack |
| Number of Interrupt levels | 7 |
| Input/Output | 32 discrete I/O pins |
| Instruction Set | Large and comprehensive |

**Table 3.2. Features of the MC68332 Integrated Microcontroller**

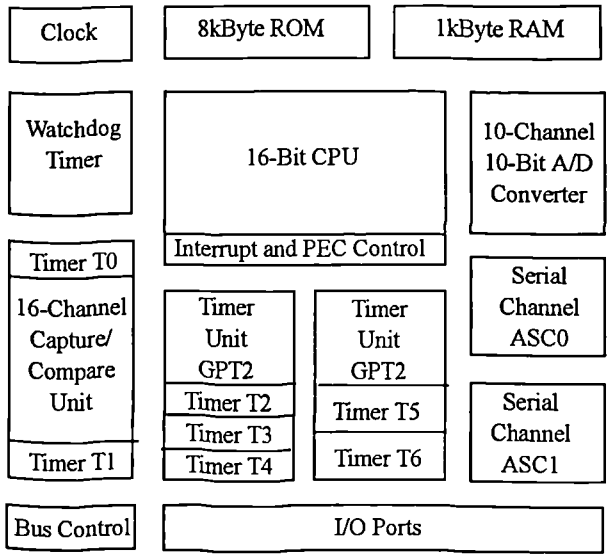


**Figure 3.3. Functional Block Diagram of the SAB80C166**

### 3.2.3 The Siemens SAB80C166

The SAB80C166 has been developed to meet the high performance requirements of real time embedded control applications [11]. The processor uses a control based, "RISC" style instruction set. The array of peripherals includes an Intelligent Peripheral Subsystem with a 16 channel Capture/Compare unit that can be used as a flexible PWM waveform generator. A block diagram of the controller is shown in figure 3.3.

The SAB80C166 is the first in Siemens' proposed new 16-bit controller family. The family will be backwardly compatible. Being the first in a new family of processors means that this controller has not suffered from the design constraints that can compromise the functions required in control applications. The future derivatives will include extra and more flexible peripherals in line with the requirements of their major customers.

| | |
|---|---|
| CPU Clock Frequency | 20MHz |
| Average Instruction time | 100ns |
| Multiply Instruction Time | 500ns (16x16) |
| Division Instruction Time | 1000ns |
| PWM output channels | 16 |
| Minimum Pulse Width | 400ns |
| Number of Timers | 6 |
| Serial Ports | 2 |
| Package | 100 pin Plastic quad flat pack. |
| Number of Interrupts | 19 (external) |
| Input/Output | 76 discrete I/O pins |
| Instruction Set | "RISC" style |

**Table 3.3. Features of the SAB80C166 Microcontroller**

The second controller in the family is the SAB80C167 [12]. This recently released processor has an expanded capture and compare unit that would allow greater accuracy for PWM waveform generation. Siemens also support the addition of customer specific on-board peripherals. These peripherals could include a dedicated PWM generation unit.

## 3.3 Choosing a Microcontroller for the Matrix Converter

### 3.3.1 The Desirable Functions for a Matrix Converter Controller

A matrix converter consists of nine independently controlled bi-directional switches. Nine PWM waveforms are therefore required to drive these switches. A controller with at least nine PWM output channels would therefore reduce the need for additional hardware. A selection of on-board event timers and interrupts would be useful in allowing the controller to react to external events. This would allow the correction of the model of the input frequency and input phase order detection.

A switching frequency of 20kHz was chosen for the converter. The reasons for this choice of frequency are explained later in this thesis. This relatively high switching frequency requires the controller to compute the pulse widths quickly. Even if the values are only updated every other switching period, the software needs to operate efficiently on a high throughput microprocessor. At a 20kHz switching frequency the controller will have 50μs to perform the PWM duty cycle computations. At this switching frequency it would be important to have a PWM waveform with a relatively high resolution and minimum pulse width. A minimum pulse width of 500ns could take advantage of the faster semiconductor switches that are currently available.

The control algorithm described in Chapter 2 requires multiplication to control the output voltage amplitude. A processor with an efficient and accurate multiplication instruction is therefore necessary. Nine is the minimum number of multiplications the control algorithm will require to give output voltage control. If the processor has a slow multiplication instruction then this will seriously decrease the time left for the lookup table routines and the correction algorithms.

### 3.3.2 The Choosing of a Micro-Controller

The need for nine PWM output channels excludes the TMS320C14/E14 as a viable controller for the matrix converter unless external hardware is used. The TMS320C14 has a fast multiplication instruction and a useful instruction set. At the time of choosing a controller, only the EPROM version of this controller was available. This hardware restriction would have impeded the software development.

The MC68332 has a long multiplication instruction time, 3.2μs. If the nine multiplications required by the control algorithm were to be implemented using this processor then there would only be 18μs left in any one instruction cycle. This would make it impossible to update of the compare registers every switching cycle.

| Function | TMS320C14 | MC68332 | SAB80C166 |
|---|---|---|---|
| **Multiplication Instruction Time** | 160ns | 3200ns | 500ns |
| **Average Instruction Time** | 160ns | 400ns | 100ns |
| **PWM Output Channels** | 6 | 16 | 16 |
| **PWM Pulse Width Resolution** | 40ns | 1920ns | 400ns |
| **Minimum PWM Pulse Width** | 40ns | 60ns | 400ns |

**Table 3.4. Comparison of Processor Functions Critical to The Matrix Converter**

The minimum pulse width for the PWM generation unit on the MC68332 is 1920ns. This long minimum pulse width would lead to inaccuracies in the control waveforms. The pulse width restriction would not allow this processor to take advantage of any future faster semiconductor switch technologies. The MC68332 has the advantage of having an automatic PWM compare register update function that saves the software overhead required in the updating of these registers.

The SAB80C166 has an instruction set that is written with control requirements in mind. There are sixteen PWM output channels with a minimum pulse width of 400ns. The multiplication takes 500ns, leaving 45.5μs for other software functions. For these reasons the SAB80C166 was chosen to control the matrix converter.

## 3.4 The Modulation Matrix

In Chapter 2 a control matrix for the matrix converter was proposed. To implement this control matrix on a microprocessor, the continuous control waveforms must be converted into duty cycles. This implementation will require the normalisation of the control functions and sampling of the control functions every switching cycle. The safe operation of the switches must also be considered to avoid open circuits on the output lines and short circuits between the input lines. This section looks at the manipulation of the control matrix to obtain a modulation matrix in a suitable form for software implementation.

### 3.4.1 The Switch Function

If a converter implemented with perfect switches is assumed then a function, m(t), can be defined to describe the switch operation, as shown in equation 3.1. A perfect switch has zero propagation delay, zero switching time and zero conduction losses [16].

$$\begin{aligned} m(t) &= 1 \quad \text{(when the switch is closed)} \\ m(t) &= 0 \quad \text{(when the switch is open)} \end{aligned} \tag{3.1}$$

A three by three matrix of these functions, **M(t),** can then be defined to describe the switch function of all nine switches in the matrix converter. The indices refer to the switch numbers shown in figure 3.1

$$\mathbf{M(t)} = \begin{bmatrix} m_1(t) & m_4(t) & m_7(t) \\ m_2(t) & m_5(t) & m_8(t) \\ m_3(t) & m_6(t) & m_9(t) \end{bmatrix} \tag{3.2}$$

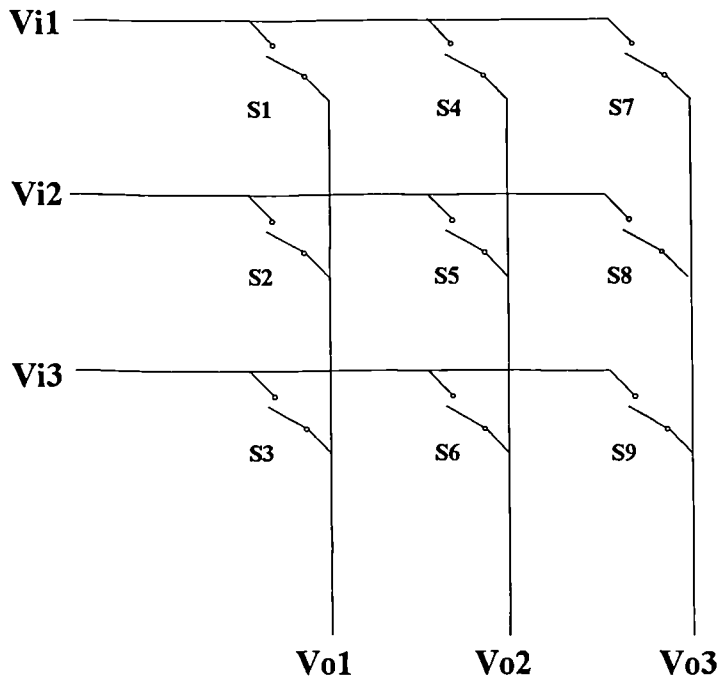


**Figure 3.4. The Matrix Converter Switch Layout**

### 3.4.2 Safe Switch Operation with Perfect Switches

The switches in the converter must be controlled in such a way that two input lines are never connected to the same output line. It is also important that every output line is always connected to an input line as open circuiting a phase of the motor will give rise to large voltage spikes due to the inductive nature of the load. To avoid open circuits on the output lines, all output lines must always be connected to an input line. These restrictions will give a set of 27 legal matrices for **M(t),** as shown in table 3.1, [17].

$$\begin{bmatrix}1&1&1\\0&0&0\\0&0&0\end{bmatrix}\ \begin{bmatrix}1&1&0\\0&0&1\\0&0&0\end{bmatrix}\ \begin{bmatrix}1&1&0\\0&0&0\\0&0&1\end{bmatrix}\ \begin{bmatrix}1&0&1\\0&1&0\\0&0&0\end{bmatrix}\ \begin{bmatrix}1&0&1\\0&0&0\\0&1&0\end{bmatrix}\ \begin{bmatrix}0&1&1\\1&0&0\\0&0&0\end{bmatrix}$$

$$\begin{bmatrix}0&1&1\\0&0&0\\1&0&0\end{bmatrix}\ \begin{bmatrix}0&0&0\\1&1&1\\0&0&0\end{bmatrix}\ \begin{bmatrix}1&0&0\\0&1&1\\0&0&0\end{bmatrix}\ \begin{bmatrix}0&0&0\\0&1&1\\1&0&0\end{bmatrix}\ \begin{bmatrix}0&1&0\\1&0&1\\0&0&0\end{bmatrix}\ \begin{bmatrix}0&0&0\\1&0&1\\0&1&0\end{bmatrix}$$

$$\begin{bmatrix}0&0&1\\1&1&0\\0&0&0\end{bmatrix}\ \begin{bmatrix}0&0&0\\1&1&0\\0&0&1\end{bmatrix}\ \begin{bmatrix}0&0&0\\0&0&0\\1&1&1\end{bmatrix}\ \begin{bmatrix}0&0&1\\0&0&0\\1&1&0\end{bmatrix}\ \begin{bmatrix}0&0&0\\0&0&1\\1&1&0\end{bmatrix}\ \begin{bmatrix}0&0&0\\0&1&0\\1&0&1\end{bmatrix}$$

$$\begin{bmatrix}0&1&0\\0&0&0\\1&0&1\end{bmatrix}\ \begin{bmatrix}1&0&0\\0&0&0\\0&1&1\end{bmatrix}\ \begin{bmatrix}0&0&0\\1&0&0\\0&1&1\end{bmatrix}\ \begin{bmatrix}0&1&0\\1&0&0\\0&0&1\end{bmatrix}\ \begin{bmatrix}1&0&0\\0&0&1\\0&1&0\end{bmatrix}\ \begin{bmatrix}1&0&0\\0&1&0\\0&0&1\end{bmatrix}$$

$$\begin{bmatrix}0&1&0\\0&0&1\\1&0&0\end{bmatrix}\ \begin{bmatrix}0&0&1\\1&0&0\\0&1&0\end{bmatrix}\ \begin{bmatrix}0&0&1\\0&1&0\\1&0&0\end{bmatrix}$$

**Table 3.1. Legal Forms for the Modulation Matrix, M(t)**

### 3.4.3 The Switch Duty Cycles

Chapter 2 introduced a possible control matrix for a matrix converter ,**G(t)**. Each element of this control matrix consists of the sum of six sinusoidal functions. To operate the switches a duty cycle for each must be defined. This duty cycle matrix, **D(t)**, may be obtained by the addition of a constant to each element of the control matrix. The constant is the sum of two elements. The first element is a fixed value to ensure that the duty cycle will never take a negative value.

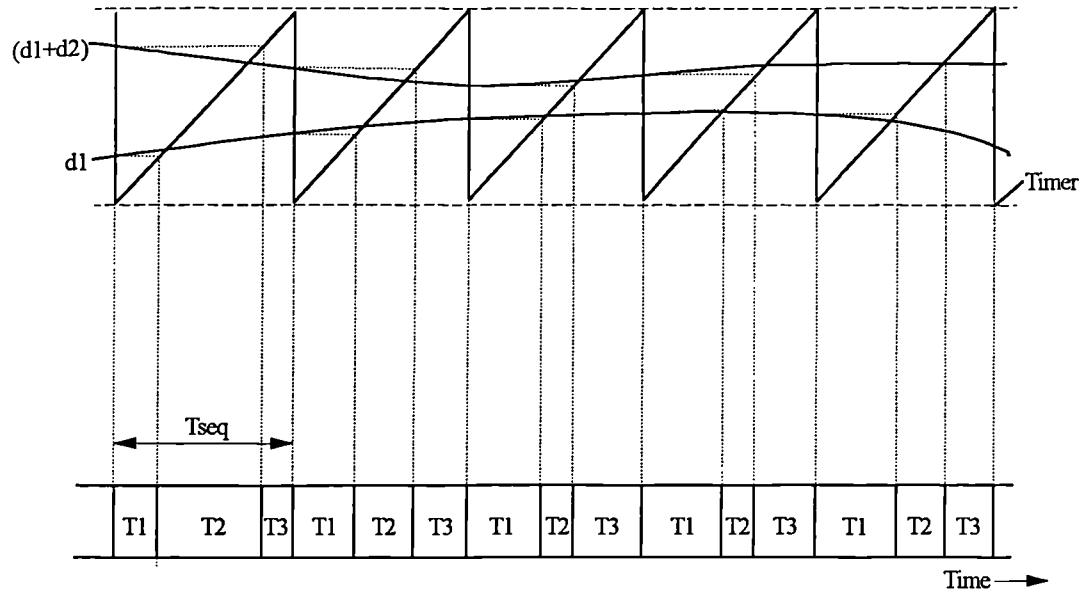


**Figure 3.5. Timing Diagram for One Output Line of a Matrix Converter**

The second element is required to balance the currents drawn from the input lines when the matrix converter is not operating at maximum output voltage. This combined constant has no effect on the operation of the control matrix because it does not effect the nature of the control functions.

$$\mathbf{D(t)} = \begin{bmatrix} d_1 & d_2 & d_3 \\ d_4 & d_5 & d_6 \\ d_7 & d_8 & d_9 \end{bmatrix} = \begin{bmatrix} (1-q) & (1-q) & (1-q) \\ (1-q) & (1-q) & (1-q) \\ (1-q) & (1-q) & (1-q) \end{bmatrix} + \begin{bmatrix} 0.5 & 0.5 & 0.5 \\ 0.5 & 0.5 & 0.5 \\ 0.5 & 0.5 & 0.5 \end{bmatrix} + \mathbf{G(t)} \tag{3.3}$$

The duty cycle matrix is sampled to define the closed time of each switch in the converter. This may be achieved by calculating each duty cycle and comparing it to a saw-tooth timer waveform. This waveform has a period $T_{seq.}$ that is the switching period for the converter. The compare process for this PWM waveform generation is shown for one output phase in figure 3.5. T1 is the connection time of the output line to input line 1; T2 the connection time to line 2; and so on.

## 3.5 The Implementation of the Control Matrix

The duty cycle matrix in equation 3.3 may be computed using a microprocessor. The PWM waveforms for each switch are then generated. These waveforms can then be used to drive the bi-directional switches in any matrix converter.

### 3.5.1 The Program Design

The basic layout of the core program for the matrix converter control algorithm is given in figure 3.6. Before the control algorithm can be calculated, the control program must set up the various timers, analogue to digital converters and I/O channels that are required. The capture and compare unit has to be configured as a PWM generator and the generation modes for each output signal have to be set . These initialisations are achieved by writing to the relevant special function registers (SFRs).

The controller then reads in the required output frequency, magnitude and displacement factor from the user interface. These values are used to set up the control frequencies. The value of the control function can then be found using lookup tables.

There are three sine wave lookup tables, one for each of the control waveform magnitudes. This *pre-scaling takes up memory, but allows faster calculation of the* control functions. In this application, time may be at a higher premium than memory. The time step for the next switching period is also calculated. These time steps are added to the current position in the lookup table. The larger the time step, the higher the control frequency.

From the value of the control function, the switching times for the PWM output waveforms can be established. The switching times are sent to a buffer to be used to update the PWM compare registers when the current switching cycle has finished. This updating can be set to happen automatically when the relevant interrupt is present. This is done using the onboard data moving function.

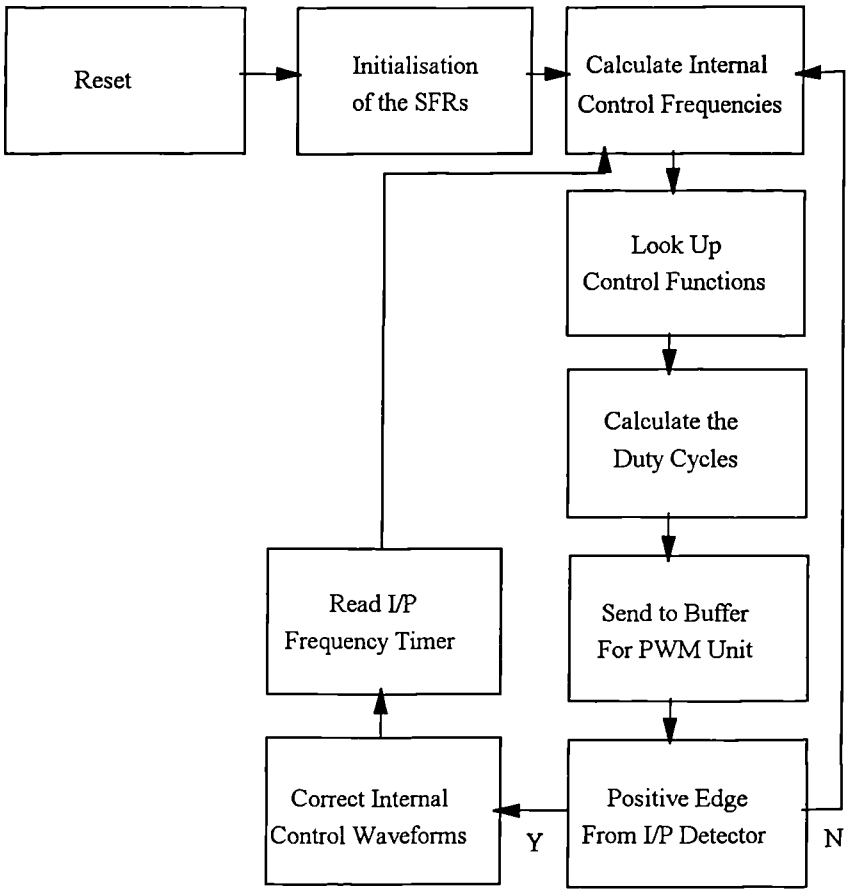


**Figure 3.6. A Brief Outline of the Main Program Layout**

The final step in the program allows the controller to correct the phasing of the internal control functions. These internal control functions must be kept in phase with the actual input waveforms. The correction routines are activated when a positive edge has occurred in the signal from the zero input voltage crossing detector. This task could be accomplished using interrupts, but the main body of the program is a critical zone as far as the control functions are concerned. The input frequency is very low in comparison to the switching frequency and hence there will be no measurable loss in accuracy.

### 3.5.2 Correction of Controller Phasing Errors

The control functions (equation 2.14) which deal with the 2nd and 4th harmonics of the input frequency are easily phase corrected. These two waveforms will pass through zero at the same time as the input voltage waveform. It is therefore a relatively easy task to correct any small error in these functions by setting them to zero when a positive edge from the zero crossing detector is present. The control functions containing harmonics involving the output frequency will not be passing through zero at this time. A way of correcting the time phasing of these remaining functions must therefore be found.

Consider the two control functions that are the sum and the difference of the input and output frequencies for switch 1.

$$\begin{aligned} g_{11}(t) &= \cos((\omega_i + \omega_o)t) \\ g_{12}(t) &= \cos((\omega_i - \omega_o)t) \end{aligned} \tag{3.4}$$

These two functions may be expanded:

$$\begin{aligned} g_{11}(t) &= \cos(\omega_i t).\cos(\omega_o t) + \sin(\omega_i t).\sin(\omega_o t) \\ g_{12}(t) &= \cos(\omega_i t).\cos(\omega_o t) - \sin(\omega_i t).\sin(\omega_o t) \end{aligned} \tag{3.5}$$

When the input voltage waveform is passing through zero:

$$\cos(\omega_i t) = 0$$

and:

$$\sin(\omega_i t) = 1$$

Equation 3.5 can therefore be rewritten:

$$\begin{aligned} g_{11}(t) &= \sin(\omega_o t) \\ g_{12}(t) &= -\sin(\omega_o t) \\ &= \sin(-\omega_o t) \end{aligned} \tag{3.6}$$

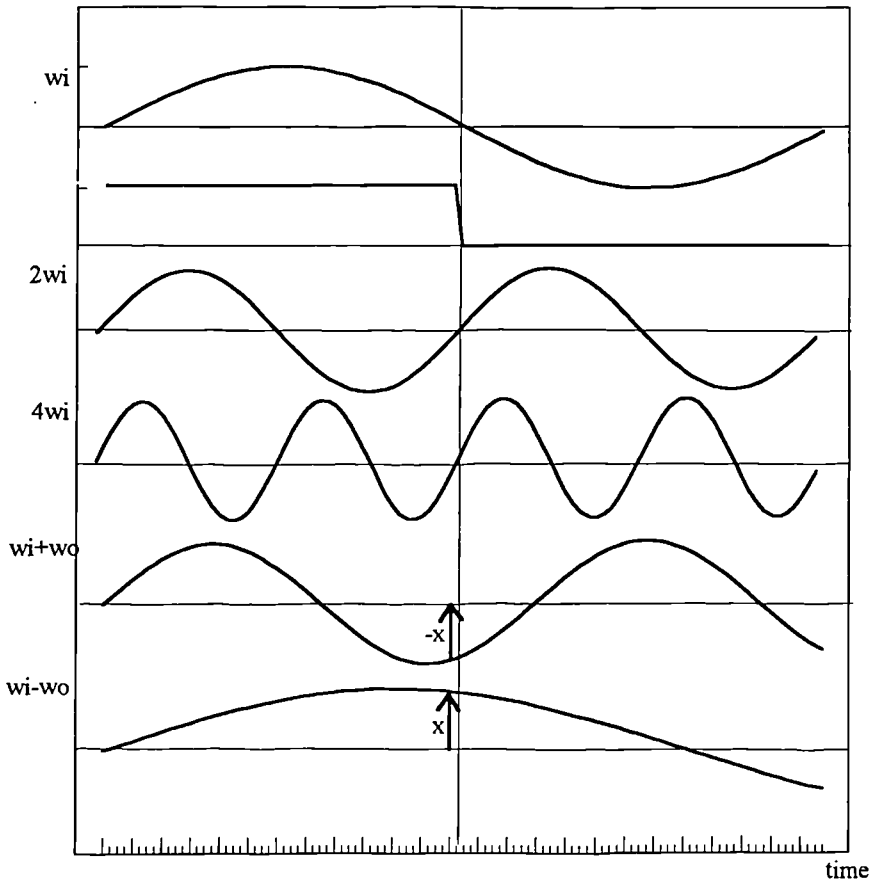


**Figure 3.7. The Relationship Between the Input Voltage Waveform and the Control Waveforms**

When the input voltage waveform is passing through the zero point, the two control functions are at the same point as each other on their particular sinusoid function, but have the opposite sign. This can be used to correct any small phasing error that may have occurred between them. This theory can be applied to any of the control functions that contain the output frequency or the third harmonic of the output frequency. The correction process is shown in figure 3.7.

The controller also uses the input voltage information to measure the input frequency to the matrix converter. Multiple zero crossing hazards can occur in the signals from the zero voltage detector. To prevent these hazards affecting the per-

formance of the converter either a phase locked loop or some crude filtering of the signal must be implemented.

The order of the three phases of the input voltage waveforms to the matrix converter affects the operation of the control matrix. The controller's model of the input voltage waveform model must agree with the voltages applied to the matrix converter. A second zero crossing detector is required to provide the controller with this input voltage phase order information. The controller can then detect the phase order of the input voltages and correct the internal model accordingly. This simple operation saves the necessity of checking the phase ordering of the mains every time a matrix converter is installed in a new location.

## 3.6 Conclusions

The microcontroller family of processors are well suited to the task of controlling power converters such as the matrix converter. The latest 16-bit processors with their associated peripherals minimise the software overheads involved in the generation of PWM waveforms. The SAB80C166 was chosen for the implementation of the prototype matrix converters due to the suitability of the processor and peripherals.

The manipulation of the control matrix into a duty cycle matrix has been described. The safe operation of the switches in a matrix converter must always be considered. With these restrictions in mind, the basic design of a digital implementation has been described. Problems associated with the accumulation of small phase errors between the input voltage waveforms and the controller's model of the input waveforms must always be addressed in the implementation of a matrix converter.

# Bibliography


[1] Lipo T.A., "Recent Progress in the Development of Solid State AC Motor Drives", IEE Trans. on Power Electronics, Vol.3, No.2, April 1988, pp.105-117.

[2] "The New Reference Class: The SAB80C166 Microcontroller", Seimens A.G., 1990.

[3] TMS32010 Users Guide, Texas Instruments, 1983.

[4] TMS320C14/TMS320E14 Users Guide, Texas Instruments, 1988.

[5] TMS320C14/TMS320E14 DSP Microcontroller Product Bulletin, Texas Instruments, 1988.

[6] TPU MC68300 Embedded Control Family Reference Manual, Motorola, 1989.

[7] MC68332 SIM Users Manual, Motorola, 1989.

[8] SIM MC68332 Manual, Motorola, 1989.

[9] QSM MC68300 Manual, Motorola, 1989.

[10] CPU Reference Manual, Motorola, 1989.

[11] Microcontroller SAB80C166 User's Manual, Seimens, 1990.

[12] "On the Road Towards High Performance", Drives and Control, March 1993.

[13] Karsten P, "16-bit Controller Core 'Minimum' Design", Electronic Project Design, September 1991.

[14] Product Information - SAB80C166, Seimens, 1990.

[15] Data Sheet - SAB80C166, Siemens, 1990.

[16] Beasant R.R, Beatie W.C and Refsum A, "An Approach to the Realisation of a High Power Venturini Converter ", IEEE, April 1990, pp.291-297.

[17] Huber L, Borojevic D and Buràny N, "Analysis, Design and Implementation of the Space Vector Modulator for Forced Commutated Cycloconverters", IEE Proceedings, Part B, 1992, pp.

Chapter 4

# Switching Devices and Gate Drivers

## 4.1 Introduction

This Chapter considers the implementation of the practical bi-directional switch required for the implementation of a matrix converter. The choice of controllable switching device is considered in the light of recent semiconductor developments. The construction of a switch from discrete components is described and an optimum design within the limits of present technology suggested.

The ratings for the devices used in the construction of the converter are calculated. Data for the device ratings is given for a range of converter sizes and the method of calculation is shown. The building of the hardware required to drive the chosen switching device is explained. Minimisation techniques for this hardware are reviewed and the optimum solution is presented.

The building of a general purpose gate driver for voltage controlled devices is described in detail. Practical results for device characteristics for IGBTs using this gate driver are given.

## 4.2 The Choice of Switching Device

Any switching frequency converter requires the use of some form of controllable or semi-controllable switching devices. Recent years have seen a rapid increase in the use and performance of semiconductor switching devices, particularly the use of silicon based technologies. These technological advances have opened the door to solutions that could not have been implemented fifteen years ago [1]. This section will take a brief look at present switching device technologies and consider their suitability for use in matrix converters.

### 4.2.1 Thyristors

This was the first and most rugged of the semiconductor power switching devices. It has a four layer npnp structure. The device is turned on by a current pulse to the gate. Once on the device will remain latched on until the current carried by the device falls to zero. Thyristors are capable of very high current and voltage

carrying capabilities, with devices available with ratings of 6000Volts and 3500Amps.

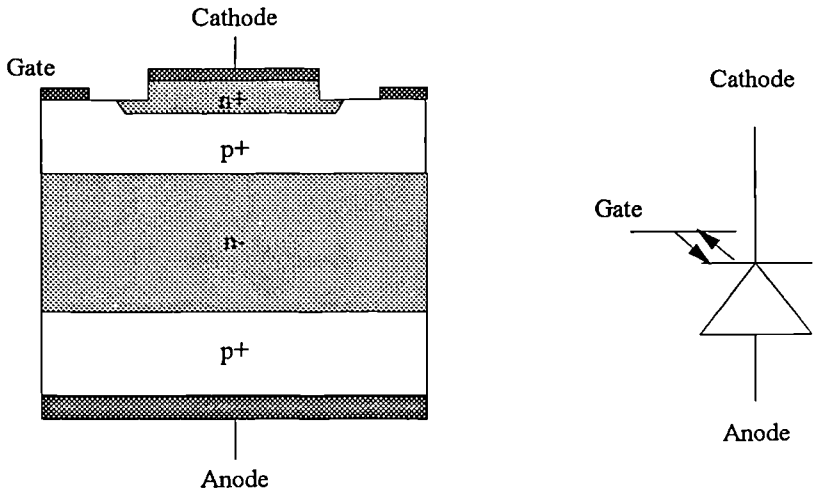


**Figure 4.1. The Element Structure and Circuit Symbol for a GTO Thyristor**

If two thysistor structures are connected in inverse parallel then a triac is formed. This is a bi-directional device, but suffers from the same lack of turn off control as the thyristor.

### 4.2.2 Gate Turn-off Thyristors

The GTO is used in many high power applications due to thyristor-like current carrying capacity. The device offers low on-state losses, a high voltage blocking capability and full gate control [4]. The device is manufactured as an array of cathode elements to permit good gate access to the conducting regions to facilitate the turn-off process. Unbalanced current sharing during turn off due to variations in characteristics across the device can lead to high local dissipation. For this reason a GTO must have a snubber circuit to restrict the rate of rise of the anode voltage. This snubber arrangement causes high switching losses and hence the GTO can only be used at low switching frequencies. The structure and circuit symbol for the GTO are shown in figure 4.1.

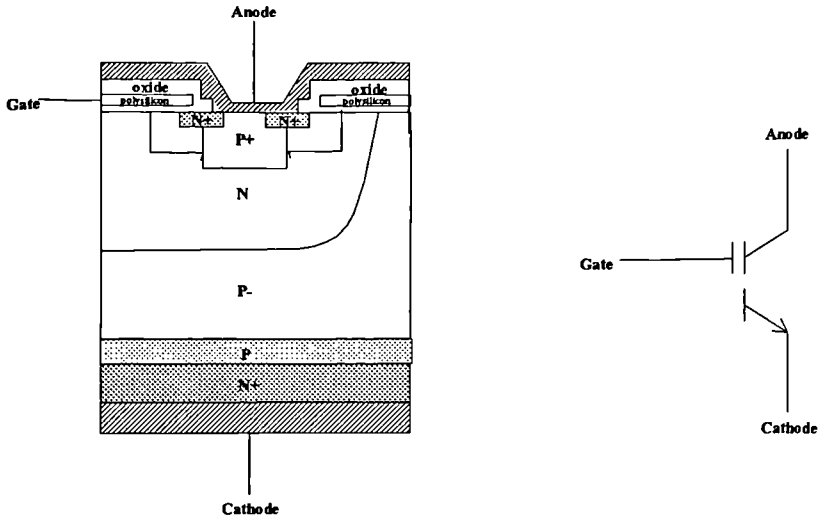


**Figure 4.2. The Structure and Circuit Symbol for an MCT**

### 4.2.3 Mos Controlled Thyristors

The MCT is a thyristor type device that can be triggered on or off by a short pulse on the MOS gate. It is comparable to the IGBT in switching speed, but has a lower forward voltage drop leading to lower conduction losses. The devices have high peak current carrying capabilities and very high dv/dt and di/dt ratings, typically about 5000V/μs and 1000A/μs [6]. They may be suitable for use in resonant converters, which have zero current switching. The MCT will be available on a large scale commercial basis in the near future. The first devices will be available with ratings of 1000Volts and 30Amps.

### 4.2.4 Static Induction Transistors

The structure of this device was first proposed as far back as 1950. Developments in the fabrication of silicon devices allowed the practical manufacture of these devices. The SIT is a normally on device and this may cause protection problems under gate driver fault conditions. The SIT requires a higher gate drive potential than MOS gate voltage controlled devices.

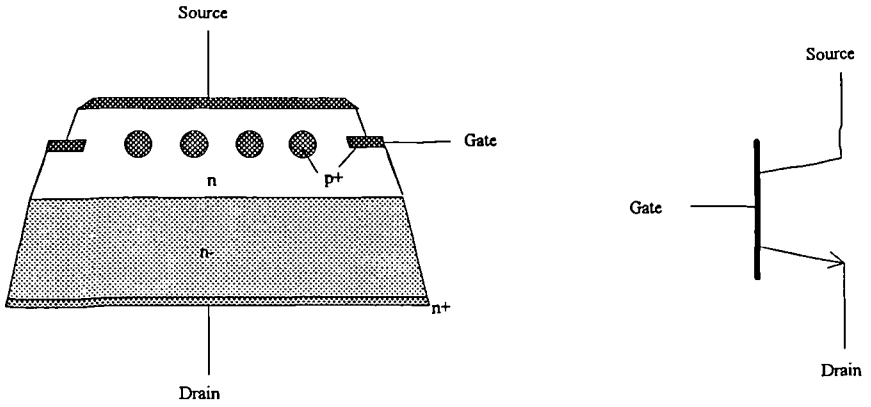


**Figure 4.3. Structure and Circuit Symbol of a SIT**

Since the SIT is a majority carrier device, conduction losses are higher than in IGBTs and other conductivity modulated devices, although the switching times are lower. This restriction makes the SIT unsuitable for general purpose power electronics. The SIT has however been used in Japan for induction heaters and uninterruptable power supplies [5].

### 4.2.5 Bipolar Junction Transistors

The BJT is a current controlled three layer device. It is faster than a thyristor type of device and has high current carrying capabilities, with devices available with ratings of 1200Volts and 800Amps. The device suffers from a characteristic second junction breakdown problem. The switching frequency of BJTs is restricted by the switching delays and the switching losses that are considerably greater than in an MOS type device. The advantages of the voltage controlled MOS style devices have led to them replacing BJTs in many power applications

### 4.2.6 MOSFETs

The power MOSFET is the fastest of all the currently available switching devices. This device is capable of operating at MHz switching frequencies. The MOSFET is a voltage controlled device that requires a high pulse of current to charge the gate capacitance at turn on.

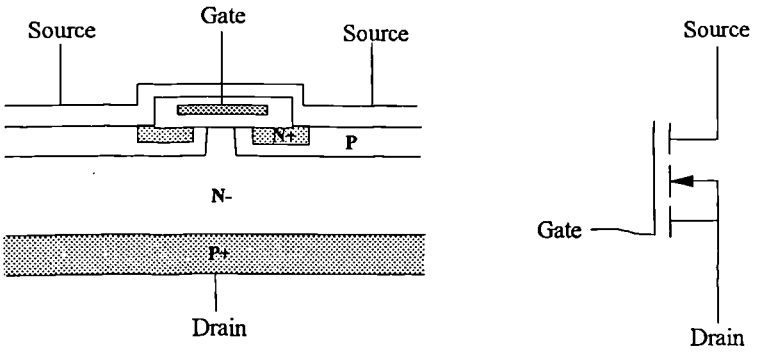


**Figure 4.4. Structure and Circuit Symbol for a MOSFET**

The switching losses in a MOSFET are low due to the fact that it is a majority carrier device and that the switching times are therefore short. The MOSFET does suffer from high conduction losses due to a relatively high, temperature dependent on-resistance. There is a parasitic parallel diode present in the device structure. It would be possible to utilise this diode in some applications but it is unfortunately relatively slow. The structure and circuit symbol for the power MOSFET are shown in figure 4.4. MOSFETs are available with power ratings up to 600Volts and 50Amps.

### 4.2.7 Isolated Gate Bipolar Transistors

An IGBT is a hybrid MOS gated BJT [7]. The device combines the attributes of MOSFETs and BJTs. The device has BJT conduction characteristics and the general drive characteristics of a MOSFET. An IGBT has good forward voltage blocking capabilities and is a normally off device. Devices are available with ratings of 1200Volts and 400Amps. The impurity concentration in the $p^+$ of the device must be carefully controlled to prevent the thyristor structure of the device from latching. The IGBT can tolerate higher current densities than MOSFETs and is rapidly replacing both MOSFETs and BJTs in high power, mid-frequency applications. The characteristics of the IGBT make it a very suitable active device for use in switching power converters such as the matrix converter. The structure and circuit symbol for the IGBT are shown in figure 4.5.

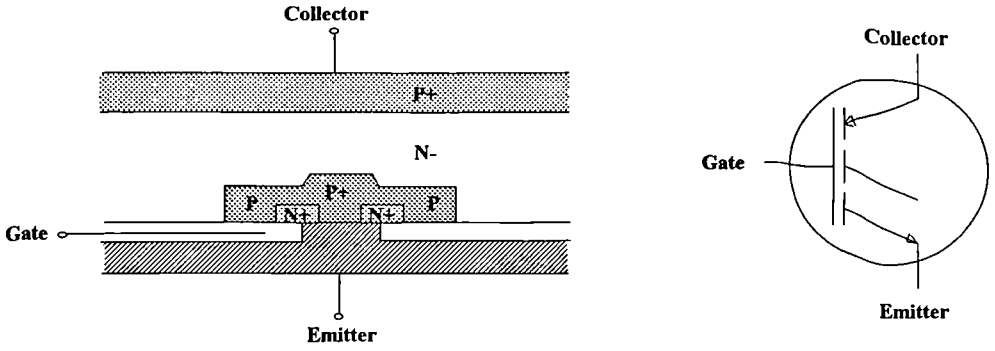


**Figure 4.5. Structure and Circuit Symbol for an IGBT**

### 4.2.8 The Future

The prospect of power devices based on Gallium Arsenide technologies in the near future may represent a major breakthrough in semiconductor technology [8]. These devices could have a greatly reduced forward voltage drop that will dramatically decrease conduction and switching losses.

A fully controllable bi-directional, high power switching device of suitable characteristics for use in switching power converters is not yet available in a practical form. This type of device is presently only available in the form of a photo-electric device [9]. In these devices a laser is used to illuminate a piece of silicon when conduction is required.

## 4.3 Bi-Direction Switch Configurations

The practical realisation of a Matrix Converter requires the use of a bi-directional switch. Until device technology progresses to the point where such a device is practical this bi-directional switch must be fabricated using discrete components [10]. There are three possible configurations for the arrangement of the semiconductor components to implement this switch:

- Diode Bridge
- Back-to-back IGBT with common collectors
- Back-to-back IGBT with common emitters

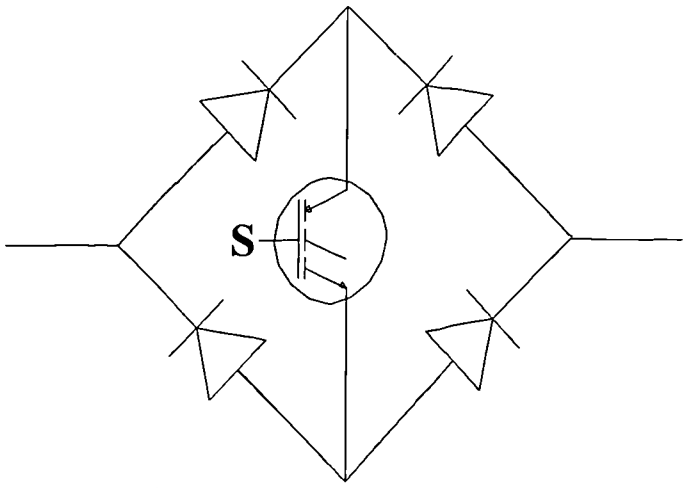


**Figure 4.6. Diode Bridge Bi-directional Switch Configuration**

### 4.3.1 The Diode Bridge Bi-Directional Switch

A switching device may be placed across a diode bridge to create a bi-directional switch, as shown in figure 4.6. This style of bi-directional switch has the advantage of only requiring one controllable device and associated gate driver circuit [11]. The main disadvantage of the diode bridge arrangement is that three devices are conducting at any given time giving rise to relatively high conduction losses. The switch would not be able to control the direction in which the current can flow. The high component count and large conduction losses may lead to a large and inefficient converter.

### 4.3.2 The Back-to-back IGBT Switch in Common Emitter Mode

Figure 4.7 shows a back-to-back IGBT arrangement for the bi-directional switch [12]. The diodes in series with each IGBT are for reverse voltage blocking. These diodes are required because IGBTs have no reverse voltage blocking capabilities. The connection between the emitters of the IGBTs is not required for the operation of the switch, but does improve the transient characteristics. The back-to-back arrangement has the advantage of a lower overall component count than the diode bridge arrangement, as shown in table 4.1.

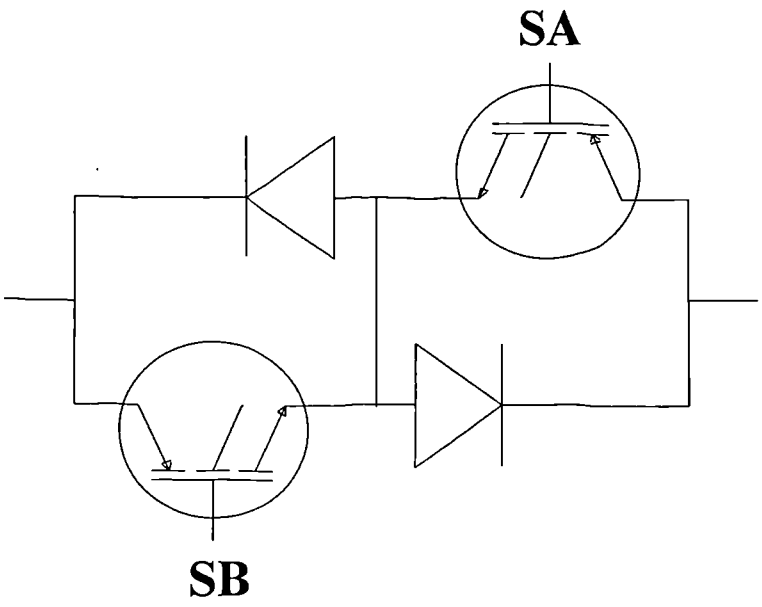


**Figure 4.7. Back-to-back IGBT in a Common Emitter Configuration**

In the back-to-back IGBT switch only two devices are conducting at any given time. Lower device conduction losses than in the diode bridge arrangement will therefore be achieved. The direction in which the current may flow in the back-to-back switch can also be controlled by independent control of the IGBT gates. This current direction control can be used to ensure the safe commutation of the current path between switches. This current commutation method will be considered in chapter 8. The connection of the devices in common emitter mode means that only one isolated gate drive could operate both devices in the switch. The subject of gate drives will be considered more fully later in section 4.6.

### 4.3.3 The Back-to-back IGBT Switch in Common Collector Mode

An alternative to the common emitter connection of the IGBTs is to connect the devices in a common collector configuration, as shown in figure 4.8. This switch configuration has all the advantages of the common emitter configuration, except that the emitter of each device will be connected to either an input or an output line of the converter.

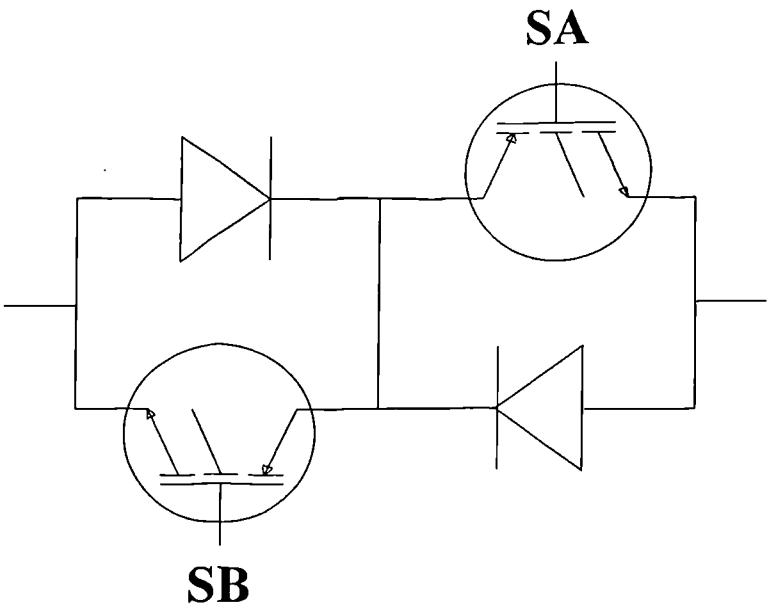


**Figure 4.8. Back-to-back IGBT in a Common Collector Configuration**

A matrix converter could be built with a separate heat sink for each bi-directional switch. Each switch can be implemented using discrete devices. If the connections for the back-to-back switch were to be made in common collector mode, then the need for device isolation from the heat sink would be removed. This situation occurs because the collector of an IGBT is usually connected to the tab in TO220 and TO3P packages. The cathodes of the diodes are also electrically common to the collectors of the IGBTs. The cathode of a discrete diode is also usually connected to the device's tab. This configuration would therefore reduce the wiring complexity and lead to lower thermal resistances between the devices and the heat sinks. The layout of this circuit on an individual switch heat-sink is shown in figure 4.9.

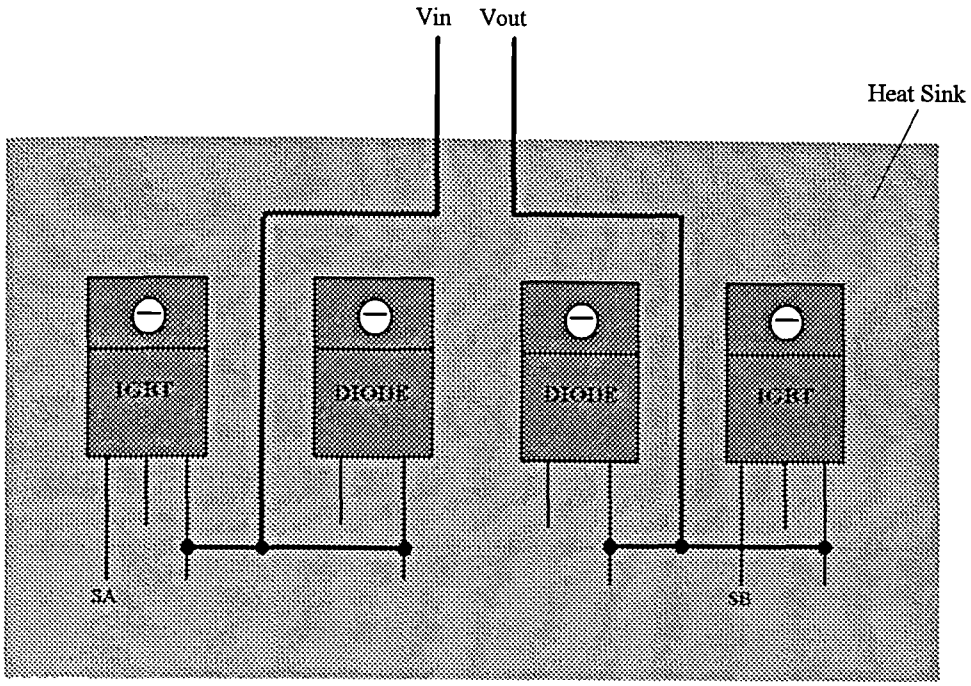


**Figure 4.9. Circuit Layout for a Back-to-back IGBT Bi-Directional Switch Arrangement Built on an Individual Heat Sink**

### 4.3.4 A Comparison of Comparative Circuit Semiconductor Costs

Table 4.1 gives a comparison of the number of semiconductor and passive devices required to implement a matrix converter with a diode bridge or a back-to-back IGBT bi-directional switch. The table also includes the component count for a rectifier/inverter circuit and an inverter with a controlled input bridge.

The diode bridge switch would give a matrix converter a high component count. The back-to-back configurations would require fewer components, but would require more IGBTs. The cost of controllable devices is greater than the cost of diodes, and hence the lower component count may not lead to the lowest semiconductor costs.

| | MATRIX CONVERTER | | INVERTER | |
|---|---|---|---|---|
| **DEVICE** | **Diode Bridge** | **Back-to-back** | **Diode Rectifier** | **Controlled Bridge** |
| **Diodes** | 36 | 18 | 12 | 12 |
| **IGBTs** | 9 | 18 | 6 | 12 |
| **Large Reactive Components** | 0 | 0 | 1 | 1 |
| **Semiconductor Device Count** | 45 | 36 | 18 | 24 |

**Table 4.1: Device Count for the Switch Configurations**

It should be noted that a matrix converter constructed with switches implemented in the diode bridge configuration would require fewer IGBTs than a controlled rectifier/inverter circuit. The controlled rectifier approach still requires a large dc link capacitor as well as inductors in the input lines [13]. The cost of this circuit may prove to be higher than the matrix converter, making the matrix converter attractive when sinusoidal input currents are required.

## 4.4 Device Ratings for Matrix Converters

The calculation of ratings for the discrete devices in the matrix converter switch is presented in this section. The maximum instantaneous current flowing in any given device for a given motor power rating is calculated. The maximum instantaneous voltage across any given transistor or diode is also considered.

An ideal matrix converter under steady state conditions has been assumed. The effects of unbalanced input voltages, starting currents, overload conditions, current commutation problems, device losses and harmonic distortion have been ignored.

### 4.4.1 Device Current Ratings

The power taken from the supply to the motor can be calculated as follows:

$$P = \sqrt{3}.V_L.I_p.\cos(\varphi) \tag{4.1}$$

By rearranging an equation for the phase current, $I_{p,}$ can be derived:

$$I_{p,rms} = \frac{P}{\sqrt{3}.V_{L,rms}.\cos(\varphi)} \tag{4.2}$$

For a matrix converter the maximum possible output line voltage can be calculated for an input voltage of 415Volts as shown in equation 4.3:

$$\begin{aligned} V_{L,rms} &= \frac{\sqrt{3}}{2}.V_{i,rms} \\ &= \frac{\sqrt{3}}{2}.415 \\ &= 360\text{Volts} \end{aligned} \tag{4.3}$$

Therefore, by substituting in equation 4.3 into equation 4.4:

$$I_{p,rms} = \frac{0.0016.P}{\cos(\varphi)} \tag{4.4}$$

The instantaneous maximum current passing through a given device in an ideal matrix converter is then the peak value of this current:

$$I_{d,\max} = \frac{0.00160.\sqrt{2}.P}{\cos(\varphi)} = \frac{0.00225.P}{\cos(\varphi)} \tag{4.5}$$

### 4.4.2 Device Voltage Ratings

The maximum peak voltage seen across any given device in the converter, $V_{d,max}$, is the maximum voltage between two lines of the three phase input voltages:

$$V_{d,\max} = 240.\sqrt{2}.\left[\cos(\omega t) - \cos(\omega t + \tfrac{2\pi}{3})\right]_{\max} \tag{4.6}$$

This maximum value may be calculated as shown in section 2.2.1.

$$V_{d,\max} = 240.\sqrt{2}.\sqrt{3} = 588\text{Volts} \tag{4.7}$$

### 4.4.3 The Semiconductor Device Ratings

For a matrix converter operating from a 415Volt three phase supply the required voltage rating of the switching devices is 588Volts. Assume the converter is connected to a motor or similar load with a power factor of 0.87. The required current rating for the switching devices is then 2.6Amps for every 1kWatt of rated output power using equation 4.5.

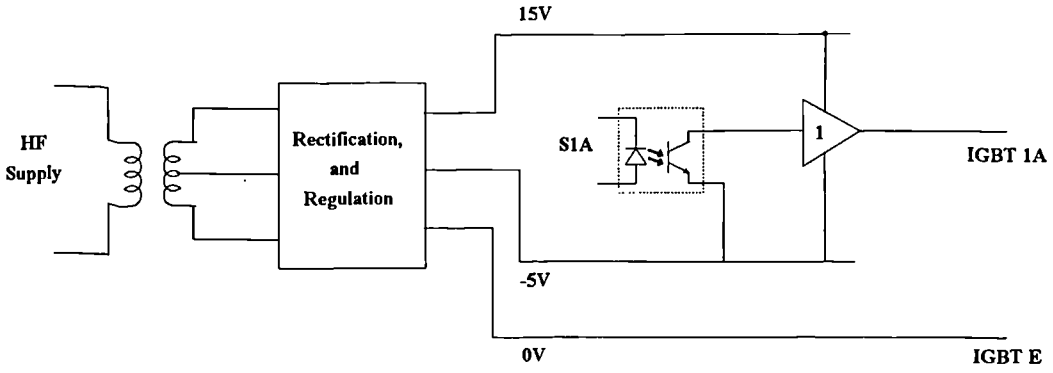


**Figure 4.10. Circuit Diagram of a Gate Drive Circuit with an Individual Isolated Power Supply**

A matrix converter designed to drive a 5kW motor would therefore require IGBTs and diodes rated to take a maximum pulsed current of 13Amps. The diodes would require a minimum reverse bias voltage blocking capability of 600Volts. The IGBTs would also be required to have a minimum forward voltage blocking capability of 600Volts.

## 4.5 The Requirement for Isolated Gate Drive Power Supplies

To switch each IGBT in the converter a voltage must be applied between the gate and the emitter of the device. Each device in the converter is floating on an input line, an output line or a connecting line. Each switching device would therefore require a gate drive circuit with an isolated power supply and an isolated control signal. Every control signal would require an independent optical link to the gate drive circuit.

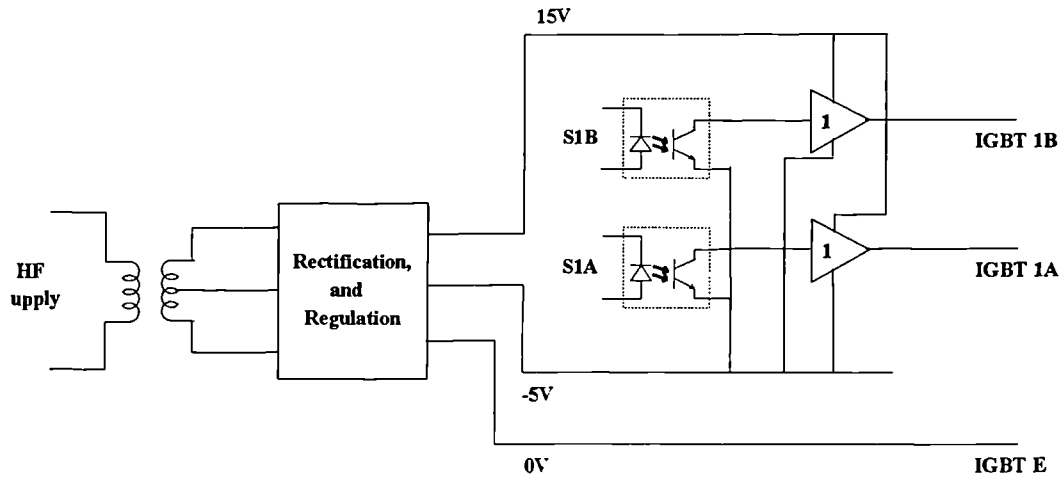


**Figure 4.11. Gate Drive Circuit for Independent Control of a Common Emitter Back-to-back Switch**

This section considers the number of isolated supplies required for the devices in the converter. Ideas on how the devices may be grouped to reduce the number of independent gate drive power supplies are discussed.

### 4.5.1 One Gate Drive Supply for Each Device

The simplest method of driving the devices is to use one independent gate drive circuit for each device in the converter. Each gate drive circuit would have to have an independent isolated power supply. The number of independent gate drive power supplies required would then be the number of controllable devices in the converter. If the back-to-back configuration was used then the converter would require eighteen independent supplies. Construction of the switches in the diode bridge form would require nine isolated supplies. Each gate drive circuit would take the form shown in figure 4.10. If a back-to-back switch configuration is used then the required number of isolated power supplies for the gate drive circuits may be reduced.

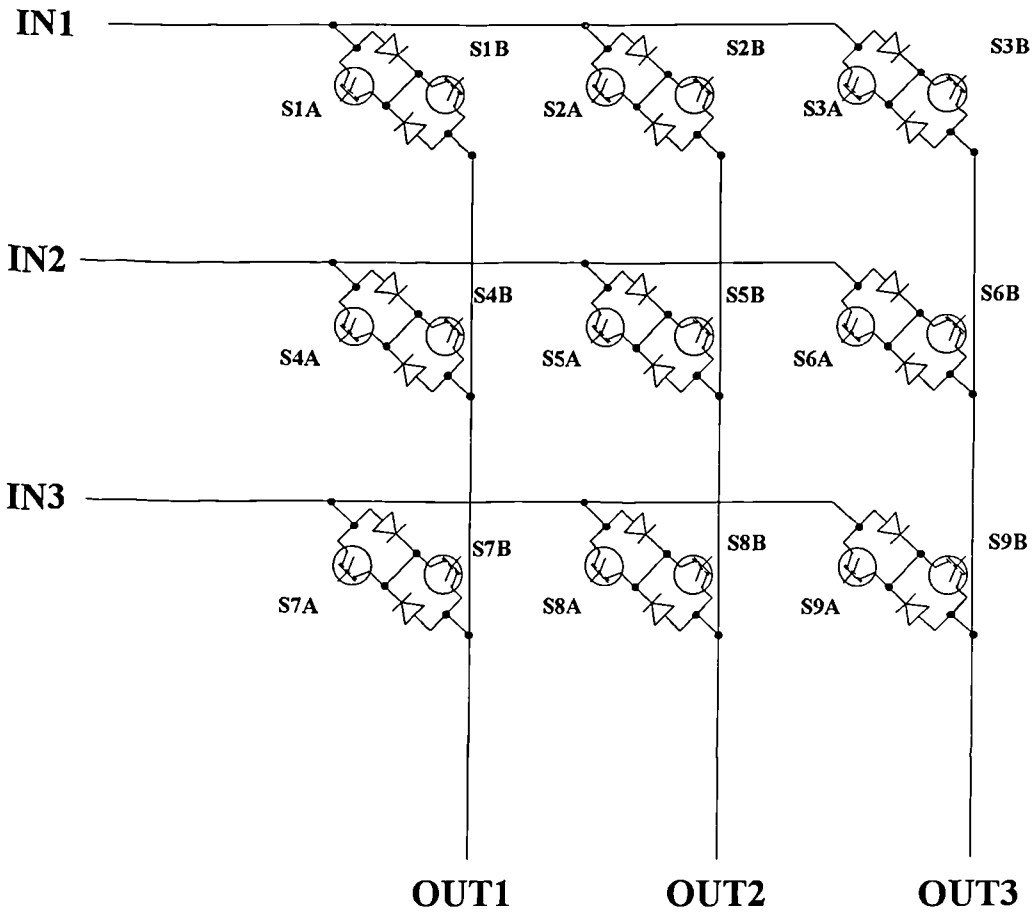


**Figure 4.12. The Switch Matrix Layout for a Complete Converter Using Back-to-back IGBT Switches in Common Collector Mode**

### 4.5.2 The Number of Isolated Gate Drive Supplies Required for a Back-to-Back Switch in Common Emitter Mode

The common emitter configuration of the bi-directional switch would allow the same isolated gate drive supply to be used in the driving of both devices. This is possible because each device requires a gate voltage with reference to the emitter voltage. The connection between the emitters allows the sharing of the isolated power supply. If independent control of the two devices in the switch is not required then the circuit shown in figure 4.10 may simply be connected to both devices.

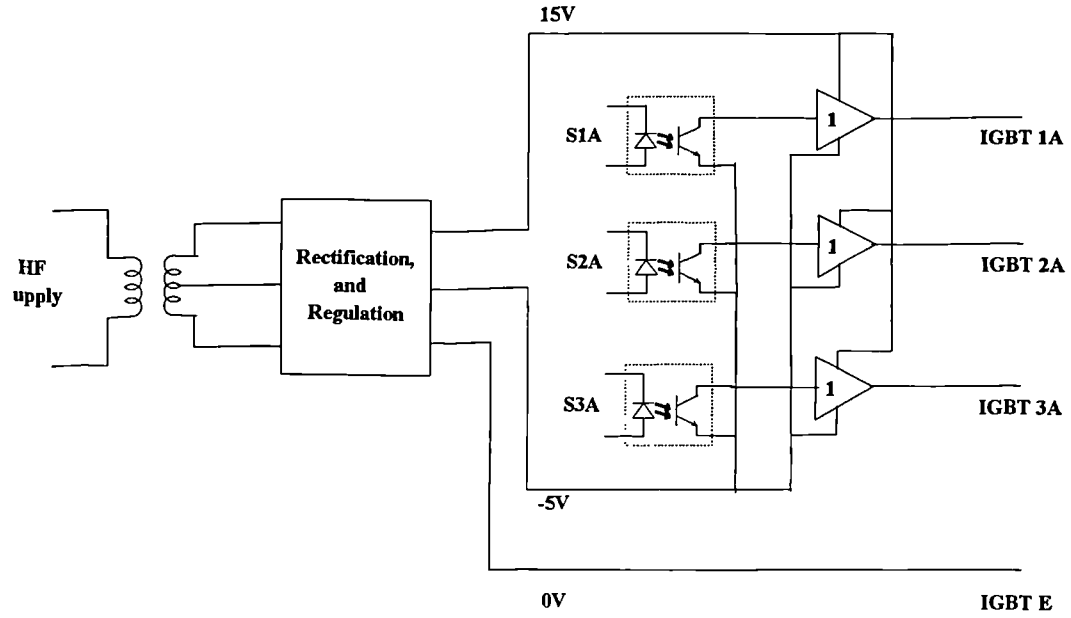


**Figure 4.13. Gate Drive Circuit a Common Collector Back-to-back Switch**

If the independent control of each device is required for current commutation then a circuit of the form shown in figure 4.11 may be used. The notation used for the control signals refers to the devices as shown in figure 4.12. This style of gate drive circuit would reduce the required number of isolated supplies to nine, whilst maintaining the ability to control the direction in which the current may flow in the switch.

### 4.5.3 The Number of Isolated Gate Drive Supplies required for a Back-to-back Switch in Common Collector Mode

The back-to-back switch may be connected in common collector mode, as described in section 4.3.3. In common collector mode the emitters of every device would be connected to either a converter input or an output line. The devices can then be grouped in sets of three with common emitters.. These sets are shown in table 4.2. The labelling of the devices refers to the labels in figure 4.11.

| Group | Switches |
|---|---|
| 1 | S1A, S2A, S3A. |
| 2 | S4A, S5A, S6A. |
| 3 | S7A, S8A, S9A. |
| 4 | S1B, S4B, S7B. |
| 5 | S2B, S5B, S8B. |
| 6 | S3B, S6B, S9B. |

**Table 4.2. IGBT Groups for a Common Collector Back-to-back Switch**

Each group of IGBTs will require only one isolated power supply for its gate drivers. A circuit such as the one described by figure 4.13 may then be used. This simplification reduces, to six, the number of isolated supplies required by a matrix converter.

A standard rectifier/inverter circuit would require only three high side gate drives. A controlled rectifier/inverter circuit would, however, require six isolated high side gate drives. The matrix converter therefore has no disadvantage in comparison to the back-to-back converter in terms of the IGBT gate driver requirements, even when switch is implemented in a back-to-back configuration.

## 4.6 The Gate Drive Circuit

This section records the design, building and performance of an isolated gate drive circuit suitable for operating IGBTs at high switching frequencies. A minimal design has been implemented to reduce the size and complexity of the driver. The driver has been tested at a high dV/dt to ensure correct operation in adverse conditions.

The gate drive has been designed for general use in driving floating IGBTs. Some compromises in the design have been made so that the gate drive is suitable for other applications besides the matrix converter.

### 4.6.1 The Operating Conditions

The gate drive is required to operate in switching power devices for a range of variable speed controllers for AC motors. These circuits may require the circuit to be able to withstand high values of dV/dt with rapid repetition rates. The driver will have the ability to operate in an electrically noisy environment. Some types of converter, such as the matrix converter, will require a large number of gate drives, and so the circuit must be relatively cheap and easy to produce in small batches. For the purposes of control, silicon management and semiconductor losses, a low propagation delay of signals through the driver circuit is desirable. Control algorithms may also be easier to implement if the turn on and turn off propagation delays are approximately equal. The ability to control the rise and fall times of the gate signal may also be useful in some applications.

An IGBT typically has a maximum gate threshold voltage of about 5Volts, with a maximum required gate charge of about 20nC. The maximum permissible gate voltage for most devices is ±20Volts. The device requires the gate to be brought down to 0Volts on turn off. To prevent the device turning on under transient conditions the gate voltage may be pulled down to -5Volts .

Under short circuit fault conditions it is possible to detect a significant rise in the voltage $V_{ce}$. This voltage rise may then be used to turn the device off in a controlled manner. In such a fault condition it is better to lower the gate voltage to 0Volts and then to -5Volts rather than attempting to snap the device off too quickly by pulling the gate rapidly down to -5volts [14].

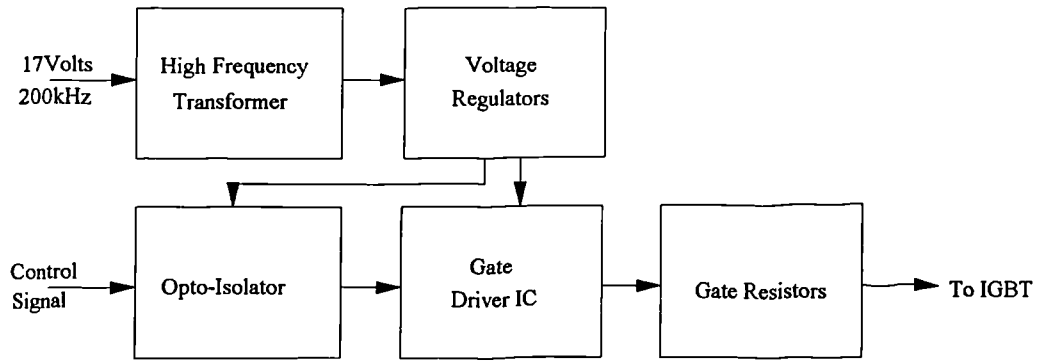


**Figure 4.14. Block Diagram of the Gate Driver**

### 4.6.2 The Circuit

Many simple circuits for driving IGBTs have been proposed [14], [15], [16]. For the purpose of this application a TSC429 driver was chosen to drive the gate of the device. The TSC429 is capable of a 6amp peak drive current and has a low output resistance [17]. This device has a maximum output voltage swing rating of 18Volts, and therefore a compromise gate voltage swing of -5Volts to +12Volts was chosen. The use of this component greatly simplifies the circuit, whilst maintaining performance. The control signal to the driver is received through an opto-isolator that incorporates a Faraday shield. The output from the opto isolator can then be used directly to drive the TSC429.

The gate driver board is powered from a high frequency isolation transformer. This transformer is small and the design allows a large number of boards to be powered from the same mains power supply. Two regulators are then used to control the rectified and smoothed voltage waveforms. The common connection for the circuit is connected to the centre tap on the high frequency transformer. The basic layout of the circuit is described in a block diagram in figure 4.14. The complete circuit diagram is shown in figure 4.15.

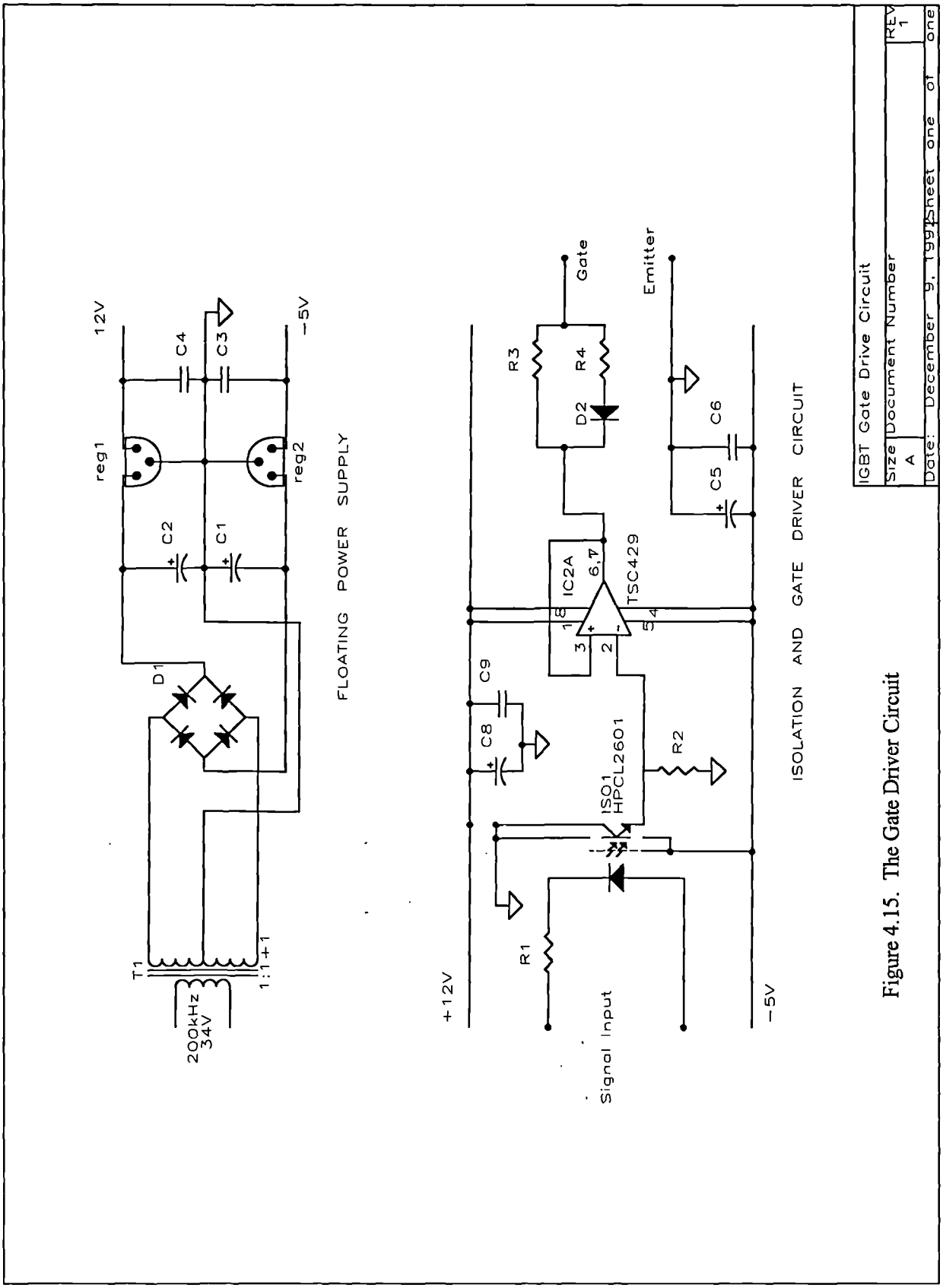


Figure 4.15. The Gate Driver Circuit

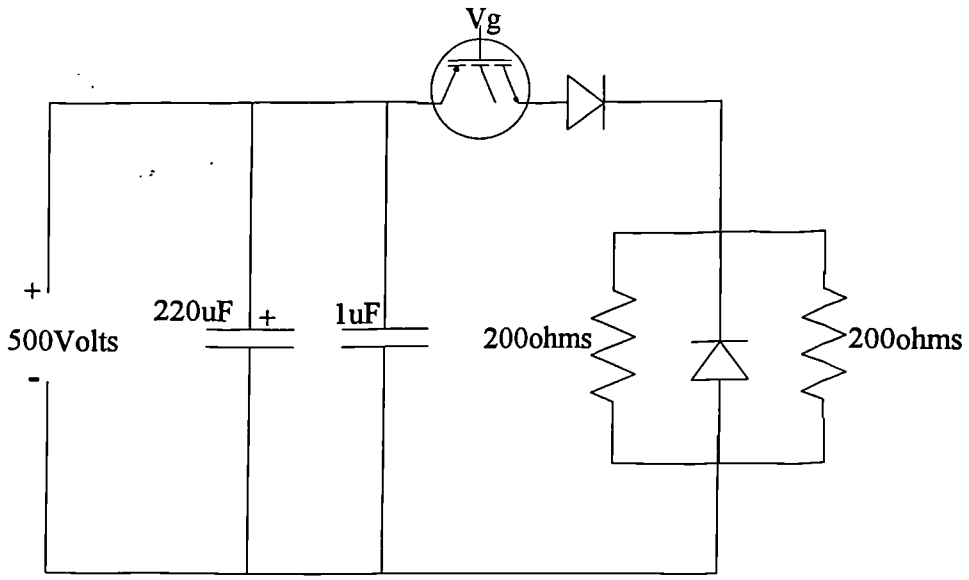


**Figure 4.16. The Test Circuit for the IGBT Gate Driver**

The gate drive is connected to the gate through a set of two resistors and a diode so that the turn on and turn off gate resistance may be varied independently. This will allow the independent shaping of both edges by the adjustment of the resistor values.

### 4.6.3 Testing the Gate Driver

The gate drive circuit was built on a small printed circuit board. A test circuit was built to test the operation of the gate drive under high values of dV/dt, as shown in figure 4.16. The board was tested using a 500Volt supply to generate a 5Amp pulse of 2μs, with a repetition rate of 5kHz and a clamped load. The propagation delays in the gate drive circuit were measured. The effect of using different values of gate resistance was examined and the propagation delay of the control signals was measured.

| | IRGBC20F Measured | IRGBC20F Data Sheet[1] | MG50Q2DS1 Measured | MG50Q2DS1 Data Sheet[1] |
|---|---|---|---|---|
| **Turn On Delay** | 25ns(180ns)[2] | 35ns | 350ns(500ns)[2] | 400ns |
| **Rise Time** | 30ns | 18ns | 320ns | 300ns |
| **Turn Off Delay** | 45ns(160ns)[2] | 90ns | 980ns(1100)[2] | 800ns |
| **Fall Time** | 210ns | 242ns | 180ns | 200ns |

**Table 4.3. Switching Delays for IGBTs Using the Designed Gate Driver**

### 4.6.4 Test Results

Figure 4.17 shows the effect of the gate drive turn-on resistance on the rise time of the load voltage. The damping of the waveforms and increased delays caused by adding more gate resistance should be noted. If the capacitance between the gate and the emitter of the device is increased then the switching times will also increase. The effect of this extra capacitance is shown in figure 4.18. Both these effects are seen because the gate drive must charge the gate capacitance before the device will be fully turned on. The higher the gate capacitance and resistance, the slower the turn on time for the device.

The propagation and state change for the delays for the gate drive driving a single IRGBC20F with 50Ω of gate resistance can be found from figure 4.18b. These delays are shown in table 4.3. The figures for the device from the manufacturer's data sheet, [18], are also included for comparison. The measured and supplied data for the Toshiba MG50Q2DS1 devices have also been included. The propagation delay of the control signals was measured. The turn on delay was found to be 155ns and the turn off delay was 115ns.

---

[1] Based on Manufacturer's Conditions

[2] Bracketed figures include the gate driver propagation delay as well as device propagation delay.

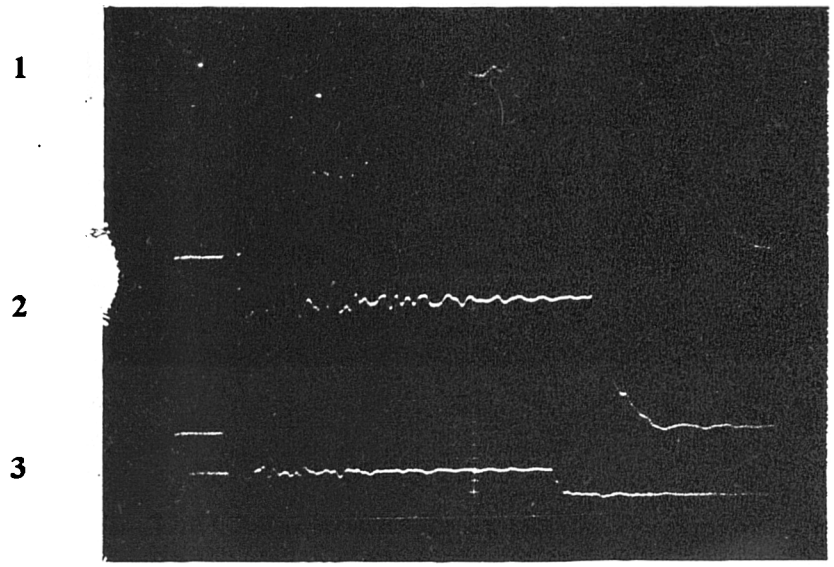


**200ns/div**

**Figure 4.17a. The Characteristics for an IRGBC20. $R_{g,on}$=0Ω, $R_{g,off}$=0Ω.**
1. Load Current, 1Amp/div. 2. Load Voltage, 200Volts/div. 3. Control Signal, 10Volts/div.

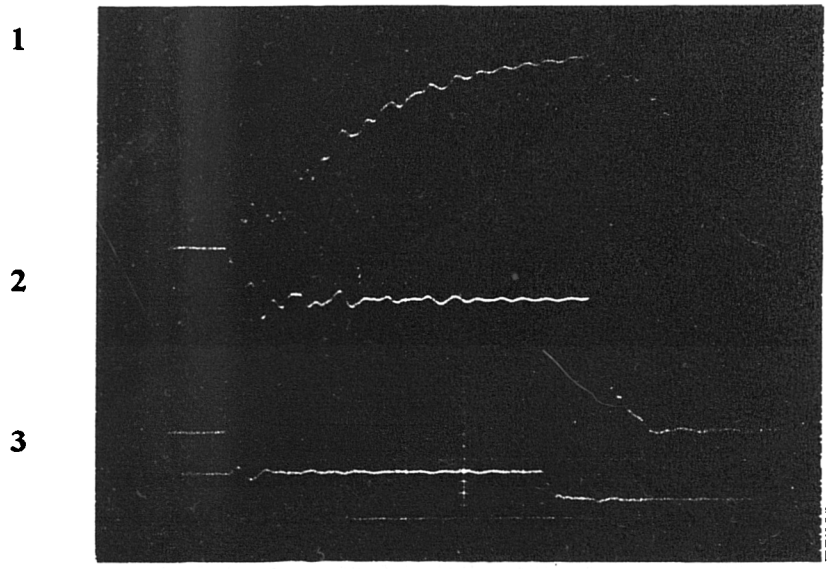


**200ns/div**

**Figure 4.17b. The Characteristics for an IRGBC20. $R_{g,on}$=33Ω, $R_{g,off}$=100Ω.**
1. Load Current, 1Amp/div. 2. Load Voltage, 200Volts/div. 3. Control Signal, 10Volts/div.

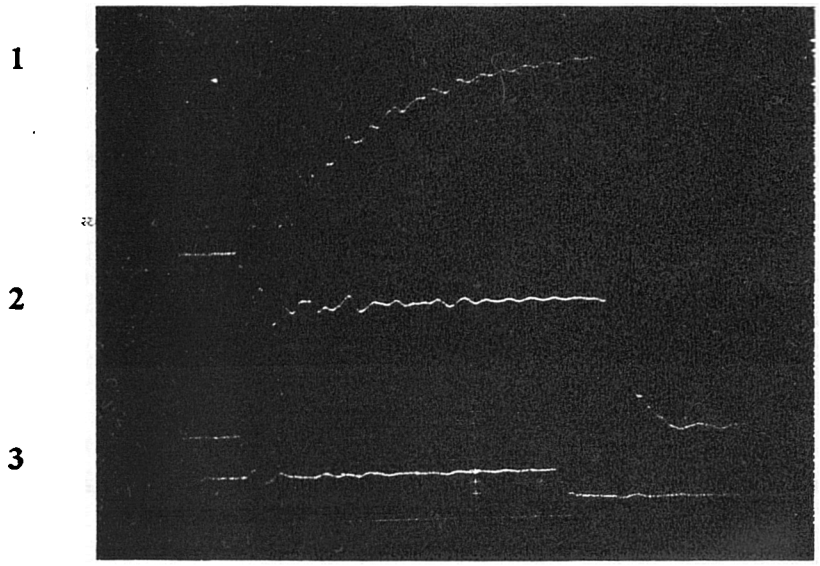


**Figure 4.17c. The Characteristics for an IRGBC20. $R_{g,on}$=100Ω, $R_{g,off}$=100Ω.**
1. Load Current, 1Amp/div. 2. Load Voltage, 200Volts/div. 3. Control Signal, 10Volts/div.

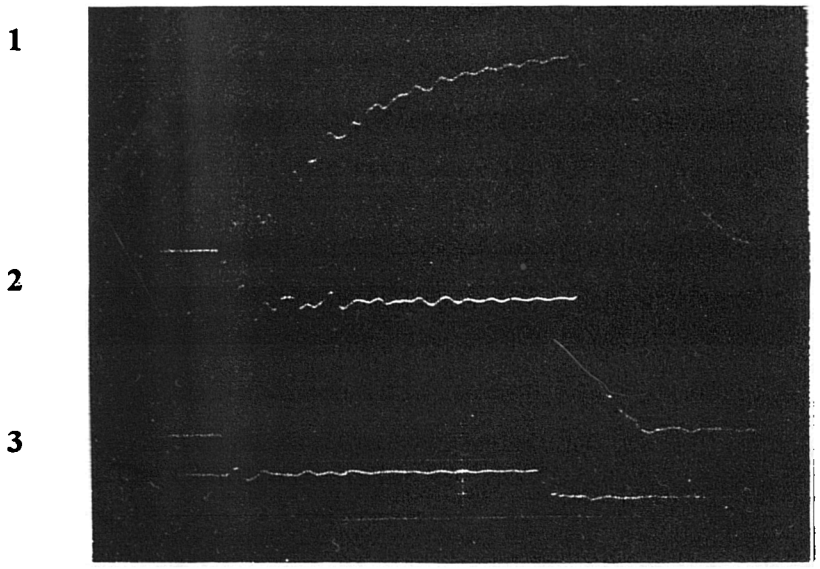


**Figure 4.18a. The Characteristics for An IRGBC20s. $R_{g,on}$=10Ω, $R_{g,off}$=100Ω**
1. Load Current, 1Amp/div. 2. Load Voltage, 200Volts/div. 3. Control Signal, 10Volts/div.

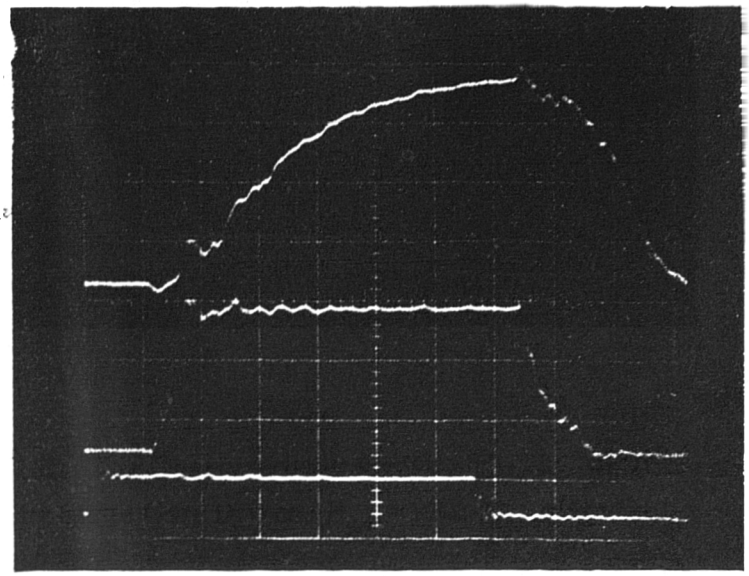


**Figure 4.18b. The Characteristics for Two IRGBC20s Driven by the Same Gate Driver. $R_{g,on}$=10Ω, $R_{g,off}$=100Ω.**
1. Load Current, 1Amp/div. 2. Load Voltage, 200Volts/div. 3. Control Signal, 10Volts/div.

### 4.6.5 The Construction of a Bi-Directional Switch for an Experimental Matrix Converter

For the building of a flexible experimental 5kWatt matrix converter, a self contained bidirectional switch unit has been designed and built. Each switch is built on a separate heat sink. The switch consists of a pair of back-to-back IGBTs in a common collector configuration, as shown in figure 4.8. No isolation is required between the devices and the heat sink because the collector of the IGBTs and the cathode of the diodes are common. Each switching device is driven by a dedicated gate driver circuit as described above. The matrix converter requires nine of these bi-directional switch units. Figure 4.19 shows a single bi-directional switch unit complete with two independent IGBT gate drivers and the device heat sink.

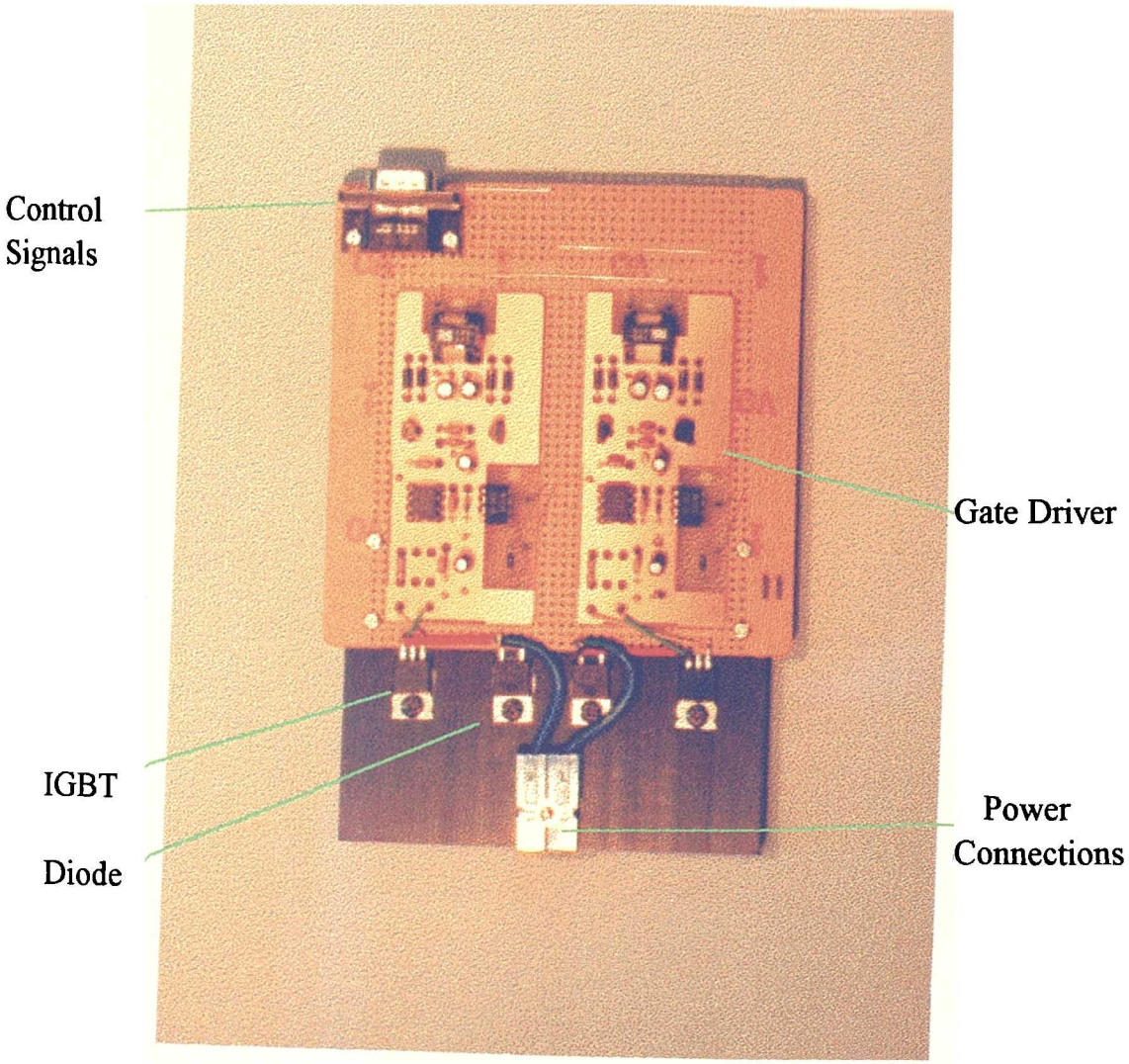


**Figure 4.19. A Bi-Directional Switch Unit with Independent IGBT Gate Drivers**

## 4.7 Conclusions

A brief overview of the state of the art semiconductor switching device technology has been presented. The IGBT has been chosen as the most suitable device for the implementation of a matrix converter at the present time. Consideration has been given to the configuration of these uni-directional switching devices to realise a practical bi-directional switch. The cost implications of the various bi-directional

switch configurations have been examined. The required device ratings for the discrete devices used in the realisation of the switch have been reviewed.

A simple, easily manufactured gate driver for prototype AC motor drives has been developed and tested. The circuit contains the minimum of components whilst maintaining high performance. It is capable of short and symmetrical propagation delays and high frequency switching. An experimental bi-directional switch unit has been built and tested using this gate driver.

# Bibliography


[1] Gjugyi L and Pelly B, "Static Power Frequency Changers", New York, Wiley, 1976.

[2] Bose B.K, "Recent Advances in Power Electronics", IEEE Transactions on Power Electronics, Vol. 7, No. 1, Jan. 1992, pp.2-17.

[3] SanRex, "Power Semiconductors Data Book 1992", Sansha Electric.

[4] Palmer P.R and Johnson C.M, "Measurement of the Redistribution of Current in GTO Thyristors During Turn-off", European Power Electronics Conference, 1989, pp.337-342.

[5] Nishizawa J et al, "Low Distortion, High Efficiency, Static Induction Transistor Type Sinusoidal PWM Inverter for Uninterruptable Power Supplies", IEEE IAS Conference Proceedings, 1986.

[6] "MCT75P60E1 Data Sheet", Harris Semiconductors, File No. 3374.1, Oct. 1992

[7] Baliga B.J, Chang M, Shafer P and Smith M.W, "The Insulated Gate Transistor: A New Power Switching Device", IEEE-IAS Conference Record, 1983, pp.794-803.

[8] Shenai K., Scott R.S. and Baliga B.J., "Optimum Semiconductors for High-Power Electronics", IEEE Transactions on Power Electronics, September 1989, pp.1811-1823.

[9] Evans G.A., Rosen A. and Stabile P.J., "Two- Dimensional Semiconductor Laser Arrays for Optically Activated Switches", Microwave Journal, Vol.35, Iss.10, Oct. 1992, pp.56-70.

[10] Lipo T.A., "Recent Progress in the Development of Solid State AC Motor Drives", IEEE Transactions on Power Electronics, Vol.3, No.2, 1998, pp.105-117.

[11] Beasant R.R., Beatie W.C. and Refsum A., "An Approach to the Realisation of a High Power Venturini Converter", IEEE, April 1990, pp.291-297.

[12] Holmes D.G. and Lipo T.A., "Implementation of a Controlled Rectifier Using AC-AC Matrix Converter Theory", IEEE Transactions on Power Electronics, Vol.7, No.1, 1992, pp.240-250.

[13] Control Techniques, "Drives and Servos Yearbook", Control Techniques plc., 1989.

[14] Bosterling W, "Non-Problematic Gate Drive of IGBT Modules", Power Conversion, April 1992, pp87-95.

[15] Edelmoser K.H et al., "Floating, Flexible and Intelligent Gate Driver Circuit for IGBT Modules", Power Conversion, April 1992, pp96-105.

[16] Smith G.A and Stevens R.G, "High Performance Drivers for IGBTs", IEE Colloquium on Active and Passive Components, Nov. 1992.

[17] "TSC429 High Speed Single CMOS Power MOSFET Driver, Data Sheet", Teledyne Semiconductors, 1985.

[18] "Toshiba GTR Module Data Book", Toshiba, 1990, Section III: IGBT Modules.

[19] Grant D.G. and Gower J., "Power MOSFETs: Theory and Applications", Wiley, 1989.

[20] "IRGBC20 IGBT Data Sheet", International Rectifiers, Data Sheet No. PD-9.626A.

# Chapter 5

# Current Commutation

## 5.1 Introduction

When controlling a matrix converter it is important to ensure that there are never any short circuits between the input lines. There must also be no uncontrolled open circuits of the output lines. If an output line was to become an open circuit it would cause voltage spikes due to the open circuiting of the motor winding. Controlling a converter with perfect switches would make avoiding these situations a relatively simple task. Safe operation with perfect switches can be achieved by ensuring that the three control signals relating to each output line have no overlaps or dead times.

When using semiconductor switches input short circuits or output open circuits may occur due to the finite switching times and propagation delays of the devices [1]. A possible effect of these delays is shown in figure 5.1. A momentary input short circuit or output open circuit may cause damage to the devices. A mechanism for preventing these situations from occurring must therefore be implemented.

This Chapter attempts to categorise and analyse existing current commutation methods. A new and more robust current commutation strategy is also proposed. This new strategy combines the advantages of the previous methods whilst reducing the effects of their disadvantages.

## 5.2 Possible Current Commutation Strategies

In the past, researchers have suggested ideas that overcome the current commutation problem by hiding it with capacitor and snubber circuits [2],[3]. Some papers have produced control methods to overcome the problem [4], [5], [6]. All these methods have significant drawbacks with the size of the required reactive components or susceptibility to failure due to non-ideal conditions. The proposed new semi-soft current commutation method reduces the probability of possible implementation problems, uses no reactive components and is simpler than some of the alternative methods.

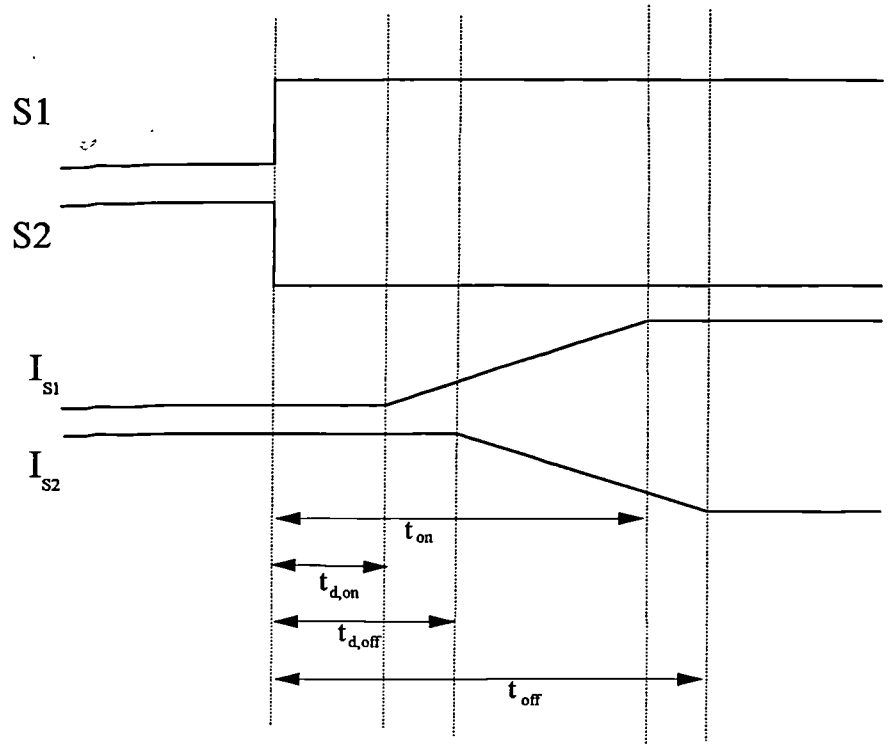


**Figure 5.1. The Control and Current Waveforms for a Transition in Current Path Between Switch 1 and Switch 2**

There are three basic current commutation strategies. Other strategies have been proposed, but they can be categorised as variations of these three.

- Dead Time.
- Overlap Time.
- Semi-Soft: a. Uni-Directional Current Flow.
  b. Bi-Directional Current Flow.

The term 'semi-soft' current commutation is introduced and defined later in this chapter.

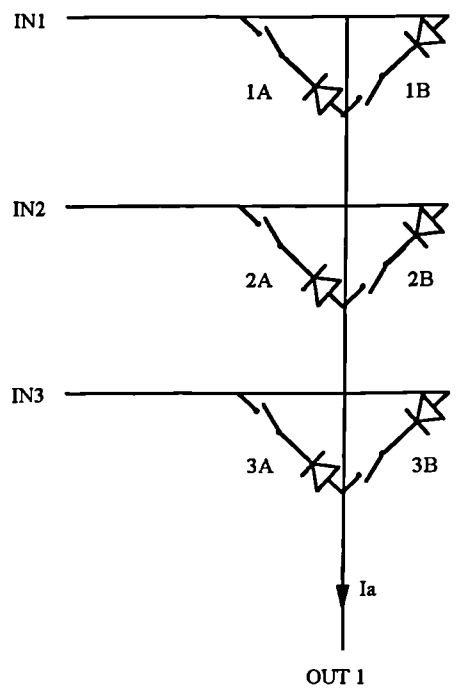


**Figure 5.2. The Bi-directional Switches for One Output Phase**

### 5.2.1 Dead Time Current Commutation

The simplest solution for preventing short circuits between input lines is to introduce dead times between the switching periods of each switch. This is the method used in standard inverter circuits [7]. The control waveforms for a current path change between switch 1 and switch 2 are shown in figure 5.3. The control waveforms for both halves of the semiconductor switch are identical. Any of the switch arrangements described in Chapter 4 can be used if this form of current control is used. The size of the dead times, $t_d$, may be altered to suit the characteristics of the devices used in the converter.

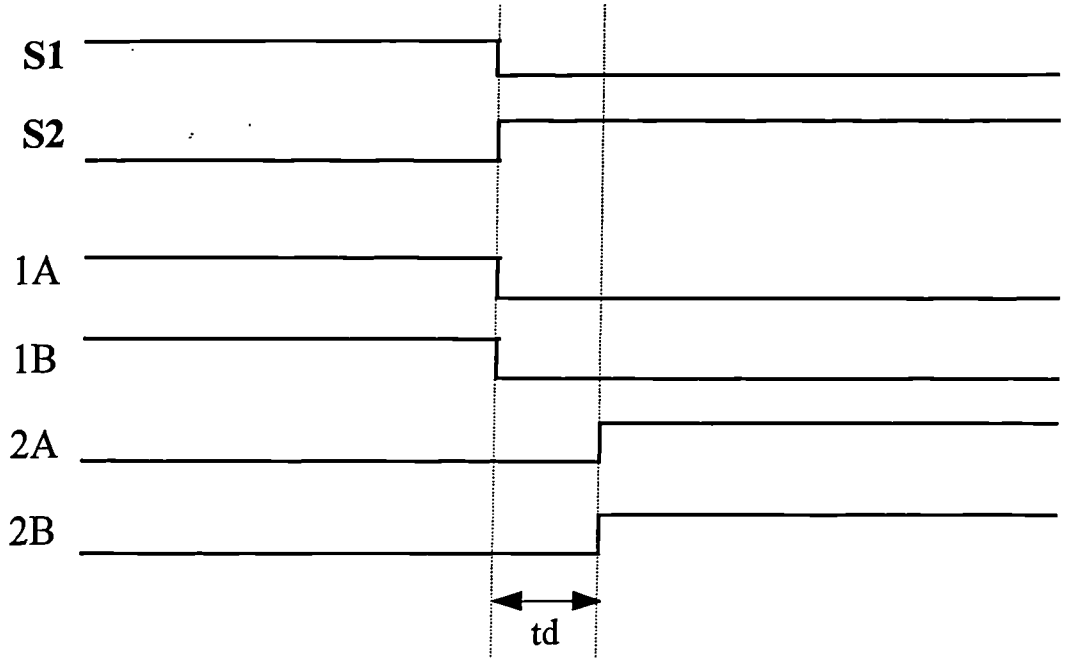


**Figure 5.3. Switch Control Waveforms for Dead Time Current Commutation**

If this method of current control is used then provision in the power circuit must be made to control the voltage spikes caused by the temporary open circuiting of the motor. This may take the form of a clamp circuit or a capacitor to limit the size of the spike.

The switch patterns for the current path hand-over between switches may be shown in the form of a state transition diagram. The state transition diagram for dead time operation is for one output phase in figure 5.4. The transitions between the states are caused by the control waveforms from the controller relating to the three switches for the given output phase. In more complex current commutation algorithms, the output current direction, Ia, is also a state transition variable. The binary numbers within each state refer to the state of each device in the converter. The notations for these state variables are defined in figure 5.4. The state transition diagrams for the other two output lines are identical, except that the control signals and current direction refer to the particular output phase.

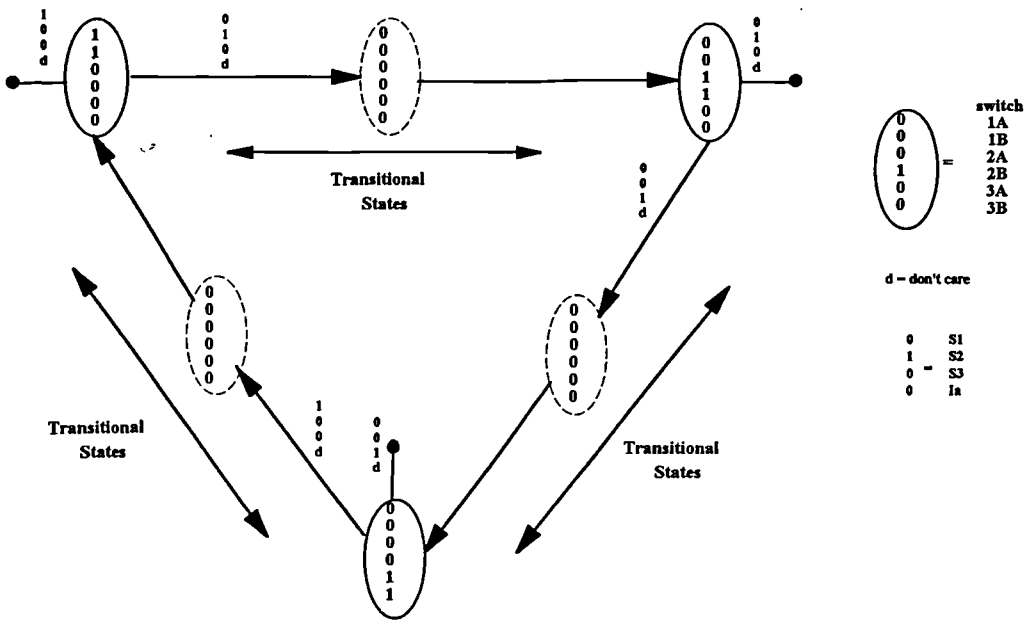


**Figure 5.4. State Transition Diagram for Dead Time Current Commutation**

### 5.2.2 Overlap Time Current Commutation

An alternative to dead time operation would be to introduce overlap times between switching periods [4]. This method would have the advantage of reduced switching losses and no open circuits on the output lines. This method of current commutation would require inductance in each of the input lines to minimise the short circuit currents between the input lines. These inductors would have to be relatively large and would produce higher converter losses. The state transition diagram for this switching period overlap scheme for one output phase is shown in figure 5.5.

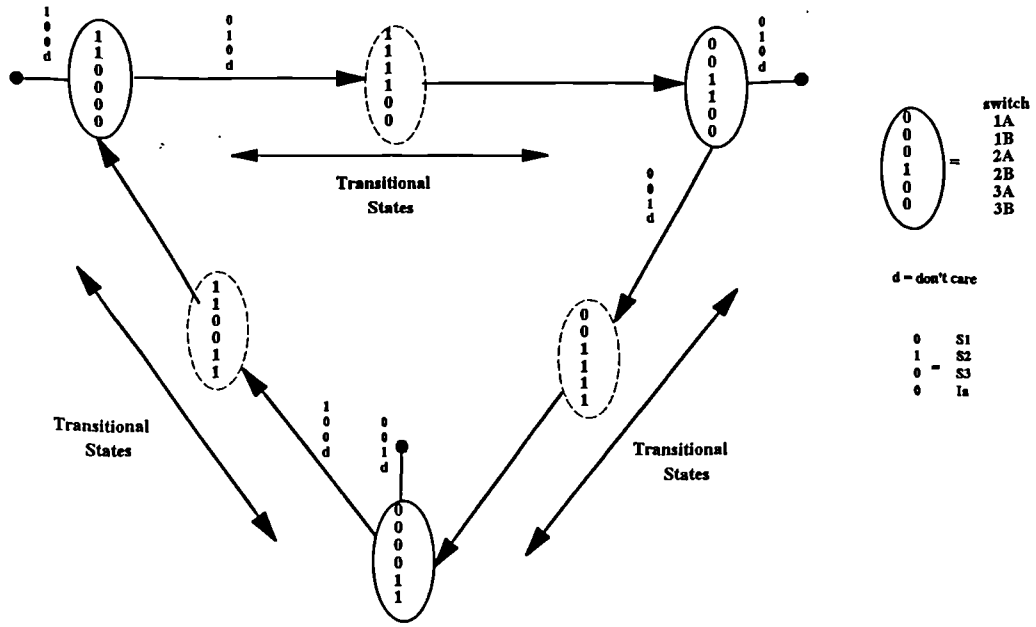


**Figure 5.5. State Transition Diagram for Overlap Time Current Commutation**

Overlap and dead time current commutation have the advantage that control of the current direction within each switch is not required. A switch implemented with just one controllable device could therefore be implemented, as shown in figure 4.6. This would reduce the number of gate driver circuits required. In the future a truly bi-directional controllable semiconductor switch may become available. Overlap or dead time operation of the converter switches would then become essential to take advantage of the circuit simplification the new technology may allow.

### 5.2.3 Semi-Soft Current Commutation With Uni-Directional Current Flow

A method of combining the advantages of both dead time and overlap time current commutation is to consider the direction of the output current at the time of switch state change. This current direction can then be used to pass the current between the switches in a controlled manner [5]. A switch implemented in such a way that the direction in which the current may flow is controllable is therefore required.

In this method, only the switch in the current carrying direction is closed. This allows the current conduction path to be passed between the switches with all the advantages of both overlap and dead time operation. There will be no short circuits between the input lines and no open circuits on the output lines. There will, however, be additional states to commutate the current between the two halves of the switch when the output current changes direction or is at a low level.

This method of current commutation has the disadvantage that the current direction must be detected correctly. Incorrect detection may occur due to factors such as electrical noise within the drive. At start-up and in low load situations the output current may be too small to guarantee correct current direction detection.

This method of current commutation therefore requires additional detection to establish when the current is entering the near zero zone. This extra information is used as part of the state changing variable and adds to the complexity of the state machine implementation. This method is shown for one output phase in the state diagram shown in figure 5.6.

The switch control signals could change state whilst the output current is in the near zero region. In this situation the state machine will wait until the current has a definite direction before allowing a change of switch state.

A variation on this would be to introduce extra states to the state machine so that the switch states can be changed in the near zero current region. These extra states could revert to dead time operation for this condition. The voltage spikes caused by the open circuiting of the motor would be smaller than at other times due to the low current flowing in the windings. This would produce a scheme of the type proposed in [6]. The state diagram for the state machine for this type of current commutation is shown in figure 5.7.

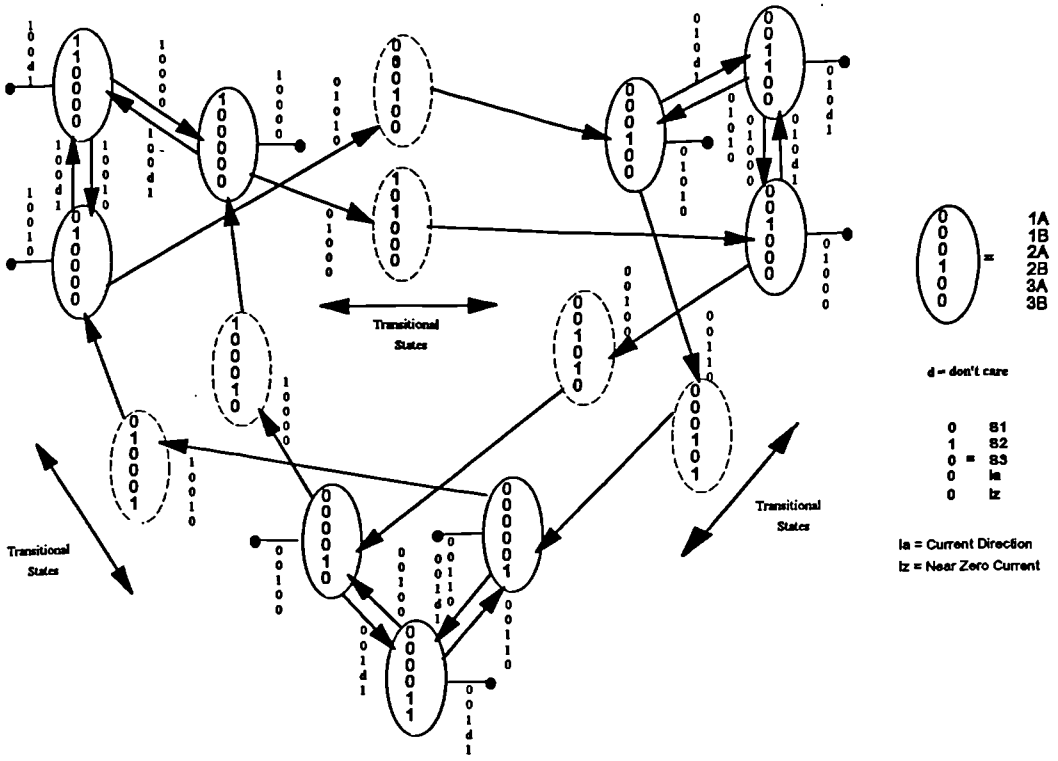


**Figure 5.6. State Transition Diagram for Semi-Soft Current Commutation with Uni-Directional Current Commutation**

### 5.2.4 Semi-Soft Current Commutation With Bi-Directional Current Flow

The current can be commutated from one switch to the next by providing an overlap in the switching periods of the conducting halves of the bi-directional switches [9]. The non-conducting half of the switch is then closed a short time after the current path hand-over has been achieved. This current path hand-over is shown in figure 5.8 for a path change from input line 1 to input line 2, with the current in a positive direction.

This method of current control will allow zero current switching of the IGBTs if the outgoing device is reverse biased by the turn on of the incoming device. This situation will occur when the voltage on the input line of the incoming switch is greater than the voltage on the input line of the outgoing switch in the conduction path.

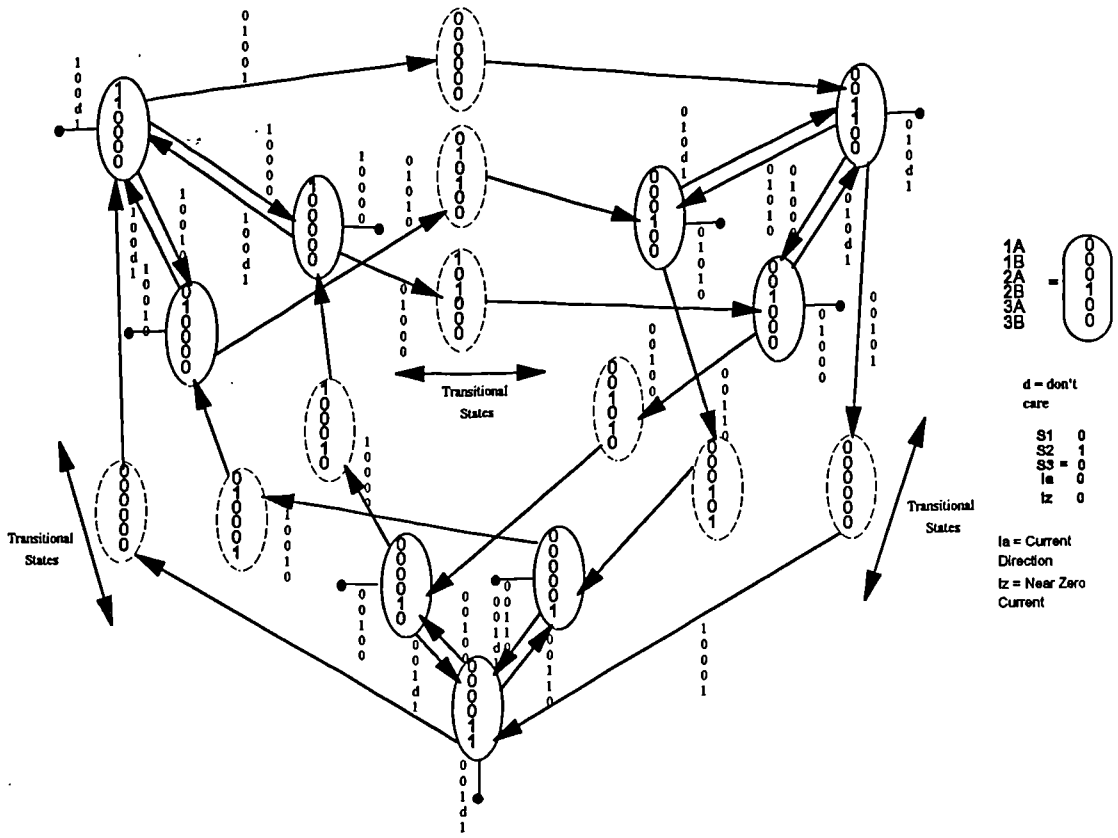


**Figure 5.7. Semi-Soft Current Commutation With Uni-Directional Current Flow and Near Zero Current Zone State Changing**

This method of current commutation will therefore achieve a 50% reduction in the average switching losses in a matrix converter because there is a 50% chance of the reverse biased situation occurring. For this reason, an appropriate term for this type of control is **semi-soft current commutation.** The State diagram for one output phase for this form of current control is shown in figure 5.9.

If the output current direction is wrongly detected, in the near zero output current region for example, then the control method will operate as if dead times had been inserted. This will occur because the switch will look open in the true current direction if the wrong half is closed first. However, this may be the best way to cope with this low current situation.

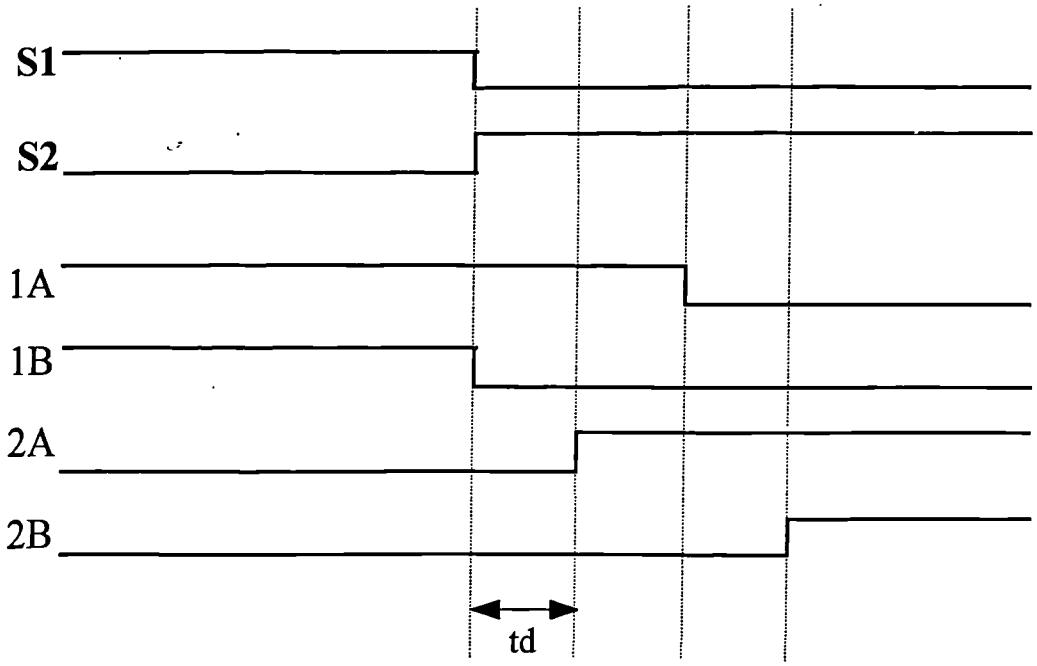


**Figure 5.8. Control Waveform Diagram for Semi-Soft Current Commutation with Bi-Directional Current Flow**

## 5.3 Implementation

The current control algorithms defined above require a quicker and more accurate response than is presently available with microprocessors. This current control must therefore be implemented externally to the processor. It is possible to implement the current control using discrete logic devices and an oscillator, but the circuit would become complex and the simplicity of the control hardware would be lost. An alternative is to use programmable logic arrays which would allow the current control for each phase to be implemented in a single device.

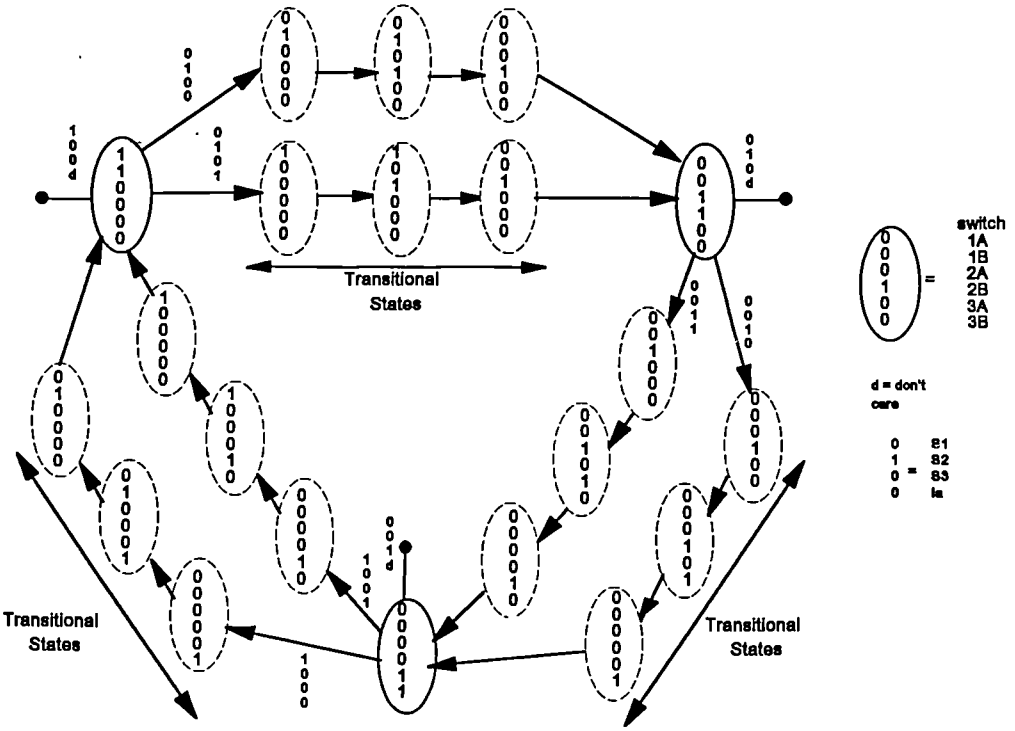


**Figure 5.9. State Transition Diagram for Semi-Soft Current Commutation With Bi-Directional Current Flow**

The use of logic arrays for the implementation of current commutation algorithms has a number of advantages. The ability to be able to program a complex algorithm with a single, low cost device would maintain hardware simplicity. The state machine approach would also ensure safe operation of the devices even if the control waveforms from the processor become corrupted.

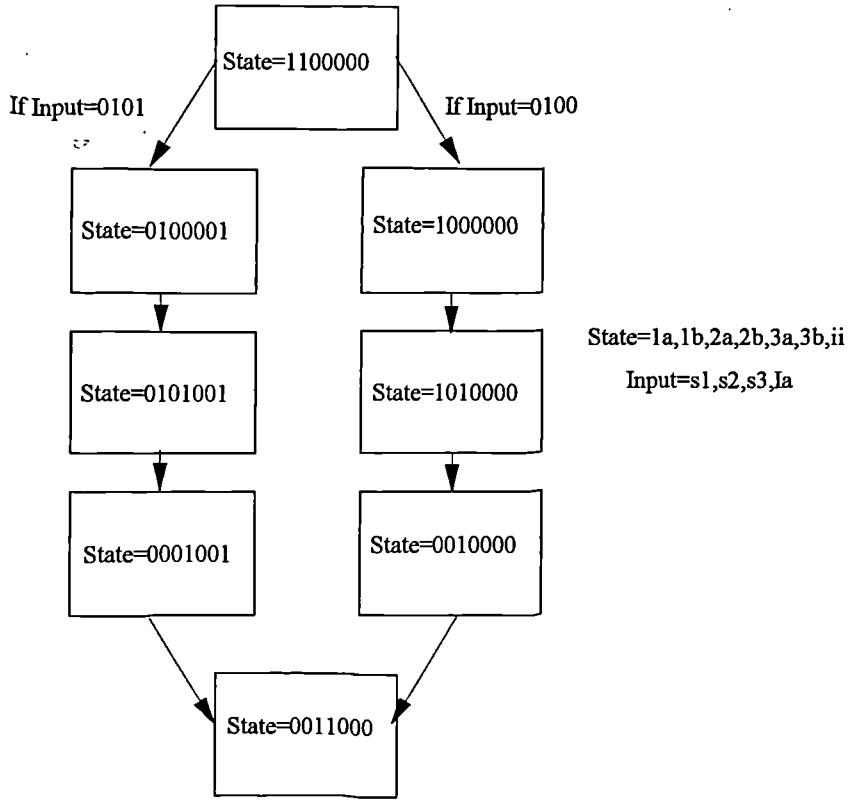


**Figure 5.10. A Flow Diagram for The GAL High Level Programing Language**

### 5.3.1 The Use of Logic Arrays

The proposed control sequences may be easily implemented using programmable logic arrays. The control sequences proposed above may be implemented using a high level programming language to program a Generic Array Logic device (GAL). Each state in the state transition diagram is assigned a seven digit binary number. This state number corresponds to the required output vector for that state plus an internal identification bit (ii). The internal identification bit distinguishes between any states with common output vectors. Using this method of assignment optimises the use of the programmable logic device because the state variables are also the output vectors.

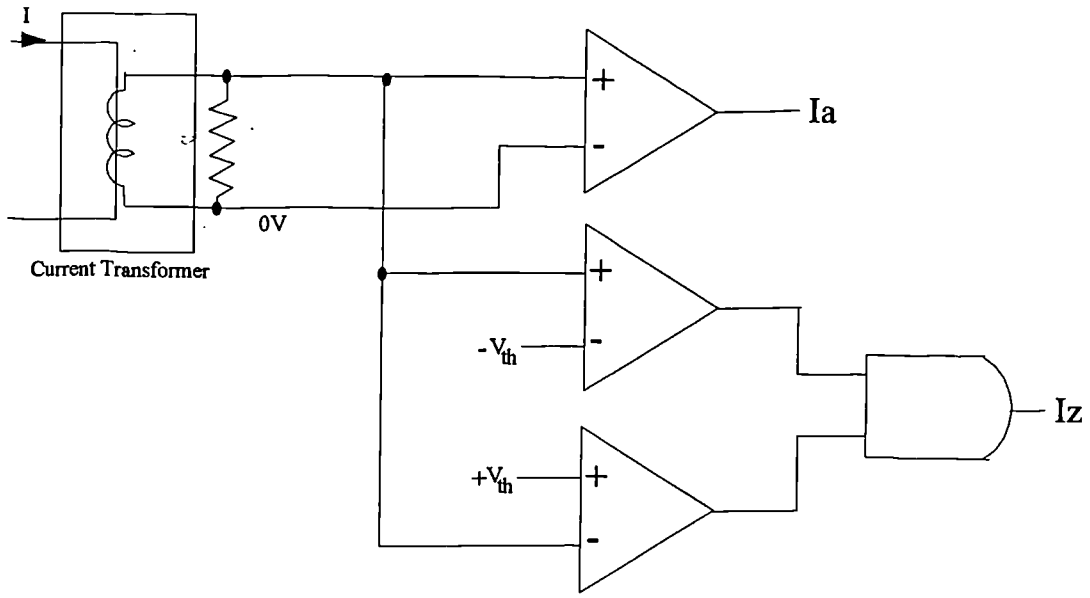


**Figure 5.11. The Current Direction and Near Zero Current Detectors for One Output Line**

The input vectors required to trigger the transitions between the states can then be defined. The input vector consists of the control signals from the controller and the current direction signal. This process is shown in the form of a flow diagram in figure 5.10 for a state change between switch 1 and switch 2 using semi-soft current commutation with bi-directional current flow.

### 5.3.2 Safe Switch operation Using a Programmable Logic Array

The possible output vectors of the logic array are fixed and transition between the states will only occur if the correct input vector is received. If the appropriate input vector is not received then the state machine will not change state. This mechanism would ensure that no short circuits between the input lines would be caused by corruption of the control waveforms from the microcontroller.

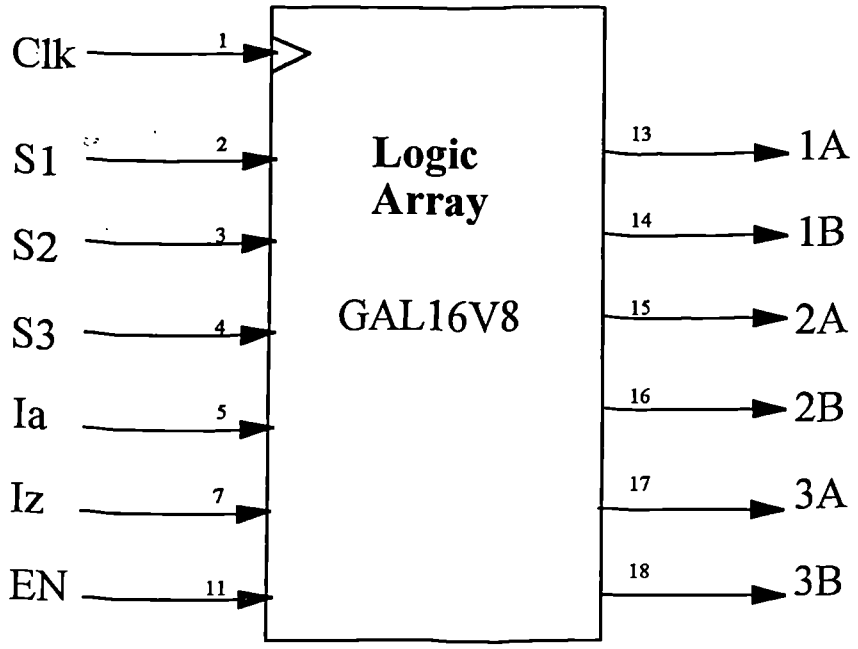


**Figure 5.12. The Connections to the Programmed Logic Array**

### 5.3.2 Programming the Logic Array

A compiler calculates the product terms and prepares a file that is used to program the device. Any current commutation algorithm that can be defined as a state diagram may be implemented using this method. The current direction and near zero current signals may be obtained from a detection circuit such as the one shown in figure 5.11.

A programmable frequency oscillator can be used to provide the clock signal for the GAL. The period of the clock is the time spent in each state. This allows the time constant of the sequencer to be altered to suit the time delays of devices used in the converter. An identical array is used for each output phase. The general GAL circuit used for the first output phase is shown in Figure 5.12. The signal EN is the chip enable signal for the GAL that may be pulled low under a fault condition to disable the output signals. In a converter implementation the three current

commutation controllers would be identically programmed but would use the control and current waveforms for the relevant output phase.

## 5.4 Conclusions

The method used to commutate the current path between the switches in a matrix converter is important. The creation of short circuits between the input lines and open circuits on the output lines due to finite switching delays in the semiconductor devices must be avoided. If these situations are allowed to occur then the converter will be unreliable due to the stress on the devices. Four fundamental methods of dealing with current commutation have been described. Some variations on these methods have been discussed.

The design and building of a state machine to allow current commutation between switches has been described. A method of semi-soft current commutation with bi-directional current control has been selected as the preferred method of current commutation due to its inherent simplicity and robustness.

# Bibliography

[1] Toshiba, "Data Book, GTR Modules", 1989

[2] Ziogas P.D., Khan S.I. and Rashid M.H., "Some Improved Forced Commutated Cycloconverter Structures", IEEE Trans. on Ind. Applications, Oct 1985, Vol.1A-21, No.5, pp.1242-1253.

[3] Lipo T.A., "Recent Progress in the Development of Solid State AC Motor Drives", IEE Trans. on Power Electronics, Vol.3, No.2, April 1988, pp.105-117.

[4] Beasant R., Beatie W. and Refsum A., "An Approach to the Realisation of a High Power Venturini Converter", Proceedings on Power Electronics, IEEE, April 1990, pp.291-297.

[5] Huber L., Borojevic D. and Burany N., "Voltage Space Vector Based PWM Control of FFCs", IECON 1989, Vol.1, pp.48-53.

[6] Svenson T. and Alakula M., "The Modulation and Control of a Matrix Converter-Synchronous Machine Drive", European Power Electronics Conference, Firenze, 1991, Vol.4, pp 469-476.

[7] Control Techniques, "Dives and Servos, Year Book 1990-1991", Control Techniques plc, 1990.

[8] Alesina A. and Venturini M., "Intrinsic Amplitude Limits and Optimum Design of 9-switches Direct PWM AC to AC Converter". Proceedings of PESC Conference Record, 1980, pp.242-252.

[9] Wheeler P.W. and Grant D.A., "Reducing the Semiconductor Losses in a Matrix Converter", Proceedings of IEE Colloquium on Power Electronics, 1992, pp.9.1-9.5.

Chapter 6

# Converter Losses

## 6.1 Introduction

This chapter presents an investigation of the semiconductor device losses in a matrix converter. The effects of different approaches to the PWM waveform generation and current commutation control on the power losses of the converter are examined. The effect of the switching frequency on the converter losses is considered. A comparison is made of the power losses and the heat sink rating for a matrix converter and a rectifier/inverter circuit.

## 6.2 The Losses in the Switching Devices

This section considers the dominant factors that influence the magnitude of the semiconductor losses in a matrix converter. This will allow examination of the size of the heat sink required to dissipate the semiconductor losses in the converter. These semiconductor losses consist of conduction and switching losses. The conduction losses due to the voltage drop across the IGBT and the diode when they are conducting. The switching losses are due to the finite switching times of the IGBTs. The magnitude of the switching losses in the matrix converter is dependent on the method of current commutation adopted in the converter and on the type of PWM generation used.

### 6.2.1 The Conduction Losses

The conduction losses in any semiconductor device are due to the forward voltage drop across the device when it is conducting. This voltage drop is variable with both junction temperature and collector current. The junction temperature is also dependent on the collector current.

$$V_{ce} \propto T_j$$
$$V_{ce} \propto \sqrt{I_c} \qquad (6.1)$$

The average power dissipated in a given device is the product of this voltage drop, the average line current and the average duty cycle of that device, $\left(t_d/t_t\right)$.

$$P_{conduction} = V_{ce}.I_c.\left(t_d/t_t\right) \tag{6.2}$$

It can be assumed that the switching times of the switches are negligible in comparison to the conduction time. The *conduction losses for one output phase of* the converter can therefore be calculated as the sum of the conduction losses in each switch in that phase, as shown in equation 6.2. The conduction loss in a given switch is the product of the forward voltage drop, the average current flowing in the switch and the duty cycle of the switch, $d_n$, as shown in equation 6.3.

$$P_{cond,phase} = \sum_{n=1}^{n=3}\left[\left(V_{cen}I_{cn}d_n\right)+\left(V_{fn}I_{fn}d_n\right)\right] \tag{6.3}$$

Where: $V_{ce}$ = Saturation voltage of the IGBT $I_c$ = Collector current in the IGBT
$V_f$ = Forward voltage of the diode $I_f$ = Forward current in the diode

At any given time only one diode/IGBT pair will be conducting for each output line. If it is assumed that the switching time delay is small in comparison to the total conduction time of the switches then the conduction loss can be calculated for one set of devices as if they are conducting all the time. This is shown in equation 6.5.

$$P_{cond,phase} \cong I_l.\left(V_{ce}+V_f\right) \tag{6.4}$$

In a rectifier/inverter circuit either the freewheeling diode or the IGBT would be conducting in the output bridge [1]. A pair of diodes would also be conducting in the input bridge as shown in figure 6.1.

$$P_{cond,phase} \cong I_c.\left(0.91.V_{ce,IGBT}+1.09.V_{ce,diode}\right) \tag{6.5}$$

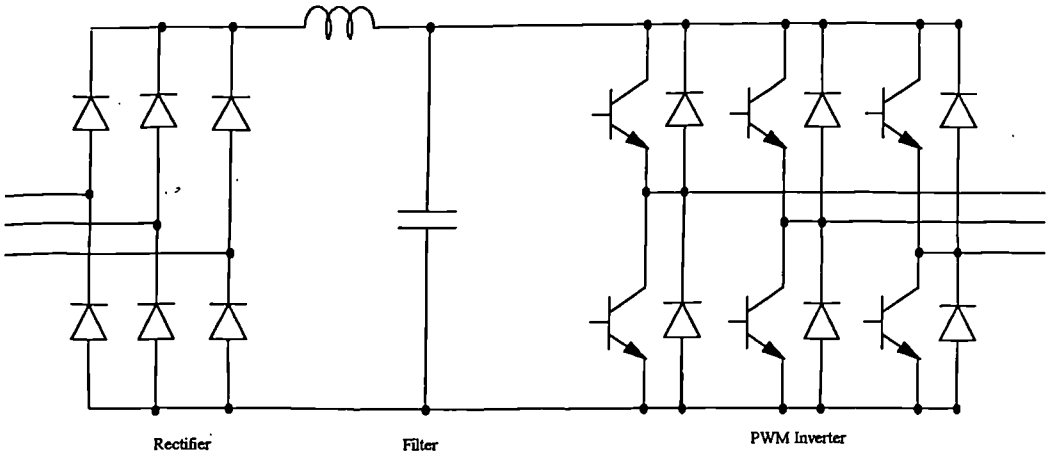


**Figure 6.1. A Rectifier/Inverter Circuit**

### 6.2.2 The Switching Losses

The switching losses per switch in the matrix converter are calculated as the product of the switching frequency and the switching energy loss per pulse, $E_{loss}$, for a given device. The switching energy loss per pulse is usually given in device data sheets for given conditions.

$$P_{switch,phase} = 3 f_s . E_{loss} \tag{6.6}$$

The total power loss for a matrix converter can then be calculated. The total losses are equal to the sum of the switching losses and the conduction losses, as shown in equation 6.7.

$$P_{total} = 3.\left(P_{cond,phase} + P_{switch,phase}\right) \tag{6.7}$$

The contribution made by the conduction losses and the switching losses to the total losses in a matrix converter are shown graphically in figure 6.2.

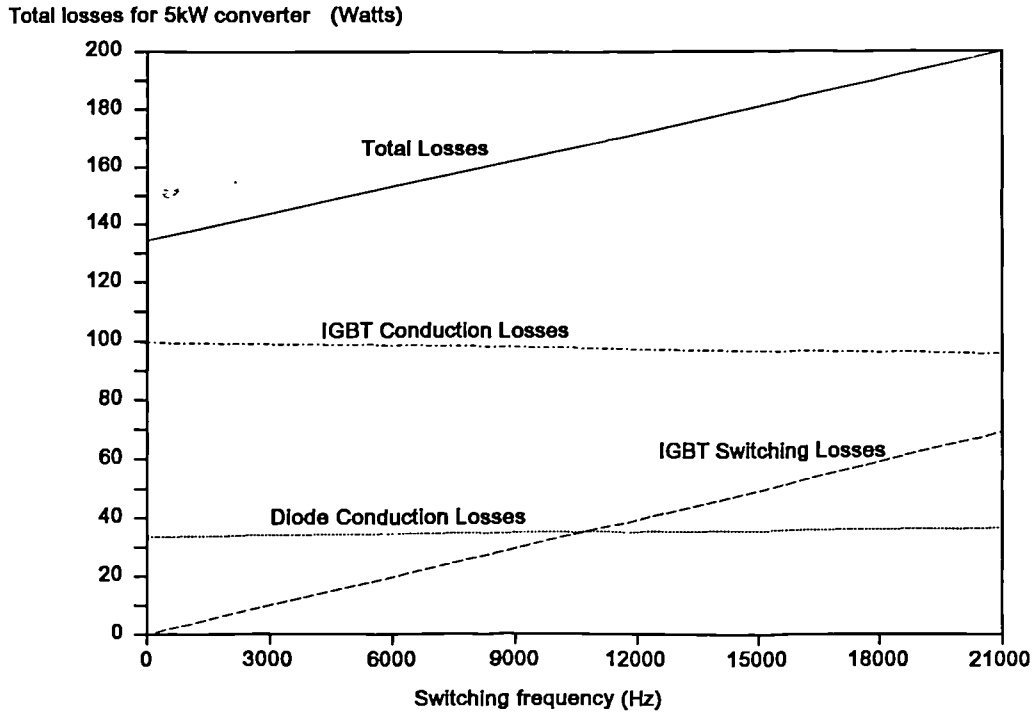


**Figure 6.2. The Composition of the Matrix Converter Semiconductor Losses**

## 6.3 Methods of Switching Loss Reduction

The characteristics of the chosen devices in a matrix converter determine the conduction losses. The switching losses may also be reduced by careful selection of devices. However the switching losses can be reduced for a given switching frequency if consideration is given to the method of current commutation employed and the PWM switching patterns used.

### 6.3.1 Switching Loss Reduction Using Semi-soft Current Commutation

The switching losses can be reduced by the implementation of a suitable method of commutating the current from one conducting switch to the next, such as semi-soft current commutation that was described in Chapter 5. This method of current control will allow zero current switching of the IGBTs if the outgoing device is reverse biased by the turn-on of the incoming device.

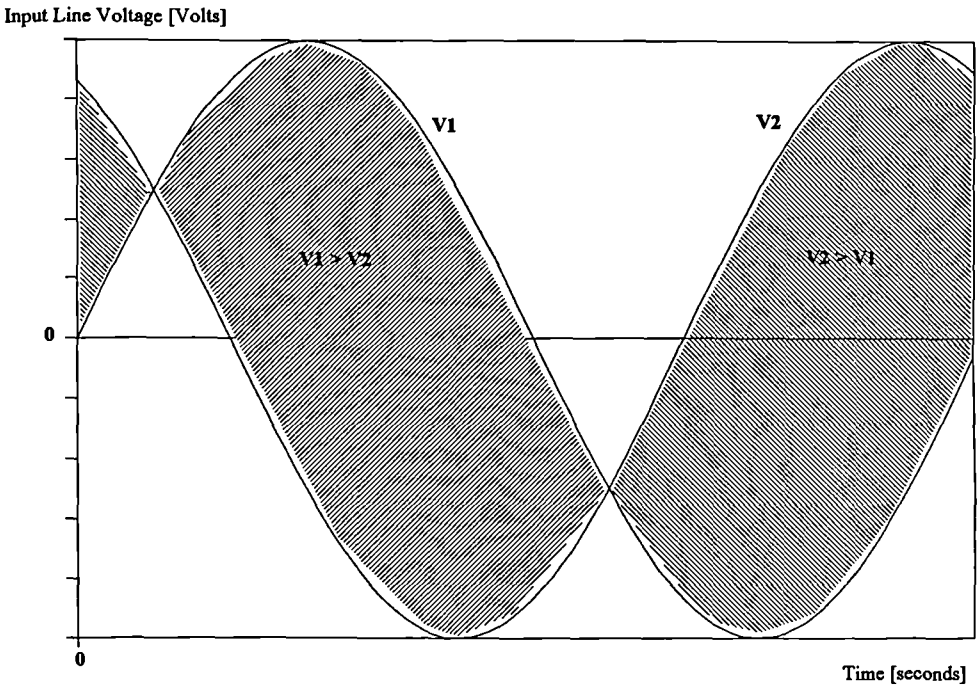


**Figure 6.3. The Areas Probability of Where One Input Phase is at a Higher Potential Than Another**

This reverse bias situation will occur when the voltage on the input line of the incoming switch is greater than the voltage on the input line of the outgoing switch in the conduction path. The probability of the incoming input line being at a greater potential than the outgoing input line is equal to the probability of a sine wave being greater in value than a sine wave with 2/3 phase shift. By inspection it can be seen that this probability will be 50%, as shown in figure 6.3. This reverse biasing will therefore occur in 50% of the switch state changes. This method of current commutation will reduce the switching losses in a matrix converter by 50%.

### 6.3.2 Switching Loss Reduction Using Semi-Symmetrical PWM Waveforms

The switching losses can also be reduced by 33% with the implementation of a PWM method in which the last in a set of three switching periods becomes the first switching period in the next set of three switching periods.

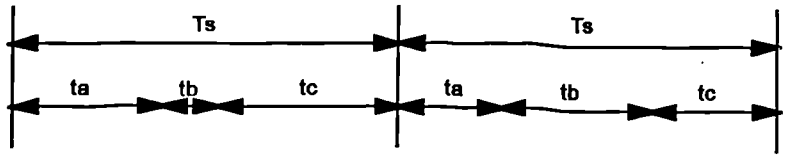


a. Non-symmetrical PWM

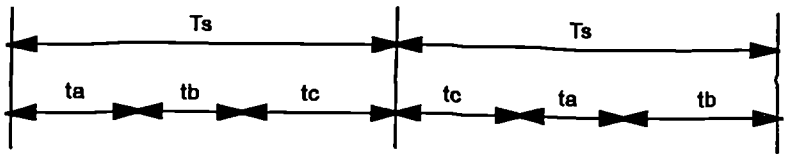


b. Semi-symmetrical PWM

**Figure 6.4. The Control Waveform Sequences for Semi-Symmetrical and Non-Symmetrical PWM**

Instead of a conventional order of switch S1, switch S2, switch S3, switch S1, switch S2, switch S3 and so on, the order becomes switch S1, switch S2, switch S3, switch S3, switch S1, switch S2 and so on. This method has been termed **semi-symmetrical PWM**. This change to the PWM generation scheme will affect the characteristics of the switching frequency harmonics. The switching sequence for semi-symmetrical PWM is shown in figure 6.4.

### 6.3.3 Total Switching Loss Reduction

The above semiconductor loss reduction methods will give four switching pattern variants for a matrix converter switching patterns:

- Basic matrix converter with dead-times and non-symmetrical PWM.
- Matrix converter using semi-symmetrical PWM.
- Matrix converter with semi-soft current commutation.
- Matrix converter using semi-symmetrical PWM and with semi-soft current commutation

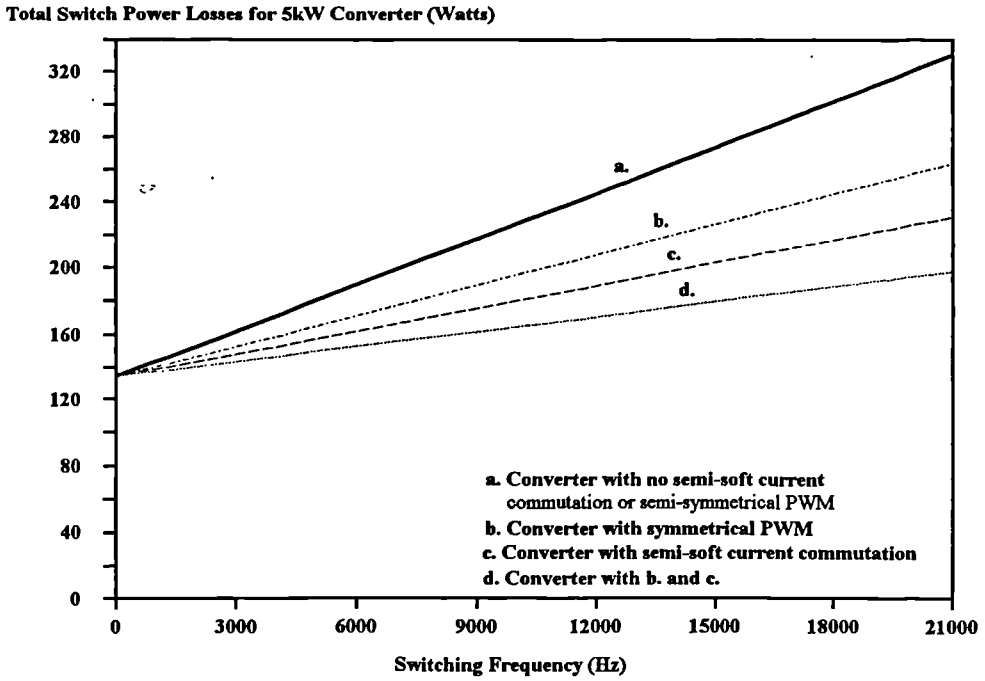


**Figure 6.5. The Effect of Switching Loss Reduction Techniques on the Total Converter Losses**

If both switching loss reduction methods are implemented on the matrix converter, the switching losses will be reduced by 66%. The average number of switch state changes giving rise to a switching loss will be reduced from nine per switching cycle to three per switching cycle.

The inverter has six hard switch state changes per switching cycle. Therefore the matrix converter could have lower switching losses than a basic inverter. Depending on the chosen switching frequency, these savings could compensate for the extra conduction losses that are inherent in the matrix converter structure. The effect of implementing both semi-soft current commutation and semi-symmetrical PWM on the switching losses of a matrix converter is shown in figure 6.5. The reduction in switching losses for each technique implemented independently is also shown.

## 6.4 Calculation of Semiconductor Losses and Heat Sink Rating

To quantify the semi-conductor losses in any circuit, assumptions have to be made about the behaviour of the device. The following equations are derived from linearizations of the characteristic graphs given in IGBT data sheets. The equations allow a good approximation of the conduction and switching losses in the matrix converter to be determined. In some cases iteration is necessary as variables are interdependent. The equations have been used to develop a spread sheet program which allows the effect of changing various variables on the converter losses and the size of the heat sink to be modelled.

The fixed variables used for the spread sheet are dependent on the supply used and on the devices chosen:

1. The Maximum Output Volts (=0.866.$V_i$). [$V_{out}$]
2. The Total Thermal Resistances in the devices. [$R_{th}$]
3. The Forward Voltage Drop at given Temperatures. [$V_{ce}$]
4. The Maximum IGBT Junction Temperature. [$T_j$]
5. The energy loss per pulse under given conditions. [$E_{loss}$]

The user defined variables on the spread sheet are dependent on the environment in which the converter is used and on the required converter performance:

1. The Ambient Air Temperature. [$T_{air}$]
2. The Power Output of the Motor. [P]
3. The Power Factor of the Motor. [$\phi$]
4. The Switching Frequency. [$f_s$]

The phase current [$I_p$] for the motor is calculated from the output power and the power factor of the motor:

$$I_p = \frac{P}{\sqrt{3}.\phi.V_{l,out}} \tag{6.8}$$

### 6.4.1 Estimation of the Switching Losses

The IGBT switching loss per pulse has to be scaled for the defined junction temperature and collector current under which it is operating. The junction temperature and the switching loss per pulse are proportional to each other and this will therefore create an iterative loop.

$$E_{switch-loss,Tj} = \left[1+\frac{(t_j - t_d)}{t_d}\right].E_{loss,d}.\left[\frac{I_p}{I_d}\right] \tag{6.9}$$

Thus the switching power loss for each hard switching on and off of a device is:

$$P_{switch} = f_s.E_{switch-loss,Tj} \tag{6.10}$$

The total switching loss depends on the PWM scheme implemented and on the current commutation methodology that is adopted. The switching losses are then proportional to the number of hard switching switch state changes per cycle in the converter [$K_S$], which are shown in table 6.1. The average switching loss in each phase can therefore be calculated.

$$P_{switch,total} = K_s.P_{switch} \tag{6.11}$$

### 6.4.2 Estimation of the Conduction Losses

The forward voltage drop across the IGBT is dependent on the phase current and the operating junction temperature of the device:

$$V_{ce,IGBT} = V_{cd,d}.\left[\left(\frac{T_j}{T_d}\right).\left(\sqrt{\frac{I_p}{I_d}}\right)\right] \tag{6.12}$$

| Switching Strategies | Number of Lossy Switch State Changes |
|---|---|
| Dead-times and non-symmetrical PWM | 9 |
| Semi-symmetrical PWM | 6 |
| Semi-zero voltage switching | 4.5 |
| Semi-symmetrical PWM with semi-zero voltage switching | 3 |

**Table 6.1. Number of Lossy Switch State Changes**

The forward voltage drop of the diode is calculated in the same way except that the junction temperature will be different from that for the IGBT. This will have to be calculated from the total power dissipated and the heat sink temperature. This creates another iterative loop.

The conduction loss per phase may then be calculated assuming that one bi-directional switch of devices is always conducting. Equation 6.3 can therefore be rewritten:

$$P_{cond,phase} = I_p.\left(V_{ce,IGBT} + V_{ce,diode}\right) \tag{6.13}$$

Because the matrix converter has three output phases the total conduction losses are given by:

$$P_{cond,total} = 3.P_{cond,phase} \tag{6.14}$$

### 6.4.3 The Total Device Losses and Heat Sink Rating

The total power loss for the converter is the sum of the total switching and conduction losses as shown in equation 6.15.

$$P_{total} = P_{switch,total} + P_{cond,total} \tag{6.15}$$

Using this total power loss and the thermal resistances of the devices it is possible to calculate the temperature of the heat sink, as shown in figure 6.6.

$$T_{sink} = \frac{P_{total} \cdot R_{th,IGBT} \cdot R_{th,diode} + T_{j,IGBT} \cdot R_{th,diode} + T_{j,diode} \cdot R_{th,IGBT}}{R_{th,diode} + R_{th,IGBT}} \tag{6.16}$$

Where:

$R_{th} = R_{th,CS} + R_{th,JC}$

$R_{th,CS}$ = Case to Sink Thermal Resistence

$R_{th,JC}$ = Junction to Case Thermal Resistence

From this information the minimum total heat sink rating can be calculated:

$$\text{Heat Sink Rating} = \frac{T_{sink} - T_{air}}{P_{total}} \text{ K / Watt} \tag{6.17}$$

## 6.5 Comparison of Losses for a Matrix Converter and an Inverter

This section compares the semiconductor losses in a matrix converter and an inverter that employs similar semiconductor components. The calculations are based on a 5kWatt experimental matrix converter described in Chapter 9. The IGBTs used are IRGBC20 600Volt, 13Amp devices. The diodes used are MUR860 600Volt, 8Amp devices.

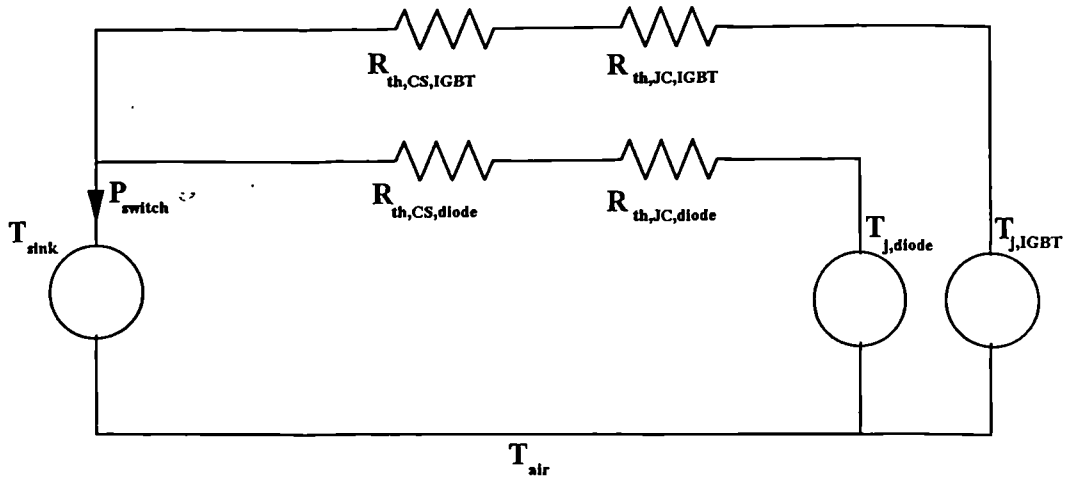


**Figure 6.6. Thermal Resistance's for a Bi-Directional Switch**

The methods described above for calculating the device losses and the heat sink ratings have been used to create a spread sheet program in Lotus 123. The estimation program enables the effects of altering the switching frequency and power rating of a matrix converter employing these devices to be studied. The effect of the four switching style variants on the total converter losses has been examined as shown in figure 6.5. The effects of output power and switching frequency on the comparative losses of the matrix converter and the inverter have also been investigated, as has the effect of output power and switching frequency on the rating of the heat sink.

Besides the information given in device data sheets [3,4], the following constants have been assumed for this program:

$V_{out} = 360$Volts

$T_{air} = 30°C$

$T_{j,max} = 150°C$

$\phi = 0.866$

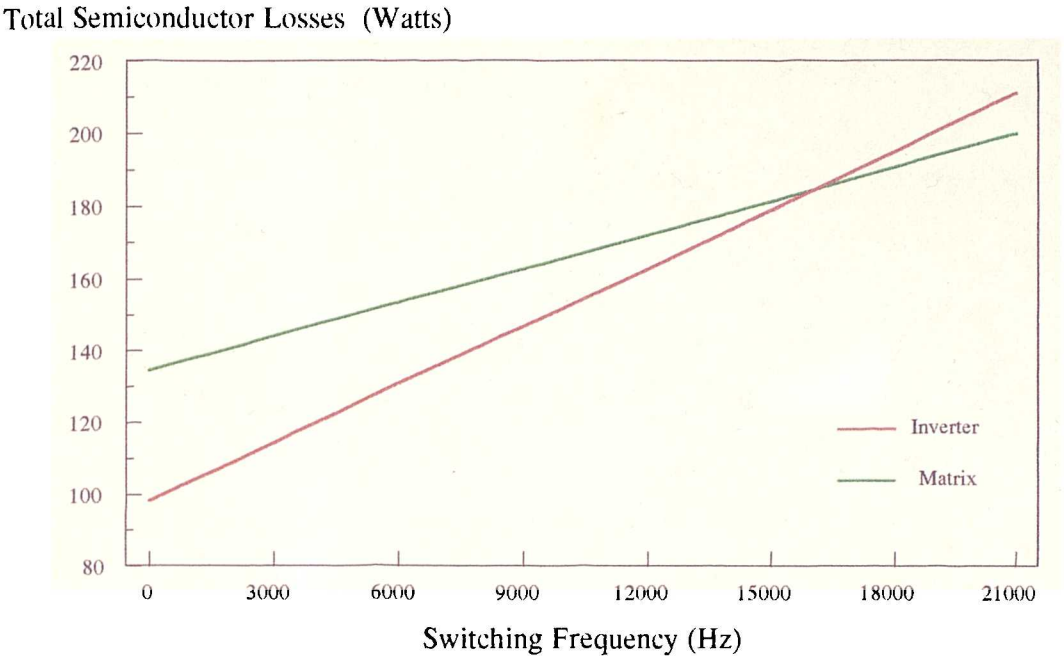


**Figure 6.7. Total Power Losses Against Switching Frequency for a 5kWatt Converter**

Figure 6.2 showed how the components of the total power loss are affected by the switching frequency of the converter. It can be seen that an increase in switching frequency has a small effect on the conduction losses due to the increase in junction temperature.

The variation of power loss with switching frequency for a matrix converter with semi-soft current commutation and semi-symmetrical PWM is shown in figure 6.7. The power losses in an inverter employing similar components are also shown for comparison. It can be seen that as the switching frequency increases, the difference between the power losses decreases. At higher switching frequencies the matrix converter will become more efficient than the inverter. It should be noted that the losses in the DC link capacitors of the inverter have not been included in these semi-conductor loss calculations.

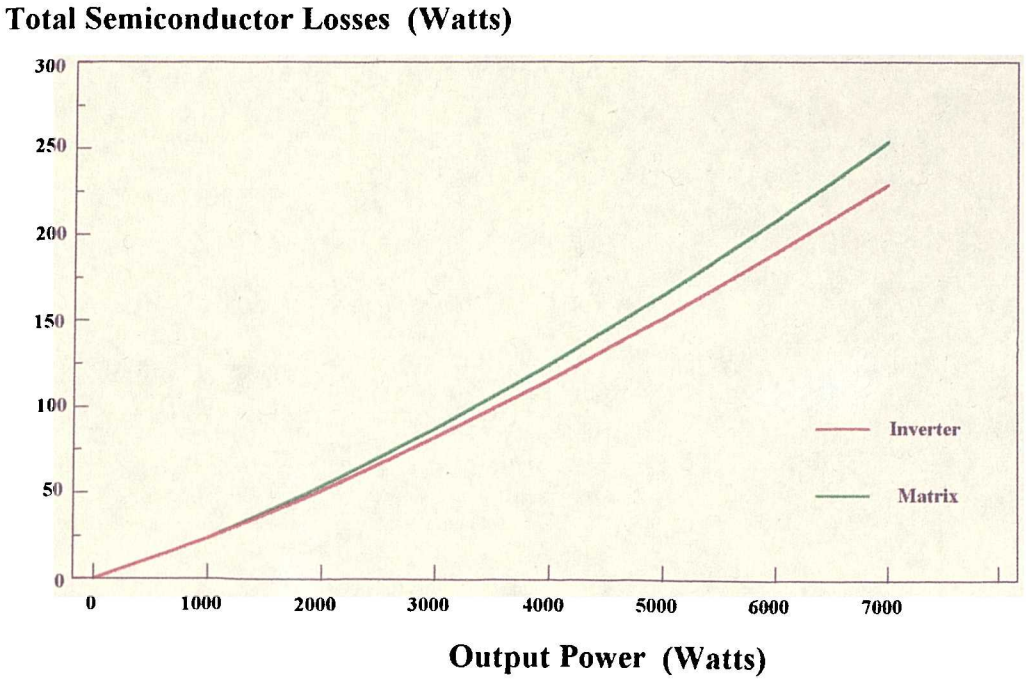


**Figure 6.8. Total Power Losses Against Output Power for a Switching Frequency of 10kHz**

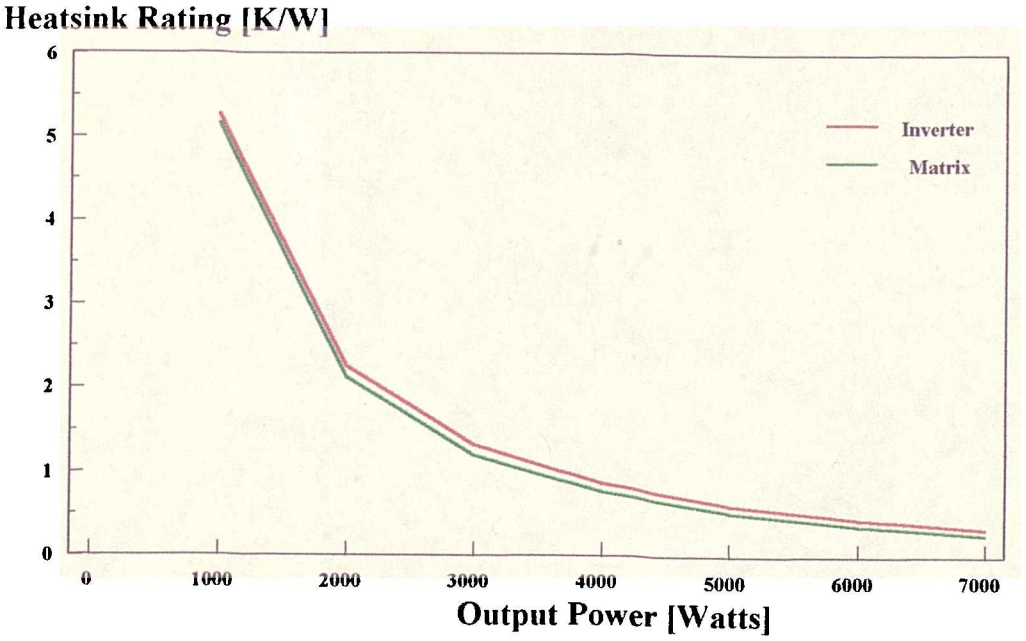


**Figure 6.9. Minimum Combined Heat Sink Rating Against Output Power for a Switching Frequency of 10kHz**

Figure 6.8 shows how the power loss varies with the output power of the converter. A comparison with the inverter is also given. The effect of this power loss on the required minimum rating of the heat-sink is shown in figure 6.9.

## 6.6 Conclusions

This chapter has described some of the work carried out to estimate the minimum ratings for the switching devices and their associated heat sink in the Matrix Converter. A series of measures to reduce the switching losses of the matrix converter have been described. The semiconductor power loss has been estimated, allowing the investigation of the converter efficiency. From these losses an estimation of the required total heat sink rating has been made. All these figures have been compared to an inverter using the same principles.

It has been shown that the matrix converter has semiconductor losses of the same order of magnitude as an inverter. If a switching frequency above 16kHz is chosen then the matrix converter becomes a more efficient converter than the rectifier/inverter circuit. The size of heat sinks required by the two converter topologies are therefore very similar if a relatively high switching frequency is chosen.

# Bibliography


[1] Grant D.A., "Using HEXFET III in PWM Inverters for Motor Drives and UPS Systems", International Rectifiers, Power MOSFETs Application Notes.

[2] "IRGBC20 Data Sheet", International Rectifier, No. PD-9.626A.

[3] "MUR860 Data Sheet", Motorola.

[4] "GTR Module Data Book", Toshiba.

[5] Tounsi S. and Dorkel J., "Thermal Environment CAD for Power Circuits", IEE Colloquium on Power Electronic Devices, Nov. 1992, pp.7.1-7.5.

[6] Bose B.K, "Recent Advances in Power Electronics", IEEE Transactions on Power Electronics, Vol. 7, No. 1, Jan. 1992, pp.2-17.

[7] RS Components Catalogue.

Chapter 7

# Switching Frequency Harmonics

## 7.1 Introduction

This chapter mathematically investigates the effects of the switching frequency in a matrix converter. A mathematical model is developed of the harmonics that the switching frequency generates in the control waveform. This is used to model the harmonics in the output voltage waveform from the converter. The results are presented graphically with the aid of spectral maps.

The use of the mathematical model can be extended to examine the possibility of harmful subharmonics to the output frequency caused if a matrix converter is operated at low switching frequencies. The harmonics associated with the switching frequency in the input current waveforms can be examined. The problems associated with providing a circulation path for the switching frequency harmonics can therefore be addressed.

## 7.2 The Calculation of the Nature of the Harmonics

### 7.2.1 The Mathematics

In order to establish the principles involved in mathematically modelling the waveforms in the converter, consider a basic sinusoidal modulation function as defined in equation 7.1

$$h_c = \tfrac{1}{2}\left(1 + M\cos(\omega_c t)\right) \tag{7.1}$$

The control function is uniformly sampled at a frequency $\omega_S$. The height, $\kappa$, of the control function above the time axis at a given sampling point will give the switch duty cycle.

Let: $x = \omega_s t$

$y = \omega_c t$ (7.2)

and: n = order of control frequency harmonics

m = order of switching frequency harmonics

This will give a periodic pulse train of pulses of width κ every τ seconds, which corresponds to the periodic variables x and y. This pulse train can therefore be expressed as a double Fourier series in terms of x and y as derived in equation 7.14. This series will give a pulse train for the uniformly sampled series derived from the modulation function. This process is shown pictorially in figure 7.1.

$$F(x,y_1)=\tfrac{1}{2}a_0(y_1)+\sum_{m=1}^{\infty}\left[a_m(y_1)\cos(mx)+b_m(y_1)\sin(mx)\right] \tag{7.3}$$

Where

$$a_m(y_1)=\frac{1}{\pi}\int_0^{2\pi}F(x,y_1)\cos(mx)dx \tag{7.4}$$

and

$$b_m(y_1)=\frac{1}{\pi}\int_0^{2\pi}F(x,y_1)\sin(mx)dx \tag{7.5}$$

These coefficients are functions of y only. These values are also periodic with respect to y and can therefore also be represented by a Fourier series for all possible values of y:

$$a_m(y)=\tfrac{1}{2}c_{0m}+\sum_{n=1}^{\infty}\left[c_{nm}\cos(ny)+d_{nm}\sin(ny)\right] \tag{7.6}$$

$$c_{nm}=\frac{1}{\pi}\int_0^{2\pi}a_m(y)\cos(ny)dy$$

$$d_{nm}=\frac{1}{\pi}\int_0^{2\pi}b_m(y)\sin(ny)dy \tag{7.7}$$

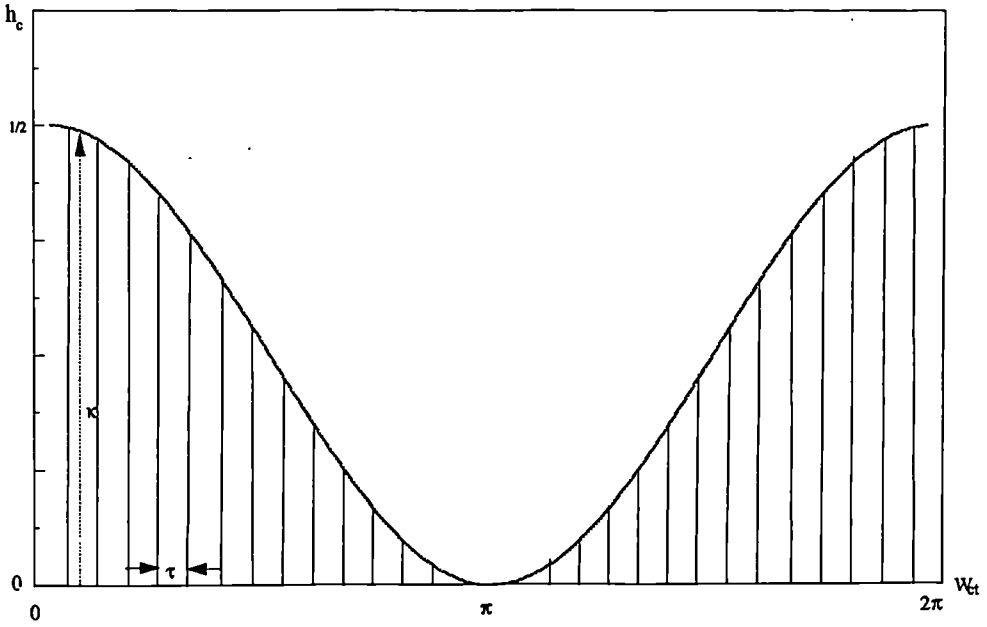


$$\tau = \frac{2\pi}{\omega_s}$$

**Figure 7.1. The Control Waveform**

$$b_m(y) = \tfrac{1}{2} e_{0m} + \sum_{n=1}^{\infty} \left[ e_{nm} \cos(ny) + f_{nm} \sin(ny) \right] \tag{7.8}$$

$$e_{nm} = \frac{1}{\pi} \int_0^{2\pi} b_m(y) \cos(ny) dy$$

$$f_{nm} = \frac{1}{\pi} \int_0^{2\pi} b_m(y) \sin(ny) dy \tag{7.9}$$

If the equations for $a_m(y_1)$ and $b_m(y_1)$ given in equations 7.4 and 7.5 are substituted into the series given in equations 7.7 and 7.9 then the expanded equations become:

$$c_{mn} = \frac{1}{\pi}\int_0^{2\pi}\frac{1}{\pi}\left[\int_0^{2\pi} F(x,y)\cos(mx)dx\right]\cos(ny)dy]$$
$$= \frac{1}{\pi^2}\iint F(x,y)\cos(mx)\cos(ny)dxdy$$
$$= \frac{1}{2\pi^2}\left[\iint F(x,y)\cos(mx+ny)dxdy + \iint F(x,y)\cos(mx-ny)dxdy\right] \tag{7.10}$$

$$d_{mn} = \frac{1}{\pi}\int_0^{2\pi}\frac{1}{\pi}\left[\int_0^{2\pi} F(x,y)\cos(mx)dx\right]\sin(ny)dy]$$
$$= \frac{1}{\pi^2}\iint F(x,y)co\sum_{y=} s(mx)\sin(ny)dxdy$$
$$= \frac{1}{2\pi^2}\left[\iint F(x,y)\sin(mx+ny)dxdy + \iint F(x,y)\sin(mx-ny)dxdy\right] \tag{7.11}$$

$$e_{mn} = \frac{1}{\pi}\int_0^{2\pi}\frac{1}{\pi}\left[\int_0^{2\pi} F(x,y)\sin(mx)dx\right]\cos(ny)dy]$$
$$= \frac{1}{\pi^2}\iint F(x,y)\sin(mx)\cos(ny)dxdy$$
$$= \frac{1}{2\pi^2}\left[\iint F(x,y)\sin(mx+ny)dxdy + \iint F(x,y)\sin(mx-ny)dxdy\right] \tag{7.12}$$

$$f_{mn} = \frac{1}{\pi}\int_0^{2\pi}\frac{1}{\pi}\left[\int_0^{2\pi} F(x,y)\sin(mx)dx\right]\sin(ny)dy]$$
$$= \frac{1}{\pi^2}\iint F(x,y)\sin(mx)\sin(ny)dxdy$$
$$= \frac{1}{2\pi^2}\left[\iint F(x,y)\cos(mx-ny)dxdy - \iint F(x,y)\cos(mx-ny)dxdy\right] \tag{7.13}$$

Equations 7.6 and 7.8 are substituted into equation 7.13; then equations 7.10 to 7.13 substituted into this new equation; and then like terms are collected to produce:

$$\begin{aligned} F(x,y) = & \frac{1}{4\pi^2}\iint F(x,y)dxdy \\ & + \frac{1}{2\pi^2}\sum_{n=1}^{\infty}\left[C_{ny}\cos(ny) + S_{ny}\sin(ny)\right] \\ & + \frac{1}{2p^2}\sum_{m=1}^{\infty}\left[C_{mx}\cos(mx) + S_{mx}\sin(mx)\right] \\ & + \frac{1}{2p^2}\sum_{m=1}^{\infty}\sum_{n=\pm1}^{\pm\infty}\left[C_{mx+ny}\cos(mx+ny) + S_{mx+ny}\sin(mx+ny)\right] \end{aligned} \tag{7.14}$$

Where:

$$C_\theta = \iint F(x,y)\cos(\theta)dxdy$$
$$S_\theta = \iint F(x,y)\sin(\theta)dxdy$$

The first term of equation 7.14 gives the DC component of the PWM waveform. The second component will represent the control frequency and its associated harmonics. The third term relates to the fundamental of the switching frequency and its harmonics. The final term models the harmonics of the control frequency associated with each of the switching frequency harmonics. To evaluate equation 7.14 it is necessary to find a solution to the double integrals.

### 7.2.2 The Solutions

To achieve a real solution to the equation the terms $S_\theta$ and $C_\theta$ are combined:

$$C_\theta + iS_\theta = \int_0^{2\pi}\int_0^{2\pi} F(x,y)e^{i\theta}dxdy \tag{7.15}$$

The height of the pulses in the pulse train will be considered to be unity. The first integral represents the area of a given pulse. In evaluating this area it must be remembered that the pulse width is sampled at the beginning of the cycle.

$$C_{mx+ny} + iS_{mx+ny} = \int_0^{2\pi h_c}\int_0 e^{i(mx+ny)}dxdy$$
$$= -\frac{i}{my}\int_0^{2\pi}\left[e^{i(mx+ny)h_c} - e^{iny}\right]dy \qquad (7.16)$$

Where $n \neq 0$ and $m \neq 0$

The term $e^{iny}$ in equation 7.16 can be ignored as it is periodic with respect to y. Equation 7.16 can then be compared to the form equation 7.17, which is the definition of a Bessel function of the first kind:

$$J_n(Z) = \frac{i^{-n}}{2\pi}\int_0^{2\pi} e^{iZ\cos\Phi}e^{in\Phi}d\Phi \qquad (7.17)$$

Equation 7.16 can then be written in terms of a Bessel function:

$$C_{mx+ny} + iS_{mx+ny} = -\frac{2\pi y i}{m}e^{\frac{i}{2}(mx+ny+n\pi)}J_n\left(\frac{(mx+ny)M}{2y}\right) \qquad (7.18)$$

By separately equating the real and imaginary parts of equation 7.18:

$$C_{mx+ny} = -\frac{2\pi y}{m}J_n\left(\frac{(mx+ny)M}{2y}\right)\cos\left(\frac{mx+ny}{2y}+\frac{n\pi}{2}\right)$$
$$S_{mx+ny} = \frac{2\pi y}{m}J_n\left(\frac{(mx+ny)M}{2y}\right)\sin\left(\frac{mx+ny}{2y}+\frac{n\pi}{2}\right) \qquad (7.19)$$

If equations 7.19 are substituted into the last term of equation 7.14 then a time domain model of the control frequency harmonics of the switching frequency may be evolved:

$$F_4(x,y)=\frac{1}{2\pi^2}\sum_{m=1}^{\infty}\sum_{n=\pm1}^{\pm\infty}\left[C_{mx+ny}\cos(mx+ny)+S_{mx+ny}\sin(mx+ny)\right]$$
$$=\frac{-x}{\pi}\sum_{m=1}^{\infty}\sum_{n=\pm1}^{\pm\infty}\frac{J_n\left[\frac{\pi}{2y}(mx\pm ny)\right]}{(mx\pm ny)}\sin\left\{(mx\pm ny)+\frac{(mx+ny)}{2y}-\frac{n\pi}{2}\right\}$$
$$=\frac{-\omega_s}{\pi}\sum_{m=1}^{\infty}\sum_{n=\pm1}^{\pm\infty}\frac{J_n\left[\frac{\pi}{2\omega_c}(m\omega_s\pm n\omega_c)\right]}{(m\omega_s\pm n\omega_c)}\sin\left\{(m\omega_s t\pm n\omega_c t)+\frac{(m\omega_s+n\omega_c)}{2\omega_c}-\frac{n\pi}{2}\right\} \tag{7.20}$$

If either n or m is set to zero in equation 7.20 then the remainder of the equation will represent the second and third terms of equation 7.14 respectively:

$$F_2(x,y)=\frac{-\omega_s}{\pi}\sum_{n=1}^{\infty}\frac{J_n\left[\frac{n\pi\omega_c}{2\omega_s}\right]}{(n\omega_c)}\sin\left(n\omega_c t-\frac{n\omega_c}{2\omega_s}-\frac{n\pi}{2}\right) \tag{7.21}$$

$$F_3(x,y)=\frac{1}{\pi}\sum_{m=1}^{\infty}\frac{1-J_0\left[\frac{m}{2}\right]}{m}\sin(m\omega_s t) \tag{7.22}$$

Combining equations 20, 21, 22 we obtain the result:

$$F(t)=\frac{1}{2\pi}$$
$$-\frac{\omega_s}{\pi}\sum_{n=1}^{\infty}\frac{J_n\left[\frac{n\pi\omega_c}{2\omega_s}\right]}{(n\omega_c)}\sin\left(n\omega_c t-\frac{n\omega_c}{2\omega_s}-\frac{n\pi}{2}\right)$$
$$+\frac{1}{\pi}\sum_{m=1}^{\infty}\frac{1-J_0\left[\frac{m}{2}\right]}{m}\sin(m\omega_s t)$$
$$-\frac{\omega_s}{\pi}\sum_{m=1}^{\infty}\sum_{n=\pm1}^{\pm\infty}\frac{J_n\left[\frac{\pi}{2\omega_c}(m\omega_s+n\omega_c)\right]}{(m\omega_s+n\omega_c)}\sin\left\{(m\omega_s t+n\omega_c t)-\frac{(m\omega_s+n\omega_c)}{2\omega_c}-\frac{n\pi}{2}\right\} \tag{7.23}$$

### 7.2.3 Evaluation of the Solutions

By evaluating the Bessel functions for a given harmonic it is possible to calculate the magnitude of that harmonic at any given frequency. The magnitude of given harmonics may be useful in examining subharmonics of the output frequency when the converter is under low switching frequency operation. The magnitudes of harmonics are also required when considering the bandwidth required by a band-pass input filter stage and in evaluating other EMC related problems. A more complex control algorithm can be evaluated by the superposition of suitably scaled control frequencies substituted into equation 7.23. This has been done for the PMW control algorithm described in chapter 2.

## 7.3 The Subharmonics of the Output Frequency

### 7.3.1 The Magnitude of the Harmonics

Consider a simple matrix converter using the control function $h_c/2$. The ideal output voltage waveform for one of the three output lines can be calculated:

$$
\begin{aligned}
V_{ol} &= \begin{bmatrix} F(t) & F(t+\frac{4\pi}{3}) & F(t+\frac{2\pi}{3}) \end{bmatrix} \begin{bmatrix} V\cos(\omega_i t) \\ V\cos(\omega_i t+\frac{2\pi}{3}) \\ V\cos(\omega_i t+\frac{4\pi}{3}) \end{bmatrix} \\
&= \frac{V\omega_s}{2\pi}\sum_{n=1}^{\infty}\frac{J_n\left[\frac{n\pi\omega_c}{2\omega_s}\right]}{(n\omega_c)}\sin\left(n\omega_c t-\omega_i t-\frac{n\omega_c}{2\omega_s}-\frac{n\pi}{2}\right) \\
&+\frac{V}{2\pi}\sum_{m=1}^{\infty}\frac{1-J_0\left[\frac{m}{2}\right]}{m}\sin\left(m\omega_s t-\omega_i t+\frac{\pi}{2}\right) \\
&+\frac{V\omega_s}{2\pi}\sum_{m=1}^{\infty}\sum_{n=\pm 1}^{\pm\infty}\frac{J_n\left[\frac{\pi}{2\omega_c}(m\omega_s+n\omega_c)\right]}{(m\omega_s+n\omega_c)}\sin\left\{(m\omega_s+n\omega_c-\omega_i)t-\frac{(m\omega_s+n(1+\pi\omega_c))}{2\omega_c}\right\}
\end{aligned}
\tag{7.24}
$$

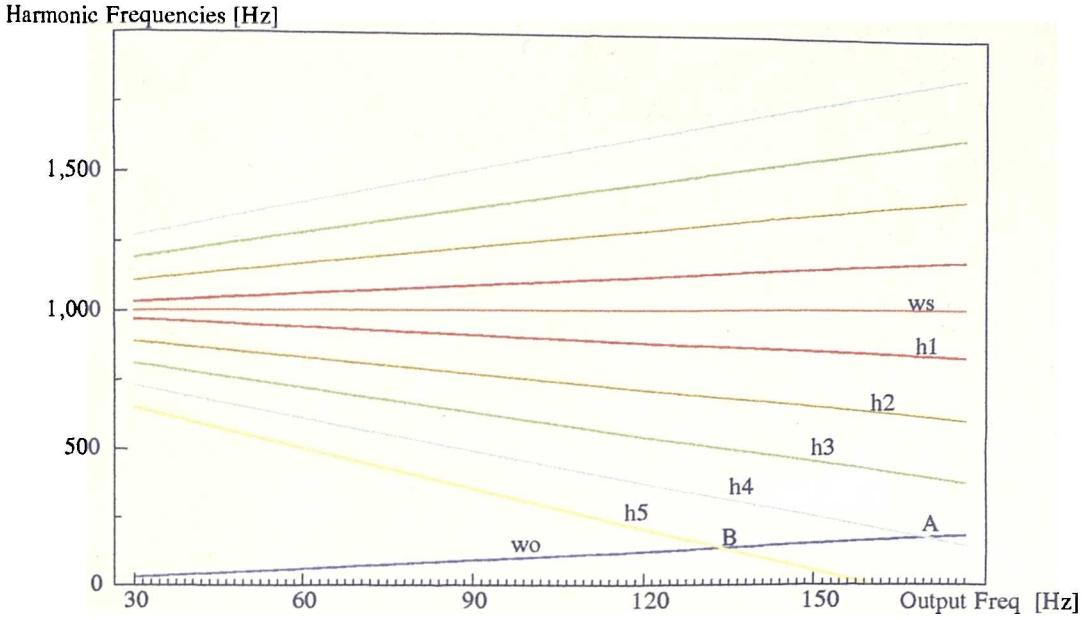


**Figure 7.2. The harmonics to the Switching Frequency**

From equation 7.24 the magnitude of any harmonic in the output voltage can be calculated. As can be seen from equation 7.24, the line to line output voltage frequency spectrum will consist of:

- The required output frequency
- Harmonics of the required output frequency
- The switching frequency
- Harmonics of the switching frequency
- Side bands of the switching frequency[1] relating to the output frequency and harmonics of the output frequency
- Side bands of the harmonics of the switching frequency relating to the output frequency and harmonics of the output frequency

---

[1] This phrase is used throughout this thesis to describe the harmonics which occur at frequencies described by $(\omega_s \pm n\omega_o)$.

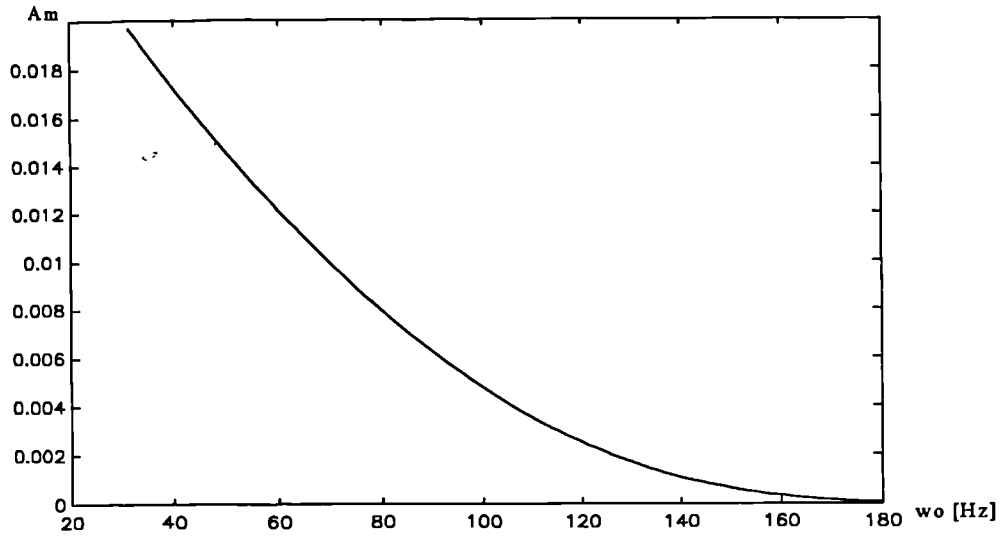


**Figure 7.3. The Magnitude of the Harmonic $h_4$ Against $\omega_0$**

Consider a matrix converter operating with a low switching frequency (for example 1kHz) and a high output frequency (for example 150Hz). In this situation the side bands of the switching frequency relating to the fourth and fifth order harmonics of the output frequency would be subharmonics of the output frequency. This effect is shown in figure 7.2.

To assess the effect of these subharmonics on the quality of the output voltage waveforms their magnitudes can be calculated. By inspection it can be seen from equation 7.24 that the maximum magnitude of these subharmonics will occur when the output frequency is set so that the frequency of the harmonic is equal to the required output frequency. For example the fourth and fifth side band harmonics of the switching frequency at points A and B in figure 7.2.

### 7.3.2 The Maximum Magnitude of the subharmonics of the Output Voltage Frequency in a matrix Converter Operating at a Low Switching Frequency

Consider the side band harmonic relating to the forth harmonic of the output frequency, $h_4$, as shown in figure 7.2. At a point A the output frequency is such that the harmonic will become a subharmonic of the required output frequency. Using equation 7.24 the magnitude of $h_4$ at this point can be calculated:

From figure 7.2, the output frequency at point A on $h_4$ can be found:

$$\omega_o = \omega_s - 4\omega_c + \omega_i$$
$$\omega_o = \omega_c - \omega_i$$

Therefore at point A:

$$\omega_c = 220Hz$$
$$\omega_o = 170Hz$$

If we assume that:

$$\omega_s = 1000Hz$$
$$\omega_i = 50Hz$$

Then the magnitude, $A_m$, of the harmonic relative to the output frequency magnitude at point A can be found:

$$A_m = \frac{\omega_s J_4\left[\frac{\pi\left(\omega_s - 4\omega_c\right)}{2\omega_c}\right]}{2\pi\left(\omega_s - 4\omega_c\right)}$$
$$= \frac{1000 J_4\left[\frac{\pi(1000-880)}{440}\right]}{2\pi(1000-880)}$$
$$= 7.96\times10^{-4}$$
$$= -32dB \qquad (7.25)$$

If the output frequency is increased above 170Hz then the frequency of the harmonic $h_4$ will reduce towards 0Hz and the value of the Bessel function in equation 7.25 will exponentially decrease to zero. The maximum magnitude of the given harmonic will therefore be the value found from equation 7.24. This effect is shown in the magnitude against output frequency plot given in figure 7.3.

If the above calculations are repeated for harmonic $h_5$ then the magnitude relative to the output frequency can be found for the point B in figure 7.2. This harmonic will also exponentially decease to zero as the output frequency is increased.

$$B_m = 0.187 \times 10^{-3} = -37dB \tag{7.26}$$

These subharmonics caused by the side bands of the switching frequency will therefore not have a large effect on the quality of the output waveforms, because *their magnitudes will be insignificant. As the order of the harmonics* increases, its magnitude will decrease. It can also be shown from equation 7.24 that as the switching frequency increases the magnitude of the possible subharmonics will also decrease.

### 7.3.3 The Extension of the Theory to Cover More Complex Control Algorithms

The above method can be extended using the principles of superposition to cover the complete frequency spectrum of a more complex control algorithm, such as that given in Chapter 2. The line output voltage waveform for this converter when using the extension of the above method is given in equation 7.27. In all cases the magnitude of these harmonics at the point they cross the output frequency is always the same order of magnitude or less than those given above. As the frequency of intercept decreases, the magnitude of the subharmonics will also exponentially decrease.

$$V_{ol}=\sum_{x=1}^{6}\beta_x\left[\begin{array}{l}\dfrac{\omega_s}{2\pi}\sum_{n=1}^{\infty}\dfrac{J_n\left[\frac{n\pi\omega_{cx}}{2\omega_s}\right]}{(n\omega_{cx})}\cos\left(n\omega_{cx}t-\omega_i t-\frac{n\omega_{cx}}{2\omega_s}-\frac{(n-1)\pi}{2}\right)\\ +\dfrac{1}{2\pi}\sum_{m=1}^{\infty}\dfrac{1-J_0\left[\frac{m}{2}\right]}{m}\cos(m\omega_s t-\omega_i t)\\ +\dfrac{\omega_s}{2\pi}\sum_{m=1}^{\infty}\sum_{n=\pm1}^{\pm\infty}\dfrac{J_n\left[\frac{\pi}{2\omega_c}(m\omega_s+n\omega_{cx})\right]}{(m\omega_s+n\omega_{cx})}\cos\left\{(m\omega_s+n\omega_{cx}-\omega_i)t-\dfrac{(m\omega_s+n+(n-1)\pi\omega_{cx})}{2\omega_{cx}}\right\}\end{array}\right]$$

Where: and:

$$\begin{aligned}\omega_{c1}&=\omega_o+\omega_i & \beta_1&=0.433\\ \omega_{c2}&=\omega_i-\omega_o & \beta_2&=0.433\\ \omega_{c3}&=4\omega_i & \beta_3&=0.125\\ \omega_{c4}&=-2\omega_i & \beta_4&=0.125\\ \omega_{c5}&=\omega_i+3\omega_o & \beta_5&=0.060\\ \omega_{c6}&=\omega_i-3\omega_o & \beta_6&=0.060\end{aligned} \qquad (7.27)$$

## 7.4 The Frequency and Magnitude of the Harmonics

### 7.4.1 Output Voltage Waveform

The model of the output waveform given in equation 7.27 was numerically analysed using a Matlab program. The result of this was a spectral map-like graph of the expected frequency harmonics. The spectral map shows a plot of frequency against magnitude against time. The output frequency is varied with time. These plots can then be compared to a spectral map obtained from measurements made on a real converter to check the validity of the mathematical model. Figure 7.4 shows the spectral map for one voltage output line obtained from a matrix converter operating under the algorithm set out in Chapter 2.

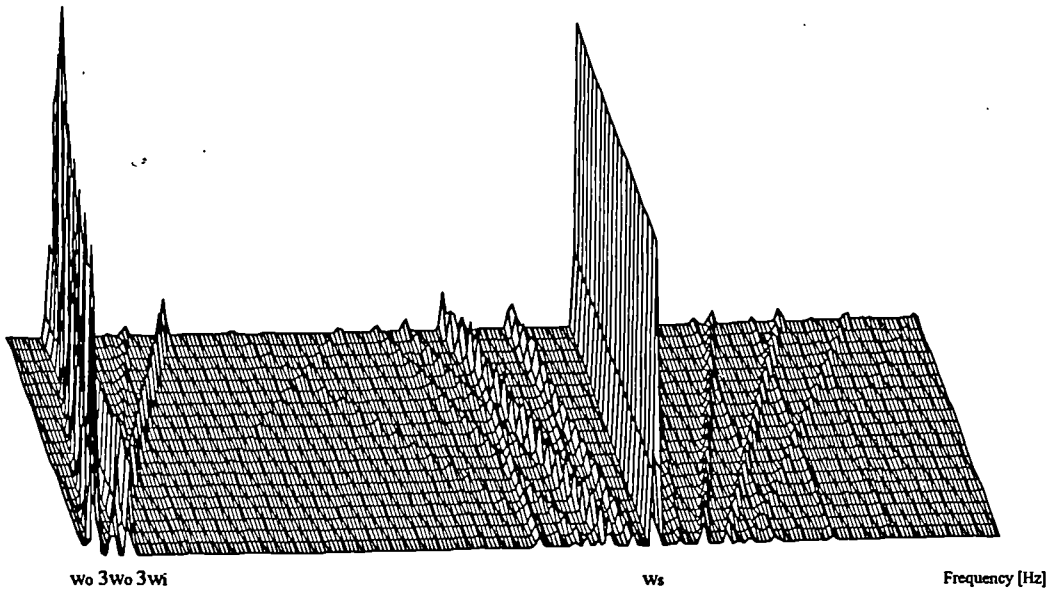


**Figure 7.4. A Spectral Map of the Output Line Voltage Created From the Mathematical Model**

A switching frequency of 1kHz was chosen to enable the output frequencies to be seen easily on the same axis as the switching harmonics. The plot shows an output frequency sweep from 30Hz to 180Hz. Only the first harmonic area of the switching frequency is shown, but the pattern will repeat with different magnitudes at $2\omega_S$, $3\omega_S$, etc.

### 7.4.2 Input Current Waveform

To investigate the switching frequency harmonics induced in the unfiltered input current of the matrix converter, the method used in equation 7.14 was adapted to produce a suitable mathematical model. The model of the input current is given in equation 7.28. This model assumes that a sinusoidal current is induced in the motor windings by the output voltage waveform from the matrix converter.

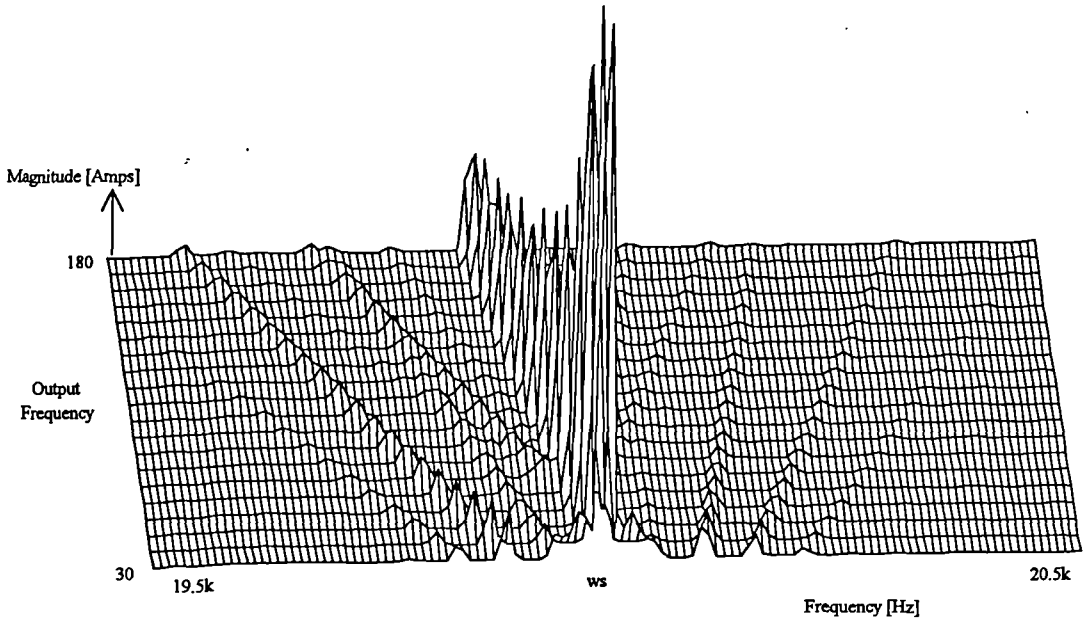


**Figure 7.5. A Spectral Map of the Harmonics to the Switching Frequency Input Line Current Created from the Mathematical Model**

$$I_{il} = \begin{bmatrix} F(t) & F(t+\frac{2\pi}{3}) & F(t+\frac{4\pi}{3}) \end{bmatrix} \begin{bmatrix} I\cos(\omega_i t) \\ I\cos(\omega_i t+\frac{2\pi}{3}) \\ I\cos(\omega_i t+\frac{4\pi}{3}) \end{bmatrix}$$

$$= \frac{I\omega_s}{2\pi}\sum_{n=1}^{\infty}\frac{J_n\left[\frac{n\pi\omega_{c1}}{2\omega_s}\right]}{(n\omega_{c1})}\cos\left(n\omega_{c1}t-\omega_o t+\frac{n\omega_{c1}}{2\omega_s}-\frac{(n-1)\pi}{2}\right)$$

$$+\frac{I}{2\pi}\sum_{m=1}^{\infty}\frac{1-J_0\left[\frac{m}{2}\right]}{m}\cos(m\omega_s t-\omega_o t)$$

$$+\frac{I\omega_s}{2\pi}\sum_{m=1}^{\infty}\sum_{n=\pm1}^{\pm\infty}\frac{J_n\left[\frac{\pi}{2\omega_{c1}}(m\omega_s+n\omega_{c1})\right]}{(m\omega_s+n\omega_{c1})}\cos\left\{(m\omega_s+n\omega_{c1}-\omega_o)t-\frac{(m\omega_s+n(1+\pi\omega_{c1}))}{2\omega_{c1}}\right\}$$

$$+\frac{I\omega_s}{2\pi}\sum_{n=1}^{\infty}\frac{J_n\left[\frac{n\pi\omega_{c2}}{2\omega_s}\right]}{(n\omega_{c2})}\cos\left(n\omega_{c2}t+\omega_o t+\frac{n\omega_{c1}}{2\omega_s}-\frac{(n-1)\pi}{2}\right)$$

$$+\frac{I}{2\pi}\sum_{m=1}^{\infty}\frac{1-J_0\left[\frac{m}{2}\right]}{m}\cos(m\omega_s t+\omega_o t)$$

$$+\frac{I\omega_s}{2\pi}\sum_{m=1}^{\infty}\sum_{n=\pm1}^{\pm\infty}\frac{J_n\left[\frac{\pi}{2\omega_{c1}}(m\omega_s+n\omega_{c2})\right]}{(m\omega_s+n\omega_{c2})}\cos\left\{(m\omega_s+n\omega_{c2}+\omega_o)t-\frac{(m\omega_s+n(1+\pi\omega_{c2}))}{2\omega_{c2}}\right\}$$

| Frequency, $f_S$ | Relative Magnitude |
|---|---|
| 50Hz | 1.000 |
| 20kHz | 0.667 |
| 40kHz | 0.068 |
| 60kHz | 0.061 |
| 80kHz | 0.018 |
| 100kHz | 0.021 |
| 120kHz | 0.008 |

**Table 7.1. Relative Maximum Magnitudes of the Input Current Switching Frequency Harmonics**

Where:

$$\omega_{c1} = \omega_o + \omega_i$$
$$\omega_{c2} = \omega_o - \omega_i \qquad (7.28)$$

The Matlab program was modified to produce a spectral map for this input current waveform. The output frequency was increased from 30Hz to 180Hz. The switching frequency was set at 20kHz with an input frequency of 50Hz. The spectral map for the switching frequency and it's side band harmonics is shown in figure 7.5. The pattern for higher order harmonics of the switching frequency is similar but with lower magnitudes, as shown in table 7.1.

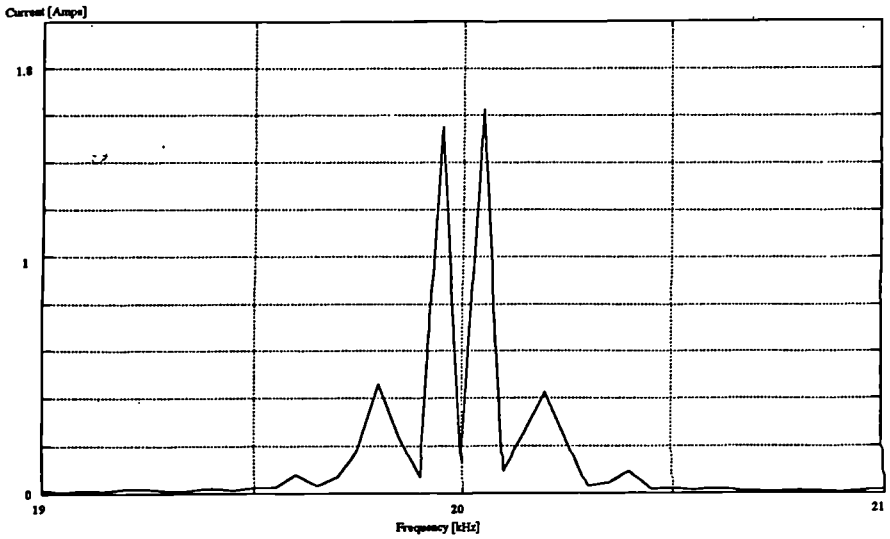


**Figure 7.6. The Input Line Current Spectra of the Harmonics to the Switching Frequency Created from a Computer Simulation, fo=30Hz**

The spectra of the harmonics to the switching frequency in the input current can also be obtained using a computer simulation. These simulation results have been obtained using the ACSL simulation program. The simulated spectral map for the same conditions as the mathematical model in figure 7.5 is shown in figure 7.6. As can be seen, there is a very good correlation in the frequency and magnitude of the mathematical model and the simulation results. The simulation results for the of the input current spectrum, for a complete frequency range up to 60kHz, is shown in *figure 7.7.*

These results have been verified against practical results from a matrix converter capable of driving a 5kWatt motor (The operation of this converter will be examined more fully in Chapter 9). The spectrum of the switching frequency and it's side band harmonics in the input current to this mains voltage converter is shown in figure 7.8. Again, good correlation can be found between this result and the predicted spectra shown in figures 7.5 and 7.6. The complete spectrum which relates to the simulated results in figure 7.7 is given in figure 7.9.

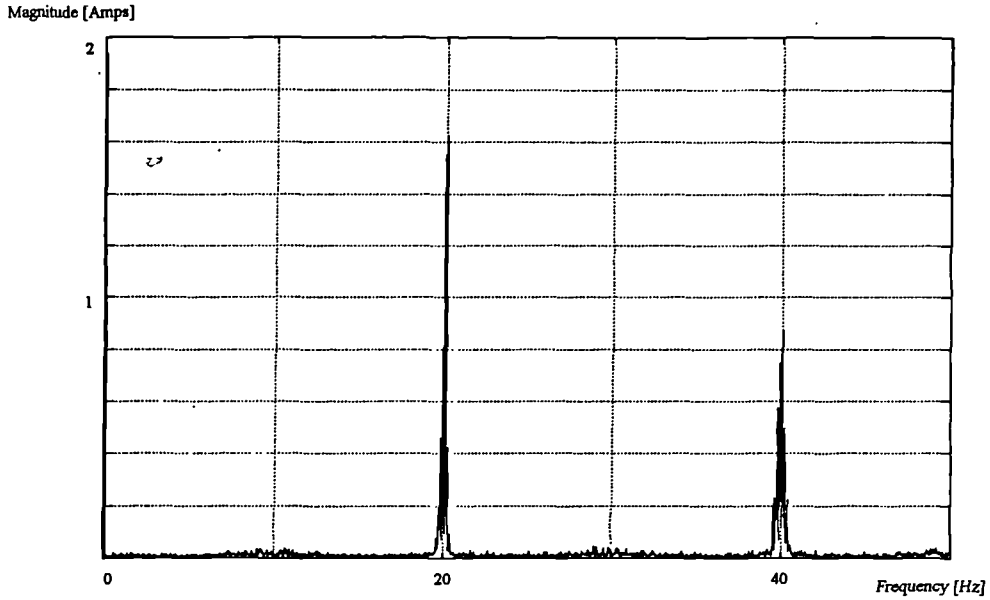


**Figure 7.7. The Input Line Current Spectra of the Created Using the Computer Simulation**

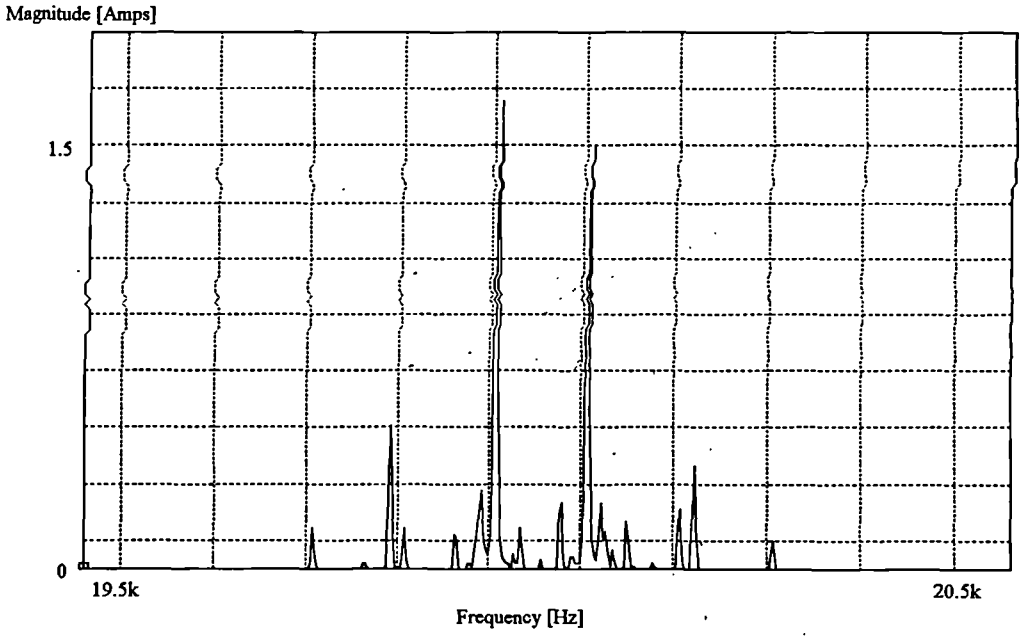


**Figure 7.8. The Input Line Current Spectra Showing the Harmonics to the Switching Frequency for a 5kWatt Matrix Converter. fo=30Hz**

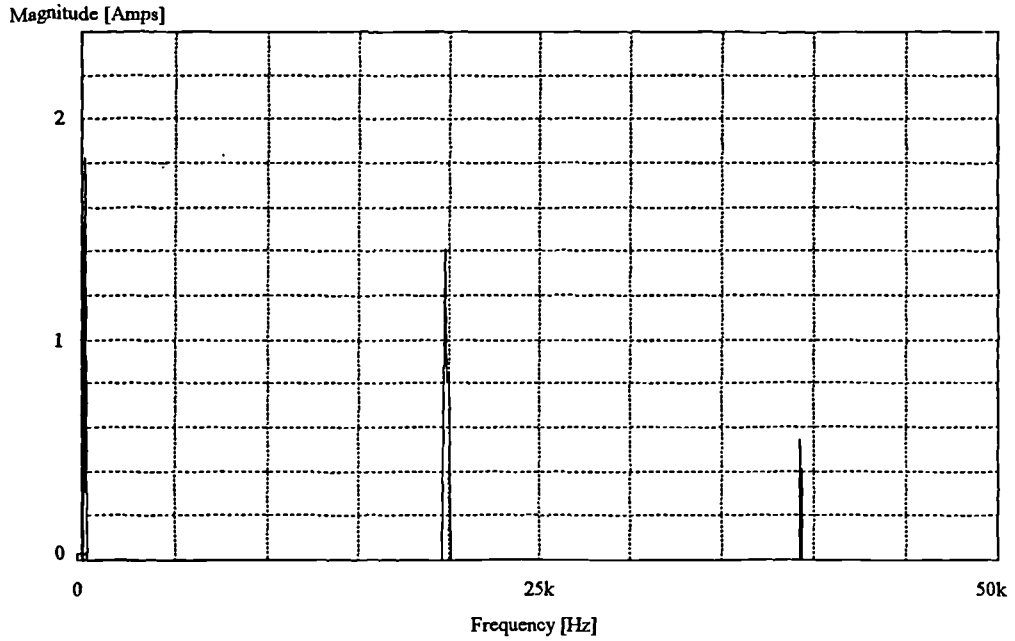


**Figure 7.9. The Input Line Current Spectra for a 5kWatt Matrix Converter**

## 7.5 Conclusions

This chapter has presented a method of mathematically modelling the harmonics generated due to the switching frequency in a matrix converter. The method has been used to assess possible subharmonics of the output frequency at low switching frequencies. These subharmonics have been found to have negligible effect.

The mathematics has also been extended to allow models of the line output voltage and the input current waveforms to be examined. The results obtained have been plotted in a similar form to a spectral map for a sweep of output frequency using the Matlab mathematical analysis package. The boundary conditions for the integrals may be changed to allow other switching strategies to be modelled. In this way the effect of semi-symmetrical switching patterns may be analysed.

The results obtained from the mathematical model have been compared with results obtained using simulations of the matrix converter. These simulations have been

found to agree very closely with the mathematical results. Both the mathematical and simulation results have also been compared to the results obtained from an experimental 5kWatt matrix converter. Again the results have been found to be consistent.

# Bibliography


[1] Mullion E.B., Pye D.R. and Southwell R.V., "Bessel Functions For Engineers", Mc.Lachlan, Oxford, 1961.

[2] Carrara G., Gardella S., Marchesoni M., Salutari R. and Sciutto G., "A New Multilevel PWM Method: A Theoretical Analysis", IEEE Transactions on Power Electronics, Vol.7, No.3, July 1992, pp.497-505.

[3] Patel H.S. and Hoft R.G., "Generalised Techniques of Harmonic Elimination and Voltage Control in Thyristor Inverter: Part 1 - Harmonic Elimination", IEE Transactions on Industrial Applications, Vol.1A-9, 1973

[4] Matlab User's Manual.

[5] Black H.S., "Modulation Theory", Van Nostrand, New York, 1953.

# Chapter 8

# *The Input Filters*

## 8.1 Introduction

This chapter looks at the requirements of the input filters of a matrix converter. The effect of the input filter on the performance of the matrix converter is considered. Also, the effects on the input current from the mains supply are examined and discussed with regards to existing and possible future regulations. Consideration is given to a converter in both motoring and regenerative modes. An explanation of the unique aspects of a matrix converter complying with conductive EMC regulations is given.

The unfiltered input current to a matrix converter consists of the fundamental input frequency and its associated harmonics, harmonics around the switching frequency and the harmonics of the switching frequency as discussed in Chapter 7. The frequencies of interest in the design of the input filters are components in the regions of the switching frequency and its harmonics. For a matrix converter operating at a switching frequency of $f_s$ the frequency regions of interest will be around $f_s$, $2f_s$, $3f_s$, $4f_s$,etc. A switching frequency of 20kHz was chosen for the initial matrix converter design.

If the supply voltage has no unwanted harmonics and is balanced then a matrix converter will draw insignificantly low harmonic currents related to the fundamental frequency. The permitted levels for these harmonics are set out by the Electricity Association [1]. It has been shown that the 3rd, 5th, etc. harmonics of the input current are at a very low level in comparison to the fundamental in a practical matrix converter. Due to the low level of these harmonics in an ideal matrix converter the recommendations for these harmonics will easily be met. They will therefore not be considered any further in this chapter.

## 8.2 The Regulations

### 8.2.1 The New EEC Regulations

The current EEC regulations on this issue came into force in all member states on January 1st 1992, although they will be operating alongside any existing regulations until January 1st 1996. After January 1st 1996 all equipment sold must comply with European Directive number 89/336/EEC. These regulations deal with harmonics of the fundamental current frequency up to 2.5kHz and with frequencies that may interfere with radio communications in the frequency range 150kHz to 30MHz. This Radio Frequency Interference (RFI) range is dealt with in the regulations set out in EN55011. These ranges give an unregulated band between 2.5kHz and 150kHz. There is a statutory duty in this frequency range not to interfere with anybody else's equipment under the Wireless and Telegraph Act [2]. EN55011 also states that the frequency range between 10kHz and 150kHz is under review. The regulations are summarised in table 8.1.

### 8.2.2 Possible Future Developments in the Regulations

*It is possible that future developments in communications may utilise* parts of the spectrum from 50kHz to 150kHz to communicate along existing mains cabling in houses and offices. These communications could be used for a range of applications such as wireless connections between computers and printers; remote baby listening devices; and remote reading of electricity meters. Future technologies are likely to take advantage of this under-utilised communication resource. The regulations in this area are therefore likely to be considered by the EEC in the near future. The filtering of the switching frequency harmonics generated by a matrix converter therefore warrants investigation. The viability of the matrix converter may depend on the effects any future legislation in this area has on the input filter requirements.

| Regulation | Dates Applicable | Country |
|---|---|---|
| BS800 | Until 1-1-96 | UK. |
| VDE0871-1 | Until 1-1-96 | Germany |
| EN55011 | Optional until 31-12-95<br>Compulsory from 1-1-96 | All EEC Member Countries |

**Table 8.1. A Summary of the European Regulations**

## 8.3 Application of Regulations to a Matrix Converter

### 8.3.1 The Standards for the 10kHz to 150kHz Frequency Range

The current European and British Standards for allowable distortion of the input voltage are shown in figures 8.1 and 8.2. The German VDE0871 part 1 defines the acceptable levels for these switching frequency harmonics as shown in figure 8.3. These German regulations may form the basis for future EEC regulations in the 10kHz to 150kHz frequency range. For the purpose of this chapter we will consider the implementations of a matrix converter complying with this German standard.

If the converter was used in regenerative mode then the switching frequency harmonics would still be being circulated in the input filter in the same way as in motoring mode. The regulations for harmonics of the input frequency would still apply as defined in G5/3 [1]. These regulations set out the size of any harmonics of the input frequency that may be generated. However the levels of inter-harmonics that may be generated are comparatively high because they are unlikely to have a cumulative effect.

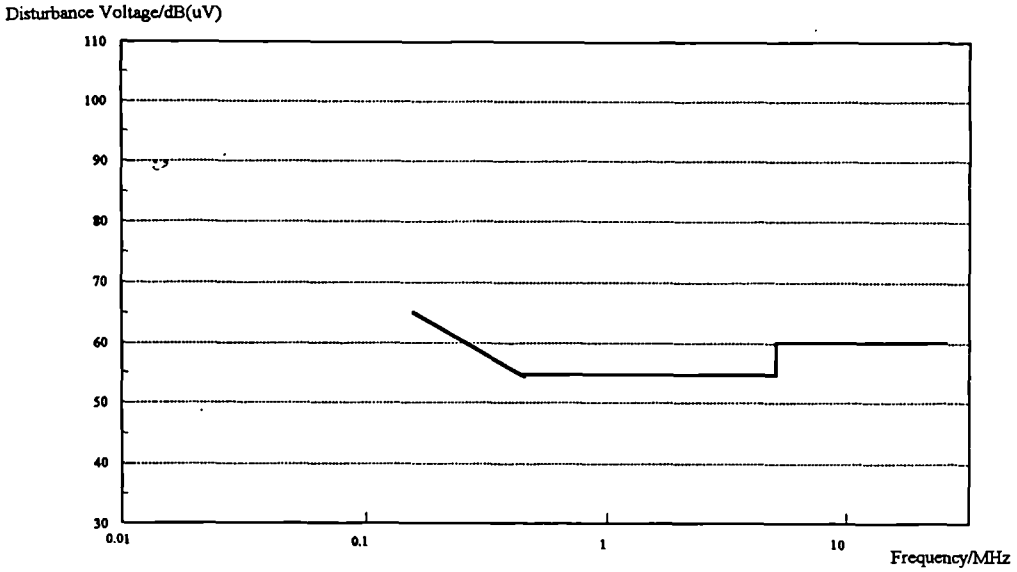


**Figure 8.1. British Standard for Interference Limits, BS800**

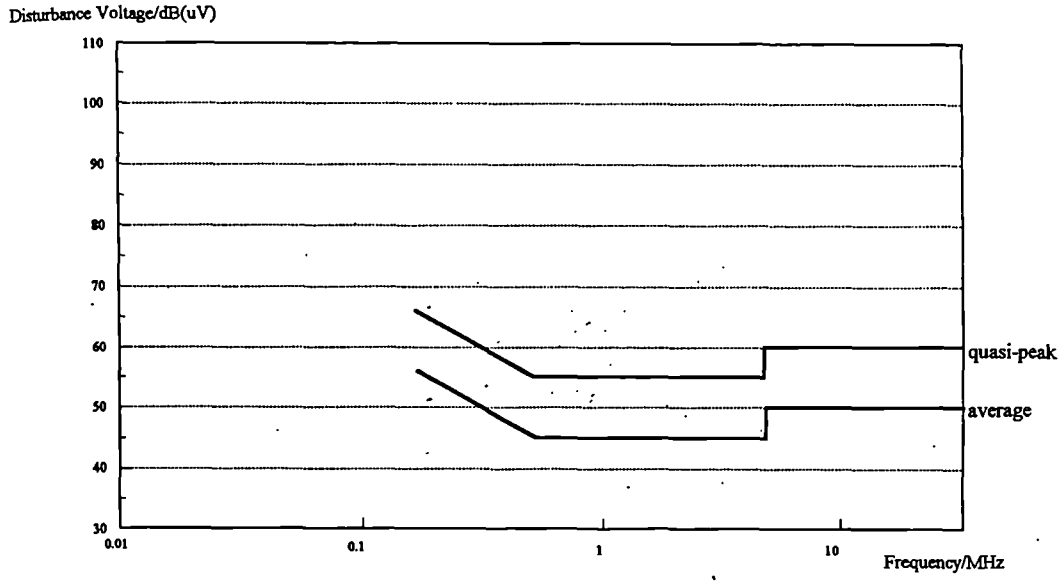


**Figure 8.2. The European Standard for Voltage Disturbance Limits, EN55011**

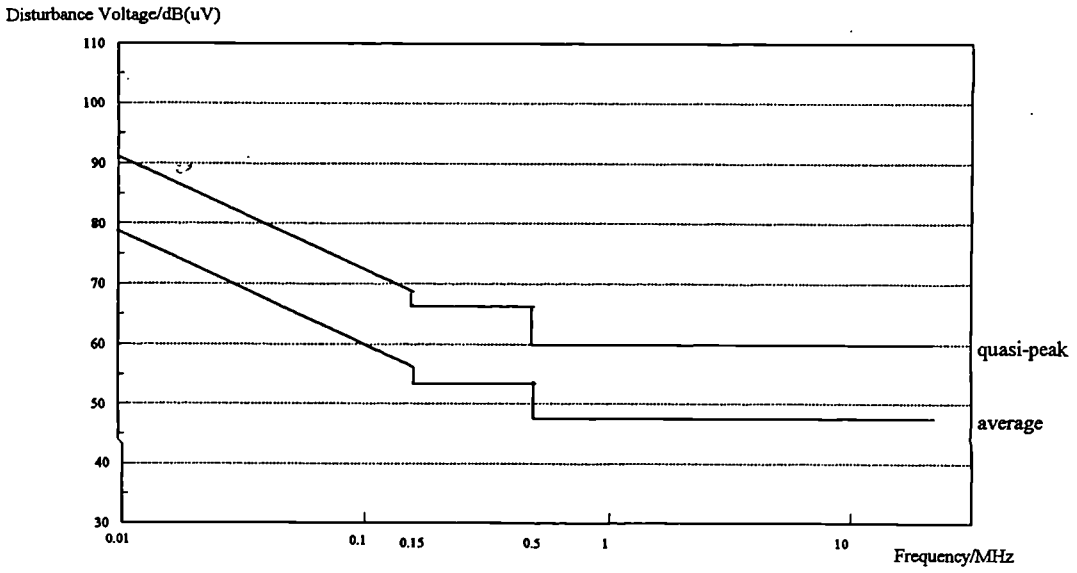


**Figure 8.3. VDE 0871 Part1, Recommended Disturbance Voltage Limits**

### 8.3.2 Implications of Complying with the Recommendations of VDE0871-1

If we consider a matrix converter operating at 20kHz, then it is possible to calculate the relative magnitudes of the switching frequency harmonics under worst case conditions, as described in Chapter 7. These harmonics will be in the differential mode. If we consider the limits described in figure 8.3, then the allowable levels of input current to the converter at these frequencies may be calculated for a given converter output power rating. From these allowable levels of input, current distortion the required attenuation of the input filters at these switching frequency harmonics may be calculated.

| Frequency, $f_S$ | Relative Magnitude |
|---|---|
| 50Hz | 1.000 |
| 20kHz | 0.667 |
| 40kHz | 0.068 |
| 60kHz | 0.061 |
| 80kHz | 0.018 |
| 100kHz | 0.021 |
| 120kHz | 0.008 |
| 140kHz | 0.0100 |
| 160kHz | 0.0050 |
| 180kHz | 0.0060 |
| 200kHz | 0.0065 |

**Table 8.2. Relative Maximum Magnitudes of the Switching Frequency Harmonics**

## 8.4 Calculating the Required Filter Attenuation

The filter attenuation may be calculated by finding the magnitude of the input current harmonics. These magnitudes can then be compared to the magnitude of the maximum harmonic current that may be drawn from the supply to keep within the disturbance voltage limits.

### 8.4.1 The Magnitude of the Harmonic Currents

Consider a matrix converter with a maximum input current of $I_i$. The largest switching frequency current harmonics around the switching frequency, $I_{fs}$, would have a maximum magnitude of $0.66 I_i$ Amps as shown in table 8.2. This maximum value occurs when the output frequency is zero at maximum input current. This worst case situation is therefore assumed for the input filter calculations in this chapter. The value of this maximum switching frequency harmonic current may be found by evaluation of the appropriate Bessel Function, as described in Chapter 7.

### 8.4.2 The Allowable Harmonic Disturbance Voltage

At 20kHz the recommended maximum disturbance voltage is 0.02Volts. This disturbance voltage is measured in terms of Quasi-peak with a bandwidth of 200Hz, as defined in [5], but for the purpose of this approximate study it will be assumed to be equal to the peak level at any given frequency. The assumption is made that the impedance of the supply can be considered as a 50Ω resistor in parallel with a 50μH inductor [5]. The level of disturbance current that may be drawn from the supply, $I_{i,disturbance}$, can be calculated:

$$I_{i,disturbance} = \frac{V_{disturbance}}{\left(\frac{1}{50} + \frac{1}{j2\pi f_s 50\times10^{-6}}\right)} Amps \tag{8.1}$$

### 8.4.3 The Required Filter Attenuation

To achieve this level the input filter must reduce the switching frequency current drawn from the supply to this level. The required filter attenuation at 20kHz may then be calculated:

$$A_{filter,20kHz} = 20\log\left(\frac{I_{fs}}{I_{i,disturbance}}\right) dB \tag{8.2}$$

This procedure may be repeated for $2f_s$, $3f_s$ and so on, although the magnitudes reduce as the frequency increases, the recommended magnitudes of the harmonics also decrease. The maximum magnitudes for these switching frequency harmonics for a switching frequency of 20kHz are shown in table 8.2. This information can then be used to develop the required filter characteristics for a given size of matrix converter.

Consider a matrix converter with a line input current of 6.5Amps, then the maximum switching frequency harmonic near 20kHz will have a magnitude of 4.3Amps. Using equation 8.1 it can be found that the maximum allowable disturbance current at this frequency will be $3{\cdot}4\times10^{-3}Amps$. Using equation 8.2 the required filter attenuation is then found to be 62dB. Repeating this procedure for 40kHz, 60kHz, etc. will enable the required filter attenuation to be calculated, as shown in table 8.2. The magnitude of the disturbance voltage created by an unfiltered matrix converter is shown in figure 8.4. The minimum required filter attenuation characteristics can then be drawn as shown in figure 8.5. The filtering is only required to reduce harmonics around the switching frequency and its harmonics. These harmonics have a maximum value as shown in figure 8.4, and have a band width that is dependant on the input and output frequencies as shown in [5].

## 8.5 Filter Configurations

If we consider filtering the differential mode switching frequency harmonics discussed above then we will require line-to-line filters designed to meet the attenuation characteristics shown in figure 8.5. These filters can be considered as circulating the switching frequency currents between the input lines.

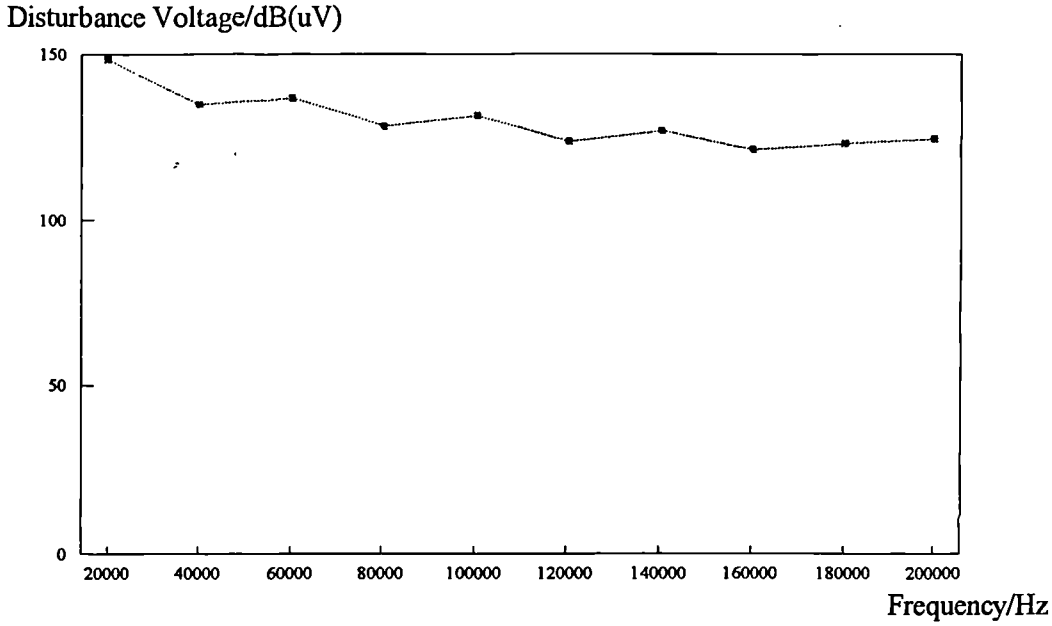


**Figure 8.4. The Magnitude of the Disturbance Voltage for an Unfiltered Converter**

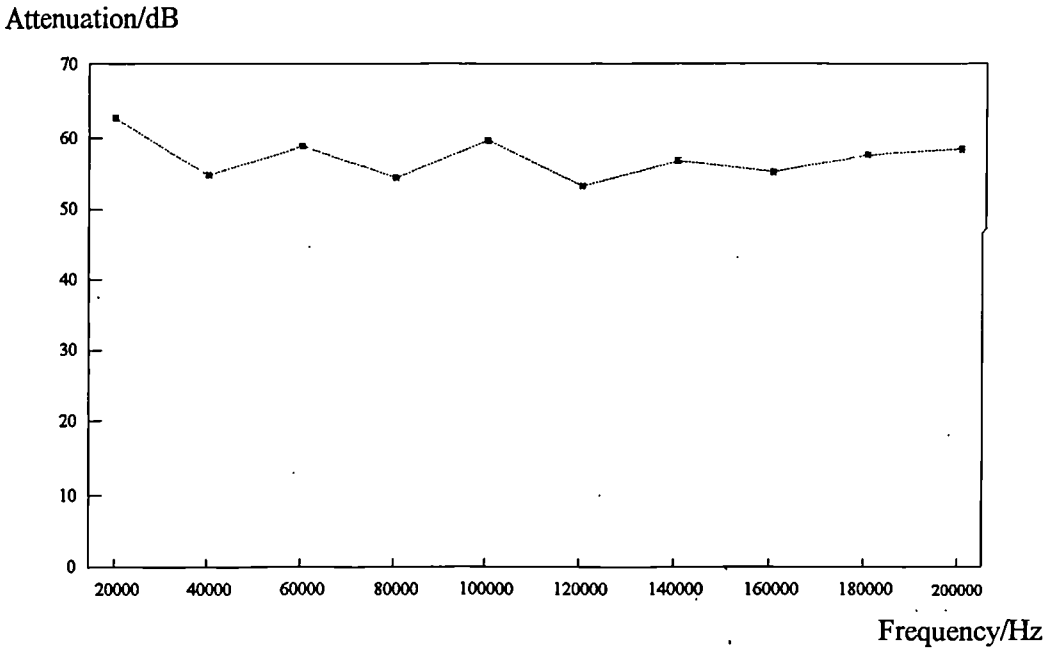


**Figure 8.5. The Required Filter Attenuation at the Switching Frequency Harmonic Frequencies**

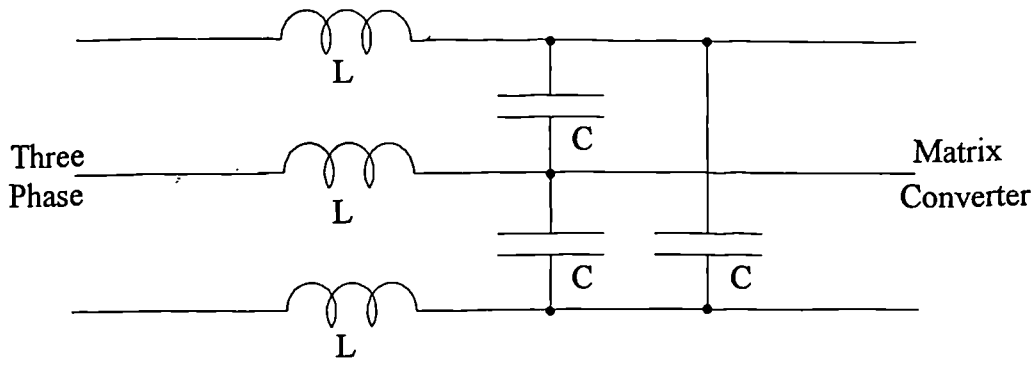


**Figure 8.6. LC Line to Line Filter**

### 8.5.1 Single Stage LC Low Pass Filter

The simplest and most widely used form of input line filter would be a simple LC filter, as shown in figure 8.6. At the frequencies of interest we are able to assume that these components will behave as ideal components and therefore we can ignore all parasitic components of the inductors and capacitors in the analysis. The ratio of the input voltage to output voltage is given in equation 8.3.

$$\frac{V_i}{V_o} = \frac{1}{1-\omega^2 LC + \frac{j\omega L}{Z_L}} \tag{8.3}$$

If we ignore the last term of the denominator, because it will be insignificant at the frequencies of interest, then this equation may be simplified:

$$\frac{V_i}{V_o} = \frac{1}{1-\omega^2 LC} \tag{8.4}$$

This equation is shown graphically, for a resonant frequency of 2kHz in terms of attenuation, in figure 8.7. As can be seen from this graph, a one stage LC filter of this kind would not be capable of the required attenuation around 20kHz, although the filter would provide sufficient attenuation at 40kHz. However, if the resonant frequency of the filter was lowered to achieve the required attenuation, the components would be large and uneconomical. A possible solution to this would be to provide a multi-stage LC filter. Possible component values for this filter are shown in table 8.3.

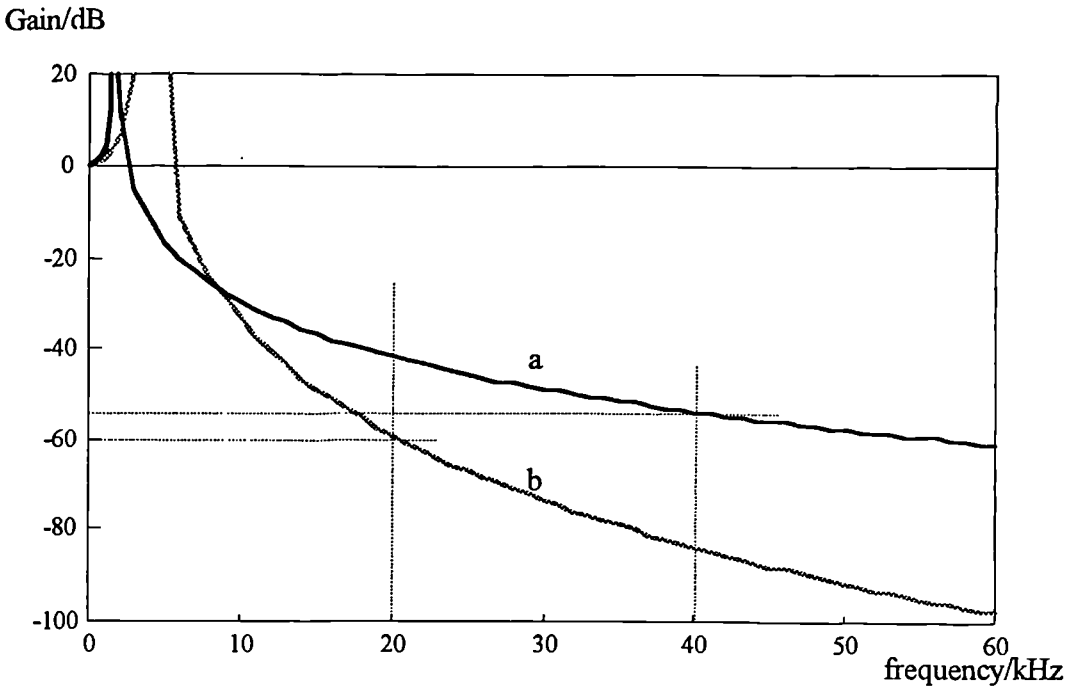


**Figure 8.7. The Attenuation Characteristics for LC Filters**
a. Single Stage LC Filter b. Two Stage LC Filter

### 8.5.2 Multi-Stage LC Low Pass Filter

A multi-stage filter would require more components, but the total value of the components could be smaller whilst still providing greater attenuation at lower frequencies. A two-stage filter using the same total inductance and capacitance as in the single-stage filter example is shown in figure 8.8. This filter would have an approximate attenuation characteristic as shown in figure 8.7b. The attenuation characteristic shows that this type of filter would have just enough attenuation at the critical frequency of 20kHz. The two stage filter would also have the advantage of a higher self resonant frequency for the same attenuation at 20kHz. For the purpose of the converter example considered earlier in this chapter this solution would seem viable.

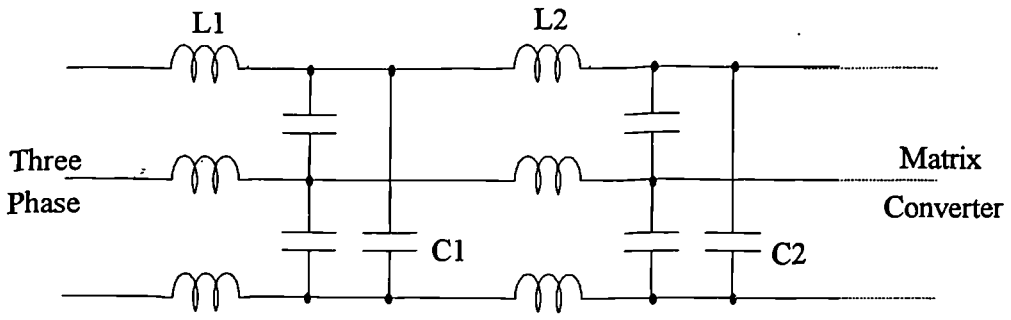


**Figure 8.8. Multi-stage LC filter Circuit**

A variation on the two stage filter is a pi-filter. The inductance in the input line is then used as the first inductor in the filter. Unfortunately, in a matrix converter the second break frequency of this filter would only be useful if an uneconomically large value of capacitance was used.

### 8.5.3 Low Pass Filter With Added Harmonic Current Diversion

For higher power converters or converters that may require a higher filter resonant frequency, it may be necessary to increase the order of the multi-stage filter. A possible alternative to this increase in size and complexity of the filter may be to provide a short circuit path for these unwanted lower order switching frequency harmonics along with the low pass single stage LC filter. A circuit for this type of filter is shown in figure 8.9.

The series line-to-line LC combination may be tuned to the frequency of the unwanted switching frequency harmonics whose level is greater than the regulations will allow if a single-stage LC filter is used alone. In the example shown in figure 8.9, this series LC path would be tuned to the switching frequency of 20kHz. The attenuation characteristics of such a filter would take the form shown in figure 8.10. The characteristic shows that this modified circuit would provide sufficient attenuation at 20kHz as well as at 40kHz.

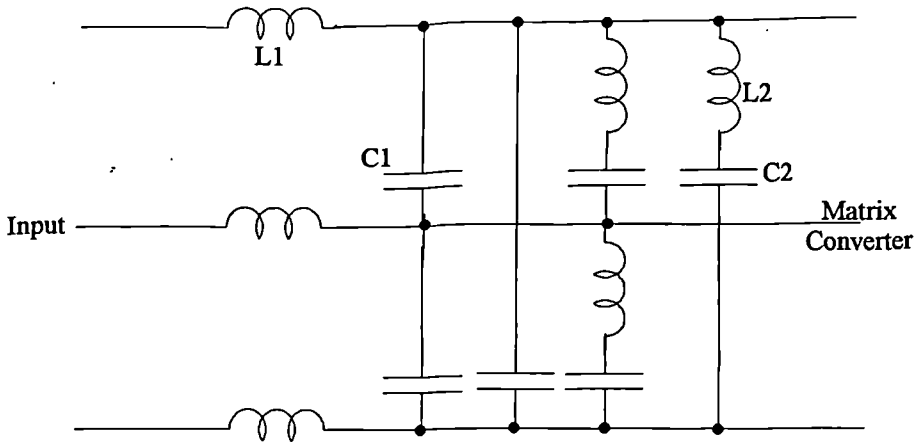


**Figure 8.9. LC Line to Line Filter With Added Harmonic Diversion**

## 8.6 Filter Costs

### 8.6.1 The Comparative Component Costs of the Filters

Calculating the comparative costs of the components for the filters is complex, due to the large number of contributory factors. In an attempt to make cost comparisons between the various possible filter configurations, it has been assumed that the cost and size of a comparable component is proportional to the component's power rating. The cost of inductive power has been taken as twice as much as capacitive power.

Using these assumptions, it is then possible to calculate the approximate comparative costs of the three filters described above using a normalised cost factor - as shown in equation 8.5. The result of this equation on the three types of filter is shown in figure 8.11. From this graph it is possible to pick component values from within a suitable range to achieve the most economical filter design. The component sizes for the example used in this chapter are given in table 8.3.

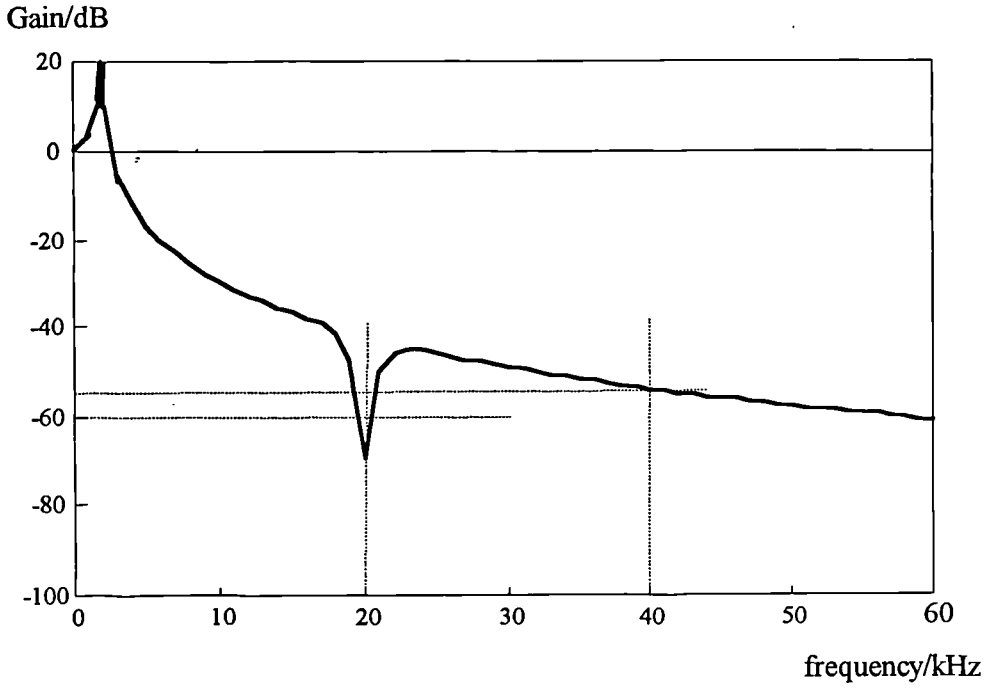


**Figure 8.10. The Attenuation Characteristics for a Low Pass LC Filter With a 20kHz Short Circuit Path**

$$Cost\ Factor = 2.05\left\{2\sum_{n=1}^{n=\infty} L_n I_{n,rms}^2 + \sum_{m=1}^{m=\infty} C_m V^2\right\} \tag{8.5}$$

Where: V = input voltage,

$I_{rms}$ = total input current

The converter side components used in such a filter would require a ripple current rating that would allow them to carry the switching frequency currents. These currents may be considered as approximately the same as the unfiltered switching frequency currents described in Table 8.2. The series inductance of such capacitors is about 30nH [12], and therefore would have a self resonance frequency of about 1MHz, which is well above the frequencies of interest.

| Filter Type | Inductance | Capacitance | Cost Factor |
|---|---|---|---|
| Single Stage LC[1] | 3mH | 1.5μF | 1 |
| Single stage LC<br>with 20kHz Diversion | 3mH<br>0.5mH | 1.5μF<br>0.16μF | 1.07 |
| Two Stage LC | 2mH<br>2mH | 1μF<br>1μF | 1.35 |
| LC capable of -60dB<br>at 20kHz | 11mH | 6μF | 3.74 |

**Table 8.3. Component Values for the Three Considered Types of Filter**
(Based on a Converter with an Input Line Current of 6.5Amps at 415Volts)
([1] does not meet required attenuation at 20kHz)

### 8.6.2 The Effect of Switching Frequency on the Size of the Input Filters

As the switching frequency is lowered, the input filter size will increase. This can be shown by calculating the cost of the filter required to meet the regulations at different converter switching frequencies. At switching frequencies below 10kHz the first switching frequency harmonic above 10kHz has been considered. The graph of switching frequency against filter cost is shown in figure 8.12. The cost factor is calculated using equation 8.5. As can be seen from this graph, the cost and size of the input filter increases dramatically as the switching frequency is lowered.

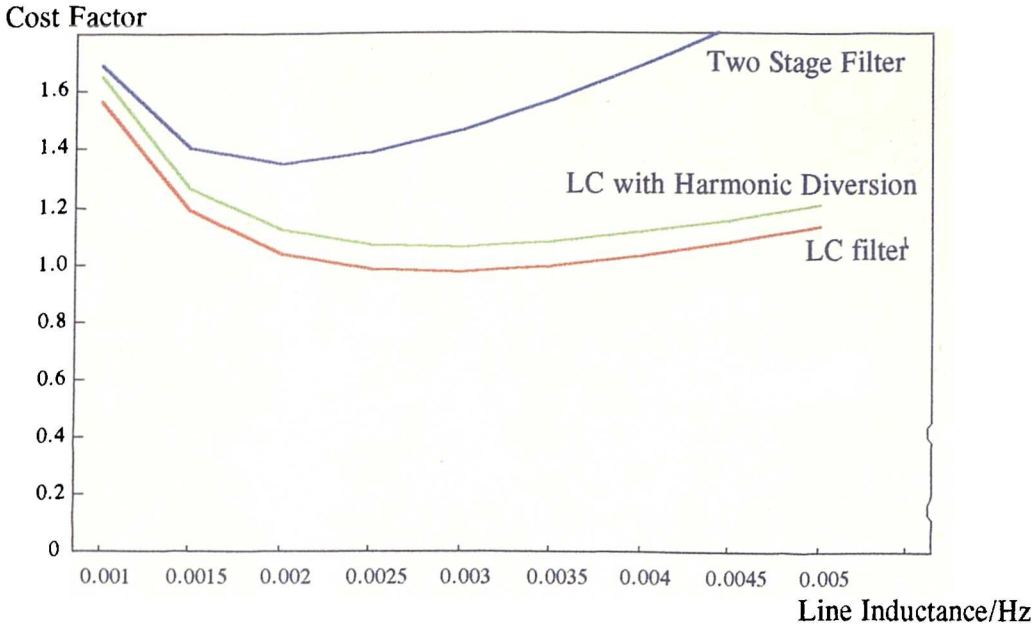


**Figure 8.11. A Graph of Comparative Filter Costs Against Inductor Size**
(The Component Values For the Harmonic Diversion Components are Optimal)
([1] Does not meet regulations at 20kHz)

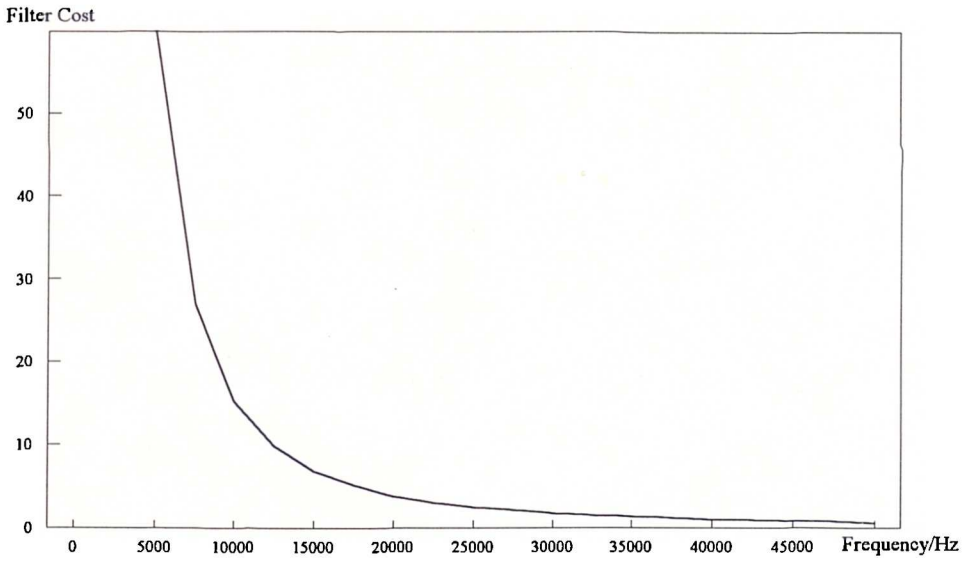


**Figure 8.12. The Effect of Switching Frequency on the Comparative Cost of the Input Filter**

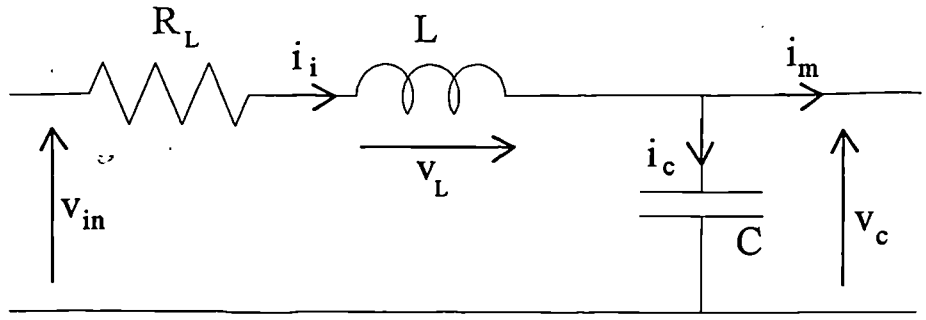


**Figure 8.13. A Single Phase LC Filter**

The information from figure 8.12 would suggest that the highest switching frequency possible should be used for the converter. However, as the switching frequency increases, the switching losses in the IGBTs will increase, as shown in figure 6.5. The switching frequency may also be limited by the capabilities of the converter's chosen microcontroller. A trade off must be made between the converter losses, with the extra heatsink costs, and the cost and size of the input filters. It should be noted that the converter switching losses are proportional to the switching frequency, whilst the input filter size is an inverse square function of the switching frequency.

## 8.7 The Effect of Filter Phase Lag and Self Resonance

This section examines the non-ideal properties of an input filter that may have a detrimental effect on the operation of a matrix converter. When reactive components are place in a power circuit a phase shift between the voltage and current may occur. The input filter of a matrix converter will exhibit this characteristic and therefore the magnitude of this phase shift should be considered. LC-type filters also exhibit self resonance at a given frequency. The effect of this resonance and possible solutions will therefore be considered.

### 8.7.1 Filter Phase Lag

The inclusion of the filter into the matrix converter structure will cause an additional phase shift between the input voltage and current waveforms at the fundamental input frequency. This phase shift will change the input displacement factor seen by the mains supply to the converter.

Consider a single phase LC low pass filter as shown in figure 8.13. If the matrix converters input displacement factor is assumed to be unity, then the impedance of the filter capacitor and the impedance of the load, $g_m$. The basic LC filter can be analysed as shown below. The phase shift can then be calculated as shown in equation 8.7.

From figure 8.13 it can be seen that:

$$\begin{aligned} i_i &= i_c + i_m \\ v_{in} &= v_r + v_L + v_c \end{aligned} \tag{8.6}$$

Rearranging and rewriting equation 8.6:

$$\begin{aligned} L\tfrac{di_i}{dt} &= -i_i R_L + v_{in} - v_c \\ C\tfrac{dv_c}{dt} &= i_i - i_m \\ j\omega L\dot{I}_i &= \dot{V}_{in} - \dot{I}_i R_L - \dot{V}_c \\ j\omega C\dot{V}_c &= \dot{I}_i - \dot{I}_m \end{aligned}$$

Therefore:

$$\frac{\dot{I}_i}{\dot{V}_{in}} = \frac{j\omega C + g_m}{j\omega L R_L + \left(1 + \omega^2 LC\right)} \tag{8.7}$$

Where: $g_m = \dfrac{\dot{I}_i}{\dot{V}_{in}}$

For the filter component values assumed in the chapter it can be seen that the phase lag will be very small if the motor is not lightly loaded, as shown in equation 8.8.

If: L=2mH, C=2.2μF, $R_L$=0.1Ω and $g_m$=0.04

Then: $$\frac{\dot{I}_i}{\dot{V}_{in}} = 0.04\tan\left(0.03^\circ\right) \tag{8.8}$$

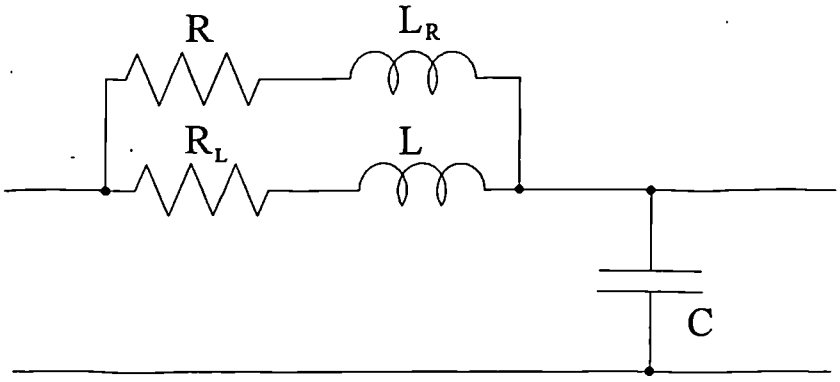


**Figure 8.14. A Single Phase LC Filter with Real Damping Resistor**

### 8.7.1 Reducing the Effect of Filter Resonance

The input filter will have a frequency or frequencies at which self resonance will occur. This unwanted resonance will cause unwanted noise on the input waveform. To reduce the effect of this resonance it may be necessary to implement a damping circuit for the filter. A possible solution for a single phase filter is shown in figure 8.14. The principle can be easily extended to a three phase converter.

The performance of this damping circuit can be seen by examining the filter characteristics. A comparison between the characteristics of an undamped filter and filter with a 100Ω damping resistor is shown in figure 8.15. It should be noted that the inclusion of this resistor decreases the filter attenuation at higher frequencies. If a small line inductance in the resistive loop is provided then this resistive current path will have a higher attenuation at higher frequencies. The effect of adding a small inductor in this resistive path is shown in figure 8.16. This inductance could be added by using a wire wound resistor that would naturally have a small amount of line inductance.

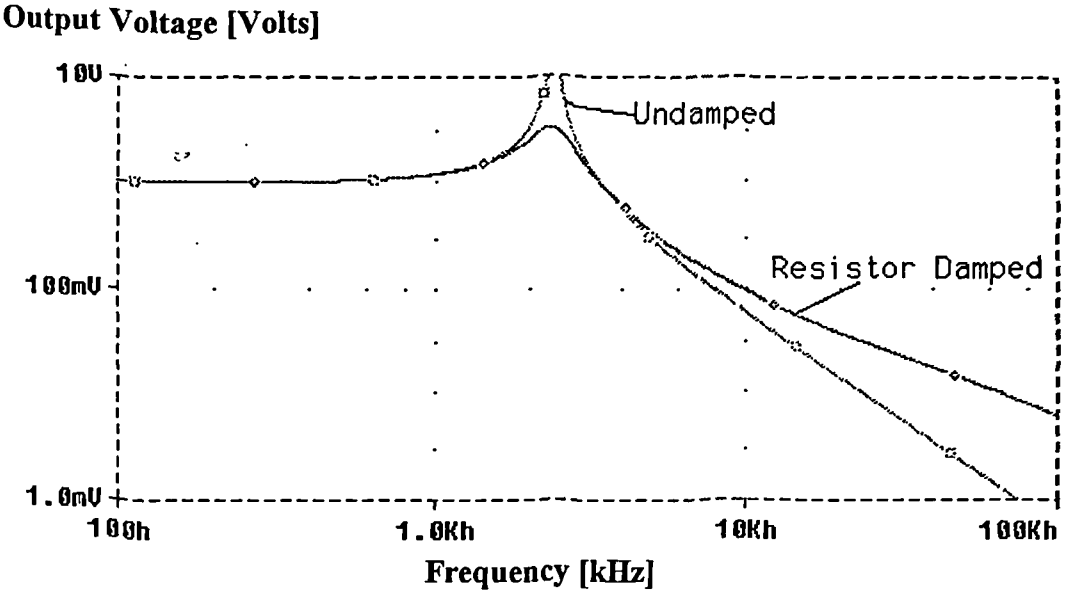


**Figure 8.15. Filter Characteristics for a Resistance Damped and an Undamped LC Filter**

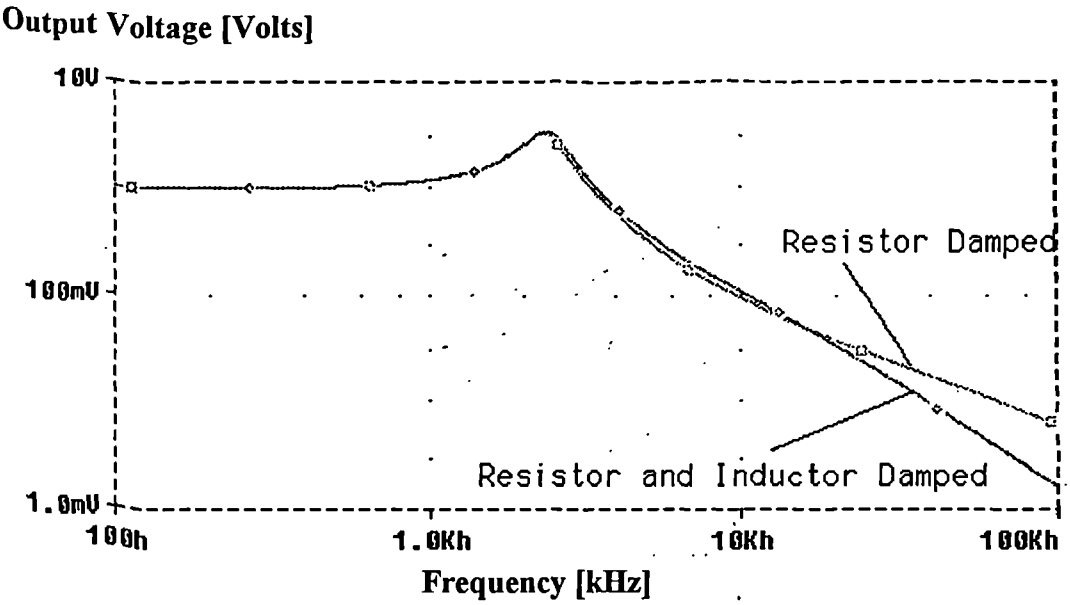


**Figure 8.16. Filter Characteristics for a Resistor Damped and a Inductor and Resistor Damped LC Filter**

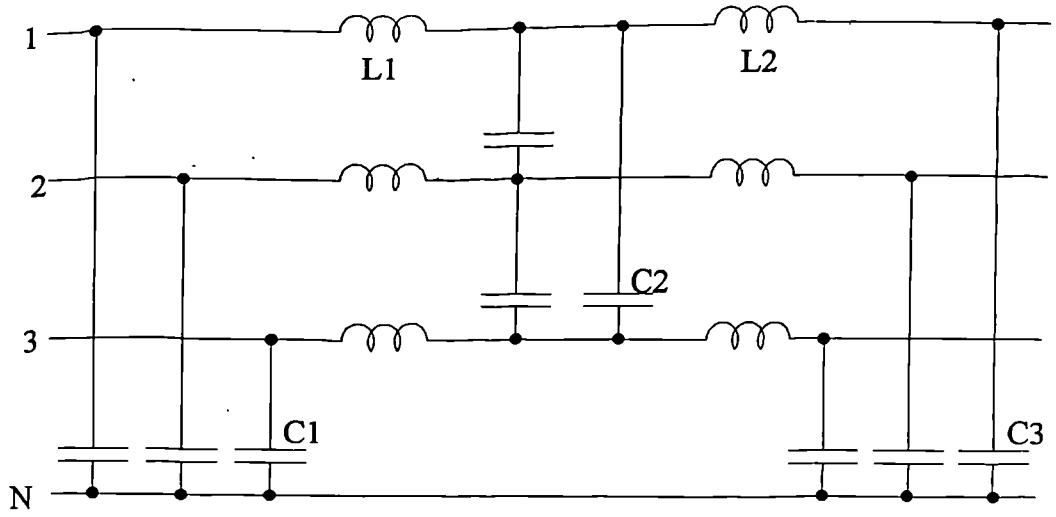


**Figure 8.17. A Possible Filter Circuit for Total EMC Compliance**

## 8.8 Complete EMC Filtering

This chapter has dealt with the differential mode noise that is unique to the structure of the matrix converter. Also in the converter there will be higher frequency common mode Radio Frequency Interference due to the action of the switches. This RFI will not differ greatly from the problems usually associated with a standard inverter, and is therefore not dealt with in any detail in this thesis. A circuit of the type shown in figure 8.17 could be used to overcome this noise and hence comply with the regulations in this higher frequency area.

## 8.9 Conclusions

The filters considered in this chapter would be used, along with the differential and common mode filters already employed, to comply with the EMC regulations at frequencies greater than 150kHz in inverter circuits. This chapter has examined the relevant regulations and recommendations in the EMC band between 10kHz and 150kHz where a matrix converter is likely to cause new differential mode noise problems. It has been shown that complying with possible future regulations will require the matrix converter switching frequency to be relatively high in order to

minimise the size of input filter components. The maximum switching frequency is limited by the acceptable switching losses in the devices used to implement the switches.

Comparisons have been made between different filter configurations. It has been shown that the most economical filter in terms of cost and size would be a simple LC filter with a harmonic diversion to reduce the magnitude of the fundamental switching frequency. The attenuation characteristics for this filter are the same as for a simple LC filter except that there is a notch at 20kHz.

# Bibliography

[1] "Engineering Recommendation G5/3: Limits for Harmonics in UK Electricity Supply System", Electricity Association, 1976.

[2] British Standards Institution, BS800, 1983.

[3] European Standards, EN55011, 1986.

[4] German Standards, VDE0871 part 1, 1981.

[5] CISPR16,

[6] Hemphill H. and Aust S., "EMC and Drives", Drives and Controls, Vol. 8, No. 8, Oct. 1992

[7] Critchley R., "New European Standards on EMC Affects Drives", Drives and Controls, Vol. 8, No. 9, Nov. 1992

[8] "IEEE Guide for Harmonic Control and Reactive Compensation of Static Power Converters", IEEE Std.519, 1981.

[9] "Principles of Solid State Power Conversion", pp.439-449.

[10] Jones R. and Jones S.R., "A unity Power Factor Sinusoidal Supply Side Converter For Industrial AC Drives", IEE Colloquium on Variable Speed Drives, Sept. 1992, pp8/1-8/5.

[11] Brichant F., "Forced Commutated Inverters", North Oxford Academic, 1984.

[12] "Capacitors for Power Electronics", Arcotronics Data Sheet.

[13] R.S. Components Catalogue, July to September 1992.

Chapter 9

# Hardware Design and Performance

## 9.1 Introduction

This chapter will describe the circuits required for the operation of a practical 5kWatt matrix converter that have not yet been presented in this thesis. These auxiliary circuits include input voltage phase detection; output current direction detection and the output voltage clamp. A block diagram giving the full matrix converter circuit is shown in figure 9.1. The operation of a 5kWatt experimental matrix converter will then be described and practical results of the waveforms obtained will be presented.

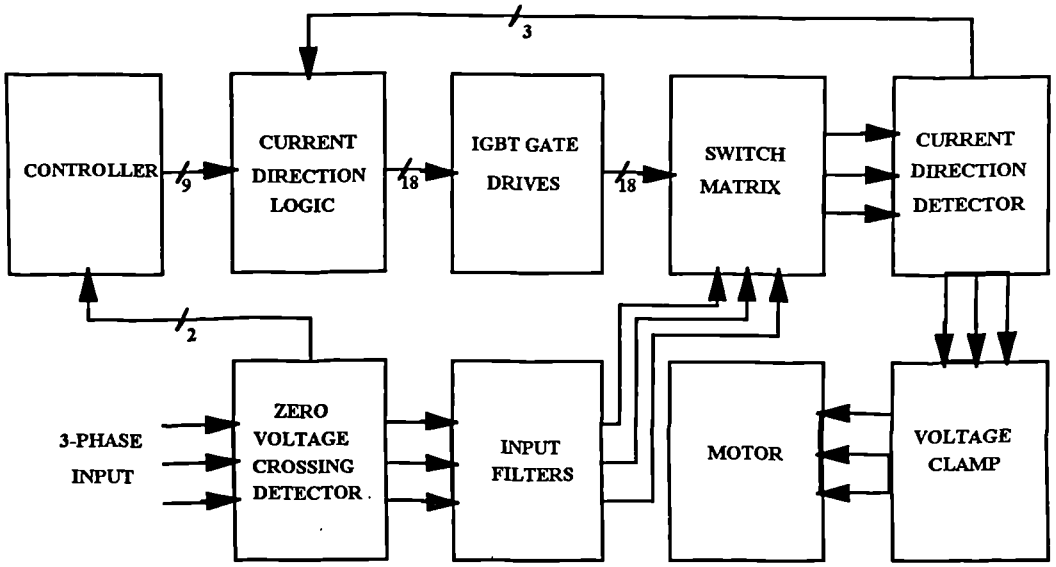


**Figure 9.1. Block Diagram of the Matrix Converter Circuits**

## 9.2 The Auxiliary Circuits

This section will examine the elements of the matrix converter structure that have not been described in previous chapters. These circuits are essential for the operation of a matrix converter under the limitations of present technology. They include an output voltage clamp, input voltage zero crossing detection and output current direction detection.

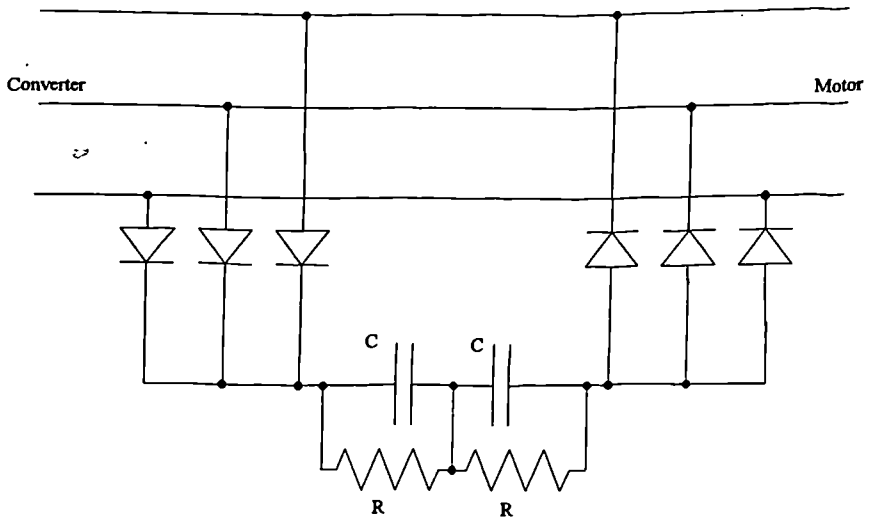


**Figure 9.2. Output Voltage Clamp for a Matrix Converter**

### 9.2.1 The Output Voltage Clamp

The output voltage clamp protects the switching devices from turn-off transients during low output current conditions. Under low current conditions there may be uncertainty in the output current detection signal and this uncertainty may cause unwanted dead time current commutation to occur. This dead time would cause an open circuit between the motor windings leading to potentially large voltage rises on the output lines. These voltage transients could damage the switching power devices.. The circuit used is shown in figure 9.2. The clamp allows current flow from the matrix converter's output lines if the voltage on these lines is greater than the clamp voltage. The monitoring of this clamp voltage provides a useful means of checking for transient switching faults in the converter.

### 9.2.2 The Output Current direction Detector

The semi-soft current commutation methods described in Chapter 5 requires knowledge of the direction of the output current at the time of current handover. This information can be obtained by looking at the voltage across a pair of back to back diodes placed in the output line of the converter [1]. However, this method increases the losses in the converter.

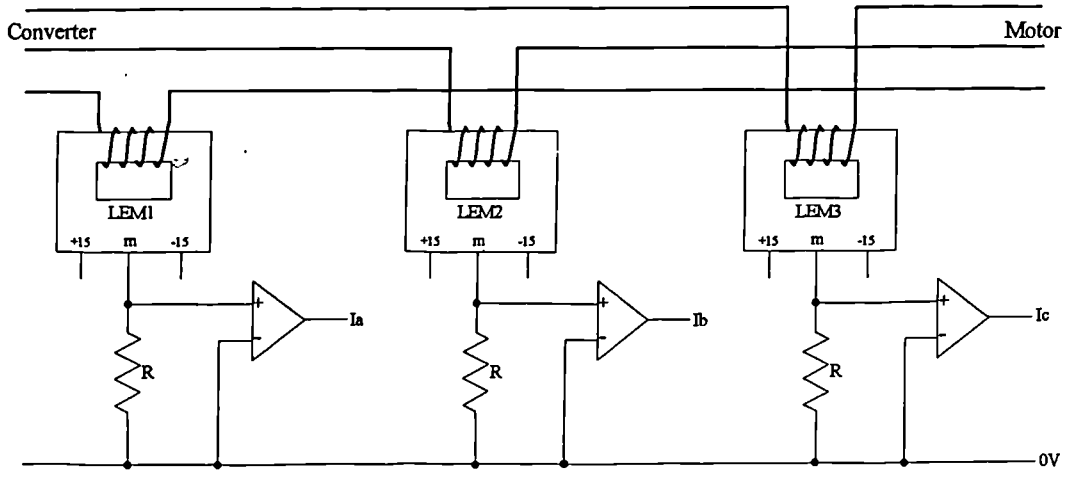


**Figure 9.3. The Output Current Direction Detection Circuit**

An alternative would be to sense the current direction in each switch by looking at the voltage drop across each of the 18 diodes already implemented in the switch matrix circuit. This method would give the most accurate indication of the current direction at any given time, but would require a large amount of additional hardware. Eighteen individual comparator circuits would have to be implemented and the information then processed to give the current direction for each output line. An extension of this idea would be to make the current commutation strategy operate semi-independently within each bi-directional switch circuit. This would have the advantage of greater accuracy in the correct commutation of current, but would require a large increase in the circuit complexity.

The current direction may be found using Hall effect current sensors [2,3]. The information from these sensors is often used in motor control techniques and there would therefore be only a small cost increase in implementing this sensing strategy. A possible circuit for the implementation is shown in figure 9.3.

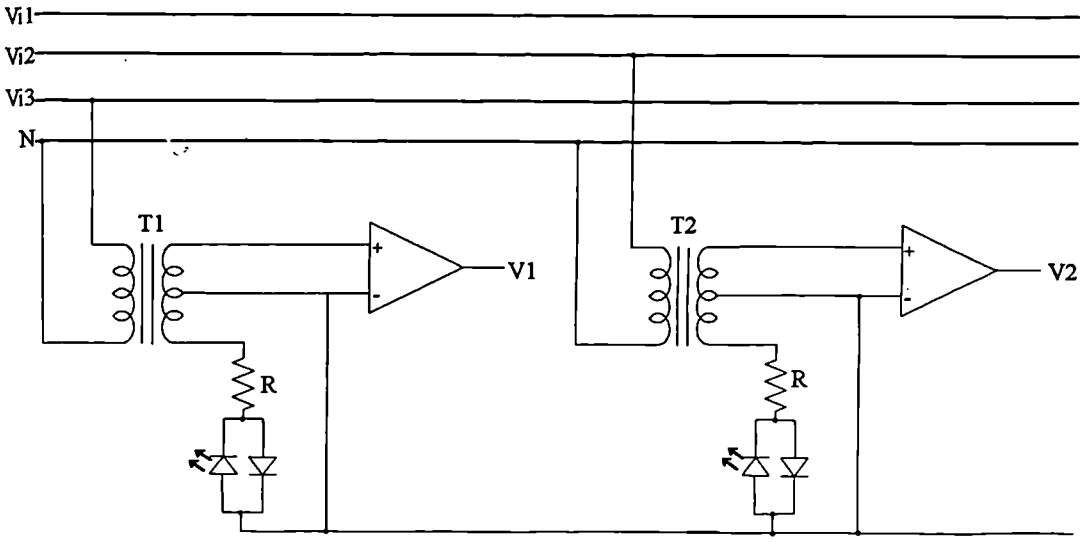


**Figure 9.4. The Input Voltage Zero Crossing Detector**

### 9.2.3 The Input Voltage Zero-Crossing Detector

The microprocessor used to control the matrix converter must track the input voltage to keep its model of the input voltage waveform in phase with the actual input voltage waveform. The circuit used is shown in figure 9.4. A 240Volt to 5Volt transformer is used to provide isolation and a compactor provides the controller with positive and negative edges that are used to trigger non-critical interrupts in control software. Two input voltage zero crossing detectors are implemented so that the controller can ascertain the phase order of the three phase supply. This phase ordering is performed as part of the software initialisation routines.

The information from these detectors is also be used to enable the controller to measure the input frequency and change the control frequencies accordingly. This method would allow the converter to be used as a constant frequency supply from a variable frequency source. The converter could also be connected to a supply of any frequency and adapt itself to the supply with no manual set-up.

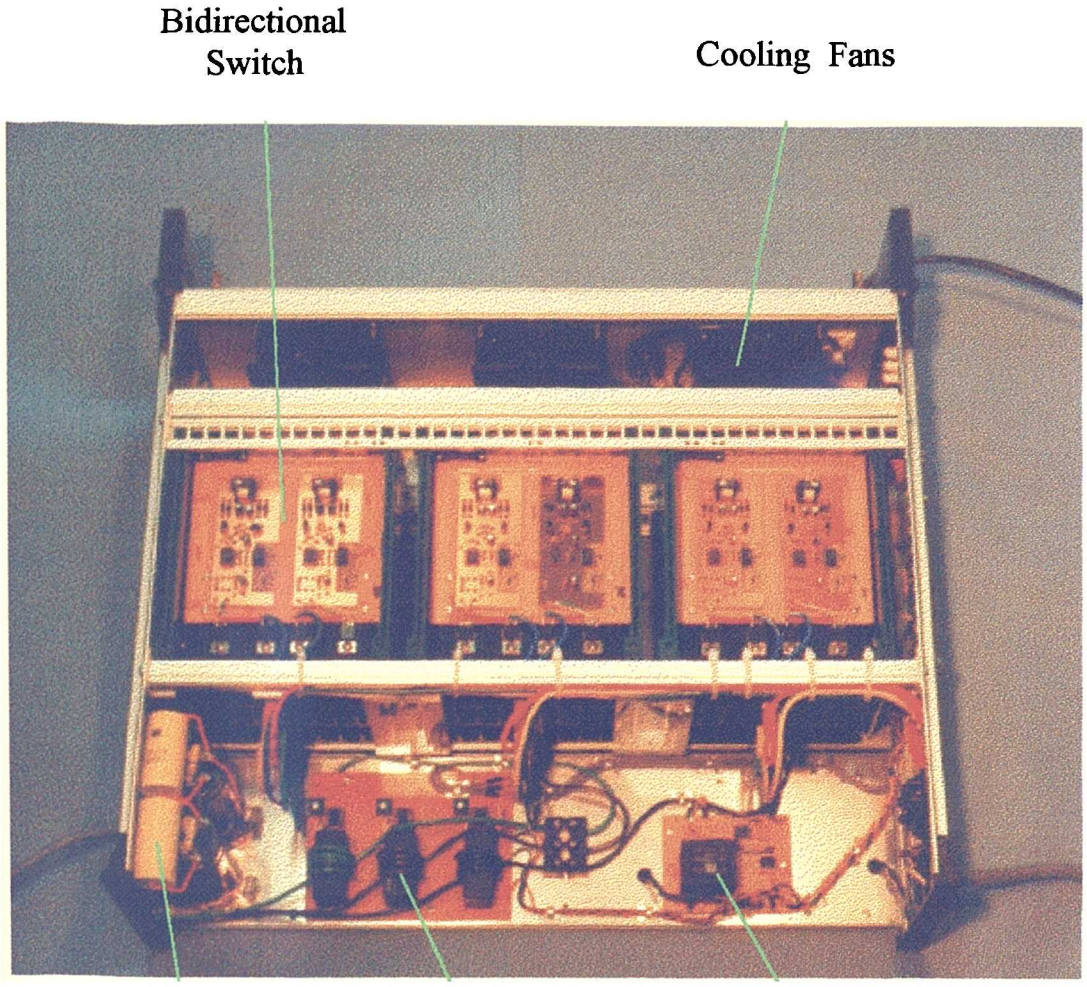


**Figure 9.5. The Experiment Matrix Converter**

## 9.3 The Building of the Experimental Matrix Converter

This section briefly considers the building of the 415Volt matrix converter that has been used to obtain the practical results given in this thesis. The converter was designed to be capable of driving a 5kWatt motor in both motoring and generating modes.

| Harmonic Number | Rectifier Harmonics | Matrix Converter Harmonics |
|---|---|---|
| 1 | 100% | 100% |
| 3 | 4.1% | 0.6% |
| 5 | 27.6% | 1.2% |
| 7 | 18.5% | 0.38% |
| 11 | 10% | 0.14% |
| 13 | 6.5% | 0.08% |

**Table 9.1: Input Current Harmonics for a Rectifier and a Matrix Converter**

The experimental matrix converter was designed to be capable of driving a 5kWatt motor from a 415Volt three phase supply. The power semiconductor devices and the input and output cabling were kept as far away as possible from the signal level circuits to minimise noise problems. Sufficient heat-sinking is provided for the power semiconductor devices to dissipate the losses described in Chapter 6. The power cables between each of the bi-directional switches is minimised to reduce the effect of the inductance in the wire. The converter was also designed to be easily repairable if there is damage to any of the power semiconductor devices.

The building of a bi-directional switch has been described in Chapter 5. Nine of these switches are then arranged in a three-by-three square to form the switch matrix in a suitable enclosure. The auxiliary circuits were built and fitted on the power side of the switch matrix. The control signals were fed from the current commutation control circuits directly to the signal side of the switch matrix. Fans were added to the front panel of the converter's enclosure to provide the required cooling for the power semiconductors. The complete experimental matrix converter is shown in figure 9.5.

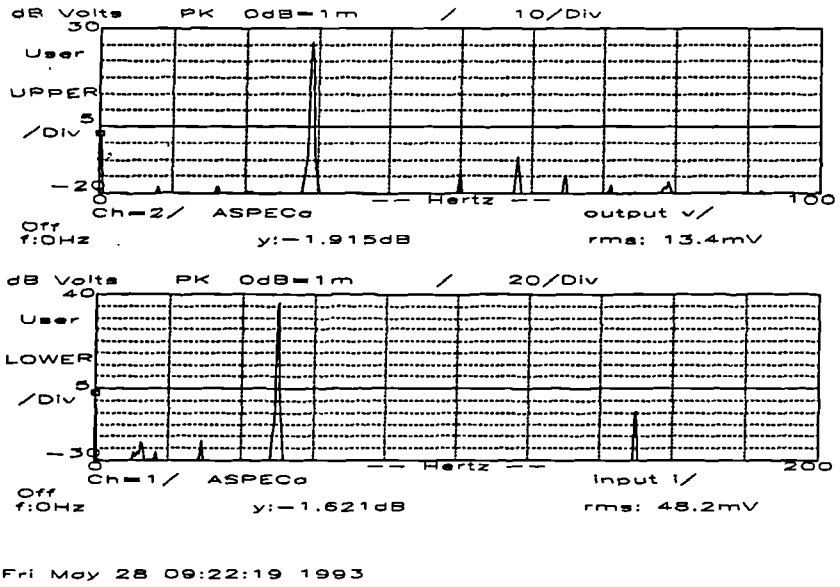


**Figure 9.6. The Output Voltage and Input Current Spectrum for a 5kWatt Matrix Converter Operating with an Output Frequency of 30Hz**

## 9.4 Practical Results

This section will give some practical waveforms obtained from the experimental matrix converter. They show both time and frequency domain results under different operating conditions.

### 9.4.1 The Input and Output Waveforms

Figure 9.6 to 9.8 show the input current and output voltage low frequency spectrum for a matrix converter with output frequencies of 30Hz, 80Hz and 120Hz. As can be seen from these waveforms there are no significant subharmonics to the output frequency. The harmonics to the input frequency are low, and the harmonics that can be seen are due to the harmonics in the lab supply on the day measurements were taken. Table 9.1 gives a summary of the input current harmonics obtained for a matrix converter in comparison to the input current harmonics for a rectifier [5]. The harmonics that are present are mainly due to distortion in the supply voltage waveforms.

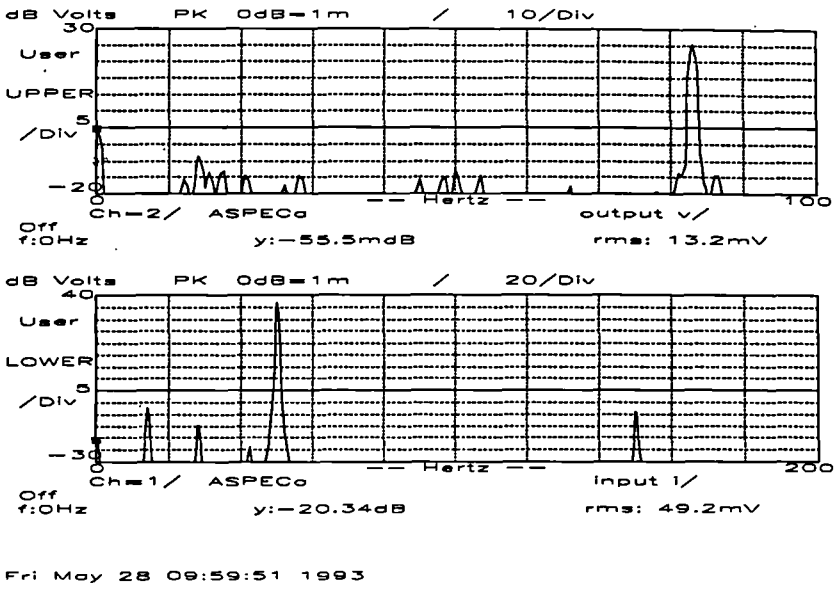


**Figure 9.7. The Output Voltage and Input Current Spectrum for a 5kWatt Matrix Converter Operating with an Output Frequency of 80Hz**

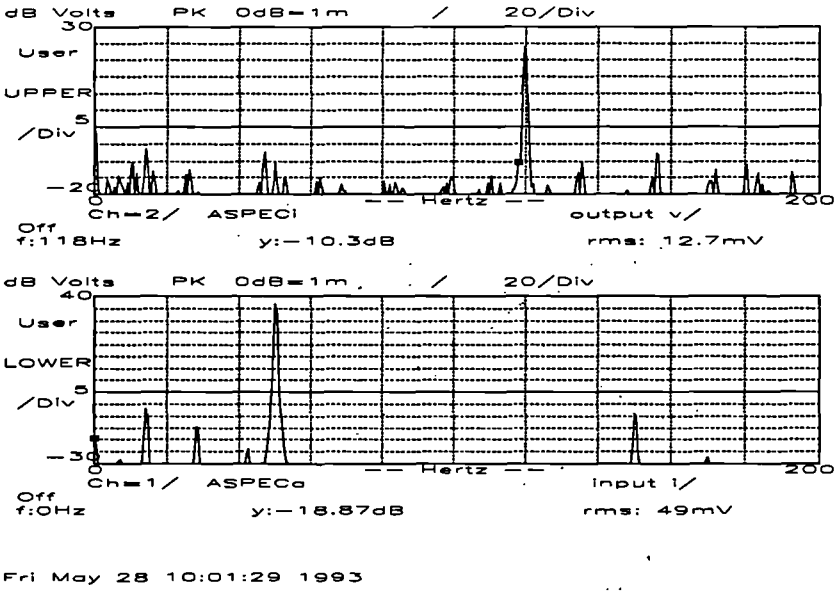


**Figure 9.8. The Output Voltage and Input Current Spectrum for a 5kWatt Matrix Converter Operating with an Output Frequency of 30Hz**

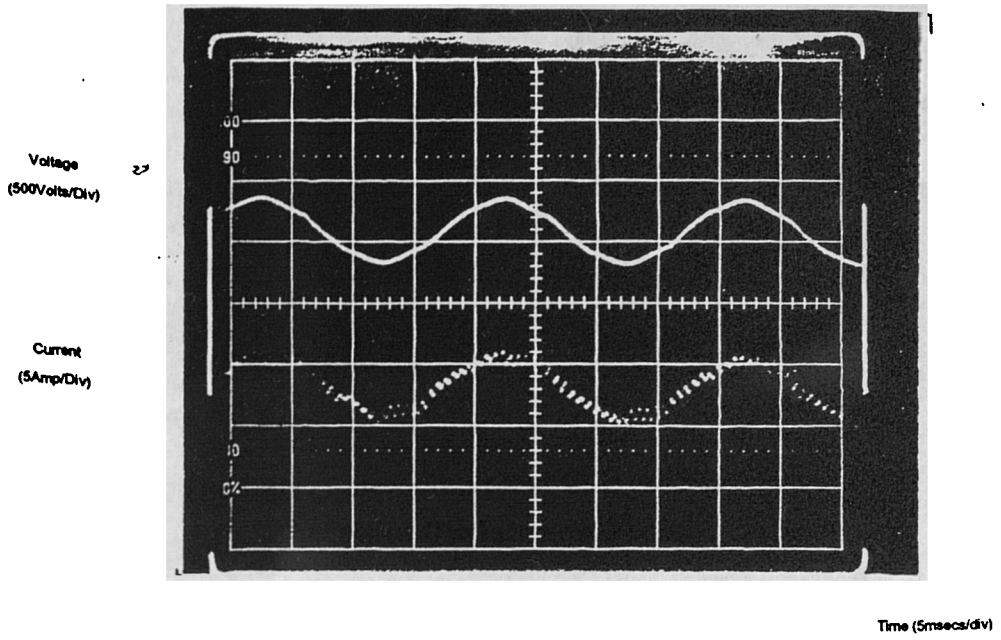


**Figure 9.9: The Input Line Voltage and Current Waveforms with Lagging Input Displacement Factor**

### 9.4.2 Input Displacement Factor Control

The input displacement factor of the converter may be varied by altering the appropriate variable in the control algorithm. This allows the displacement factor to be altered in a range from lagging at the motor's power factor to leading at the motor's power factor, including unity. Figures 9.9 and 9.10 show these two extremes. The ripple on the input current waveform is due to the resonant frequency of the input filter.

### 9.4.3 The Converter in the Regenerative Mode

The matrix converter is a naturally regenerative converter. The waveforms in figure 9.11 show the converter operating in the regenerative mode. A DC Machine operated from a Control Techniques Mentor Drive is used to drive the AC machine.

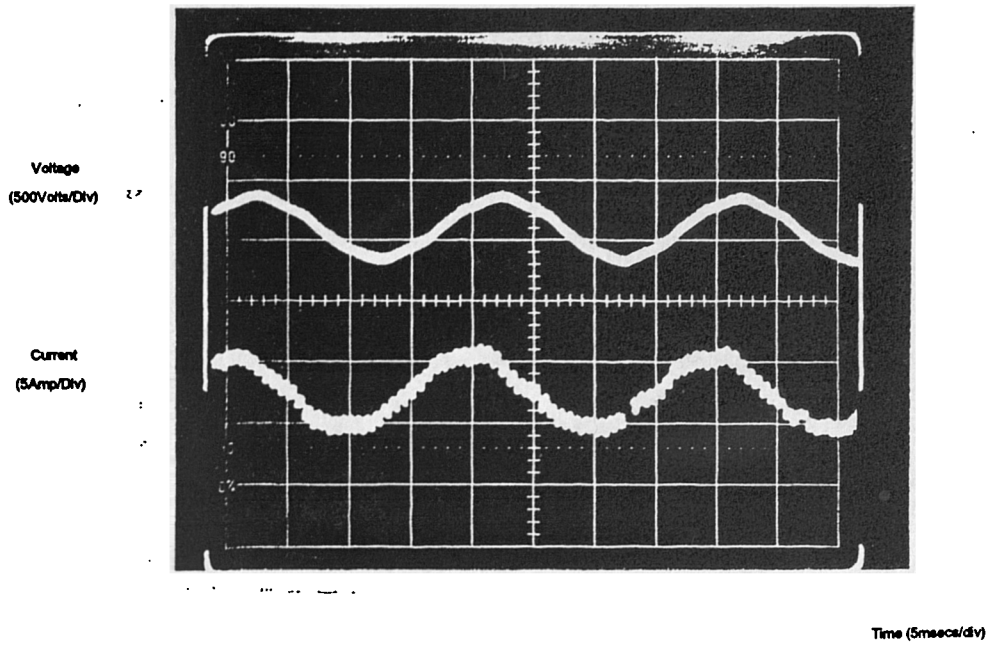


**Figure 9.10: The Input Line Voltage and Current Waveforms with Leading Input Displacement Factor**

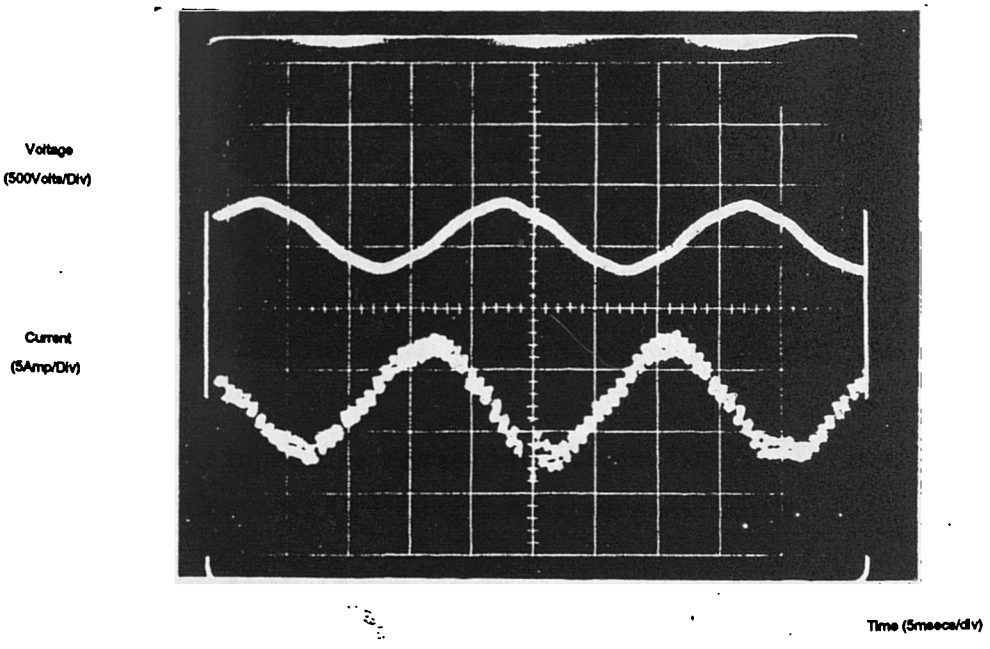


**Figure 9.11: The Input Line Voltage and Current Waveforms Showing the Converter Operating in a Regenerative Mode**

## 9.5 Conclusions

The construction of the auxiliary circuits that are required for the safe operation of a practical matrix converter has been described. The operation of a matrix converter under various operating conditions has been examined and the results presented. The converter offers sinusoidal input currents and output voltages. There are no significant subharmonics in the output voltage waveforms. The converter has been shown to be capable of operation as a four quadrant drive, with natural regeneration.

# Bibliography


[1] Huber L, Borojevic D and Burany N, "Voltage Space Vector Based PWM Control of FCCs", IECON 1989, Vol.1, pp.48-53.

[2] "LEM Module 50A, Data Sheet", LEM Sales Information.

[3] Telcon Technology Limited, "CONTEC HTP100, Data Sheet".

[4] Wheeler P.W. and Grant D.A., "Reducing the Semiconductor Losses in a Matrix Converter", Proceedings of IEE Colloquium on Power Electronics, 1992, pp.9.1-9.5.

[5] Jones R. and Jones S.R., "A Unity Power Factor Sinusoidal Supply Side Convertor for Industrial AC Drives", Proceedings of IEE Colloquium on Static Power Conversion, 1992, pp.8.1-8.5.

Chapter 10

# The Matrix Converter as the General Power Converter

## 10.1 Introduction

The structure of a generalised matrix converter can be viewed as the fundamental switching power converter [1]. From this structure it is possible to introduce restrictions and simplifications to the converter circuit to create any switching power converter circuit. Once the circuit has been established a suitable control algorithm for the given application can be found.

This chapter examines the belief that the matrix converter circuit is the most generalised converter circuit. The degeneration of the three phase matrix converter to a controlled rectifier and the degeneration to current and voltage source inverters is explained in detail. The possibility of using matrix converter control algorithms to control these converters is considered. The fundamental role played by the reactive elements in a power converter is discussed.

## 10.2 The Matrix Converter's Place in the Switching Power Converter Family

### 10.2.1 The Generalised Matrix Converter

The true unrestricted matrix converter consists of x input lines that can be connected to any of the y output lines by the closing of a perfect bidirectional switch. Such a switch is placed on every intersection node between the input lines and the output lines so that any input line may be connected to any output line at the discretion of the control mechanism of the converter. This generalised circuit is shown in figure 10.1. The circuit may be used to convert any x-phase input supply of any fundamental frequency into any y-phase output supply of any fundamental frequency.

The matrix converter considered in this thesis has been a converter in which the number of inputs and outputs have been restricted to three. Other converters may be similarly described by defining the appropriate number of input and output lines. For example, an inverter can be viewed as a two input line, three output line matrix converter with a zero input frequency.

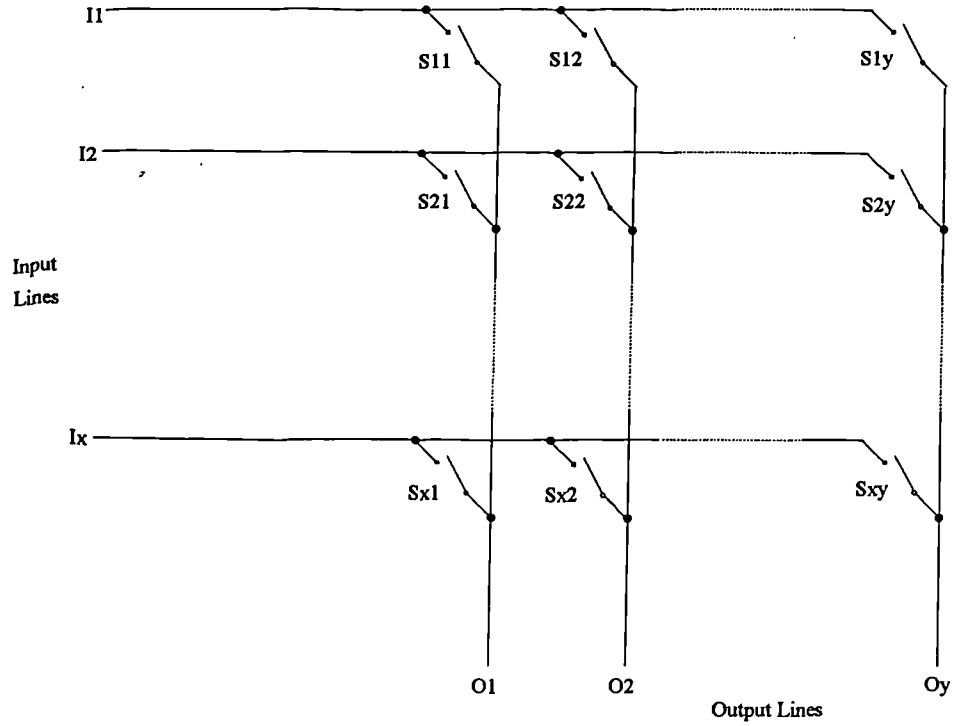


**Figure 10.1. The Generalised Matrix Converter Structure**

In some case the switches of the converter will not require the full functionality of the bidirectional switch. In these situations the circuits can be simplified by removing parts of the switch that are not required. In this way all converter topologies can be found using a single simplified matrix converter circuit or a combination of simplified matrix converter circuits.

### 10.2.2 Constraints on Simplified Converter Structures

In some cases additional restrictions may be imposed on the range of input and output frequencies due to the nature of the power switches employed. An example of this is in a Cycloconverter, [3], where the maximum output frequency is reduced to a third of the input frequency because of the inability to turn off the switching devices until they are negatively biased. This imposition of frequency restrictions is also sometimes inherent in the converter if there are fewer input lines than output lines. This situation will occur in a single phase to three phase direct conversion process.

| Converter Type | Example | Input Frequency | Output Frequency | Input Lines | Output Lines |
|---|---|---|---|---|---|
| 3AC/3AC | Matrix Converter/ Cycloconverter | any | any/<3$f_i$ | 3 | 3 |
| 3AC/AC | Single Output Phase Matrix | any | any | 3 | 2 |
| AC/3AC | AC Resonant Output Stage | any | <10$f_i$ | 2 | 3 |
| 3AC/DC | Three Phase Rectifier | any | zero | 3 | 2 |
| DC/3AC | Three Phase Inverter | zero | any | 2 | 3 |
| AC/AC | AC Chopper | any | <3$f_i$ | 2 | 2 |
| AC/DC | Single Phase Rectifier | any | zero | 2 | 2 |
| DC/AC | Single Phase Inverter | zero | any | 2 | 2 |
| DC/DC | DC Chopper | zero | zero | 2 | 2 |

**Table 10.1. Converter Types and Restrictions**

These restrictions in the degeneration of the generalised matrix converter structure are summarised with examples in table 10.1. The three-phase matrix converter can be simplified by the restriction of the number of input and output lines and the restriction of the input and output frequencies. Taken one at a time these restrictions can be used to develop a family tree of all possible switching power converter structures as shown in figure 10.2.

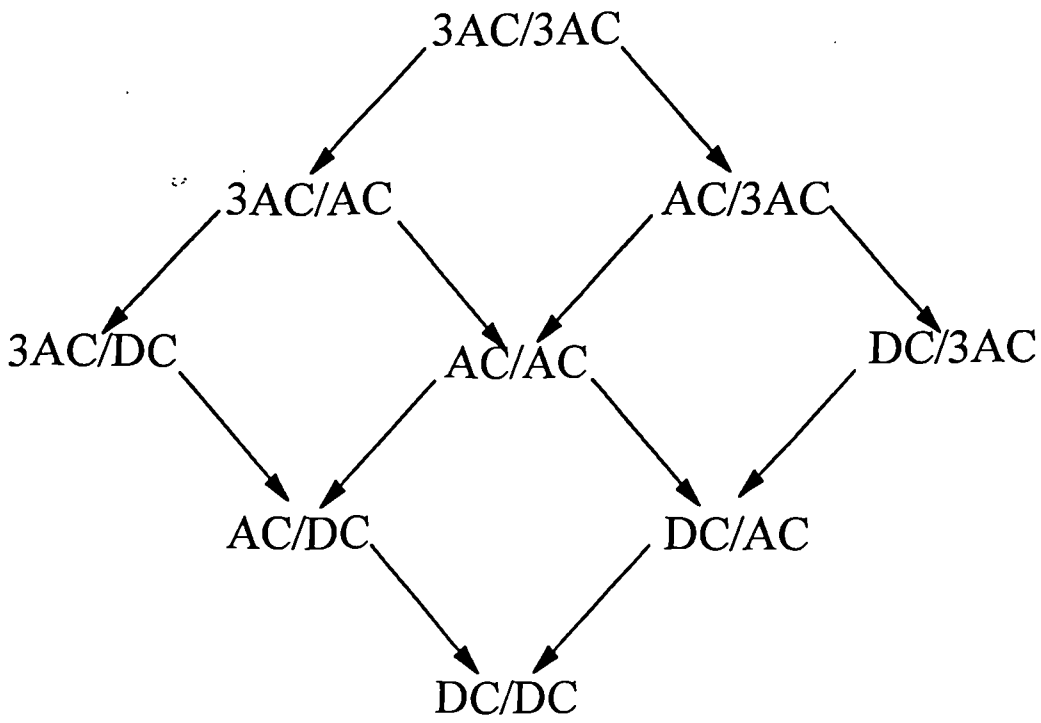


**Figure 10.2. The General Power Converter Family Tree**

More complex converters have to be considered as a combination of more than one restricted generalised converter. Passive components in converter structures can be considered as a necessity to provide each of the component generalised converters with ideal supplies.

For example, a back to back converter, [4], is a combination of a three input, two output converter with zero output frequency and a two input three output converter with zero input frequency. The bidirectional switches of the converter can be simplified by considering the circuit redundancy. The DC link capacitor in the standard converter structure can be considered as providing the first converter with a current sink and providing the second converter with a nearly ideal voltage source.

| Output Phase Angle | $V_{out1}$ | $V_{out2}$ | $V_{out3}$ |
|---|---|---|---|
| $\pi/6$ | +ve | -ve | zero |
| $11\pi/6$ | -ve | +ve | zero |

**Table 10.2. Output Voltage Variation with Output Phase Angle**

## 10.3 The Implementation of a Controlled Rectifier

If the output frequency of a matrix converter was set to 0Hz and the amplitude set to a non-zero value then the converter could operate as a controlled rectifier. This controlled rectifier would allow the control of the DC output voltage and would be capable of natural bidirectional current flow. The converter can be used as a single ended or dual ended supply. If a dual ended supply is implemented then the output voltage ratio between the two supplies can also be controlled.

### 10.3.1 The Degeneration of the Matrix Converter Control Algorithm

The control algorithm given in chapter 2 may be simplified by setting $\omega_o = 0$. This will give the output voltages defined in equation 10.1. The output voltage phase angle, $\varphi_O$, is the static operating point of the converter in the range of possible output voltages

$$\mathbf{V_o(t)} = \begin{bmatrix} 0.866V_i.\cos(\varphi_o) + 0.25.\cos(3\omega_i t) \\ 0.866V_i.\cos(\varphi_o + \frac{2\pi}{3}) + 0.25.\cos(3\omega_i t) \\ 0.866V_i.\cos(\varphi_o + \frac{4\pi}{3}) + 0.25.\cos(3\omega_i t) \end{bmatrix} \quad (10.1)$$

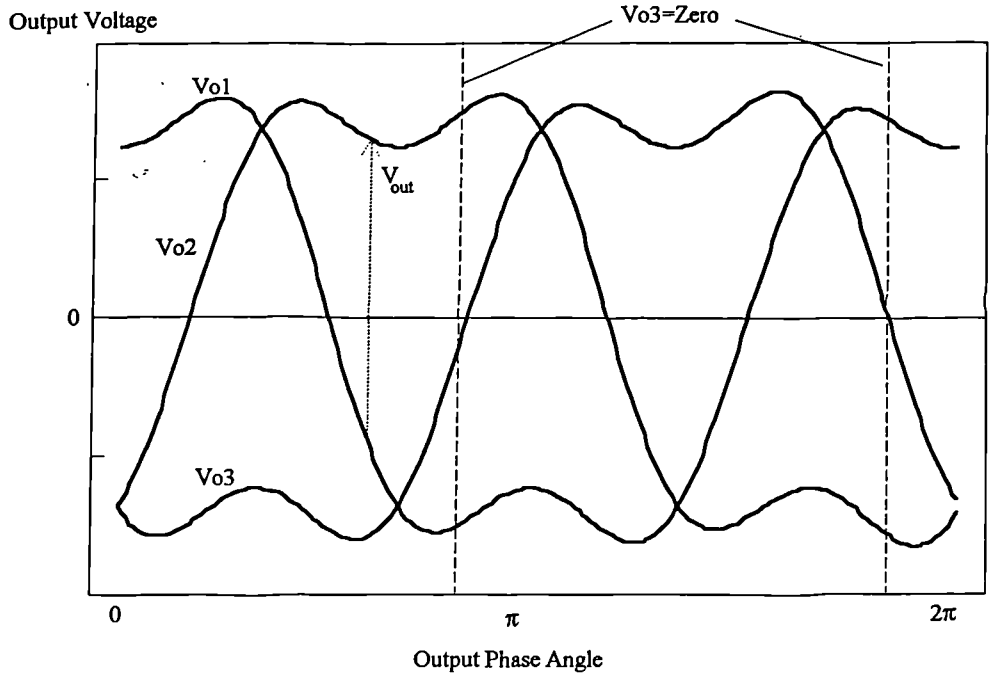


**Figure 10.3. Possible Output Voltages for Output Phase Angle Operating Points**

All the output lines will have a superimposed common mode third harmonic of the input frequency to maintain the maximum output voltage range. An operating point can be chosen such that one of the three output lines will be at zero volts, whilst the other two output lines will be at maximum negative and maximum positive potentials. This zero voltage will occur on the third output line when the operating point is set to an output phase angle of $^{5\pi}/_{6}$ or $^{11\pi}/_{6}$. At these points the first and second output line will have maximum positive and negative values as shown in table 10.2. By controlling the operating position, the ratio of the positive and negative DC potentials can be altered. This control of the potentials of the output voltages is shown in figure 10.3.

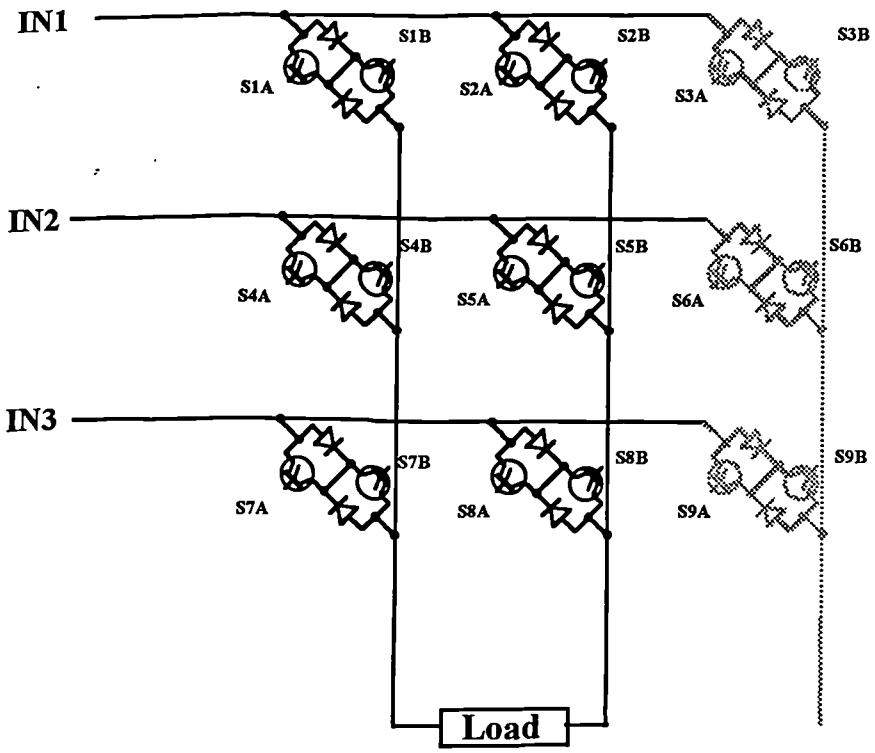


**Figure 10.4. The Degeneration of the Matrix Converter to a Single Ended Bi-Directional AC-DC Converter**

### 10.3.2 The Simplification of the Matrix Converter Power Circuit

A rectifier requires only two output lines, therefore one output phase of the matrix converter will become redundant. The switches required by this redundant phase need not be implemented. This reduces the number of bidirectional switches required from nine down to six as shown in figure 10.4. Only twelve switching devices will then be used to implement this AC-DC converter. The natural bi-directional current flow of the matrix converter circuit and control algorithm will allow the converter to provide regeneration without the need for any extra circuits or additional complex control algorithms.

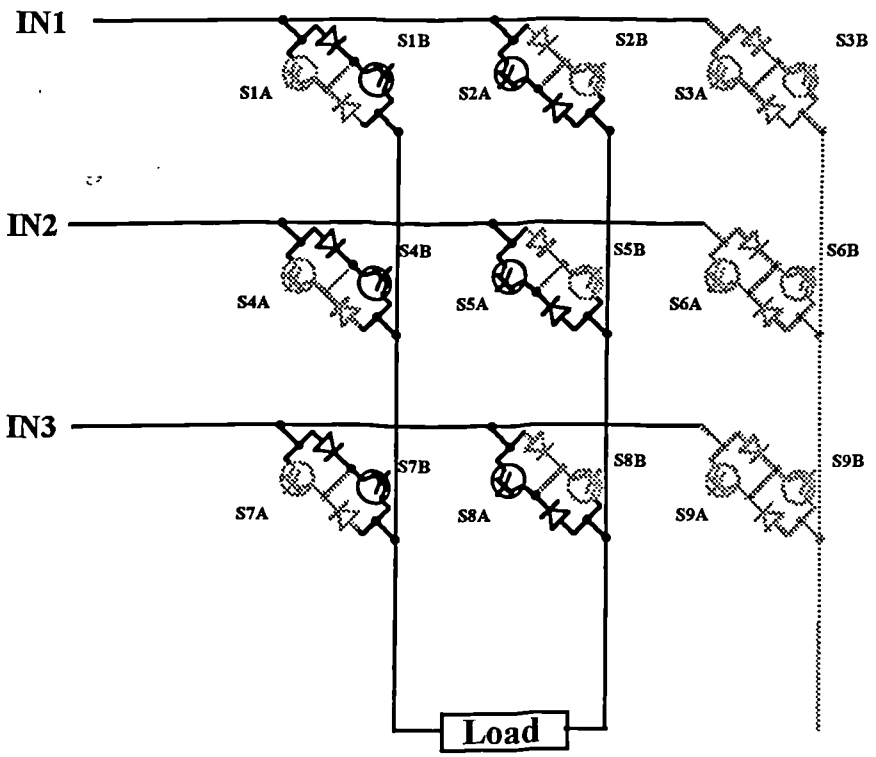


**Figure 10.5. The Degeneration of the Matrix Converter to a Single Load Uni-Directional AC-DC Converter**

This rectifier topology has the additional advantage of allowing the DC voltage to be switched between positive and negative by simply inverting the phase angle of the output voltage operating point.

If reverse current flow is not required then half of each bidirectional switch will not be required. These unused switches do not need to be implemented, therefore reducing the required number of switching devices to six. The circuit for this unidirectional current flow AC-DC converter is shown in figure 10.5. The circuit requires the same number of devices as a standard PWM bridge rectifier.

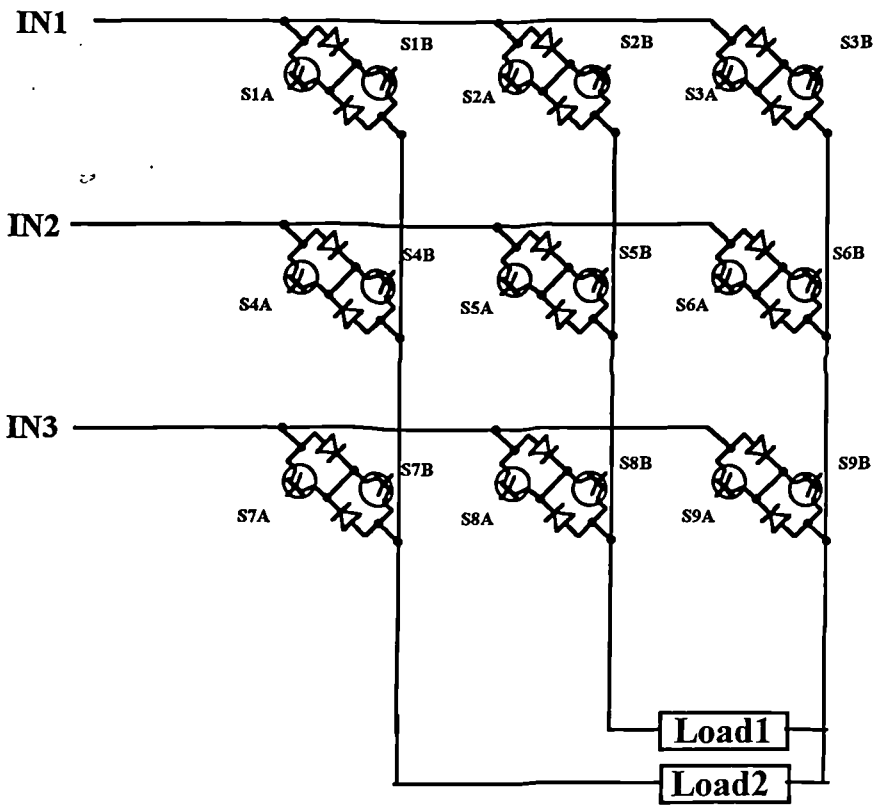


**Figure 10.6. The Degeneration of the Matrix Converter to a Double Load Bi-Directional AC-DC Converter**

The converter may be extended to a dual supply topology by the inclusion of all the switches. In this configuration the third phase becomes the effective zero voltage point in the output circuit [5-7]. This dual supply circuit will provide the supply with sinusoidal input current even if the loads are unbalanced. This is possible because of the averaging effect of the control algorithm when the input displacement factor is set to unity. This effect can be explained by considering the effective cancellation of the output power factor in the matrix converter algorithm. The imbalance in the DC current may be viewed as the same effect of the phase angle.

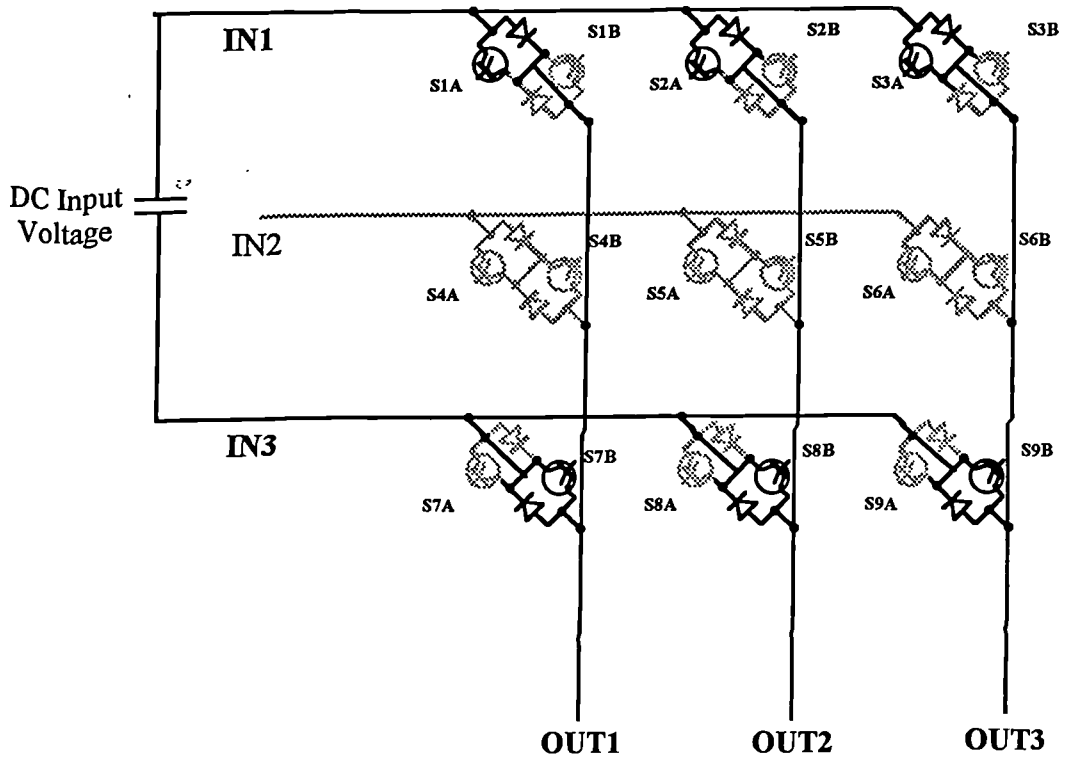


**Figure 10.7. The Degeneration of the Matrix Converter Circuit to a Voltage Source Inverter**

## 10.4 The Implementation of an Inverter

If the input frequency of the converter is set to zero then the matrix converter will function in an inverter-like fashion [8]. Some of the switches in the converter will become redundant and therefore would not be implemented. This reduction in the number of switches will lead to two possible converter configurations. These two circuit configurations correspond to a voltage source inverter (VSI) [13] and a current source inverter (CSI) [14].

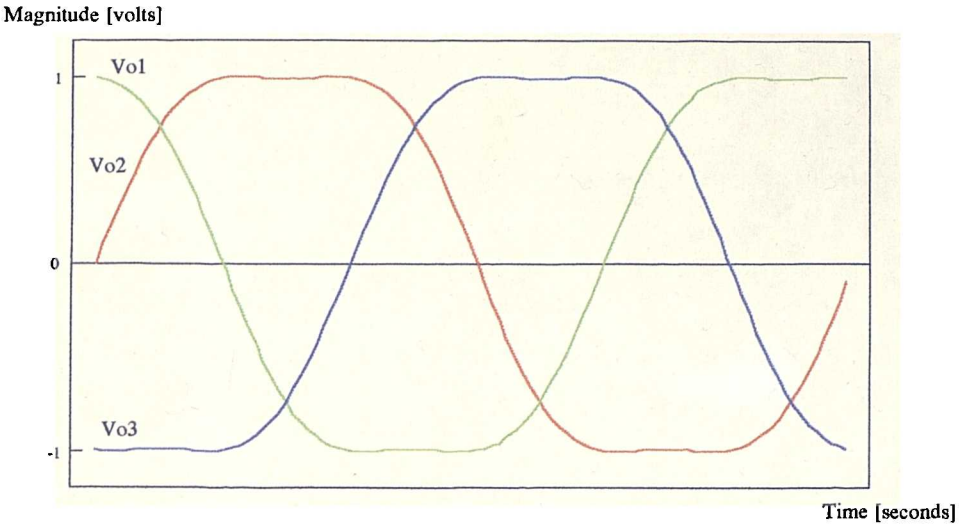


**Figure 10.8. The Average Output Voltage Waveforms from the VSI**

### 10.4.1 Simplification of the Matrix Converter to a Voltage Source Inverter

The input voltage frequency, $\omega_i$, will be set to zero. This will simplify the control equations set out in Chapter 2. Since the input is DC, only two input lines are required and the switches for one of the matrix converter input lines are not implemented. The reverse current flow in each switch does not require control as this will be dealt with by the anti-parallel diodes. The half of each switch that would carry this reverse current is therefore redundant and is not implemented. This circuit reduction is shown in figure 10.7.

The maximum output voltage of a matrix converter is restricted by the voltage of the input voltage. The inclusion of the third harmonic of the input frequency will increase the line to line voltage as shown in figure 10.8. The maximum output voltage of the converter in this VSI arrangement can therefore be calculated as shown in equation 10.2.

$$V_{o,peak} = 0.866.\frac{3V_{dc}}{2} \tag{10.2}$$

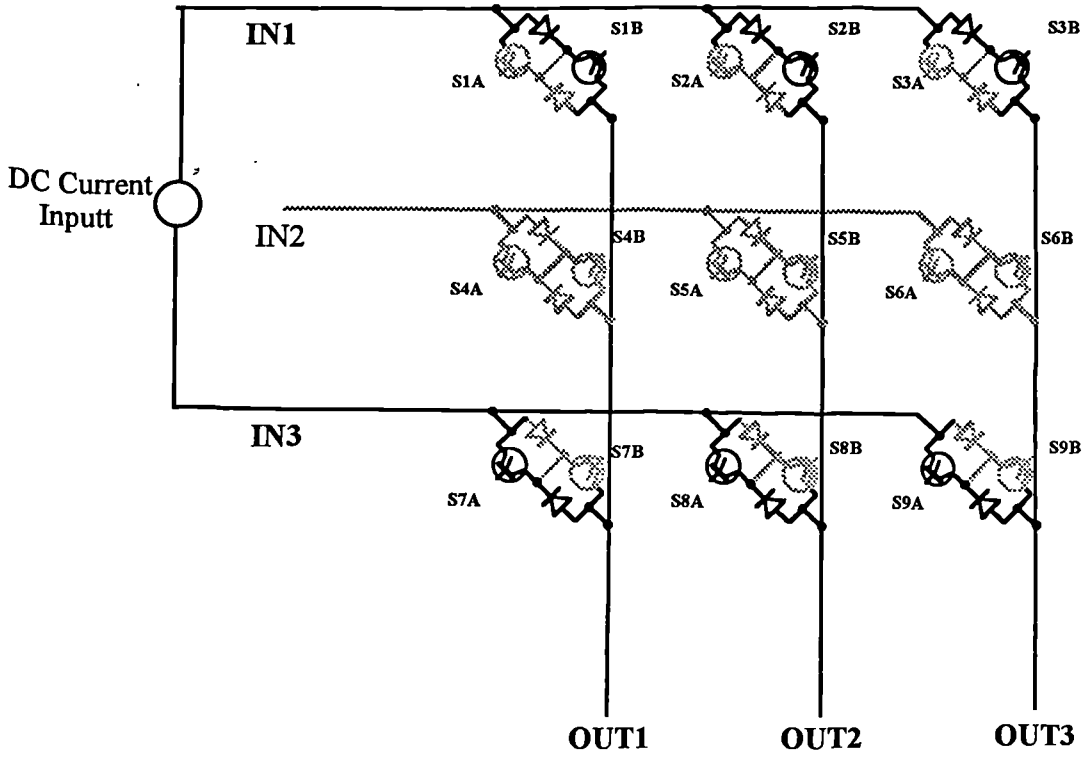


**Figure 10.9. The Degeneration of the Matrix Converter to a Circuit to a Current Source Inverter**

### 10.3.2 Simplification of the Matrix Converter to a Current Source Inverter

The control algorithm described in Chapter 2 takes a continuous input voltage and generates a discontinuous output voltage. This output voltage waveform's fundamental frequency forces a continuous current to flow in an inductive load.

To operate in a CSI configuration, the control matrix can be transposed. This transposed matrix can then be reduced by setting the input frequency, $\omega_i$, to zero. The input voltage will now be the discontinuous voltage instead of the output voltage because of the constraint of having a continuous input current. This is shown in equation 10.3

$$\mathbf{I_o(t) = M(t)^T . \begin{bmatrix} I_{DC} \\ 0 \\ -I_{DC} \end{bmatrix}} \tag{10.3}$$

The matrix converter circuit may be simplified by not implementing the unused input line of the converter in the same way as for the VSI. The DC current has to be continuous, so the halves of the bidirectional switches in the non-conducting direction are not required. This will reduce the number of switching devices in the converter to six, as shown in figure 10.9.

## 10.4 Conclusions

The most generalised form of the matrix converter has been presented and the idea of the matrix converter as the most general form of switching power converter has been proposed. The degeneration of the circuit into other presently recognised power converters has been described.

The simplification of the matrix converter circuit to a controlled rectifier, VSI and CSI circuits has been considered. It has been shown how the matrix converter control algorithms presented in this thesis can be used to control these forms of converter and their advantages have been discussed.

# Bibliography


[1] Wood P, "General Theory of Switching Power Converters", Proc. of PESC Conference Record (San Diego) 1979, pp.3-10.

[2] Lipo T.A., "Recent Progress in the Development of Solid State AC Motor Drives," IEE Trans. on Power Electronics, Vol.3, No.2, April 1988, pp.105-117.

[3] Gjugyi L and Pelly B, "Static Power Frequency Changers", New York : Wiley, 1976.

[4] Zhang H., Wheeler N. and Grant D.A, "Back to Back Converter...", Universities Power Electronics Conference, Stafford, 1993, pp.??.

[5] Holmes D.G and Lipo T.A, "Implementation of a Controlled Rectifier using AC-AC Matrix Converter Theory", Conf. Record PESC 1989, pp.353-359.

[6] Holmes D.G and Lipo T.A, "Implementation of a Controlled Rectifier using AC-AC Matrix Converter Theory ", IEEE Trans. on Power Electronics, Vol.7, No.1, January 1992, pp.240-250.

[7] Holmes D.G, "Implementation of a Controlled Rectifier using AC-AC Matrix Converter Theory", IEEE Power Electronics Specialists Conference: PESC '89, Milwaukee, 26-29 June 1989.

[8] Holmes D.G, "A New Modulation Algorithm for Voltage and Current Source Inverters, based on AC-AC Matrix Converter Theory", IEEE 1990 pp.1190-1195.

[9] Alesina A and Venturini M, "Intrinsic Amplitude Limits and Optimum Design of 9-Switches Direct PWM AC to AC Converters", PESC Conference Record 1988, pp.1284-1291.

[10] Alesina A and Venturini M, "Solid-State Power Conversion : A Fourier Analysis Approach to Generalised Transformer Synthesis," IEEE Trans. on Circuits and Systems, Vol. cas28, No.4, April 1981, pp.319-330.

[11] Alesina A and Venturini M, "The Generalised Transformer : A New Bidirectional Sinusoidal Waveform Frequency Converter With Continuous Variable Adjustable Input Power Factor", Proc. of PESC Conference Record, 1980, pp.242-252.

[12] Wood P, "Switching Power Converters", (book), Van Nostrand Reinhold Company, 1981.

[13] Control Techniques, "Drives and Servos Year Book", 1990.

[14] Enjeti P.N, Ziogas P.D. and Lindsay J.F, "A Current Source PWM Inverter with Instantaneous Current Control Capacity", IEEE Industrial Applications Society, Annual Meeting Conference Record, 1988, pp.895-902.

# Chapter 11

# Conclusions

## 11.1 Summary of the Work Undertaken

The work summarised in this thesis has covered many aspects of the matrix converter circuit and its operation. The intrinsic maximum input to output voltage ratio for the matrix converter circuit has been established and a PWM control algorithm capable of achieving this maximum ratio has been derived. This control algorithm is capable of drawing sinusoidal input current with no minimised low frequency harmonics, whilst maintaining sinusoidal output voltage waveforms and enabling the control of the input displacement factor. The input displacement factor can be set to be either leading, lagging at the same angle as the displacement factor of the load, or anywhere in between these limits including unity. These characteristics can be compared to a rectifier/inverter circuit that requires a large DC capacitor and draws non-sinusoidal input currents at a fixed, lagging power factor.

Detailed consideration has been given to the silicon devices required in a matrix converter for both control and power handling. The required characteristics of a suitable micro-processor for use in controlling switching power converters have been discussed and a suitable micro-controller identified and tested. The chosen controller has then been used for the real time implementation of a PWM matrix converter control algorithm.

The characteristics of modern semiconductor power switching devices have been examined and the IGBT established as the most suitable controllable device for this type of hard switching power converter at the present time. The design and operation of a bi-directional switch from discrete components have then been considered, and a back-to-back pair of common collector IGBTs with anti-parallel diodes has been chosen as the most suitable arrangement because of functionality and minimum conduction losses. The minimum device ratings for the devices in these switches have been calculated.

The problems associated with passing the current path between the switches in the converter has been addressed. Existing solutions have been categorised, and alternative methods proposed. The state machine design of possible solutions has

been given and the single chip implementation of these state machines on Generic Logic Arrays has been outlined.

The power losses in the matrix converter circuit have been analysed and quantified. Methods of reducing the switching losses have been introduced which include the use of semi-soft switching techniques and of semi-symmetrical PWM waveform generation. The power losses associated with the matrix converter have been compared to those in a rectifier/inverter circuit. It has been shown that at higher switching frequencies the losses in a matrix converter can be less than those in a comparable rectifier/inverter circuit and therefore a smaller heat sink can be used.

If the converter is driven from a perfectly sinusoidal supply then it will draw no harmonic currents, unlike a rectifier. However, filters may be required to reduce the levels of the switching frequency harmonic currents drawn from the supply. These filters may be required to meet future EMC regulations. The effect of these possible regulations on the size of the input filters and the unique aspects of the filter design required by the matrix converter circuit have been considered. The cost of these filters with respect to the switching frequency of the converter has also been considered. The cost of the filter would reduce with a higher switching frequency, but the switching losses in the converter will increase with frequency. A balance must therefore be found between the size of the input filter and the acceptable magnitude of the switching losses.

An experimental matrix converter for driving a 5kW three phase induction motor has been built and tested. The results from this converter have been encouraging and have helped in the refining and verification of the ideas presented in this thesis. The experimental converter has been tested in both motoring and regenerative modes and under different loading conditions.

The concept of the reduction of matrix converter circuit and control theory to inverter and controlled rectifier circuits has been discussed. This may be achieved by appropriately setting the input or output frequency to zero. The redundant switches in the circuit may then be removed, reducing the matrix converter circuit to the usual inverter or controlled rectifier circuits.

## 11.2 Potential Applications

Because of the intrinsic limit of 0.866 for the maximum input to output voltage ratio of the matrix converter it is unlikely that it will be used widely as a general purpose variable speed motor drive in the near future. It would be difficult to sell a product that could not be used as a direct replacement for an inverter drive. For this reason it would seem likely that the back-to-back converter will be used in situations where sinusoidal input currents are required instead of the matrix converter in the next few years.

However, the matrix converter may well find applications in motor drives where the absence of large capacitors would be very desirable, and would compensate for the inconvenience of having to use a lower voltage motor. Applications of this type may be found in potentially hazardous areas, such as mines, where it is desirable not to have stored energy due to the risk of explosions. Other applications may be found in areas where the physical size of the drive is important, and the all silicon solution offered by the matrix converter will provide a means of minimising the size of the drive.

The all silicon solution offered by the matrix converter circuit makes it very suitable for production in hybrid modules, with the associated cost and size improvements that hybrid technology may bring. In some applications it may be possible for the required hybrid module for a matrix converter motor drive to be mounted on or inside the casing of small motors. A possible example of this is in pump and fan applications. The case of the motor would then form the heat sink for the drive. This would give a very compact and user-friendly unit with lower installation costs.

The matrix converter can be set up to operate from any input frequency. Other applications for the circuit may therefore exist in situations where a constant frequency supply is required from a variable frequency source. An example of these applications is the generation of electricity for the national grid from natural sources such as wave power and wind turbines, where the frequency and phase of the generated electricity can not be guaranteed. The matrix converter could be set up

to alter the frequency and phase of the generated power to match the phase and frequency of the national grid.

Other potential uses could include connections between power systems of different frequencies, for example to allow power flow between 50Hz and 60Hz distribution grids. The circuit could also be used to cope with step changes in frequency. For example, in a uninterruptable power supply system the circuit can be used to ensure a constant frequency supply from either the AC supply or a backup DC supply. Matrix converters have also been suggested for use as active filters. In this application a dummy inductive load is used as the output voltages would not usually be sinusoidal.

## 11.3 Scope for Future Work

The motor control aspects of variable speed drives have not been addressed in this thesis. The principles involved have been widely developed for inverter motor drives and future work could therefore involve the extension of new inverter control techniques to the matrix converter structure.

Appendix A

# The Verification of the Control Matrix Operation

## A.1 The Notation

To minimise the size of the equations and to simplify the trigonometry involved in the verification of the matrix converter control algorithm the following shorthand notation has been adopted:

$$c(x,y,n,\phi) = \cos(x\omega_i t + y\omega_o t + \tfrac{n\pi}{3} + \phi) \tag{A.1}$$

By applying this notation to the control matrix given in Chapter 2 the control matrix may be rewritten as shown in equation A.2. These equations assume that the control matrix is set up for unity input displacement factor and that the converter is operating at maximum output voltage, but the results of the analysis are valid for all possible conditions.

$$\begin{aligned} G(t) = \tfrac{0.866}{3}.&\begin{bmatrix} c(1,1,0)+c(1,-1,0) & c(1,1,2)+c(1,-1,-2) & c(1,1,4)+c(1,-1,-4) \\ c(1,1,2)+c(1,-1,-2) & c(1,1,4)+c(1,-1,-4) & c(1,1,0)+c(1,-1,0) \\ c(1,1,4)+c(1,-1,-4) & c(1,1,0)+c(1,-1,0) & c(1,1,2)+c(1,-1,-2) \end{bmatrix} \\ +\tfrac{0.25}{3}.&\begin{bmatrix} c(4,0,0)+c(2,0,0) & c(4,0,2)+c(2,0,-2) & c(4,0,4)+c(2,0,-4) \\ c(4,0,0)+c(2,0,0) & c(4,0,2)+c(2,0,-2) & c(4,0,4)+c(2,0,-4) \\ c(4,0,0)+c(2,0,0) & c(4,0,2)+c(2,0,-2) & c(4,0,4)+c(2,0,-4) \end{bmatrix} \\ -\tfrac{0.12}{3}.&\begin{bmatrix} c(1,3,0)+c(-1,3,0) & c(1,3,4)+c(-1,3,-4) & c(1,3,2)+c(-1,3,-2) \\ c(1,3,0)+c(-1,3,0) & c(1,3,4)+c(-1,3,-4) & c(1,3,2)+c(-1,3,-2) \\ c(1,3,0)+c(-1,3,0) & c(1,3,4)+c(-1,3,-4) & c(1,3,2)+c(-1,3,-2) \end{bmatrix} \end{aligned} \tag{A.2}$$

## A.2 The Output Voltage Waveforms

If the input voltage matrix is multiplied by the control matrix then the output voltage waveforms can be verified, as described in equation A.3. This process assumes that the switching frequency is very high in comparison to both the input and output frequencies, and that the input voltage waveforms are perfect sinusoids of the supply frequency.

$$\mathrm{V_o(t)} = \begin{bmatrix} V_{o1}(t) \\ V_{o2}(t) \\ V_{o3}(t) \end{bmatrix} = \mathrm{G(t).V_i(t)}$$

$$= \mathrm{G(t).}V_i \begin{bmatrix} \mathrm{c(1,0,0)} \\ \mathrm{c(1,0,2)} \\ \mathrm{c(1,0,4)} \end{bmatrix} \tag{A.3}$$

Each output phase will be considered independently, and therefore only one line of the control matrix need be considered for each output phase. The ideal output voltage waveform for the first output phase will therefore be:

$$V_{o1}(t) = \frac{1}{3} \begin{bmatrix} 0.866.(\mathrm{c(1,1,0)} + \mathrm{c(1,-1,0)}) \\ +0.25.(\mathrm{c(4,0,0)} + \mathrm{c(2,0,0)}) \\ -0.12.(\mathrm{c(1,3,0)} + \mathrm{c(-1,3,0)}) \\ \\ 0.866.(\mathrm{c(1,1,2)} + \mathrm{c(1,-1,-2)}) \\ +0.25.(\mathrm{c(4,0,2)} + \mathrm{c(2,0,-2)}) \\ -0.12.(\mathrm{c(1,3,4)} + \mathrm{c(-1,3,-4)}) \\ \\ 0.866.(\mathrm{c(1,1,4)} + \mathrm{c(1,-1,-4)}) \\ +0.25.(\mathrm{c(4,0,2)} + \mathrm{c(2,0,-2)}) \\ -0.12.(\mathrm{c(1,3,4)} + \mathrm{c(-1,3,-4)}) \end{bmatrix}^T . \begin{bmatrix} \mathrm{c(1,0,0)} \\ \mathrm{c(1,0,2)} \\ \mathrm{c(1,0,4)} \end{bmatrix}$$

$$\begin{aligned}V_{o1}(t) = V_i.\tfrac{1}{3}.\{&0.866.(c(2,1,0)+c(2,1,2)+3.c(2,1,4)+c(0,1,0)\\&+c(2,-1,0)+c(2,-1,-4)+c(2,-1,-2)+3.c(0,-1,0))\\&+0.25.(c(5,0,0)+c(5,0,2)+c(5,0,4)+3.c(3,0,0)\\&+c(1,0,0)+c(1,0,-2)+c(1,0,-4)+3.c(-3,0,0))\\&+0.12.(c(2,3,0)+c(2,3,2)+c(2,3,4)+3.c(0,3,0)\\&+c(-2,-3,0)+c(-2,-3,-2)+c(-2,-3,-4)+3.c(0,-3,0))\}\end{aligned} \tag{A.4}$$

Using the assumption that the sum of a set of balanced three phase waveforms of equal magnitude is zero:

$$c(x_1,y_1,0)+c(x_1,y_1,2)+c(x_1,y_1,4)=0 \tag{A.5}$$

And the assumption from trigonometric laws that:

$$\begin{aligned}c(0,y_1,\phi_1) &= c(0,-y_1,-\phi_1)\\ c(x_1,0,\phi_2) &= c(-x_1,0,-\phi_2)\end{aligned} \tag{A.6}$$

Equation A.4 can be rearranged and simplified:

$$V_{o1}(t) = V_i\{0.866.c(0,1,0)+0.25.c(3,0,0)+0.12.c(0,3,0)\} \tag{A.7}$$

This analysis can be repeated for the second output phase of the converter. Only the second row of the control matrix need be considered for the second output phase:

$$V_{o2}(t)=\frac{1}{3}\begin{bmatrix} 0.866.(c(1,1,2)+c(1,-1,-4)) \\ +0.25.(c(4,0,0)+c(2,0,0)) \\ -0.12.(c(1,3,0)+c(-1,3,0)) \\ \\ 0.866.(c(1,1,4)+c(1,-1,-2)) \\ +0.25.(c(4,0,2)+c(2,0,-2)) \\ -0.12.(c(1,3,4)+c(-1,3,-4)) \\ \\ 0.866.(c(1,1,0)+c(1,-1,0)) \\ +0.25.(c(4,0,2)+c(2,0,-2)) \\ -0.12.(c(1,3,4)+c(-1,3,-4)) \\ \\ \end{bmatrix}^T \cdot \begin{bmatrix} c(1,0,0) \\ c(1,0,2) \\ c(1,0,4) \end{bmatrix}$$

$$\begin{aligned} V_{o2}(t) = V_i.\tfrac{1}{3}.\{&0.866.(c(2,1,0)+c(2,1,2)+3.c(2,1,4)+c(0,1,2) \\ &+c(2,-1,0)+c(2,-1,-4)+c(2,-1,-2)+3.c(0,-1,-4)) \\ &+0.25.(c(5,0,0)+c(5,0,2)+c(5,0,4)+3.c(3,0,0) \\ &+c(1,0,0)+c(1,0,-2)+c(1,0,-4)+3.c(-3,0,0)) \\ &+0.12.(c(2,3,0)+c(2,3,2)+c(2,3,4)+3.c(0,3,0) \\ &+c(-2,-3,0)+c(-2,-3,-2)+c(-2,-3,-4)+3.c(0,-3,0))\} \end{aligned} \quad \text{(A.8)}$$

Equation A.8 can be rearranged and simplified:

$$V_{o2}(t) = V_i\{0.866.c(0,1,2)+0.25.c(3,0,0)+0.12.c(0,3,0)\} \quad \text{(A.9)}$$

This analysis can be repeated for the third output phase of the converter. Only the last row of the control matrix need be considered for the third output phase:

$$V_{o3}(t)=\frac{1}{3}\begin{bmatrix} 0.866.(c(1,1,4)+c(1,-1,-2)) \\ +0.25.(c(4,0,0)+c(2,0,0)) \\ -0.12.(c(1,3,0)+c(-1,3,0)) \\ \\ 0.866.(c(1,1,0)+c(1,-1,0)) \\ +0.25.(c(4,0,2)+c(2,0,-2)) \\ -0.12.(c(1,3,4)+c(-1,3,-4)) \\ \\ 0.866.(c(1,1,2)+c(1,-1,-4)) \\ +0.25.(c(4,0,2)+c(2,0,-2)) \\ -0.12.(c(1,3,4)+c(-1,3,-4)) \\ \\ \end{bmatrix}^T \cdot \begin{bmatrix} c(1,0,0) \\ c(1,0,2) \\ c(1,0,4) \end{bmatrix}$$

$$\begin{aligned} V_{o3}(t) = V_i.\tfrac{1}{3}.\{&0.866.(c(2,1,0)+c(2,1,2)+3.c(2,1,4)+c(0,1,4) \\ &+c(2,-1,0)+c(2,-1,-4)+c(2,-1,-2)+3.c(0,-1,4)) \\ &+0.25.(c(5,0,0)+c(5,0,2)+c(5,0,4)+3.c(3,0,0) \\ &+c(1,0,0)+c(1,0,-2)+c(1,0,-4)+3.c(-3,0,0)) \\ &+0.12.(c(2,3,0)+c(2,3,2)+c(2,3,4)+3.c(0,3,0) \\ &+c(-2,-3,0)+c(-2,-3,-2)+c(-2,-3,-4)+3.c(0,-3,0))\} \end{aligned} \quad \text{(A.10)}$$

Equation A.10 can then be rearranged and simplified:

$$V_{o3}(t) = V_i\{0.866.c(0,1,4)+0.25.c(3,0,0)+0.12.c(0,3,0)\} \quad \text{(A.11)}$$

By combining equations A.7, A.9 and A.11 the output voltage matrix produced by the control matrix under ideal conditions can be found:

$$
\begin{aligned}
\mathrm{V_o(t)} &= \begin{bmatrix} V_{o1}(t) \\ V_{o2}(t) \\ V_{o3}(t) \end{bmatrix} \\
&= 0.866. \begin{bmatrix} \mathrm{c}(0,1,0) \\ \mathrm{c}(0,1,2) \\ \mathrm{c}(0,1,4) \end{bmatrix} + 0.25.\mathrm{c}(3,0,0) + 0.12.\mathrm{c}(0,3,0) \\
&= 0.866. \begin{bmatrix} \cos(\omega_o t) \\ \cos(\omega_o t + \frac{2\pi}{3}) \\ \cos(\omega_o t + \frac{4\pi}{3}) \end{bmatrix} + 0.25.\cos(3\omega_i \mathrm{t}) + 0.12.\cos(3\omega_o t)
\end{aligned}
\qquad \text{(A.12)}
$$

This ideal output voltage matrix formed by the control matrix corresponds to the ideal output waveforms needed to obtain the maximum output voltage magnitude, as described in equation 2.4.

## A.3 The Input Current Waveforms

The ideal output currents from the matrix converter will be sinusoidal assuming that the output voltage waveforms are ideal. These output current equations can be written in the notation form used above as shown in equation A.13.

$$
\begin{aligned}
I_o(t) &= \xi.I_i \begin{bmatrix} \cos(\omega_o t + \phi_1) \\ \cos(\omega_o t + \frac{2\pi}{3} + \phi_1) \\ \cos(\omega_o t + \frac{2\pi}{3} + \phi_1) \end{bmatrix} \\
&= \xi.I_i \begin{bmatrix} \mathrm{c}(0,1,0,\phi_1) \\ \mathrm{c}(0,1,2,\phi_1) \\ \mathrm{c}(0,1,4,\phi_1) \end{bmatrix}
\end{aligned}
\qquad \text{(A.13)}
$$

Where $\xi$ is a scaling factor determined by the magnitude and nature of the load.

The ideal input current will be the output currents modulated by the control matrix. The currents can be considered as being modulated in the opposite direction through the converter as the voltages. The ideal input currents can therefore be

described by the output currents multiplied by the transpose of the modulation matrix, as shown in equation A.14.

$$\mathrm{I_i(t)} = \begin{bmatrix} I_{i1} \\ I_{i2} \\ I_{i3} \end{bmatrix} = \mathrm{G^T(t).I_o(t)} \tag{A.14}$$

Again each phase will be examined separately. If the first input line current is considered then only the first column of the control matrix applies:

$$I_{i1}(t) = \xi.I_i.\begin{bmatrix} 0.866.\big(c(1,1,0)+c(1,-1,0)\big) \\ +0.25.\big(c(4,0,0)+c(2,0,0)\big) \\ -0.12.\big(c(1,3,0)+c(-1,3,0)\big) \\ \\ 0.866.\big(c(1,1,2)+c(1,-1,-4)\big) \\ +0.25.\big(c(4,0,0)+c(2,0,0)\big) \\ -0.12.\big(c(1,3,0)+c(-1,3,0)\big) \\ \\ 0.866.\big(c(1,1,4)+c(1,-1,-2)\big) \\ +0.25.\big(c(4,0,0)+c(2,0,0)\big) \\ -0.12.\big(c(1,3,0)+c(-1,3,0)\big) \\ \\ \end{bmatrix}^T .\begin{bmatrix} c(1,0,0,\phi_1) \\ c(1,0,2,\phi_1) \\ c(1,0,4,\phi_1) \end{bmatrix}$$

$$
\begin{aligned}
I_{i1}(t) = I_i.\xi.\{&0.866.(c(1,2,0,\phi_1)+c(1,2,2,\phi_1)+3.c(1,0,0,\phi_1)+c(1,2,4,\phi_1)\\
&+c(1,-2,0,-\phi_1)+c(1,-2,-4,-\phi_1)+c(1,-2,-2,-\phi_1)+3.c(1,0,0,-\phi_1))\\
&+0.25.(c(4,1,0)+c(4,1,2)+c(4,1,4)+c(4,-1,0)+c(4,-1,-2)+c(4,-1,-4)\\
&+c(2,1,0)+c(2,1,-2)+c(2,1,-4)+c(2,-1,0)+c(2,-1,2)+c(2,-1,4))\\
&+0.12.(c(1,4,0)+c(1,4,2)+c(1,4,4)+c(-1,-4,0)+c(-1,-4,-2)+c(-1,-4,-4)\\
&+c(-1,-2,0)+c(-1,-2,-2)+c(-1,-2,-4)+c(1,2,0)+c(1,2,2)+c(1,2,4))\}
\end{aligned}
\tag{A.15}
$$

Equation A.15 can then be rearranged and simplified:

$$
I_{i1}(t) = \xi.I_i.0.866.c(1,0,0) \tag{A.16}
$$

The second input line current may then be examined in the same way. Only the second column of the control matrix needs to be considered:

$$
I_{i2}(t) = \xi.I_i.\begin{bmatrix}
0.866.(c(1,1,2)+c(1,-1,-4))\\
+0.25.(c(4,0,2)+c(2,0,2))\\
-0.12.(c(1,3,2)+c(-1,3,2))\\
\\
0.866.(c(1,1,4)+c(1,-1,-2))\\
+0.25.(c(4,0,2)+c(2,0,-2))\\
-0.12.(c(1,3,2)+c(-1,3,-2))\\
\\
0.866.(c(1,1,0)+c(1,-1,0))\\
+0.25.(c(4,0,2)+c(2,0,-2))\\
-0.12.(c(1,3,2)+c(-1,3,-2))
\end{bmatrix}^T
\begin{bmatrix}
c(1,0,0,\phi_1)\\
c(1,0,2,\phi_1)\\
c(1,0,4,\phi_1)
\end{bmatrix}
$$

$$
\begin{aligned}
I_{i2}(t) = I_i.\xi.\{&0.866.(c(1,2,0,\phi_1)+c(1,2,2,\phi_1)+3.c(1,0,2,\phi_1)+c(1,2,4,\phi_1)\\
&+c(1,\text{-}2,0,-\phi_1)+c(1,\text{-}2,\text{-}4,-\phi_1)+c(1,\text{-}2,\text{-}2,-\phi_1)+3.c(1,0,-4,-\phi_1))\\
&+0.25.(c(4,1,0)+c(4,1,2)+c(4,1,4)+c(4,\text{-}1,0)+c(4,\text{-}1,\text{-}2)+c(4,\text{-}1,\text{-}4)\\
&+c(2,1,0)+c(2,1,\text{-}2)+c(2,1,\text{-}4)+c(2,\text{-}1,0)+c(2,\text{-}1,2)+c(2,\text{-}1,4))\\
&+0.12.(c(1,4,0)+c(1,4,2)+c(1,4,4)+c(\text{-}1,\text{-}4,0)+c(-1,\text{-}4,\text{-}2)+c(-1,\text{-}4,\text{-}4)\\
&+c(\text{-}1,\text{-}2,0)+c(-1,-2,\text{-}2)+c(-1,-2,\text{-}4)+c(1,2,0)+c(1,2,2)+c(1,2,4))\}
\end{aligned}
\tag{A.17}
$$

Equation A.17 can then be rearranged and simplified:

$$
I_{i2}(t) = \xi.I_i.0.866.c(1,0,2) \tag{A.18}
$$

The third input line current may then be examined in the same way. Only the third column of the control matrix needs to be considered:

$$
I_{i3}(t) = \xi.I_i.\begin{bmatrix}
0.866.(c(1,1,4)+c(1,-1,-2))\\
+0.25.(c(4,0,4)+c(2,0,-2))\\
-0.12.(c(1,3,4)+c(-1,3,-2))\\
\\
0.866.(c(1,1,0)+c(1,-1,0))\\
+0.25.(c(4,0,4)+c(2,0,-2))\\
-0.12.(c(1,3,4)+c(-1,3,-2))\\
\\
0.866.(c(1,1,2)+c(1,-1,-4))\\
+0.25.(c(4,0,4)+c(2,0,-2))\\
-0.12.(c(1,3,4)+c(-1,3,-2))
\end{bmatrix}^T
\begin{bmatrix}
c(1,0,0,\phi_1)\\
c(1,0,2,\phi_1)\\
c(1,0,4,\phi_1)
\end{bmatrix}
$$

$$
\begin{aligned}
I_{i3}(t) = I_i.\xi.\{&0.866.(c(1,2,0,\phi_1)+c(1,2,2,\phi_1)+3.c(1,0,4,\phi_1)+c(1,2,4,\phi_1)\\
&+c(1,-2,0,-\phi_1)+c(1,-2,-4,-\phi_1)+c(1,-2,-2,-\phi_1)+3.c(1,0,4,-\phi_1))\\
&+0.25.(c(4,1,0)+c(4,1,2)+c(4,1,4)+c(4,-1,0)+c(4,-1,-2)+c(4,-1,-4)\\
&+c(2,1,0)+c(2,1,-2)+c(2,1,-4)+c(2,-1,0)+c(2,-1,2)+c(2,-1,4))\\
&+0.12.(c(1,4,0)+c(1,4,2)+c(1,4,4)+c(-1,-4,0)+c(-1,-4,-2)+c(-1,-4,-4)\\
&+c(-1,-2,0)+c(-1,-2,-2)+c(-1,-2,-4)+c(1,2,0)+c(1,2,2)+c(1,2,4))\}
\end{aligned}
\tag{A.19}
$$

Equation A.19 can then be rearranged and simplified:

$$
I_{i3}(t) = \xi.I_i.0.866.c(1,0,4) \tag{A.20}
$$

The input current matrix may now be formed by substituting equations A.16, A.18 and A.20 into equation A.14 and decoding the notation:

$$
\begin{aligned}
I_i(t) &= \begin{bmatrix} I_{i1} \\ I_{i2} \\ I_{i3} \end{bmatrix} = \xi.I_i.\begin{bmatrix} c(1,0,0) \\ c(1,0,2) \\ c(1,0,4) \end{bmatrix} \\
&= \xi.I_i.\begin{bmatrix} \cos(\omega_o t) \\ \cos(\omega_o t + \frac{2\pi}{3}) \\ \cos(\omega_o t + \frac{4\pi}{3}) \end{bmatrix}
\end{aligned}
\tag{A.20}
$$

These ideal input currents are of the same form as the input voltages and are in phase with the input voltage waveforms, as required.

The analysis presented in this appendix has assumed that the converter has a perfect three phase supply with no impedance. The load has been considered as a perfect current source capable of absorbing current without any change in characteristics. The nine bi-directional power switches in the converter have been taken as perfect switches with no delays or losses. The switching frequency of the converter has

been considered as infinite in comparison to the input output and control frequencies.

## Appendix B

# List of Symbols

The following is a list of the symbols used in this thesis and their meanings. Chapter numbers have been given after the symbol definition in situations where the use of a variable may be unclear.

| | |
|---|---|
| A | Filter attenuation |
| $a_m(y)$ | Fourier function of y |
| $b_m(y)$ | Fourier function of y |
| C | Capacitance |
| $C_\theta$ | Double integral with product cosine function |
| $c_m(y)$ | Fourier function of y |
| $\cos(\varphi)$ | Power factor |
| $d_m(y)$ | Fourier function of y |
| $dx$ | Duty cycle of switch x |
| $E_{loss}$ | Energy lost per device switching cycle for a given device |
| $e_m(y)$ | Fourier function of y |
| **F(t)** | Sub-division of Control Matrix, rectifier process matrix |
| F(x,y) | Function of x and y |
| $f_i$ | Fundamental input frequency |
| $f_m(y)$ | Fourier function of y |
| $f_o$ | Fundamental output frequency |
| $f_s$ | Switching frequency |
| **G(t)** | Control Matrix |
| $\mathbf{G_1(t)}$ | Sub-division of Control Matrix, leading displacement factor |
| $\mathbf{G_2(t)}$ | Sub-division of Control Matrix, lagging displacement factor |

| | |
|---|---|
| $g_m$ | Input voltage to current ratio (Chapter 8) |
| $g_{xy}$ | Element x,y of the control matrix |
| **H(t)** | Sub-division of Control Matrix, inverter process matrix |
| $h_x$ | Harmonic of order x |
| $I_a$ | Current Direction |
| $i_{ac}$ | Instantaneous AC current |
| $i_c$ | Capacitor current (Chapter 8) |
| $I_c$ | Collector current in a IGBT |
| $I_f$ | Forward current in a diode |
| $I_{ix}$ | Input line current in arbitrary input line x |
| $i_m$ | Motor current |
| $\mathbf{I_o(t)}$ | Input current matrix |
| $\mathbf{I_o(t)}$ | Output current matrix |
| $I_{ox}$ | Output line current in arbitrary output line x |
| $J_n(Z)$ | Bessel Function of the first kind of Z, order n |
| $K_s$ | Number of hard switching cycles per switching period |
| L | Inductance |
| m | Order of switching frequency harmonics (Chapter 7) |
| m | Output signal from a current sensor (Chapter 9) |
| **M(t)** | matrix of switch functions |
| m(t) | switch function (Chapter 3) |
| n | Order of control frequency harmonics |
| P | Average power |

| | |
|---|---|
| q | Modulation index |
| R | Resistance |
| $R_L$ | Resistance of a real inductor |
| $R_{th}$ | Thermal residence in a device |
| $S_\theta$ | Double integral with product sine function |
| S*x* | Switch number x |
| S*x*A | Forward current direction switch control signal |
| S*x*B | Reverse current direction switch control signal |
| Sxy | Switch connected to input line x and output line y |
| t | Time variable |
| T1,T2 | Transformers (Chapter 9) |
| $T_{air}$ | Ambient air temperature |
| $T_j$ | Device junction temperature |
| $T_{seq}$, $T_s$ | Switching period |
| T*x* | Closed period of switch number x |
| $v_{ac}$ | Instantaneous AC voltage |
| $V_c$ | Voltage across a capacitor |
| $V_{ce}$ | Saturation voltage of an IGBT |
| $V_{dc}$ | DC voltage |
| $V_f$ | Forward voltage of a diode |
| $V_{ix}$ | Input line voltage on arbitrary input line x |
| $V_{o,max}$ | Maximum output voltage magnitude in a given period |
| $V_{o,min}$ | Minimum output voltage magnitude in a given period |

| | |
|---|---|
| $\mathbf{V_0(t)}$ | Input voltage matrix |
| $\mathbf{V_0(t)}$ | Output voltage matrix |
| $V_{ox}$ | Output line voltage on arbitrary output line x |
| x | Proportional factor for unbalanced supply calculations (Chapter 2) |
| y | Proportional factor for unbalanced supply calculations (Chapter 2) |
| $\frac{di}{dt}$ | Rate of change of current |
| $\frac{dv}{dt}$ | Rate of change of voltage |
| $\xi$ | Current scaling factor dependant on nature of the converter load |
| $\gamma$ | Displacement factor between voltage and current waveforms |
| $\alpha$ | Displacement factor control variable |
| $\beta$ | Proportional factor for harmonic distortion calculations |
| $\omega_c$ | Angular control frequency |
| $\omega_i$ | Angular frequency of input waveform |
| $\omega_o$ | Angular frequency of output waveform |
| $\omega_s$ | Angular Switching frequency |
| $\beta_x$ | Magnitude of function number x |

## Appendix C

# Alphabetical Bibliography

Alesina A. and Venturini M., "The Generalised Transformer : A New Bidirectional Sinusoidal Waveform Frequency Converter With Continuous Variable Adjustable Input Power Factor", Proc. of PESC Conference Record, 1980, pp.242-252.

Alesina A. and Venturini M., "Solid-State Power Conversion : A Fourier Analysis Approach to Generalised Transformer Synthesis", IEEE Trans. on Circuits and Systems, Vol. cas28, No.4, April 1981, pp.319-330.

Alesina A. and Venturini M., "Intrinsic Amplitude Limits and Optimum Design of 9-Switches Direct PWM AC to AC Converters", PESC Conference Record 1988, pp.1284-1291.

Arcotronics, "Capacitors for Power Electronics", Arcotronics Data Sheet.

Asher G.M., Davis R.M. and Vasquez-Borquez, "Operation of the Naturally Commutating Hidden Link Converter Feeding a Cage Induction Motor", Conf. on Power Electronics and Variable Speed Drives, 1988, pp.130-133.

Baliga B.J, Chang M, Shafer P and Smith M.W, "The Insulated Gate Transistor: A New Power Switching Device", IEEE-IAS Conference Record, 1983, pp.794-803.

Beasant R.R., Beatie W.C. and Refsum A., "An Approach to the Realisation of a High Power Venturini Converter", IEEE, April 1990, pp.291-297.

Beauregard F, Roy G and April G.E, "Design Consideration Related to the Use of Power MOSFETs in High Performance AC to AC Converters", Proc. of Powercon, Munich, May 11-13, 1987.

Beckhard A.J., "Nikola Tesla: Electrical Genius", 1953.

Bedford B.D and Hoft R.G, "Principles of Inverter Circuits", New York: Wiley, 1964.

Black H.S., "Modulation Theory", Van Nostrand, New York, 1953.

Bose B.K, "Recent Progress in Power Electronics", IEEE Transactions on Power Electronics, Jan. 1992, pp.2-17.

Bosterling W, "Non-Problematic Gate Drive of IGBT Modules", Power Conversion, April 1992, pp87-95.

Braun M and Hasse K, "A Direct Frequency Changer with Control of Input Reactive Power", Proc. IFAC, Control in Power Electronics and Electrical Drive, 1983, pp.187-194.

Brichant F., "Forced Commutated Inverters", North Oxford Academic, 1984.

British Standards Institution, BS800, 1983.

Burany N, "Safe Control of Four Quadrant Switches", IEEE IAS Annual Meeting, 1989, pp.1190-1194.

Carrara G., Gardella S., Marchesoni M., Salutri R. and Sciutto G., "A New Multilevel PWM Method: A Theoretical Analysis", IEEE Transactions on Power Electronics, Vol.7, No.3, July1992, pp.497-505.

Cho J.G, Kim H.S. and Cho G.H., "Novel Soft Switching PWM Converter Using A New Parallel Resonant DC-Link", PESC 1991, pp.241-247.

Cho J.G., Hu D.Y. and Cho G.H., "Three Phase Sine Wave Voltage Source Inverter Using the Soft Switched Resonant Poles", IECON 1989, Vol.1, pp.48-53.

CISPR16,

Control Techniques, "Drives and Servos Year Book, 1990-1991", 1989.

Critchley R., "New European Standards on EMC Affects Drives", Drives and Controls, Vol. 8, No. 9, Nov. 1992

Daniels A.R and D.T.Slattery D.T, " New Power Converter Technique Employing Power Transistors", Proc. IEE, Vol.125, No.2, Feb. 1978, pp.146-150.

Daniels A.R and Slattery D.T, " Application of Power Transistors to Polyphase Regenerative Power Converters", Proc. IEE, Vol.125, No.7, July 1978, pp.643-647.

Divan D.M., "The Resonant DC Link Converter - A New Concept in Static Power Conversion", IEEE Trans. on Ind. Applications, Vol.25, No.2, March 1989, PP.317-325.

Divan D.M., Venkataramanan G and De Doneker R.W, "Design Methodologies for soft Switched Inverters", Conf. Record of the IAS Annual Meeting, 1988, pp.758-766.

Divan D.M. and Skibinski G., "Zero Switching Loss Inverters For High Power Applications", Conf. Record of the IAS Annual Meeting, 1987, pp.627-634.

Divan D.M. and Skibinski G., "Zero Switching Loss Inverters For High Power Applications", IEEE Trans. on Ind. Applications, Vol.25, No.4, 1989, pp.634-643

Edelmoser K.H et al., "Floating, Flexible and Intelligent Gate Driver Circuit for IGBT Modules", Power Conversion, April 1992, pp96-105.

Electricity Association, "Limits for Harmonics in the UK Electricity Supply System", G.5/3, Engineering Publications, 1976.

Enjeti P. and Shireen W., "A New Technique to Reject DC-Link Voltage Ripple for Inverters Operating on Programmed PWM Waveforms", IEEE, 1990, pp.705-712.

Enjeti P.N, Ziogas P.D. and Lindsay J.F, "A Current Source PWM Inverter with Instantaneous Current Control Capacity", IEEE Industrial Applications Society, Annual Meeting Conference Record, 1988, pp.895-902.

European Standards, EN55011, 1986.

German Standards, VDE0871 part 1, 1981.

Gjugyi L and Pelly B, "Static Power Frequency Changers", New York : Wiley, 1976.

Grant D.A., "Using HEXFET III in PWM Inverters for Motor Drives and UPS Systems", International Rectifiers, Power MOSFETs Application Notes.

Grant D.G. and Gower J., "Power MOSFETs: Theory and Applications", Wiley, 1989.

Habetler T.G., "Rectifier/Inverter Reactive Component Minimisation", IEEE Transactions on Industrial Applications, Vol.25, No.2, March 1989, pp.307-316

Habetler T.G. and Divan M.D., "Angle Controlled Current Regulated Rectifiers For AC/AC Converters", PESC. 1989, Vol.2, pp.704-710.

Harris Semiconductors, "MCT75P60E1 Data Sheet", File No. 3374.1, Oct. 1992

Hemphill H. and Aust S., "EMC and Drives", Drives and Controls, Vol. 8, No. 8, Oct. 1992

Holmes D.G, "A New Modulation Algorithm for Voltage and Current Source Inverters, based on AC-AC Matrix Converter Theory", IEEE 1990 pp.1190-1195.

Holmes D.G, "A Unified Modulation Algorithm for Voltage and Current Source Inverters based on AC-AC Matrix Converter Theory", IEEE 1992 pp.31-40.

Holmes D.G and Lipo T.A, "Implementation of a Controlled Rectifier using AC-AC Matrix Converter Theory", Conf. Record PESC 1989, pp.353-359.

Holmes D.G and Lipo T.A, "Implementation of a Controlled Rectifier using AC-AC Matrix Converter Theory ", IEEE Trans. on Power Electronics, Vol.7, No.1, January 1992, pp.240-250.

Holmes D.G., " the General Relationship between Regular-Sampled Pulse Width Modulation and Space Vector Modulation for Hard Switching Converters" Space Vector Modulation", IEEE, 1992, pp.-.

Holmes D.G. and Lipo T.A., "Implementation of a Controlled Rectifier Using AC-AC Matrix Converter Theory", IEEE Transactions on Power Electronics, Vol.7, No.1, 1992, pp.240-250.

Huber L, Borojevic D and Burany N, "Voltage Space Vector Based PWM Control of FCCs", IECON 1989, Vol.1, pp.48-53.

Huber L, Borojevic D and Burany N, "Analysis, Design and Implementation of the Space Vector Modulation for Forced Commutated Cycloconverters", IEE Proceedings Part B 1992.

Huber L, Borojevic D, Zhuang X F and Lee F C, "Design and Implementation of a Three Phase Matrix Converter with Input Power Correction", IEEE 1993 pp.860-865.

Huber L and Borojevic D, "Space Vector Modulation for Forced Commutated Cycloconverters", IEEE, 1989, pp.871-876.

Huber L., Borojevic D and Burany N, "Digital Implementation of the Space Vector Modulator for Forced Commutated Cycloconverters", Conf. Record on Power Electronics and Variable Speed Drives, July 1990, pp.63-68.

Huisman H., "A Three Phase to Three Phase Series Resonant Power Converter With Optimal Input Current Waveforms. Part.2: Application and Results", IEEE Transactions on Power Electronics, Vol.35, No.2, May 1988, pp.269-277.

Huisman H., "A Three Phase to Three Phase Series Resonant Power Converter With Optimal Input Current Waveforms. Part.1: Control Strategy", IEEE Transactions on Power Electronics, Vol.35, No.2, May 1988, pp.263-268.

IEEE , "Guide for Harmonic Control and Reactive Compensation of Static Power Converters", IEEE Std.519, 1981.

International Rectifiers, "IRGBC20 IGBT Data Sheet", Data Sheet No. PD-9.626A.

Ishida M, Iwasaki M, Ohkuma S and Iwata K, "Waveform Control of PWM Cycloconverters with Sinusoidal Input Current, Sinusoidal Output Voltage and Variable Input Displacement Factor", Electrical Eng. in Japan, Vol.107, No.3, 1987, pp.95-103.

Ishiguro A and Furuhashi T, "A Novel Control Method for Forced Commutated Cycloconverters Using Instantaneous Values of Input Line-to-Line Voltages ", IEEE Trans. on Ind. Electronics, Vol.38, No.3, June 1991, pp.166-172.

Ishiguro A et al., "A new method of PWM control for forced commutated Cycloconverters using microprocessors", Conf Record, IEEE-IAS Annual Meeting, 1988, pp.712-721.

Jarc D.A. and Novorny D.W., A Graphical Approach to AC Drive Classification", IEEE Transactions on Industrial Applications, Vol.1A-23, No.6, 1987, pp.1029-1035.

Jones R. and Jones S.R., "A unity Power Factor Sinusoidal Supply Side Converter For Industrial AC Drives", IEE Colloquium on Variable Speed Drives, Sept. 1992, pp8/1-8/5.

Joos G., Zargari N.R. and Ziogas P.D., "A New Class of Current Controlled Suppressed-Link AC to AC Frequency Changers", IEEE, 1991, pp.830-837.

Khan S.I, Ziogas P.D and Rashid M.H, "Forced Commutated Cycloconverters for High Frequency Link Applications", IEEE Trans. on Ind. Applications, Vol.1A-23, 1987, pp.661-672.

Khoei A and Yuvarajan S, "Single Phase AC-AC Converters Using Power MOSFET's", IEEE Trans. on Industrial Electronics, Vol.35, No.3, 1988, pp.442-443.

Kim Y and Ehsani M, "New Modulation Methods for Forced Commutated Direct Frequency Changers", IEEE, 1989, pp.798-809.

Klaassens J.B., "DC to AC Series Resonant Converter System with High Freq. Generating Multiphase AC Waveforms for Multi-kilowatt Power Levels", IEEE Trans. on Power Electronics, Vol.2, No.3, July 1987, pp.247-256.

Klaassens J.B. and Beer F., "Three-Phase AC to AC Series Resonant Converter With a Reduced Number of Thyristors", Conf. Record PESC 1989, pp.376-384.

Kwon W.H and Cho G.H, "Analysis of Non-Ideal Step Down Matrix Converter Based on Circuit DQ Transformation", PESC 1991, pp.825-829.

Kwon W.H and Cho G.H, "Static and Dynamic Characteristics of Non-Ideal Step Up Nine Switch Matrix Converter", EPE Firenze, 1991, Vol.4, pp.418-423.

Lai J.S. and Bose B.K., "An Improved Resonant DC Link Inverter For Induction Motor Drives", Conf. Record IAS Annual Meeting, Vol.1, Oct. 1988, pp.742-748.

Lai J.S. and Bose B.K., "An Induction Motor Drive Using An Improved High Frequency Resonant D.C. Link Inverter", Conf. Record PESC 1990, pp.792-799.

LEM , "LEM Module 50A, Data Sheet", LEM Sales Information.

Lipo T.A., "Resonant Link Converters: A New Direction in Solid State Power Conversion", Second International Conference on Electrical Drives, 1989.

Ma X, " High Performance PWM Frequency Changers ", IEEE Trans. Industrial Applications, Vol. 1a-22, Mar./Apr. 1986, pp.267-280.

Madangpal S and Cathey J.J, "Suppression of Converter Introduced Harmonics Currents Using a FFC", IEEE Trans. on Energy Conversion., Vol.5, No.4, 1990, pp.643-649.

Matlab User's Manual.

Maytum K.J and Colman D, "The Implementation and Future Potential of the Venturini Converter", Proc. of Drives, Motors and Controls, 1983, pp.108-117.

MC68332 SIM Users Manual, Motorola, 1989.

Merwe D.J.van der, "A New System for Controlling the Speed, Direction and Torque of the Squirrel Cage Induction Motor", Patent Application No. 864255, April 1986.

Motorola, "MUR860 Data Sheet".

Mullion E.B., Pye D.R. and Southwell R.V., "Bessel Functions For Engineers", Mc.Lachlan, Oxford, 1961.

Murai Y., Abeyratne S.G., Lipo T.A. and Caldeira P., "Dual Flow Pulse Trimming Concept for a Series Resonant DC Link Power Conversion", PESC 1991, pp.254-260.

Murai Y. and Lipo T.A., "High Frequency Series Resonant DC Link Conversion", Conf. Record IAS Annual Meeting, Vol.1, Oct. 1988, pp.772-779.

Neft C.L and Schaudere C.D, "Theory and Design of a 30-Hp Matrix Converter", IEEE-IAS, Vol.1 , 1988, pp.934-939.

Nishizawa J et al, "Low Distortion, High Efficiency, Static Induction Transistor Type Sinusoidal PWM Inverter for Uninterruptable Power Supplies", IEEE IAS Conference Proceedings, 1986.

Nomura H, Fujiwara K and Kawakami H, "A Power Factor Compensator Using a Forced Commutated Cycloconverter", IEEE Trans. on Ind. Applications, Vol.26, No.4, 1990, pp.769-775.

Ohm D.Y., "Principles of Vector Control: Part1", PCIM, August 1990, pp.41-44.

Ohm D.Y., "Principles of Vector Control: Part2", PCIM, September 1990, pp.32-36.

Oyama J et al, "New Control Strategy for Matrix Converter", Conf Record PESC 1989, pp.360-367.

Palmer P.R and Johnson C.M, "Measurement of the Redistribution of Current in GTO Thyristors During Turn-off", European Power Electronics Conference, 1989, pp.337-342.

Patel H.S. and Hoft R.G., "Generalised Techniques of Harmonic Elimination and Voltage Control in Thyristor Inverter: Part 1-Harmonic Elimination", IEE Transactions on Industrial Applications, Vol.1A-9, 1973

QSM MC68300 Manual, Motorola, 1989.

R.S. Components Catalogue, July to September 1992.

Rajashekara K.S., Rajagopalan V., Sévigny A. and Vithayathil J., "DC Line Filter Design Considerations in Three-Phase Voltage Source Inverter-Fed Induction Motor Drive Systems", IEEE Transactions on Industrial Applications, Vol.1A-23, No.4, 1987, pp.673-680.

Rodriguez J, "A new control technique for AC-AC converters", Proc. IFAC, Control in Power Electronics and Electrical Drive, 1983, pp.203-208.

Rogers G.J., "Linearised Analysis of Induction Motor Transients", Proc. IEE, Vol.122, No.10, Oct. 1965, pp1917-1926.

Roy G and April G.E, "Cycloconverter Operation under a New Scalar Control Algorithm", Conf. Record PESC 1989, pp.368-375.

Roy G et al., "Asynchronous Operation of Cycloconverter with Improved Voltage Gain by Employing a Scalar Control Algorithm", IEEE-IAS, Oct.1987, pp.891-898.

SanRex, "Power Semiconductors Data Book 1992", Sansha Electric.

Seimens A.G., "The New Reference Class: The SAB80C166 Microcontroller", 1990.

Shenai K., Scott R.S. and Baliga B.J., "Optimum Semiconductors for High-Power Electronics", IEEE Transactions on Power Electronics, September 1989, pp.1811-1823.

SIM MC68332 Manual, Motorola, 1989.

Smith G.A and Stevens R.G, "High Performance Drivers for IGBTs", IEE Colloquium on Active and Passive Components, Nov. 1992.

Sood P.K., Lipo T.A. and Hansen I.G., "A Versatile power Converter for High Frequency Link Systems", IEEE Trans. On Power Electronics, Vol.3, No.4, Oct. 1988, pp.383-390.

Sood P.K. and Lipo T.A., "Power Conversion Distribution System Using a High Frequency AC Link", IEEE Trans. on Ind. Applications, Vol.24, No.2, March 1988, pp.288-299.

Spath H and Sohner W, "The Unrestricted Frequency Changer for Feeding Induction Machines", Arch. Electrotech, Vol.71, 1988, No.6, pp.441-450.

Sul S.K. and Lipo T.A., "Design and Performance of a High Freq. Link Induction Motor Drive Operating at Unity Power Factor", IEEE Trans. on Ind. Applications, Vol.26, No.3, May 1990, pp.434-440.

Sul S.K. and Lipo T.A., "Design and Performance of a High Frequency Link Induction Motor Drive Operating at Unity Power Factor", Conf. Record IAS Annual Meeting, Vol.1, Oct. 1988, pp.308-313.

Svenson T. and Alakula M., "The Modulation and Control of a Matrix Converter-Synchronous Machine Drive", European Power Electronics Conference, Firenze, 1991, Vol.4, pp 469-476.

Telcon Technology Limited, "CONTEC HTP100, Data Sheet".

Teledyne Semiconductors, "TSC429 High Speed Single CMOS Power MOSFET Driver, Data Sheet",1985.

Tenti P, Malesani L and Rossetto L, "Optimum Control of PWM Multi-converter Systems", IEEE-IAS, 1988, pp.888-894.

Tenti P, "Optimum Control of N-input K-Output Matrix Converters", IEEE Transactions on Power Electronics, Vol. 7, No. 4, Oct. 1992, pp.707-713.

TMS32010 Users Guide, Texas Instruments, 1983.

TMS320C14/TMS320E14 DSP Microcontroller Product Bulletin, Texas Instruments, 1988.

TMS320C14/TMS320E14 Users Guide, Texas Instruments, 1988.

Toshiba, "Toshiba GTR Module Data Book", 1990, Section III: IGBT Modules.

Tounsi S. and Dorkel J., "Thermal Environment CAD for Power Circuits", IEE Colloquium on Power Electronic Devices, Nov. 1992, pp.7.1-7.5.

TPU MC68300 Embedded Control Family Reference Manual, Motorola,

Valle J.del, Arias D, Yeves F and Martinez P.M, "Four Quadrant Speed Control Of Induction Motor by Unrestricted Frequency Changer", IECON 1987, Vol.1, pp.422-429.

Vas P., "Vector Control of AC Machines", Claredon: Oxford, 1990.

Venturini et al., "Method and apparatus for the conversion of a polyphase voltage system", U.S. Patent no.4628425, Dec.1986.

Venturini M, "A New Sine Wave in Sine Wave Out, Conversion Technique Which Eliminates Reactive Elements", Proceedings Powercon 7 (San Diego,CA), 1980, pp.E3_1-E3_15.

Venturini M, "Convertitore diretto AC-AC di elevata potenza", Italian Patent 20777a-79, Mar.6,1979.

Wheeler P.W. and Grant D.A., "Reducing the Semiconductor Losses in a Matrix Converter", Proceedings of IEE Colloquium on Power Electronics, 1992, pp.9.1-9.5.

Wood P, "General Theory of Switching Power Converters", Proc. of PESC Conference Record (San Diego) 1979, pp.3-10.

Wood P, "Switching Power Converters", (book), Van Nostrand Reinhold Company, 1981.

"Principles of Solid State Power Conversion", pp.439-449.

Zhang H:, Wheeler N. and Grant D.A, "Control of a Back to Back Converter", Universities Power Electronics Conference, Stafford, 1993, pp.

Ziogas P.D, Khan S.I and Rashid M.H, "Some Improved Forced Commutated Cycloconverter Structures", IEEE Trans. on Ind. Applications, Oct 1985, Vol.1A-21, No.5, pp.1242-1253.

Ziogas P.D, Khan S.I and Rashid M.H, "Analysis and Design of Forced Commutated Cycloconverter Structures With Improved Transfer Characteristics", IEEE Trans. on Ind. Electronics, Vol.1E-33, No3, Aug.86, pp.271-280.

## Appendix D

# Author's Publications

Publications which have been co-written by the author, and have been presented or have been accepted for presentation or publication are appended to this thesis on the following pages. Details of these publications are set out below.

Wheeler P.W. and Grant D.A., "Reducing the Semiconductor Losses in a Matrix Converter", IEE Colloquium on Variable Speed Drives, 1992.

Wheeler P.W. and Grant D.A., "A Low Loss Matrix Converter for Variable-Speed Drives", European Power Electronics Conference, Brighton, September 1993.

Wheeler P.W., Zhang H. and Grant D.A., "A Theoretical and Practical Investigation of Switching Frequency Harmonics in a Matrix Converter", Universities Power Electronics Conference, Stafford, September 1993.

(Winner of the Prize for Best Paper at the Conference)

# REDUCING THE SEMICONDUCTOR LOSSES IN A MATRIX CONVERTER

P. W. Wheeler and D. A. Grant[1]

## Abstract

This paper looks at the implementation of a matrix converter switching strategy under microprocessor control and using IGBTs. The effects of different switching methodologies for the converter are investigated. The power losses in the switching devices of a matrix converter are analysed and quantified. The effects of different switching frequencies and approaches to PWM generation are considered. Comparisons are drawn with a conventional inverter in terms of efficiency and relative cost.

With the price of semiconductors falling and the reduction in device switching times it may not be long before the matrix converter's silicon solution to AC motor control may be commercially viable.

## 1 Introduction

The matrix converter is an alternative to an inverter drive for 3-phase frequency control. The converter consists of nine bi-directional switches arranged as three sets of three so that any of the three input phases can be connected to any of the three output lines (see figure 1). The switches are then controlled in such a way that the average output voltage is a sinusoid of the required frequency. This circuit was considered in the late 1970's [1] and further work carried out by Venturini [2] in 1981. Some of the limitations of the matrix converter have subsequently been overcome [3], [4] making it a more viable commercial proposition.

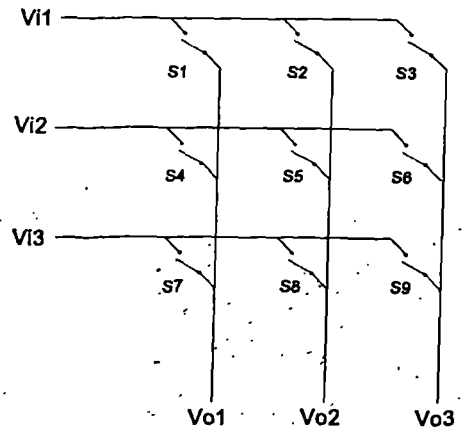


**Figure 1: The Matrix Converter Switch Layout**

## 2 The Semiconductor Losses

Since a suitable bi-directional semiconductor switch has not yet been developed the matrix converter can be realised using a switch constructed from discrete components. The switch can be realised in two ways as shown in figure 2. The back to back IGBT arrangement was chosen as it allows independent control of the current in

[1]P. W. Wheeler and D. A. Grant are with the Industrial Electronics Group, Department of Electrical and Electronic Engineering, University of Bristol, UK.

both directions within each switch. This control would not be possible if the diode bridge circuit was used. The diode bridge circuit also has a greater conduction loss since there are two diodes in series with the IGBT.

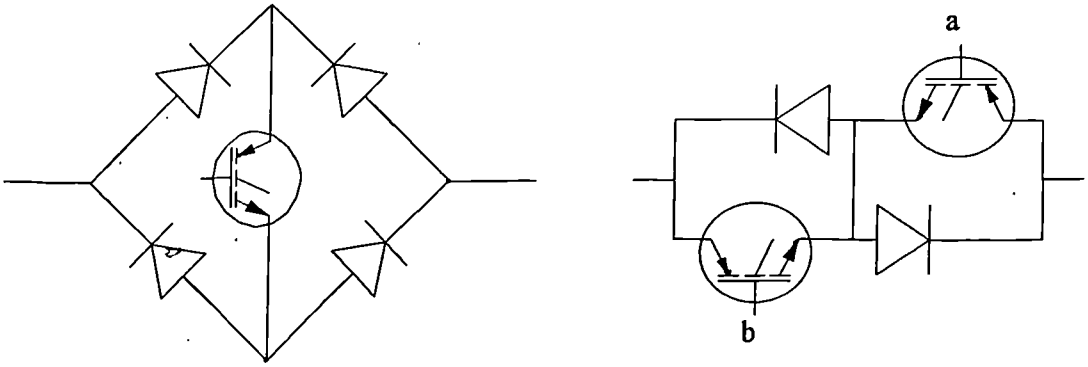


**a. Diode Bridge Bi-directional Switch** **b. Back to Back IGBT**

**Figure 2: Possible Bi-directional Switch Configurations**

The losses in a matrix converter consist of conduction losses and switching losses. The conduction losses are proportional to the forward voltage drop across the device and the current carried by the device. The forward voltage drop is dependant upon the junction temperature of the device and the current carried by the device. These relationships require an iterative calculation since the device losses and the junction temperatures are interdependent. The conduction loss per switch is calculated as the sum of the conduction losses in the IGBT and in the associated diode. The conduction loss in a matrix converter is therefore slightly greater than in an inverter in which either the IGBT or the diode would carry the load current.

The switching losses in the IGBT are due to the finite time taken for the device to change state. These losses are dependent on the junction temperature, giving a further complication to the iterative loop between the losses and the junction temperature. The switching losses are also proportional to the switching frequency at which the converter is operating.

## 3 Calculation of the Converter Losses

If the assumption is made that the switching time of the switches is negligible in comparison to the conduction time, then the conduction losses for one output phase of the converter can be calculated as the sum of the conduction losses in each switch in that phase, as shown in equation 1. The conduction loss in a given switch is the product of the forward voltage drop, the average current flowing in the switch and the duty cycle of the switch, $a_n$, as follows:

$$P_{cond,phase} = \sum_{n=1}^{n=3}\left[\left(V_{cen}I_{cn}d_n\right)+\left(V_{fn}I_{fn}d_n\right)\right] \cong I_l.\left(V_{ce}+V_f\right) \quad (1)$$

Where: $V_{ce}$ = Saturation voltage of the IGBT $I_c$ = Collector current carried by the IGBT

$V_f$ = Forward voltage of the diode $I_f$ = Forward current carried by diode

The switching losses per switch in the matrix converter are calculated as the product of the switching frequency and the energy loss per pulse, $E_{loss}$, for the given device.

$$P_{switch,phase} = 3f_s.E_{loss} \quad (2)$$

This will give a total power loss for the matrix converter equal to the sum of the switching losses and the conduction losses, as follows:

$$P_{total} = 3.\left(P_{cond,phase} + P_{switch,phase}\right) \quad (3)$$

The contribution made by each component of the power loss to the total matrix converter power losses are shown graphically in figure 3 for a range of switching frequencies. The figures are based on a 5kWatt converter using IRGBC20 600Volt, 13Amp IGBTs and MUR860 600Volt, 8Amp diodes. The graph was computed using an iterative process set up on a computer spread sheet.

This value of the total converter power loss assumes that every current path change in the converter results in a switching loss. A possible method of reducing the converter losses could therefore be to reduce the number of switch state changes that produce switching losses.

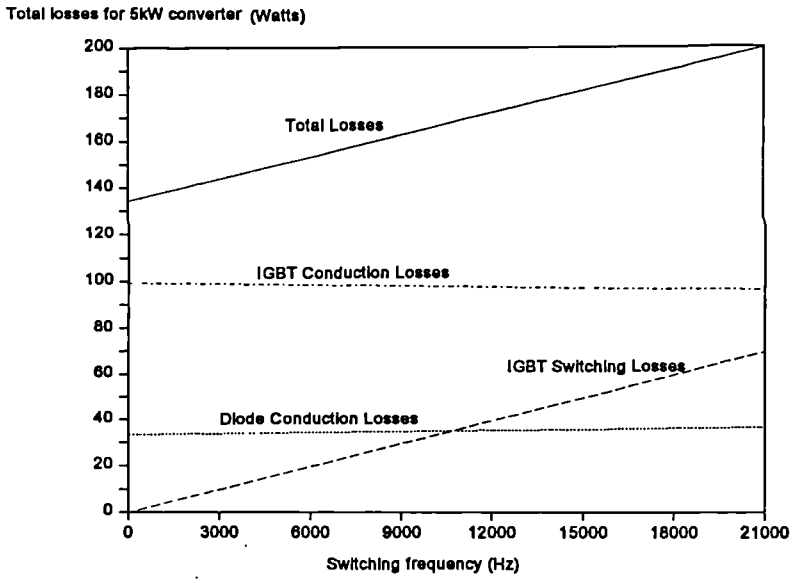


**Figure 3: The Composition of the Matrix Converter Semiconductor Losses**

## 4 Methods of Reducing Semiconductor Losses

The conduction losses in the matrix converter are determined by the forward drop characteristics of the chosen devices. However the switching losses may be reduced by selecting devices with short switching times. The switching losses may also be reduced by adopting an appropriate method of commutating the current from one conducting switch to the next. It will be shown that switching losses can be further reduced by the use of a method of Partially Symmetrical PWM.

Switching losses can be reduced by providing an overlap in the switching periods of the conducting halves of the bi-directional switches. This method of current commutation allows zero current switching if the outgoing device is reversed biased by the turn on of the incoming device. This situation will occur when the voltage on the input line of the incoming switch is greater than the voltage on the input line of the outgoing switch in the conduction path. There is a 50% probability of the zero current switching occurring at any given current path changeover. This method of current commutation will therefore achieve a 50% reduction in the average switching losses in a matrix converter. For this reason an appropriate term for this type of control is **semi-soft current commutation**. Figure 4 shows the control waveforms for semi-soft current commutation between switch S1 and switch S2 assuming the output current is flowing in the a direction as defined in figure 2.

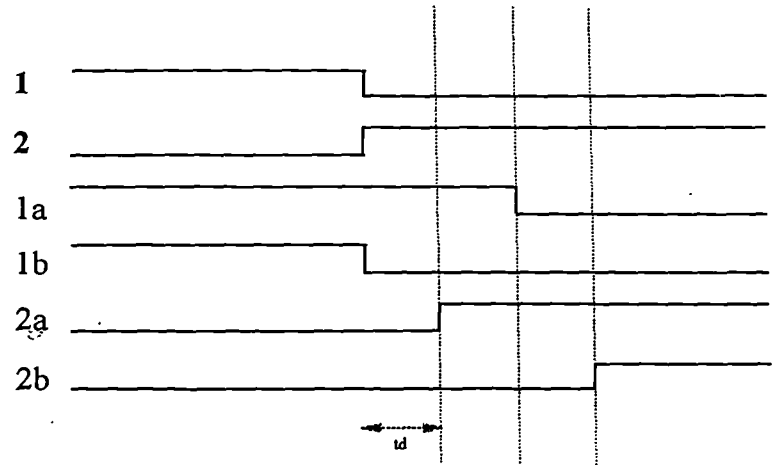


**Figure 4: The Timing Diagram for the Switch Control Functions During Semi-Soft Current Commutation**

The switching losses can also be reduced using a PWM method in which the order of the closing of the switches is considered. Instead of operating the switches in a conventional order of switch S1, switch S2, switch S3, switch S1, switch S2, switch S3 and so on, the last switch in the set of three becomes the first in the next set of three. The switching order therefore becomes switch S1, switch S2, switch S3, switch S3, switch S1, switch S2, switch S2, switch S3 and so on. This method of PWM has been termed semi-symmetrical PWM. A reduction of 33% in the required number of switch commutations is achieved using this method.

If both of the switch loss reduction techniques described above are implemented, then a reduction of 66% in the switching losses can be achieved. If the total semiconductor losses in the matrix converter are compared to total losses (rectifier and inverter stages) of an inverter drive, it can be shown that this reduction in switching losses will compensate for the extra conduction losses inherent in the matrix converter structure. Figure 5 shows that at higher switching frequencies the matrix converter can be more efficient than an inverter drive.

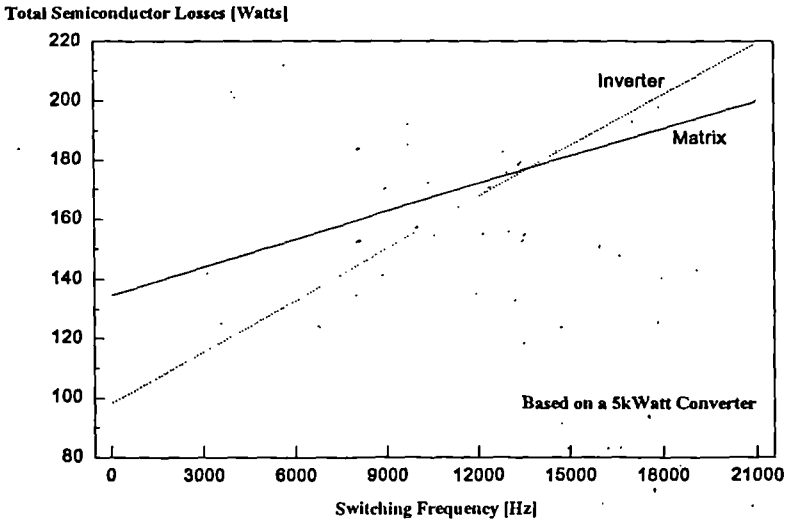


**Figure 5: A Comparison of Inverter and Matrix Converter Losses Against Switching Frequency**

## 5 Conclusions

The semiconductor losses in a matrix converter have been examined. The conduction losses in the matrix converter have been found to be higher than the conduction losses in a standard inverter. Methods of reducing the switching losses in a matrix converter have been proposed. The implementation of these methods means that the total losses in the matrix converter can be less than those in an inverter drive at high switching frequencies. It has been shown that even at lower switching frequencies the losses in the matrix converter are not significantly greater than those in an inverter drive.

## 6 References


[1] Gjugyi L. and Pelly B.,"Static Power Frequency Changers". New York, Wiley, 1976

[2] Venturini M., "A New Sinewave In Sinewave Out, Conversion Technique Which Eliminates Reactive Elements". Proceedings Powercon 7 (San Diego), 1980, pp.E3_1-E3_15.

[3] Alesina A. and Venturini M., "Intrinsic Amplitude Limits and Optimum Design of 9-switches Direct PWM AC to AC Converter". Proceedings of PESC Conference Record, 1980, pp.242-252.

[4] Beasant R., Beatie W. and Refsum A., "An Approach to the Realisation of a High Power Venturini Converter". IEEE, April 1990, pp.291-297.


## Acknowledgements


The support of the Science and Engineering Research Council for this work is gratefully acknowledged (Grant No. GR/H23436).

# A LOW LOSS MATRIX CONVERTER FOR AC VARIABLE-SPEED DRIVES

P.W. Wheeler and D.A. Grant

Industrial Electronics Group, University of Bristol, England.

Abstract. This paper reports the construction and testing of a matrix converter in which novel switching methods are employed to minimise the losses in the switching devices. A mixture of hard and soft commutation is used during each cycle of the output waveform. This permits losses to be reduced to a minimum while waveform quality is enhanced. It is demonstrated that at elevated switching frequencies the efficiency of a matrix converter can be comparable to that of the traditional inverter drives. IGBTs are used as the switching devices and a microcontroller is used to generate the switching waveforms and provide control. Reactive components have been minimised so that the matrix converter is now approaching an all-silicon solution to ac-ac power conversion. Practical results are presented.

Keywords. Matrix Converter, Forced Commutated Cycloconverters, Variable Speed Drives, Current Commutation.

## INTRODUCTION

The matrix converter is an alternative to an inverter drive for 3-phase frequency control. The converter consists of nine bi-directional switches arranged as three sets of three so that any of the three input phases can be connected to any of the three output lines (see figure 1). The switches are then controlled in such a way that the average output voltage between the output lines is a sinusoid of the required frequency. This circuit was first considered in the late 1970's [1] and further work carried out by Venturini [2] in 1981. Some of the limitations of the matrix converter have subsequently been overcome [3], [4] making it a more viable commercial proposition.

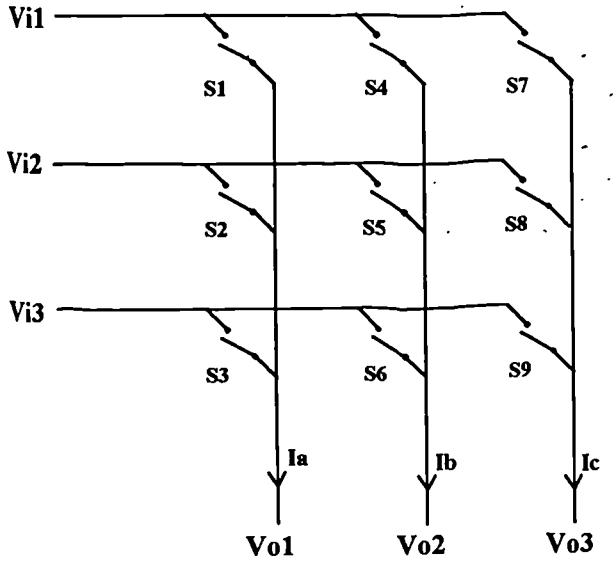


**Figure 1: The Matrix Converter Switch Layout**

The matrix converter has a number of advantages over conventional variable speed drives. A matrix converter requires no large reactive components as there is no DC link. This makes the matrix converter an all silicon solution for variable speed drives. A matrix converter also draws sinusoidal input currents after the filtering of switching frequency harmonic. Most control algorithms also allow the input displacement factor to be set at unity or even leading.

## INTRINSIC MAXIMUM OUTPUT VOLTAGE

The output voltage of a matrix converter is limited to 0.866 of the input voltage. This limitation is because the maximum peak to peak output voltage cannot be greater than the minimum voltage difference between two phases of the input. This is an intrinsic limit on the performance of any matrix converter.

The maximum output voltage may be achieved by introducing third harmonics of the input and output frequencies on to the output waveform to make full use of the available input voltage. These third harmonics will give the line output voltages described by equation 1.

$$V_o(t) = 0.866.\begin{bmatrix} \cos(\omega_o t) \\ \cos(\omega_o t + \frac{2\pi}{3}) \\ \cos(\omega_o t - \frac{2\pi}{3}) \end{bmatrix} + 0.25.\cos(\omega_o t) + 0.12.\cos(\omega_o t) \quad (1)$$

## A PRACTICAL BI-DIRECTIONAL SWITCH

The practical realisation of a Matrix Converter requires the use of a bi-directional switch. Until device technology progresses to the point where such a device is practical this bi-directional switch must be fabricated using discrete components. The switches may be constructed using diodes and transistors. IGBTs have been chosen as the controllable devices due to their high switching speeds and current handling capabilities. There are three possible configurations for this bi-directional switch:

- Diode Bridge with a Single IGBT
- A Pair of Back to Back IGBTs in Common Collector Mode
- A Pair of Back to Back IGBTs in Common Emitter Mode

### Diode Bridge Switch Configuration

Figure 2 shows the a diode bridge arrangement with one switching device providing the current path at all times. This style of bi-directional switch has the advantage of only requiring one IGBT and its associated gate driver circuit. The main disadvantage of the diode bridge arrangement is that three devices are conducting at any given time giving rise to relatively high conduction losses.

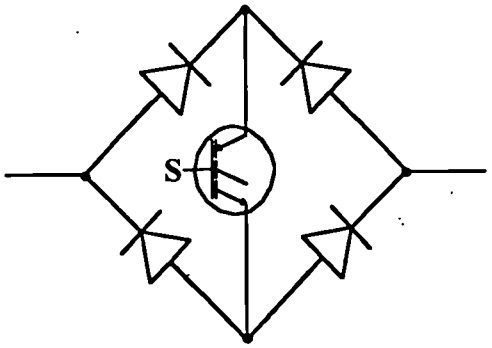


**Figure 2: The Diode Bridge Bi-Directional Switch Configuration**

### Back to Back IGBT Switch Configurations

Figures 3 and 4 show how a back to back arrangement of IGBTs may be used to implement the bi-directional switch for a matrix converter. The two diodes are used to provide the reverse voltage blocking capability. This arrangement was chosen as it allows independent control of the current in both directions within each switch. This control can then be used in current commutation between switches to reduce the switching losses. The back to back arrangement also has lower conduction losses than a diode bridge switch arrangement as fewer devices are conducting at any given time.

If the devices in the switch are connected in common emitter mode then only one isolated gate drive is required to drive each switch. In common collector mode the emitter of each device is connected to either an input of an output line of the converter. With this configuration the number of isolated gate drive supplies for the converter is reduced to six.

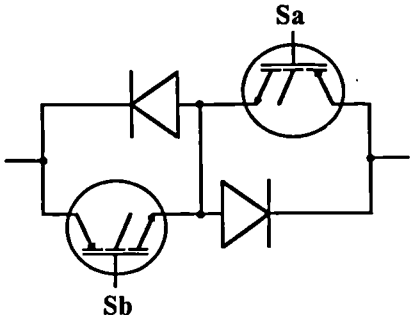


**Figure 3: Back to Back IGBT Bi-Directional Switch in a Common Emitter Configuration**

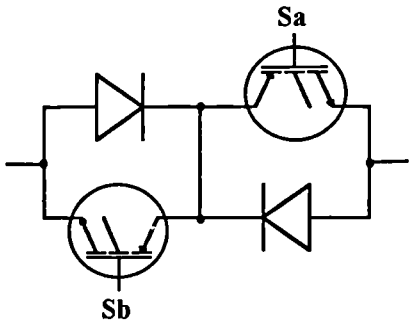


**Figure 4: Back to Back IGBT Bi-Directional Switch in a Common Collector Configuration**

## SAFE CURRENT COMMUTATION

The switches in the converter must be controlled in such a way that two input lines are never connected to the same output line. It is also important that every output line is always connected an input line to avoid open circuiting the motor. These conditions may occur due to the finite switching times in semiconductor switches. A method of avoiding these situations is therefore required.

### Dead Time Current Commutation

Matrix converters have been built using dead times [5] to overcome the shorting of the input lines due to the finite switching times of the devices. If dead times are used then some form of voltage clamping or an alternative current path must be provided to avoid an uncontrolled open circuit of the motor. The introduction of dead times also increases the losses in the converter. The switch control waveforms for dead time operation are shown in figure 5 for the passing of the current path between switch 1 and switch 2.

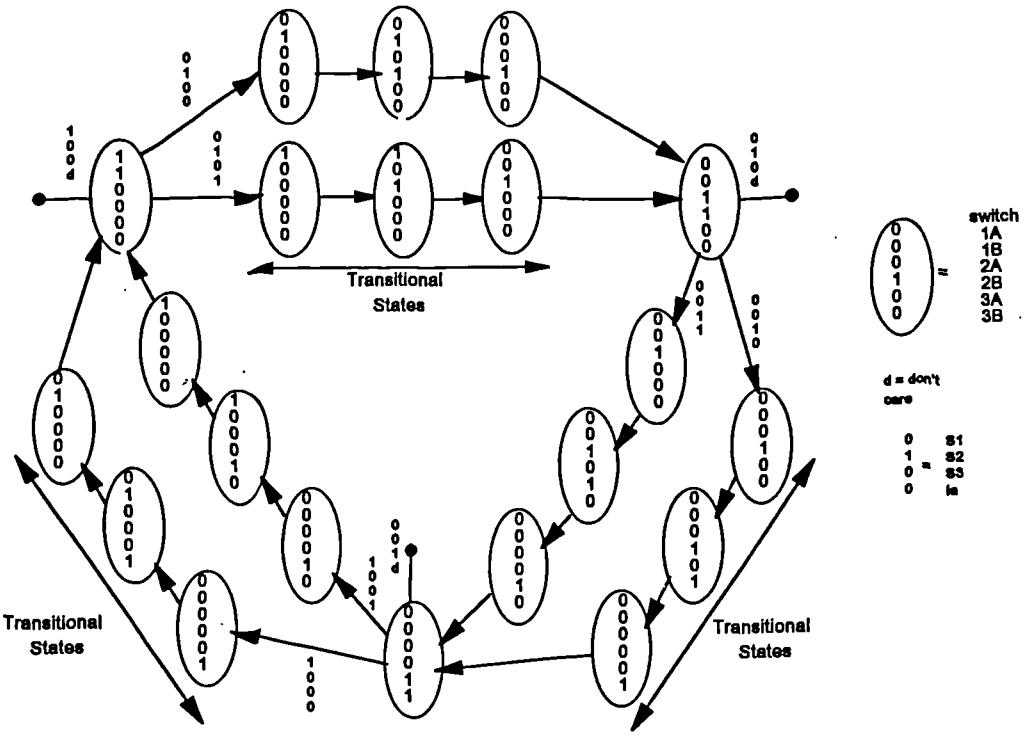


**Figure 7: The State Diagram for the Semi-Soft Current Commutation Strategy**

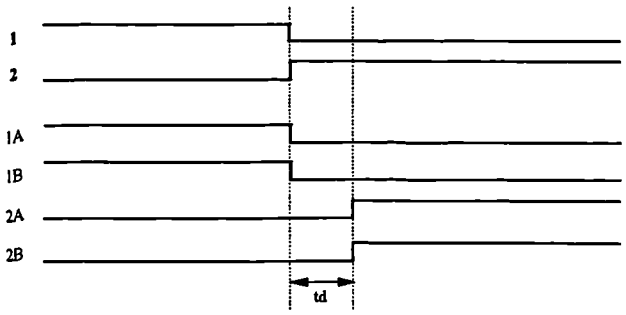


**Figure 5: Switch Control Waveforms for Dead Time Current Commutation**

### Overlap Time Current Commutation

Overlap between the switching periods of switches has been used as an alternative to dead times [6], with inductance introduced in the input lines to minimise the short circuit currents. The inductors required to minimise these currents would be large and expensive. This paper presents an alternative that minimises the switching losses and requires minimal voltage clamping.

### Semi-Soft Current Commutation

The current can be commutated from one switch to the next by providing an overlap in the switching periods of the conducting halves of the bi-directional switches. This method of current control will allow zero current switching of the IGBTs if the outgoing device is reversed biased by the turn on of the incoming device. This situation will occur when the voltage on the input line of the incoming switch is greater than the voltage on the input line of the outgoing switch in the conduction path. There is a 50% chance of the reverse biased situation occurring. For this reason an appropriate term for this type of current control is **semi-soft current commutation**. Figure 6 shows the control waveforms for semi-soft current commutation between switch S1 and switch S2, with A and B denoting the two independent halves of the switch.

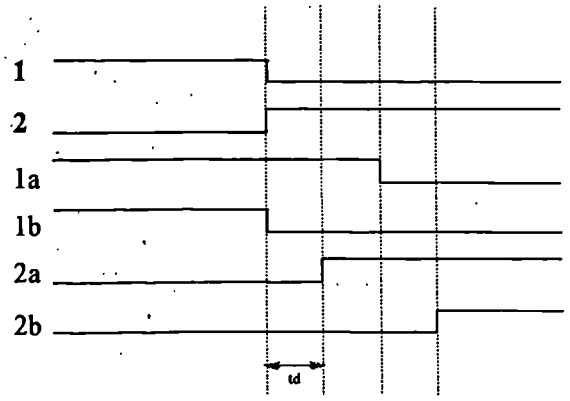


**Figure 6: The Timing Diagram for the Switch Control Functions for Semi-Soft Current Commutation**

Figure 7 shows the semi-soft current commutation control in the form of a state diagram for one output phase of the matrix converter. This state diagram may

then be used to program a logic device such as a GAL. The clock frequency for the logic device may be a used to adjust the existence time for each transition state. The existence time of each state can then be set to match the characteristic propagation and switching delays of the devices used in the converter. This approach to the implementation of the current commutation strategy gives a simple and flexible solution to the safe operation of the matrix converter switches.

## THE CONVERTER LOSSES

The semiconductor losses in a matrix converter consist of conduction losses and switching losses. The switching losses are due to the finite time taken for the IGBT to change state. The conduction losses are proportional to the forward voltage drop across the device and the current carried by the device. Figure 7 shows graphically the composition of the total losses in a matrix converter. The graph was generated using iterative routines on a computer spread sheet. The figures are based on a 5kWatt converter using IRGBC20 600Volt, 13Amp IGBTs and MUR860 600Volt, 8Amp diodes.

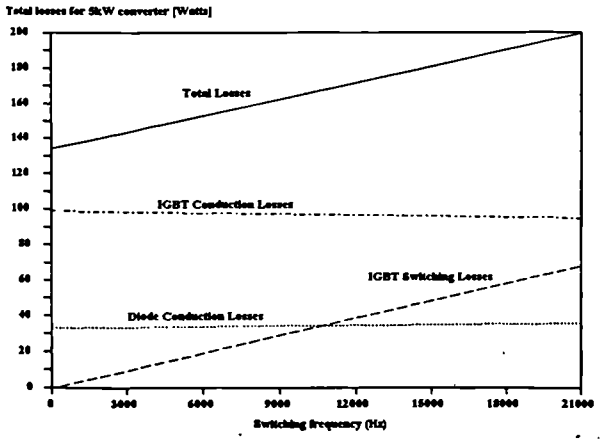


**Figure 7: The Composition of the Matrix Converter Semi-conductor Losses**

## REDUCTION OF SWITCHING LOSSES

The characteristics of the chosen devices in a matrix converter determine the conduction losses. The switching losses may also be reduced by careful selection of devices. However the switching losses may be reduced by considering the method of current commutation employed and the switching patterns.

### Switching Loss Reduction Using Semi-soft Current Commutation

The switching losses can also be reduced by the implementation of a suitable method of commutating the current from one conducting switch to the next. Semi-Soft current commutation will achieve a 50% reduction in the average switching losses in a matrix converter because there is a 50% chance of the reverse biased situation occurring.

### Switching Loss Reduction Using Semi-Symmetrical PWM Waveforms

The switching losses can also be reduced by 33% with the implementation of a PWM method in which the last in a set of three switching periods becomes the first switching period in the next set of three switching periods. Instead of a conventional order of switch S1, switch S2, switch S3, switch S1, switch S2, switch S3 and so on, the order becomes switch S1, switch S2, switch S3, switch S3, switch S1, switch S2 and so on. This method has been termed semi-symmetrical PWM. The switching sequence for semi-symmetrical PWM is shown in figure 8.

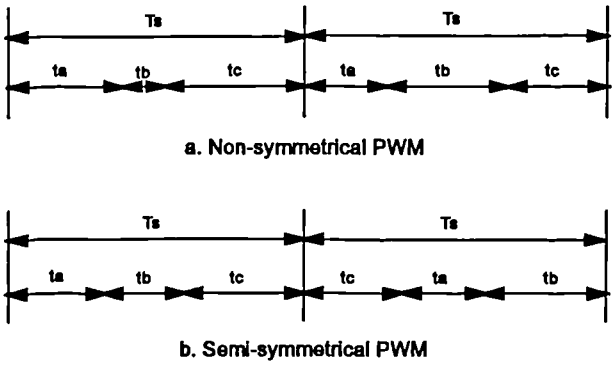


**Figure 8: The Control Waveform Sequences for Semi-Symmetrical and Non-Symmetrical PWM**

### Total Switching Loss Reduction

The effect of implementing both semi-soft current commutation and semi-symmetrical PWM on the switching losses of a matrix converter is shown in figure 9. The reduction in switching losses for each technique implemented independently is also shown.

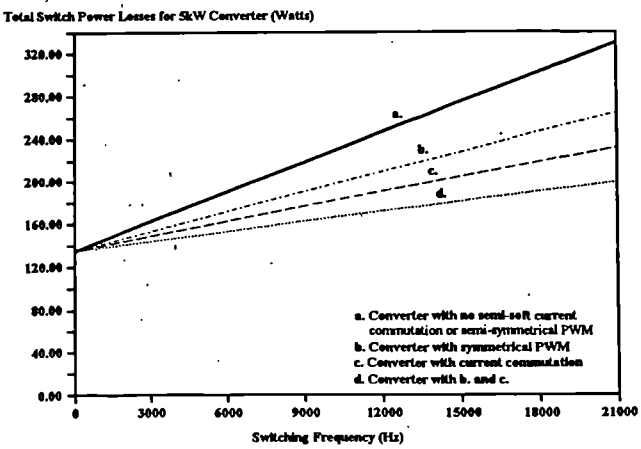


**Figure 9: The Effect of Switching Loss Reduction Techniques on the Total Converter Losses**

The semi-conductor losses for a rectifier/inverter circuit employing similar components may also be calculated. These losses for this inverter circuit can be compared to the losses in a matrix converter as shown in figure 10. At higher switching frequencies it may be seen that a matrix converter offers lower semi-conductor losses than the inverter.

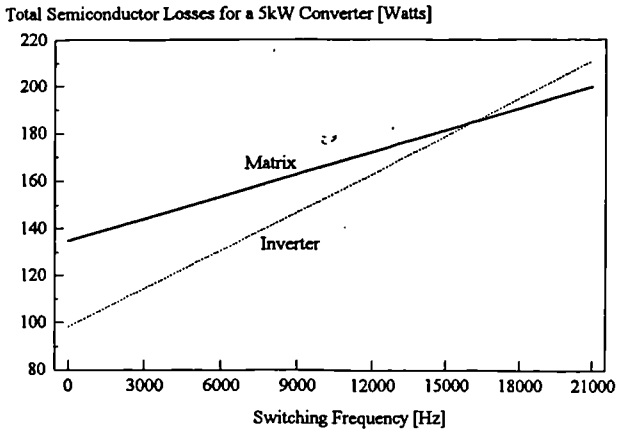


**Figure 10: A Comparison of the Total Converter Losses for a Matrix Converter and an Inverter**

## RESULTS

A 1kWatt, 415Volt matrix converter has been built and tested. The system uses a Seimens SAB80C166 micro-controller to provide the control signals. GALs have been used as the programmable logic devices for the implementation of the current commutation strategy.

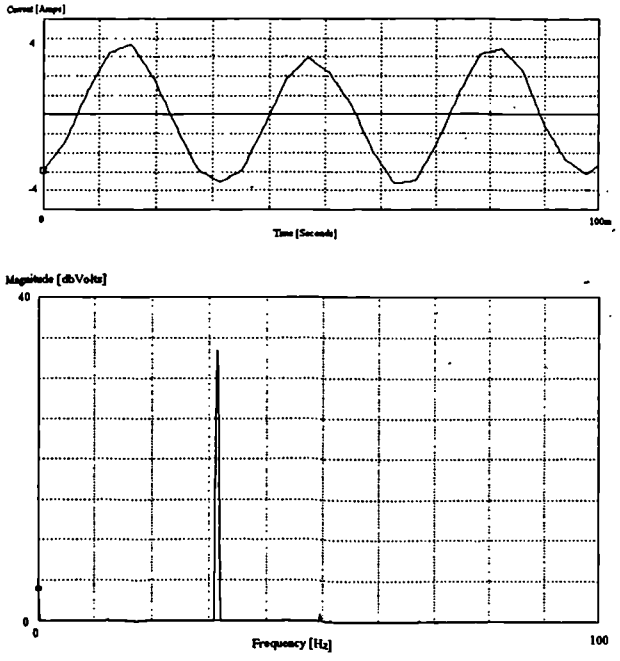


**Figure 11a: The Output Current Waveform and the Output Voltage Spectrum, 32Hz Output frequency.**

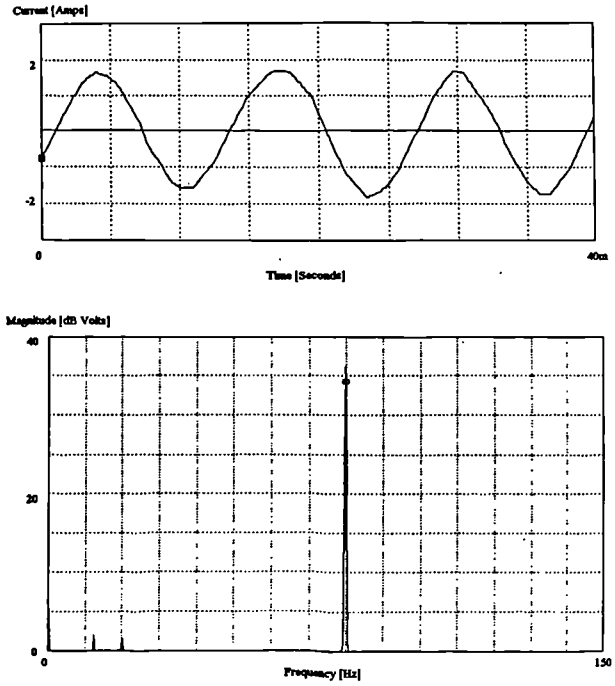


**Figure 11b: The Output Current Waveform and the Output Voltage Spectrum, 80Hz Output Frequency.**

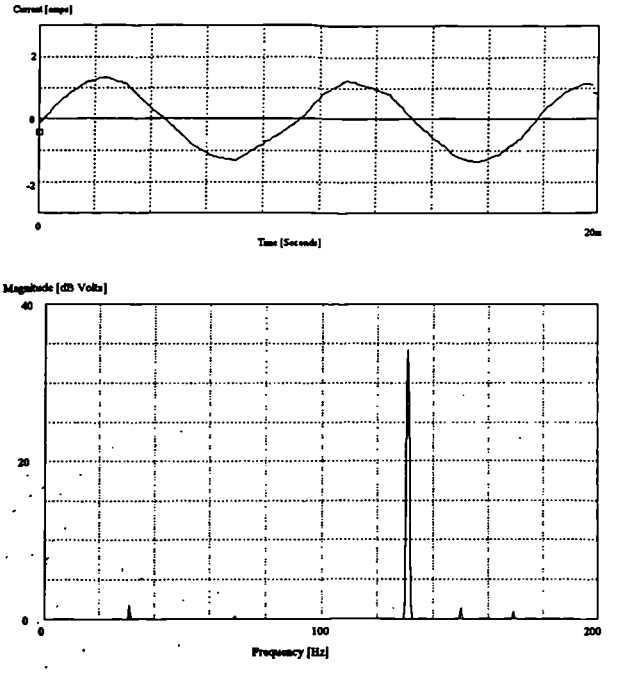


**Figure 11c: The Output Current Waveform and the Output Voltage Spectrum, 130Hz Output Frequency.**

A switching frequency of 20kHz has been chosen for the converter to minimise the size of the input filters whilst keeping switching losses at an acceptable level. The converter has been designed to give output frequencies between 0Hz and 200Hz. Figure 11 shows the output waveforms obtain from the converter. The input current frequency spectrum is shown in figure 12.

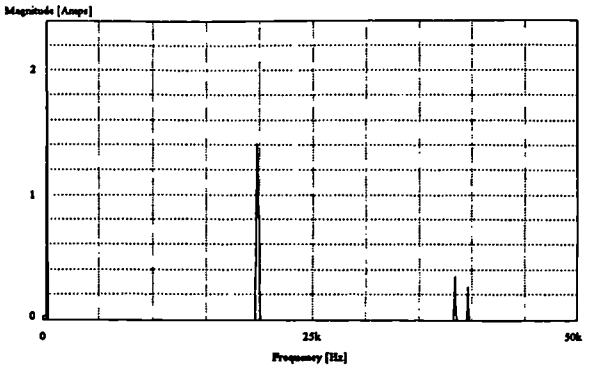


**Figure 12a: The Input Current Voltage Spectrum Showing the Fundamental and First Harmonic of the Switching Frequency. 30Hz Output Frequency**

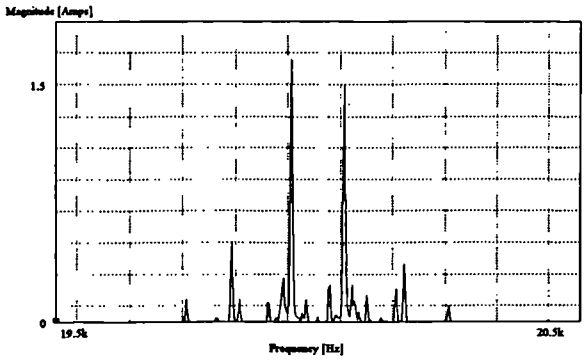


**Figure 12b: The Input Current Voltage Spectrum Showing the Harmonics to the Switching Frequency. 50Hz Input Frequency, 30Hz Output Frequency**

## CONCLUSIONS

This paper has examined the design and limitations of a matrix converter, with particular emphasis on losses in the power semiconductor devices. New methods of minimising switching losses have been described. It has been shown that total losses in a matrix converter can be comparable to those in the conventional inverter drive. Practical results obtained from a 1kWatt, 415Volt matrix converter have been presented, showing that good waveform quality can be obtained, and that the matrix converter is a serious challenger to the inverter in ac variable-speed drives.

## ACKNOWLEDGEMENTS

The support for this work from the Science and Engineering Research Council and Control Techniques plc. under the PEDDS LINK scheme is gratefully acknowledged (Grant No. GR/H23436).

## REFERENCES

1 Gjugyi L. and Pelly B., 1976, "Static Frequency Changers," New York, Wiley.

2 Venturini M., 1980, Proceedings Powercon 7 (San Diego), E3_1-E3_15.

3 Alesina A. and Venturini M., 1980, Proceedings of PESC Conference Record, 242-252.

4 Lipo T.A., 1988, IEEE Trans. on Power Electronics, 105-117.

5 Huber L., Borojevic D. and Burany N., 1989, IECON. 48-53.

6 Beasant R., Beatie W. and Refsum A., 1990, IEEE, .291-297.

7 Ueda R., Sonoda T. and Takata S., 1986, IEEE, 196-202.

# A THEORETICAL AND PRACTICAL INVESTIGATION OF SWITCHING FREQUENCY HARMONICS IN A MATRIX CONVERTER

**P.W. Wheeler, Dr. H. Zhang and Dr. D.A. Grant**

Industrial Electronics Group, University of Bristol, UK.

## ABSTRACT

This paper considers the switching frequency harmonics drawn from the supply by a matrix converter. The magnitude and frequencies of the switching frequency harmonics are examined. The problems associated with input current filtering to comply with existing and possible future EMC regulations are investigated. Possible solutions to these filtering requirements are evaluated. The paper compares results from mathematical theory, computer simulation, and a power level converter under microprocessor control.

With the price of semiconductors falling and the reduction in device switching times it may not be long before the matrix converter's all silicon solution to AC motor control may be commercially viable.

## 1 INTRODUCTION

The matrix converter is an alternative to an inverter drive for 3-phase frequency control. The converter consists of nine bi-directional switches arranged as three sets of three so that any of the three input phases can be connected to any of the three output lines (see figure 1). The switches are then controlled in such a way that the average output voltage between the output lines is a sinusoid of the required frequency.

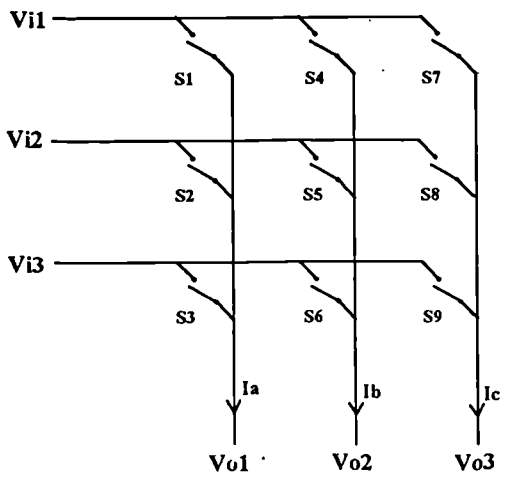


**Figure 1: The Matrix Converter Switch Layout**

This circuit was first considered in the late 1970's [1] and further work carried out by Venturini [2] in 1981. Some of the limitations of the matrix converter have subsequently been overcome [3], [4] making it a more viable commercial proposition.

### 1.1 Advantages of a Matrix Converter

The matrix converter has a number of advantages over conventional variable speed drives. A matrix converter requires no large reactive components as there is no DC link. Reactive components are therefore minimised so that the matrix converter is now approaching an all-silicon solution to ac-ac power conversion. A matrix converter also draws sinusoidal input currents after the filtering of switching frequency harmonic. Most control algorithms also allow the input displacement factor to be set at unity or even leading if the converter is connected to a load with a lagging power factor. IGBTs are used as the switching devices and a microcontroller generates the switching waveforms and provides control.

### 1.2 Intrinsic Maximum Output Voltage

The output voltage of a matrix converter is limited to 0.866 of the input voltage. This limitation is because the maximum peak to peak output voltage cannot be greater than the minimum voltage difference between two phases of the input. This is an intrinsic limit on the performance of any matrix converter. The maximum output voltage may be achieved by introducing third harmonics of the input and output frequencies on to the output waveform to make full use of the available input voltage. These third harmonics will give the line output voltages described by equation 1. This voltage restriction is the only significant restriction on the performance of a matrix converter.

$$V_o(t) = 0.866 \begin{bmatrix} \cos(\omega_o t) \\ \cos(\omega_o t + \frac{2\pi}{3}) \\ \cos(\omega_o t - \frac{2\pi}{3}) \end{bmatrix} + 0.25.\cos(\omega_o t) + 0.12.\cos(\omega_o t) \quad (1)$$

### 3.1 Computer Simulation

The operation of the converter may be modelled using a computer simulation. A suitable program has been written using ACSL. The simulation program may be used to generated the input current spectrum for the converter. The input current spectrum for an output frequency of 30Hz is shown in figure 4.

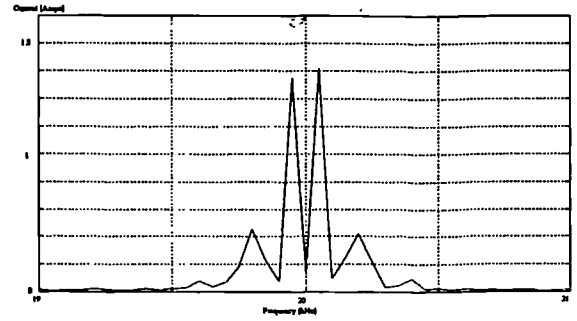

**Figure 4: A Simulated Input Current Spectrum**

### 3.1 Practical Results

A 2kWatt, 415Volt matrix Converter has been built. The unfiltered input current frequency spectrum is shown in figure 5 for an output frequency of 30Hz. The switching frequency and it's second harmonic at 40kHz can be seen. Figure 6 shows the harmonics to the switching frequency that are of the form predicted above.

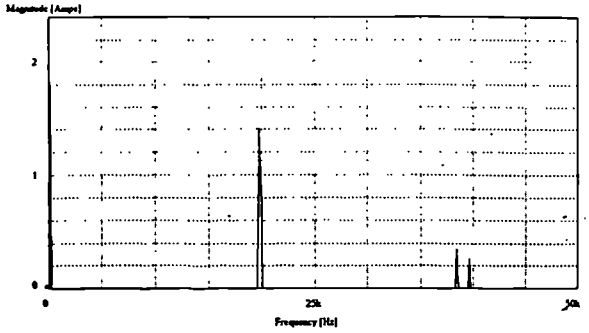

**Figure 5: The Input Current Spectrum Showing the Switching Frequency and 2nd Harmonic**

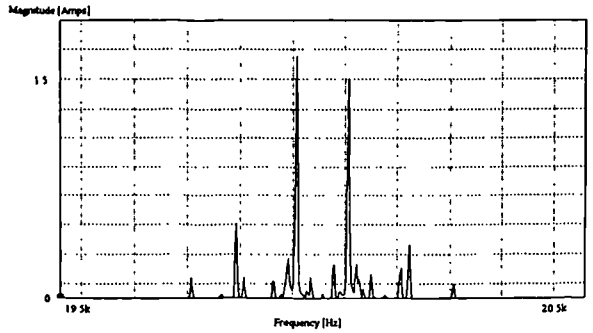

**Figure 6: The Input Current Voltage Spectrum Showing Harmonics to the Switching Frequency.**

## 4 REQUIRED FILTER CHARACTERISTICS

The mathematical model of the input current waveform may be used to determine the maximum magnitudes of the switching frequency harmonics. This worst case condition will occur when the converter is driving a motor at zero speed with maximum torque. The disturbance voltage caused by the input current of the converter drawn from a standard supply can then be calculated [8]. Once this disturbance voltage spectrum is known the attenuation characteristics for the input filter can be found. The switching frequency current has the largest magnitude of all the switching frequency harmonics. The minimum size filter would therefore be required to provide the necessary attenuation at the switching frequency.

### 4.1 Filter Circuit Design

A single stage LC filter could be used to provide the required attenuation. However to meet the regulations a single stage filter would become large. A more economical solution could be to use a multistage filter or a single stage filter with a tuned harmonic diversion as shown in figure 7.

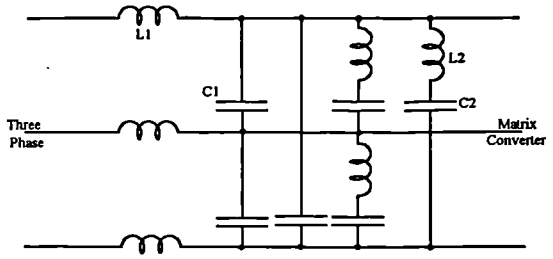


**Figure 7: LC Line to Line Filter With Added Harmonic Diversion**

### 4.2 Filter Component Costing

In an attempt to make cost comparisons between the various possible filter configurations it has been assumed that the cost and size of a comparable component is proportional to the component's power rating. The cost of inductive power has been taken as twice as much as capacitive power. Using these assumptions it is possible to calculate the approximate comparative costs of any filter configuration using a normalised cost factor as shown in equation 2.

$$Cost\ Factor = 2.05\left\{2\sum_{n=1}^{n=\infty} L_n I_{n,rms}^2 + \sum_{m=1}^{m=\infty} C_m V^2\right\} \qquad (2)$$

V = input voltage, $I_{rms}$ = total input current

The cost factor can also be used to optimise the proportions of inductance and capacitance in the filter. The component sizes for the a range of filter configurations can then be calculated and compared as shown in table 1. The figures given are based on a 415Volt converter with a maximum input line current of 6.5Amps and a switching frequency of 20kHz.

| Filter Type | L | C | Cost Factor |
|---|---|---|---|
| Single Stage LC[1] | 3mH | 1.5μF | 1 |
| Single stage with 20kHz Diversion | 3mH<br>0.5mH | 1.5μF<br>0.16μF | 1.07 |
| Two Stage LC | 2mH<br>2mH | 1μF<br>1μF | 1.35 |
| LC capable of 60dB @ 20kHz | 11mH | 6μF | 3.74 |

**Table 1: The Component Values for the Three Considered Types of Filter**
([1] does not meet required attenuation at 20kHz)

The effect on the input current spectrum of the addition of an input filter is shown in figure 8. This current spectrum can be compared to the unfiltered spectrum shown in figure 6.

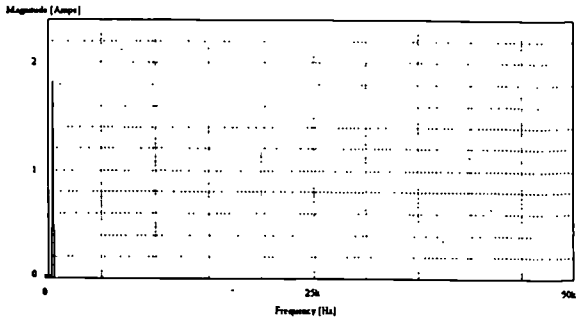

**Figure 8: Input Current Spectrum After Filtering**

If the switching frequency of the converter were to be reduced then the relative size of the filter increases as shown in figure 9. This increase in filter size must be compared to the reduction in switching losses achieved by use of a lower switching frequency.

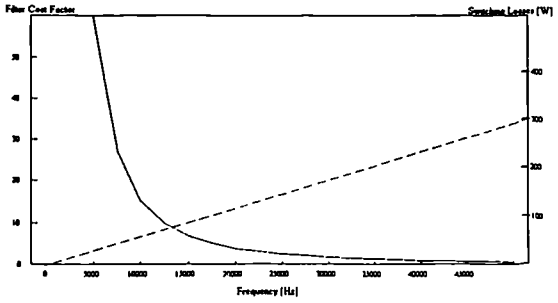

**Figure 9: The Effect of Switching Frequency on the Comparative Cost of the Input Filter**

## 5 CONCLUSIONS

The filters considered in this chapter would be used along with the existing measures employed to solve higher frequency EMC problems in inverter circuits. This paper has examined the relevant regulations and recommendations in the EMC band between 10kHz and 150kHz where a matrix converter is likely to cause new differential mode noise problems. It has been shown that complying with possible future regulations will require the matrix converter switching frequency to be relatively high to minimise the size of input filter components. Comparisons have been made between different filter configurations. It has been shown that the most economical filter for cost and size would be a simple LC filter with a harmonic diversion to reduce the harmonics to the fundamental switching frequency.

## 6 ACKNOWLEDGEMENTS

The support for this work from SERC and Control Techniques plc. under the PEDDS LINK scheme is gratefully acknowledged (Grant No. GR/H23436).

## 7 REFERENCES

[1] Gjugyi L and Pelly B, "Static Frequency Changers", Wiley, New York, 1976.

[2] Venturini M, "A Sine Wave In Sine Wave Out Converter", Proceedings Powercon 7, pp.E3_1-E3_15, 1980.

[3] Alesina A and Venturini M, "A New Bi-Directional Sinusoidal Waveform Frequency Converter", Proceedings of PESC Conference Record, pp.242-252, 1980.

[4] Lipo T.A, "Recent Progress in the Development of Solid State AC Motor Drives", IEEE Trans. on Power Electronics, pp.105-117, 1988.

[5] European Standards, EN55011, 1986.

[6] Hargis C, "Electromagnetic Corruption and Drives", Drives and Controls, Vol. 8, No. 9, Nov. 1992

[7] German Standards, VDE0871 part 1, 1981.

[8] CISPA 16

[9] Critchley R, "New European Standards on EMC Affects Drives", Drives and Controls, Vol. 8, No. 9, Nov. 1992

[10] Black H.S, "Modulation Theory," D. Van Nostrand, New York, 1953.

## 8 ADDRESS OF LEAD AUTHOR

P.W. Wheeler, Industrial Electronics Group, Dept. of Elec. Eng., Queens Building, University Walk, Bristol, BS8 1TR.